NORTHWESTERN UNIVERSITY

Determinants of Antero-Posterior Polarity in Planarian Regeneration

A DISSERTATION

SUBMITTED TO THE GRADUATE SCHOOL
IN PARTIAL FULFILLMENT OF THE REQUIREMENTS

for the degree

DOCTOR OF PHILOSOPHY

Field of Biological Sciences

By

David Ian Gittin

EVANSTON, ILLINOIS

December 2022

Abstract

Determinants of Antero-Posterior Polarity in Planarian Regeneration

David Gittin

The ability to regenerate lost tissues or organs is widespread in the animal kingdom, but the mechanistic basis underpinning this process is incompletely understood. The planarian flatworm *Schmidtea mediterranea* has an incredibly robust and flexible capacity for regeneration, able to regenerate an entire organism from arbitrary starting points. This makes it an ideal model for the study of how regenerating fragments retain body-axis polarity and use this information to correctly pattern their regeneration.

The findings presented here identify a role for Wnt11 and Dvl signaling in encoding AP axis information within the planaria, enabling a proper head/tail regeneration decision. Importantly, these factors are shown to act prior to injury to establish latent polarity mechanisms that are read out after injury through asymmetric expression of the Wnt signaling antagonist *notum*. This process differentiates the anterior and posterior ends of the regenerating fragment, allowing restoration of posterior Wnt11 expression to reinscribe AP polarity and enable future regeneration. Additionally, findings are presented establishing a function for the kinase *src-1* as a global patterning regulator and suppressor of anterior identity. Together, these findings provide new insights into the mechanisms body-axis patterning during planarian regeneration.

Thesis Advisor: Christian P. Petersen

Acknowledgements

First and foremost, I wish to thank my thesis advisor, Dr. Christian Petersen. Chris, you have been a continual source of support and guidance throughout my Ph.D. journey. You have provided not only invaluable scientific advice, but an unfailingly friendly and enthusiastic perspective which motivated me to keep working when I felt lost or overwhelmed. Thank you for making me a better scientist and a better person.

I would also like to thank all other members of the Petersen lab, past and present. Eric Hill, Cony Vásquez-Doorman, Rachel Lander and Alex Karge, thank you for welcoming me into the lab when I joined and providing support and training. An additional thanks to Erik Schad, for providing protocols, reagents, and proofreading assistance. Special credit is owed to Dr. Nicolle Bonar, who mentored me during my rotation and collaborated with me on investigations into *src-1* which yielded a second author paper and contributed a chapter to this thesis. To current lab members Xavier Anderson, Kathrine Lo, Eleanor Clark, Kyle Krueger and Elias Guan, thank you for making the second half of my time in the Petersen lab just as fun and engaging as the first half, and for validating my experience as the senior, and supposedly most knowledgeable, graduate student. Thanks also to the undergraduates who have spent time in the Petersen lab, in particular Julia Dierksheide who I had the pleasure of training in experimental techniques.

Finally, thank you to my parents, and to my brothers Taylor and Adam. I could not have completed this process without the support of my family. Your continual interest in my work helped me look above the daily grind of research tasks and see the broader value in my research.

Table of Contents

ABSTRACT.....2

ACKNOWLEDGEMENTS 3

TABLE OF CONTENTS 4

LIST OF FIGURES AND TABLES.....7

CHAPTER 1

GENERAL INTRODUCTION.....10

Regeneration biology……...11

Vertebrate Models……..15

Invertebrate Models……...18

Planarian biology and regeneration.....20

Anatomy.....21

Neoblasts……23

Stages of Regeneration……...27

Role of muscle cells in PCG expression and regeneration……..30

Wnt signaling in AP patterning and polarity determination.....33

Asymmetric injury-induced *notum* expression demarcates wound polarity.....37

Dvls are a hub for canonical and non-canonical Wnt signals.....40

AIM OF THIS THESIS 43

CHAPTER 2

Wnt11/Dishevelled signaling acts prior to injury to control wound polarization for the onset of planarian regeneration.....44

Abstract.....45

Introduction.....46

Results.....51

Dvl inhibition leads to mispolarization of injury-induced *notum* from longitudinal muscle.....51

Dvl inhibition disrupts AP patterning and muscle morphology……62

Distinct Wnts promote or inhibit polarized *notum* expression……..69

Inhibition of two Wnt11 factors can induce posterior head regeneration……..82

Wnt11/Dishevelled act prior to injury and through growth to control injury-induced *notum*…...86

Discussion.....101

Materials and Methods.....107

CHAPTER 3

Src acts with Wnt signaling to pattern the planarian anteroposterior axis...110

Abstract.....111

Introduction.....112

Results.....115

Planarian *src-1* suppresses head and trunk identity.....115

src-1 can pattern the AP axis independently from pole identity……..126

src-1 regulates expression of body-wide AP patterning factors……..129

src-1 likely acts independently of *notum/wnt11-6* in head patterning…….135

src-1 inhibition broadly sensitizes animals to AP pattern disruption……..141

Possible relationships between *src-1* and AP polarity…….147

Discussion.....149

Materials and Methods.....154

CHAPTER 4

General Discussion.....158

Scope of thesis.....159

Determinants of Antero-Posterior Polarity in Planarian Regeneration……...160

Dvl/Wnt11 signaling restricts *notum* expression at posterior-facing wounds through a βcatenin independent mechanism……160

This mechanism is dependent on the growth of polarity-informing muscle cells……...161

src-1 acts downstream of multiple planarian Wnts to control tissue patterning……..162

Significance of Work.....163

Future Directions.....163

References……167

List of Figures and Tables

Figure 1.1 Conceptual Modes of Regeneration……...13
Figure 1.2 Fingertip Regeneration in Human Children ……..14
Figure 1.3 Phylogenetic Distribution of Regenerative Capacity…….16
Figure 1.4 Planarian Anatomy…….22
Figure 1.5 Neoblasts are Irradiation Sensitive Pluripotent Stem Cells Required for Regeneration……..25
Figure 1.6 Neoblasts Contain a Subpopulation of Totipotent Stem Cells which can give rise to all Planarian Cell Types……..26
Figure 1.7 Time course of Planarian Regeneration…….28
Figure 1.8 Positionally Controlled Genes are Expressed in Muscle and Act as a Patterning Coordinate System……31
Figure 1.9 Canonical WNT Signaling Controls Anterior-Posterior Pole Determination……34
Figure 1.10 Two FGFRL-Wnt circuits control AP Regional Identity in Planaria ……....36
Figure 1.11 *notum* is the Only Planarian Gene with Asymmetric Injury Induced Expression…38
Figure 1.12 Model for Canonical Wnt Signaling Control of Head/Tail Fate Decision……...39
Figure 1.13 Dishevelled acts in Multiple Cellular Signaling Pathways…….41

Figure 2.1 Pre-existing Model of Wnt Signaling Control of *notum* expression……..52
Figure 2.2 Inhibition of the Dvls Leads to Ectopic *notum* Expression……....53
Figure 2.3 Inhibition of the Dvls Leads to Ectopic *notum* Expression in Muscle at Wound Sites, in Non-Muscle Cells Throughout the Body…….54
Figure 2.4 A Minority of Ectopic *notum* Expressing Cells Generated by Dvl Inhibition are *chat*$^{+}$ neurons…….56
Figure 2.5 Inhibition of the Dvls Depolarizes *notum* Expression with Respect to AP Wound Site…….57
Figure 2.6 Ectopic *notum* Expression in Muscle is Injury Induced……59
Figure 2.7 Non-muscle *notum* Expression Driven by Dvl Inhibition is not Injury Responsive…….60
Figure 2.8 Under Dvl Inhibition, *notum* is Expressed in Longitudinal Muscle……..61
Figure 2.9 Dvl Inhibition Causes Regeneration Defects, Including Polarity Reversal……....63
Figure 2.10 Dvl Inhibition Leads to Anterior Pole Identity at Regenerating PFWs……..64
Figure 2.11 *dvl-1* and *dvl-2* are Broadly Expressed Before and After Injury……....66
Figure 2.12 *dvl-1* and *dvl-2* are Expressed in Multiple Cell Types, Including Muscle.……67
Figure 2.13 Inhibition of Dvls Disorganizes Muscle Morphology.……...68
Figure 2.14 *wnt-1* and *wntP-2* Promote *notum* Expression at Anterior-facing Wounds……...70
Figure 2.15 *wnt1* and *wntP-2* Promote Posterior Fate……...71
Figure 2.16 *wnt1* and *wntP-2* are Expressed in the Posterior, *wnt1* is also Injury Induced……73
Figure 2.17 Inhibition of Multiple Wnts Produces Minor or Regionalized Effects ……..74
Figure 2.18 *wnt11-1* and *wnt11-2* Restrict *notum* Expression at Posterior-facing Wounds…...76
Figure 2.19 Extended RNAi Administration Strengthens Wnt11-1 Wnt11-2 Inhibition Phenotype……...77

Figure 2.20 Under *wnt11-1 wnt11-2* Double Inhibition, *notum* is Expressed in Longitudinal Muscle……79
Figure 2.21 Inhibition of the Dvls, but not the Wnt11s, Decreases Longitudinal Muscle Density ……..80
Figure 2.22 *wnt11-1* and *wnt11-2* are Expressed in Muscle Cells in the Posterior ……..81
Figure 2.23 *wnt11-1* and *wnt11-2* Promote Posterior Identity and Regeneration ……83
Figure 2.24 Inhibition of *wnt11-1* and *wnt11-2* over 18 Days Does Not Affect Pole Identity.84
Figure 2.25 Inhibition of the Wnt11s Disrupts Muscle Morphology in the Posterior but not the Anterior……..85
Figure 2.26 Extended Inhibition of the Wnt11s Leads to Posterior Head Regeneration……..87
Figure 2.27 Dvl Inhibition Phenotypes Strengthen with Longer RNAi Administration ……..89
Figure 2.28 Sublethal Irradiation During a Critical Window Inhibits *dvl-1;dvl-2(RNAi)* phenotype of *notum* Expression at Posterior-facing Wounds……90
Figure 2.29 Sublethal Irradiation Reduces *notum* Expression at Anterior-Facing Wounds….92
Figure 2.30 Irradiation Partially Rescues Dvl Inhibition Phenotype of Muscle Disorganization…….93
Figure 2.31 Sublethal Irradiation Inhibits *wnt11-1;wnt11-2(RNAi)* phenotype of *notum* Expression at Posterior-facing Wounds…….94
Figure 2.32 Irradiation Affects RNAi Phenotypes at Posterior Wounds of Head Fragments As it Does Trunk Fragments……...……...95
Figure 2.33 Irradiation Suppresses Morphological Changes Driven by Dvl or Wnt11 Inhibition……96
Figure 2.34 Irradiation Does not Alter Expression of Dvls or Wnt11s ……98
Figure 2.35 Re-expression of *wnt11-1* and *wnt11-2* During Regeneration Occurs After Expression of Injury-induced *notum*……100
Figure 2.36 Model of Antero-Posterior Polarity Determination During Regeneration……102

Figure 3.1 Phylogeny of *Schmidtea mediterranea* Src Family Kinases……116
Figure 3.2 *src-1* RNAi Knockdown……...117
Figure 3.3 *src-1* is a Regulator of Head Identity……...118
Figure 3.4 Further Evidence *src-1* is a regulator of Head Identity……119
Figure 3.5 *src-1* is a Regulator of Trunk Identity……..121
Figure 3.6 *src-2* is a Regulator of Head Identity……...122
Figure 3.7 *src-1* is Broadly Expressed in Both Muscle and Non-Muscle Cells……123
Figure 3.8 *src-1* Inhibition Does Not Affect Muscle Integrity……..125
Figure 3.9 *src-1* Restricts the Anterior Pole……..127
Figure 3.10 *src-1* Inhibition Does Not Affect the Posterior Pole……128
Figure 3.11 *src-1* Restricts Anterior Positionally Controlled Genes……...131
Figure 3.12 *src-1* Suppresses Trunk Positionally Controlled Genes……...132
Figure 3.13 *src-1* Effects Expression of Medial-Posterior Genes……...133
Figure 3.14 *src-1* Regulates Posterior Positionally Controlled Genes in Regeneration…….134
Figure 3.15 Simultaneous Inhibition of *notum* and *src-1* Creates a Synthetic Eye Phenotype…….137

Figure 3.16 Simultaneous Inhibition of *notum* and *src-1* Creates an Intermediate Brain Size Phenotype……138
Figure 3.17 Simultaneous Inhibition of *notum* and *ndk* Creates a Synthetic Eye Phenotype.139
Figure 3.18 Simultaneous Inhibition of *notum* and *ndk* Creates an Intermediate Brain Size Phenotype……..140
Figure 3.19 Simultaneous Inhibition of *src-1* and *ndk* Leads to Dramatic Posterior Photoreceptor Phenotype…….142
Figure 3.20 Simultaneous *src-1* Inhibition with Anterior Suppressors Can Cause a Polarity Reversal……143
Figure 3.21 Simultaneous *src-1* Inhibition with Anterior Suppressors Expands Trunk Identity……..144
Figure 3.22 Simultaneous *src-1* Inhibition with Trunk Identity Suppressors does not Enhance Brain Size…….145
Figure 3.23 Simultaneous *src-1* Inhibition with Regulators of Trunk Identity Enhances the Formation of Ectopic Pharynges……..146
Figure 3.24 Simultaneous *src-1* inhibition with Several PCGs can Enhance Polarity Reversal……..148
Figure 3.25 SRC: A Suppressor of Anterior Identities……....150

Chapter 1

General Introduction

Regeneration biology

All animal species face the risk of injury, and consequently have evolved various wound healing mechanisms to enable recovery from non-lethal wounds. In most mammalian species, including humans, the injury response is capable of fully healing minor injury, but more significant wounds lead to loss of the affected tissue and replacement with scar tissue lacking the same functionality (Illingworth 1974). If an organ or structure is removed entirely (i.e. the amputation of a limb) the human body is simply unable to restore what has been lost. By contrast, a number of animal species possesses an enhanced form of injury repair known as regeneration, defined as the ability to replace lost or damaged tissue in a way which recapitulates the original function and restores the animal's form and proportionality (Sanchez Alvarado 2003, Agata, Saito et al. 2007, Reddien 2018). The definition of regeneration is also sometimes expanded to include the homeostatic turnover of cell/tissue types which undergo continuous degradation and renewal, such as the stomach epithelium or hematopoietic cells (Tanaka and Reddien 2011).

Regeneration is distinct from wound healing in that regeneration allows the de novo synthesis of an entirely absent organ or tissue (Morgan 1901). This requires the presence of multi or totipotent stem cells which can proliferate and differentiate into all specialized cell types constituting the new structure (Reddien 2018). The differentiation and organization of these cells must be guided by signaling programs directing assembly of the new structure, often paralleling those used in the initial creation of the organ during embryonic development (Reddien and Sanchez Alvarado 2004, Tao, Yokota et al. 2005, Stoick-Cooper, Moon et al. 2007).

Regenerative processes can be broadly grouped into two categories (Agata, Saito et al. 2007) (Figure 1.1). The first, termed epimorphosis, involves production of new tissue at the injury sight (Morgan 1901, Elliott and Sanchez Alvarado 2013). This tissue is initially composed of

undifferentiated progenitors migrating to the injury site and grouping into an un-patterned outgrowth, known as a blastema (Tanaka and Reddien 2011). As regeneration proceeds, cells within the blastema differentiate and reorganize into a replacement for the lost tissue. The second process, known as morphalaxis, occurs within the uninjured tissues left behind after injury (Agata, Saito et al. 2007, Forsthoefel, Park et al. 2011). Loss of tissue through injury distorts the animal's overall proportions, and newly regenerated structures are often smaller than the lost original, causing retained structures to be disproportionately large within the regenerated organism (Pellettieri, Fitzgerald et al. 2010, Hill and Petersen 2015). Morphalaxis remodels and rescales the uninjured tissue to restore proportionality to the new, post-regeneration body plan (Agata, Saito et al. 2007). Some regeneration contexts, such as regrowth of a salamander's limb after amputation, appear to primarily regenerate through epimorphosis, though most involve some input from old tissue (Stocum 2004).

The regenerative capacity of different species can be compared in regards to the flexibility of regeneration and reliance on endogenous structures as a starting point. Many animal species are capable of regenerating only a limited set of tissues from defined injury types, in which positional and tissue information from the wound site guides the recreation of adjacent tissue (Sanchez Alvarado and Tsonis 2006). In contrast, some species possess a capability known as whole-body regeneration, the ability to regenerate any part of the organism from (almost) any starting point (Sanchez Alvarado 2003, Elliott and Sanchez Alvarado 2013).

In many regenerating species, capacity to regenerate is greater in younger animals and declines or disappears entirely with aging. Tadpoles can regenerate limbs and nervous tissues but not adult frogs (Stocum 2004). *Drosophila* larvae replace damage to imaginal discs, but adult flies cannot regenerate the organs derived from these structures (Hariharan and Serras 2017). This trend

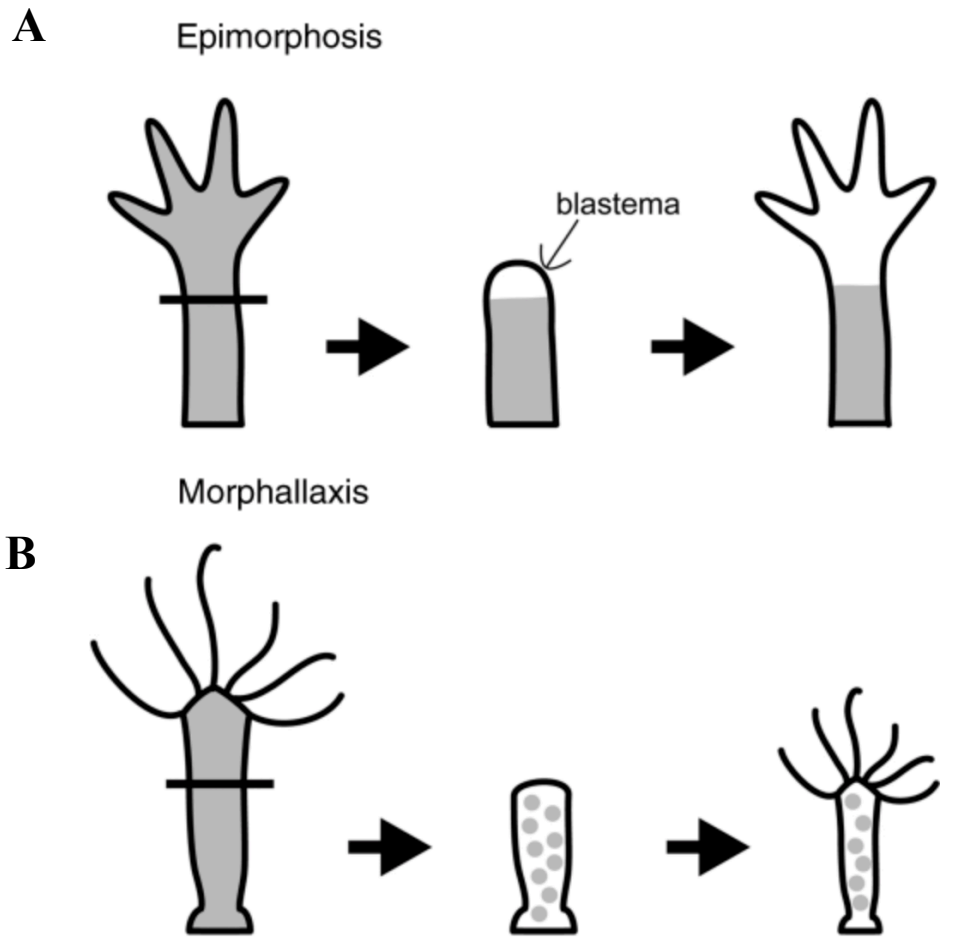

Fig 1.1 Conceptual modes of Regeneration

A) the production of new tissue at the wound site is called epimorphosis. The new tissue is known as a blastema, shown above through the example of a regenerating salamander arm. B) the reorganization of tissues away from the wound site, shown through the example of a regenerating *Hydra*. Image adapted from (Agata, Saito et al. 2007).

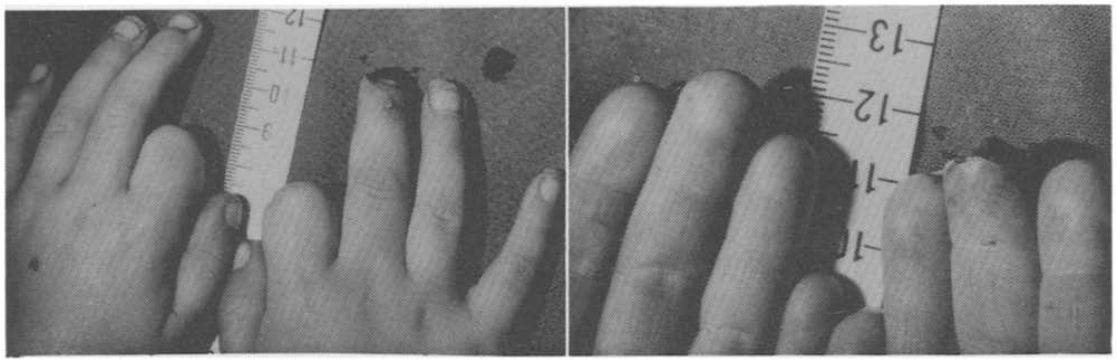

Fig. 7. A case with type II tissue loss of right middle finger.

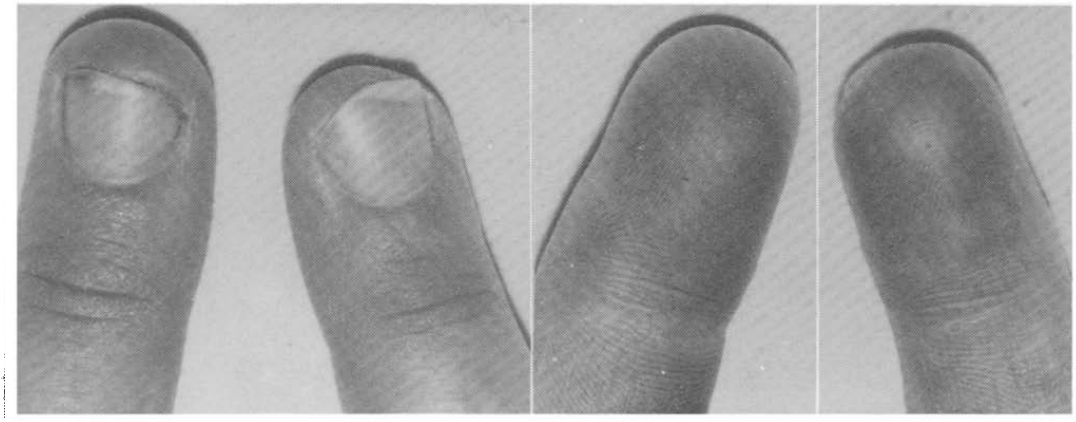

Fig. 10. Case illustrated in Figure 7. When healed and at 9 months follow up. Note almost near normal resotration of the finger tip. No residual nail deformity in this case.

Fig 1.2 Fingertip Regeneration in Human Children

Photographs show regeneration of the fingertip in a human child. Images from (Das and Brown 1978).

also holds true in humans. Young children can regenerate the tips of their fingers after injury, a capacity that is lost around onset of puberty (Douglas 1972, Illingworth 1974) (Figure 1.2). The overlap between genetic programs involved in regeneration and those used during development, as well as regenerative capacity being greatest early after development supports the idea that "regeneration recapitulates development" (Wang and Conboy 2010).

Regeneration is widespread in the animal kingdom (Figure 1.3): the Cnidarian hydra can regenerate half its body after transection (Bode 2009), the zebrafish *Danio rerio* can regenerate parts of its heart and tail fin after injury (Jopling, Sleep et al. 2010), the Axolotol can regenerate limbs after amputation (Kragl, Knapp et al. 2009), as can the Echnioderm starfish (Morgan 1901), and various lizard species can regenerate their tails (Morgan 1901). Within the mammalian lineage, members of the family *Cervidae* can regenerate their antlers (Kierdorf, Kierdorf et al. 2007). In addition to the aforementioned childhood fingertip regeneration, adult humans can regenerate the liver after partial hepatectomy (Sanchez Alvarado and Tsonis 2006).

Here we provide an overview of the regenerative capacity of select model organisms from across various phylogenetic taxa, before focusing on a description of the regenerative ability of the planarian flatworm *Schmidtea mediterranea*.

Vertebrate models

The zebrafish *Danio rerio* has a high regenerative capacity compared to most vertebrate species, able to restore damage to the heart (Poss, Wilson et al. 2002), CNS (Kroehne, Freudenreich et al. 2011, Marz, Schmidt et al. 2011), liver (Burkhardt-Holm, Oulmi et al. 1999), pancreas (Moss, Koustubhan et al. 2009), and fins (Tu and Johnson 2011). Regeneration of the heart and fins involves dedifferentiation and repurposing of cardiomyoctes and osteoblasts,

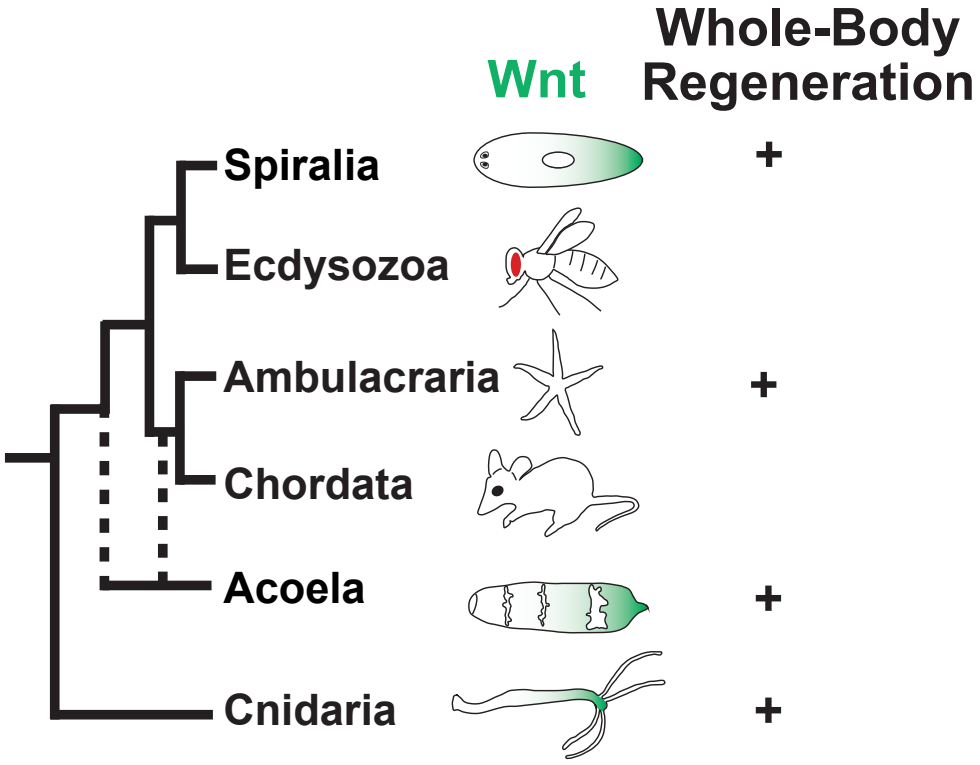

Fig 1.3 Phylogenetic Distribution of Regenerative Capacity

Capacity for whole-body regeneration is present in diverse animals diverged by at least 500 million years of evolution. Use of posteriorly expressed Wnt genes to drive axial regeneration is a common feature of multiple organisms. Figure courtesy of Dr Chris Petersen

respectively (Jopling, Sleep et al. 2010, Kikuchi, Holdway et al. 2010, Tu and Johnson 2011). Fin regeneration is under the control of Wnt signaling, with expression of multiple Wnt ligands upregulated in the distal fin tip during regeneration, and inhibition of Wnt signaling effector βcatenin blocking regeneration (Stoick-Cooper, Weidinger et al. 2007). Zebrafish are a well-established laboratory model organism which can quickly produce large numbers of progeny and can be modified through CRISPR-Cas9 to generate transgenic lines (Hwang, Fu et al. 2013, Marques, Lupi et al. 2019), providing a resource for screening genetic contributions to regeneration in a highly regenerative vertebrate.

Salamanders, including newts and axolotls, are noted for their ability to regenerate limbs following amputation. A regeneration blastema is formed at the site of injury through dedifferentiation of adjacent tissues (Stocum 2004, Kragl, Knapp et al. 2009). Lineage tracing experiments indicate that newly formed muscle, cartilage and Schwann cells are derived from the equivalent cell type, but axolotl dermal cells are able to dedifferentiate to a more potent state, contributing to multiple new cell types in the regeneration blastema (Kragl, Knapp et al. 2009). This process is directed by signals from nerve cells, and uses canonical Wnt signaling to direct patterning of the new tissue, with overexpression of Wnt signaling inhibitor *axin-1* resulting in impaired regeneration (Kawakami, Capdevila et al. 2001, Kawakami, Rodriguez Esteban et al. 2006). Other signaling pathways, including Fgf and BMP signaling also play essential roles, recapitulating mechanisms used to properly pattern limbs during embryonic development (Stoick-Cooper, Moon et al. 2007). The amphibian's ability to carry out regeneration through dedifferentiation is of great interest to the field of regenerative medicine, as it may suggest ways to therapeutically induce regeneration of adult mammalian tissues (Stocum 2004).

Invertebrate models

The cnidarian *Hydra* is one of the longest studied regenerative model organisms (Morgan 1901). These simple animals are composed of two myoepithelial cell layers, one endodermal, one ectodermal, sandwiching interstitial stem cells. *Hydra* can regenerate from severe injuries, including even disaggregation, so long as the regenerating fragment contains one cell of each type (Tanaka and Reddien 2011). The main body axis, known as the oral-aboral axis, is organized through Canonical Wnt signaling, with the ligand *wnt3* constitutively expressed in the head (oral) and activated at oral-facing wound sites during injury (Bode 2009). Experimental perturbation to increase Wnt signaling activity can initiate ectopic head formation, while inhibition of *wnt3* expression impairs regeneration (Bode 2009). *Hydra* is an excellent example of a simple animal which utilizes multiple stem cell types and canonical Wnt signaling to regenerate.

The cnidarian *Nematostella vectensis* serves as a useful model for regeneration in comparison to *Hydra*. While it possesses a more complex body plan, it is still composed of only two germ layers (Fritzenwanker, Saina et al. 2004, Layden, Rentzsch et al. 2016). *Nematostella* lack *Hydra's* extreme ability to regenerate from disaggregation, but can restore injuries to the pharynx, oral opening, or tentacles (Layden, Rentzsch et al. 2016). Similar to *Hydra,* canonical Wnt signaling promotes development and regeneration or oral axis structures, as evidenced by regeneration of ectopic oral openings after Wnt signaling hyperactivation (Trevino, Stefanik et al. 2011). Comparisons between the two cnidarians can allow us to draw conclusions about evolutionarily ancient mechanisms underlying regeneration.

One of the organisms most recently adapted as a model for studying regeneration is the aceol *Hofstenia miamia*, known as the three banded panther worm. These worms have a complex body plan derived from three germ layers, including nervous system, musculature, and epidermis,

and can undergo whole-body regeneration (Srivastava, Mazza-Curll et al. 2014). Regeneration is enabled by a population of pluripotent stem cells marked by expression of *piwi* homologs (Tewari, Owen et al. 2019). The anterior-posterior axis is patterned by activity level of canonical Wnt signaling, with Wnt ligands expressed in gradients from the posterior, and Wnt signaling antagonists expressed at the anterior (Srivastava, Mazza-Curll et al. 2014, Ramirez, Loubet-Senear et al. 2020). The dorsal-ventral axis is patterned by a bmp-admp signaling gradient, with *bmp* expressed in dorsal tissues and *admp* on the ventral side (Srivastava, Mazza-Curll et al. 2014). Both sets of patterning molecules are expressed almost exclusively in muscle cells (Raz, Srivastava et al. 2017). The acoel *Hofstenia miamia* superficially resembles the platyhelminth *Schmidtea mediterranea* in morphology and behavior, as well as sharing many conserved genetic pathways involved in regeneration (Tewari, Owen et al. 2019). However, these two species are separated by over 500 million years of evolutionary divergence (Raz, Srivastava et al. 2017). Thus, comparisons between the two worms can be informative for understanding the evolution of regeneration.

Planarian biology and regeneration

The freshwater planarian flatworm *Schmidtea mediterranea* is an ideal model organism for investigating the molecular basis of whole-body regeneration (Elliott and Sanchez Alvarado 2013). Planarians possess an incredibly robust and flexible regenerative capacity, able to create a new animal from fragments as small as 10,000 cells isolated from almost anywhere within the body (Reddien and Sanchez Alvarado 2004). The applicability of planaria for the study of regeneration has been recognized for over a century (Morgan 1898), facilitated by the fact that newly regenerated tissue emerges un-pigmented, visually distinct from pre-existing tissue. Planaria can be easily mass-cultured in a laboratory setting (Salo 2006), are amenable to a wide range of surgical intervention (Reddien and Sanchez Alvarado 2004), and fully regenerate from any injury within 3-4 weeks (Sanchez Alvarado 2003).

Over the last two decades the field has drawn increased interest as a variety of molecular tools have been developed that allow more detailed interrogation of gene expression, stem cell proliferation and differentiation, and apoptosis during wound healing and regeneration. A key development in the use of planaria as a model organism was the application of dsRNA-mediated RNA interference, which can be introduced to the animal through injection or feeding (Sanchez Alvarado and Newmark 1999). This allows for large-scale RNAi screens of gene function (Reddien, Bermange et al. 2005). Techniques have been developed to detect gene expression through whole mount *in situ* hybridization (WISH) using colorimetric readouts, or through fluorescent *in situ* hybridization (FISH) (Pearson, Eisenhoffer et al. 2009). Whole-mount detection of apoptotic cells can be performed using TUNEL staining (Pellettieri, Fitzgerald et al. 2010). The planarian genome was recently sequenced (Grohme, Schloissnig et al. 2018), and several researchers have assembled transcriptomes through single-cell RNAseq (Fincher, Wurtzel et al.

2018, Swapna, Molinaro et al. 2018, Zeng, Li et al. 2018). Immunostaining can be performed in planarians (Robb and Sanchez Alvarado 2002, Forsthoefel, Waters et al. 2014, Ross, Omuro et al. 2015), and can be used to assess cell proliferation through detecting activated phosphor-histone H3 (Newmark and Sanchez Alvarado 2000). However, to date relatively few antibodies are available for determining protein localization by immunostaining in this organism, and it is not yet possible to generate transgenic planaria (Forsthoefel, Waters et al. 2014).

Anatomy

Unlike other organisms with such robust regeneration, the planarian has a complex triploblastic body plan with multiple organ systems, which in turn possess a high degree of internal organization of different tissue types (Figure 1.4). The body can be examined along three axes, the anterior-posterior (AP), dorsal-ventral (DV) and medial-lateral (ML). The body is organized around a central digestive system, consisting of an intestine, mouth and pharynx. The intestine contains a primary anterior branch and two main posterior branches, with smaller secondary and tertiary branches innervating the body, allowing for waste and nutrient exchange with all tissues (Forsthoefel, Park et al. 2011). The pharynx is a muscular organ which transmits food from the mouth to gut, and subsequently processes undigested matter in the opposite direction for excretion (Forsthoefel, Park et al. 2011). Excretion is also carried out by a branched duct system of protonephridia which balance osmolarity between the planarian body cavity and its surrounding medium (Rink, Vu et al. 2011). The central nervous system is composed of a bi-lobed brain with anterior lateral branches connected to two ventral nerve cords, which innervate with a branching peripheral nervous system (Inoue, Hayashi et al. 2007). Two eyes containing photoreceptor neurons and pigment cells connect to the brain via axonal tracks (Lapan and Reddien 2012).

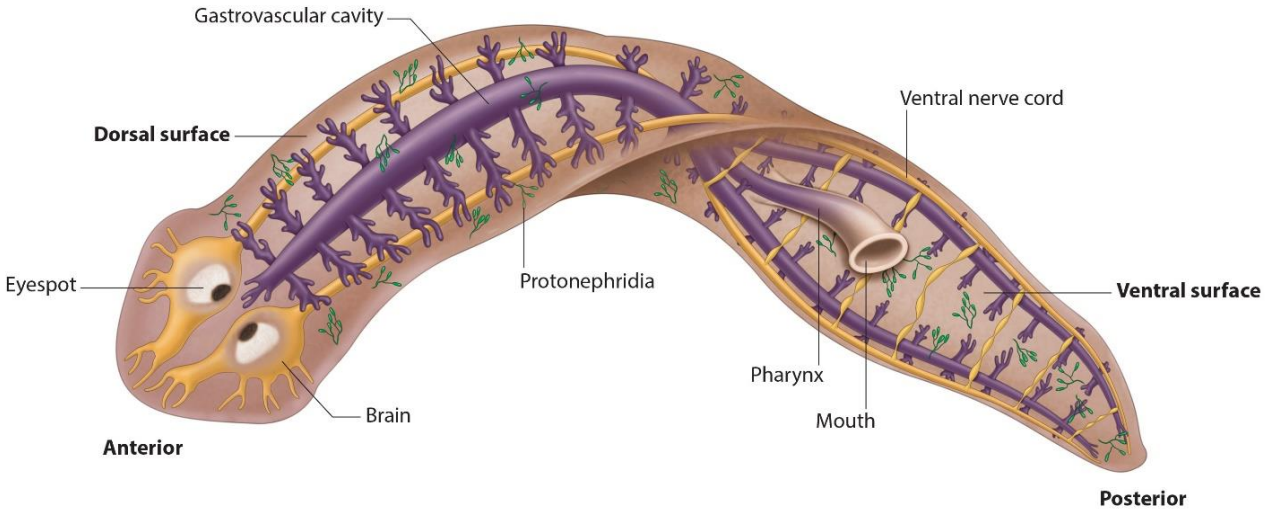

Fig 1.4 Planarian Anatomy

Planarians have a complex anatomy that includes a central nervous system, digestive system, excretory system, photoreceoptors and muscle (not shown). Image taken from (https://cuttingclass.stowers.org.node.121409)

Motility and structural support are provided by three distinct muscle layers, known as circular, longitudinal and diagonal muscle fibers, named after their orientation with respect to the main body axis (Cebria 2016). The outer layer of muscle is directly attached to the epidermis, which is ciliated on the ventral surface to assist in movement (Vu, Mansour et al. 2019). Wild planarians are naturally hermaphrodites which reproduce sexually, though natural isotypes have been isolated which lack the sexual organs and reduce exclusively through fissioning (Newmark, Wang et al. 2008). Experiments discussed in this document were exclusively conducted on one such asexual strain. Single-cell RNA sequencing has identified at least 150 distinct cell types in the organism (Fincher, Wurtzel et al. 2018). All of these cells are derived from a population of stem cells, known as neoblasts, which are the only mitotically active cells within the adult organism, responsible for maintaining homeostasis through turnover of all tissues (Wagner, Wang et al. 2011). Given their extreme importance to the planaria and its ability for regeneration, neoblasts will be discussed in more detail below.

Neoblasts

The neoblast stem cell population is housed within a parenchymal compartment extending throughout the body, except for the very anterior tip (Vasquez-Doorman and Petersen 2014). These cells comprise a large fraction of the total cells within planaria, as much as 20% (Newmark and Sanchez Alvarado 2000, Wagner, Wang et al. 2011). Neoblasts were first identified based on their cellular morphology, small in size (5-8um in diameter), with a relatively large nucleus and scant cytoplasm (Reddien and Sanchez Alvarado 2004). Their status as the only proliferating cells allows isolation of neoblasts from other cell populations through FACS sorting using DNA binding

dyes to obtain the 4N population (Hayashi, Asami et al. 2006). Neoblasts also uniquely express a set of factors including *piwi*-1 (also called *smedwi*-1), encoding a PIWI-like RNA-binding protein present in high concentrations within these cells (Reddien, Oviedo et al. 2005).

The status of neoblasts as the only mitotically active cells within the worm was first hinted at by observations that ionizing radiation, which generates double-stranded DNA breaks, selectively ablates this cell population (Hayashi, Asami et al. 2006) (Figure 1.5). Subsequent experiments examining the uptake of nucleotide analog BrdU, and presence of M-phase marker H3P confirmed neoblasts unique mitotic status (Newmark and Sanchez Alvarado 2000). The status of neoblasts as the only dividing cells inherently suggested that the neoblast class as a population must be totipotent, in order to continually maintain the organism, but for many years it was unclear whether individual totipotent neoblasts existed, or instead the neoblast population contained multiple sub-classes of specific potency (van Wolfswinkel, Wagner et al. 2014). Recently, this debate was solved through a series of experiments in which a host animal had its endogenous neoblast population completely ablated through radiation, followed by transplantation with a single donor neoblast (Wang, Wagner et al. 2018) (Figure 1.6). Complete neoblast ablation is normally lethal (Hayashi, Asami et al. 2006, Elliott and Sanchez Alvarado 2013), but in 5% of animals the single donor stem cell rescued lethality and reenabled regeneration, indicating its descendants were able to restore the entire neoblast compartment and go on to differentiate into all cell types within the worm's body (Wang, Wagner et al. 2018, Zeng, Li et al. 2018).

Neoblasts provide the raw material for new cell formation during planarian regeneration, but for regeneration to occur successfully the proliferation, migration, and differentiation of neoblasts must be tightly controlled by a complex and multi-stage signaling process. To provide context for this process, we will now describe planarian regeneration chronologically.

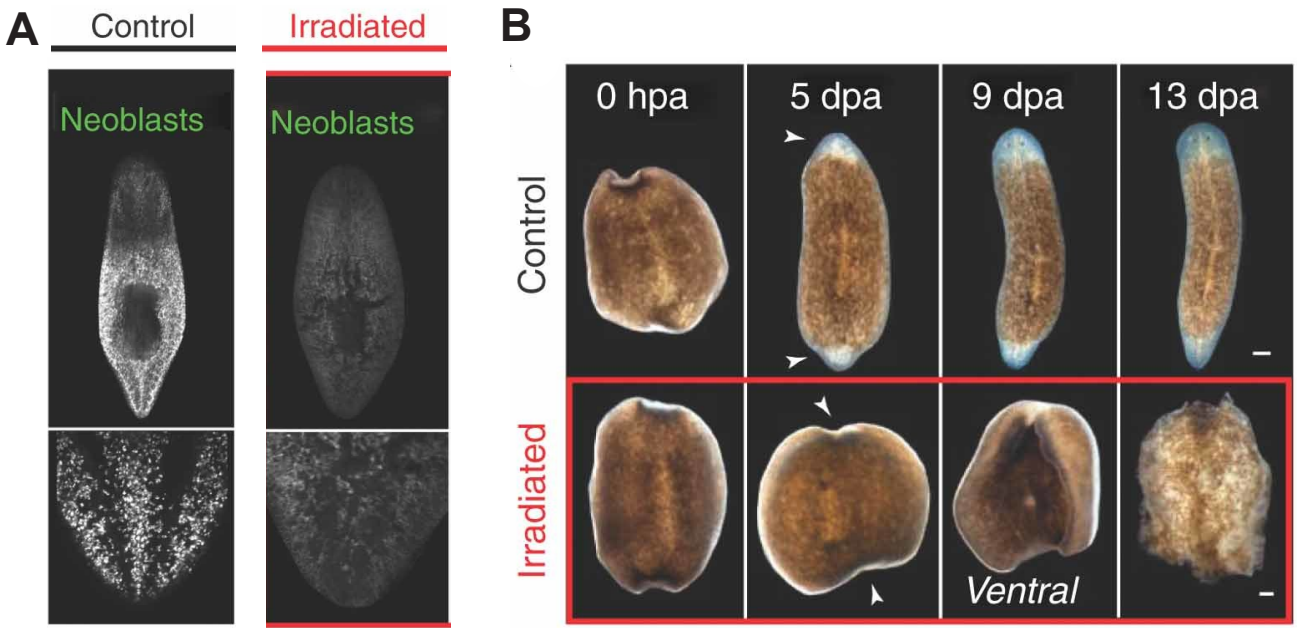

Fig 1.5 Neoblasts are Irradiation Sensitive Pluripotent Stem Cells Required for Regeneration

A) Neoblasts are irradiation-sensitive cells found throughout the animal.
B) depletion of neoblasts through irradiation prevents regeneration and leads to animal death.
Images adapted from (Elliott and Sanchez Alvarado 2013).

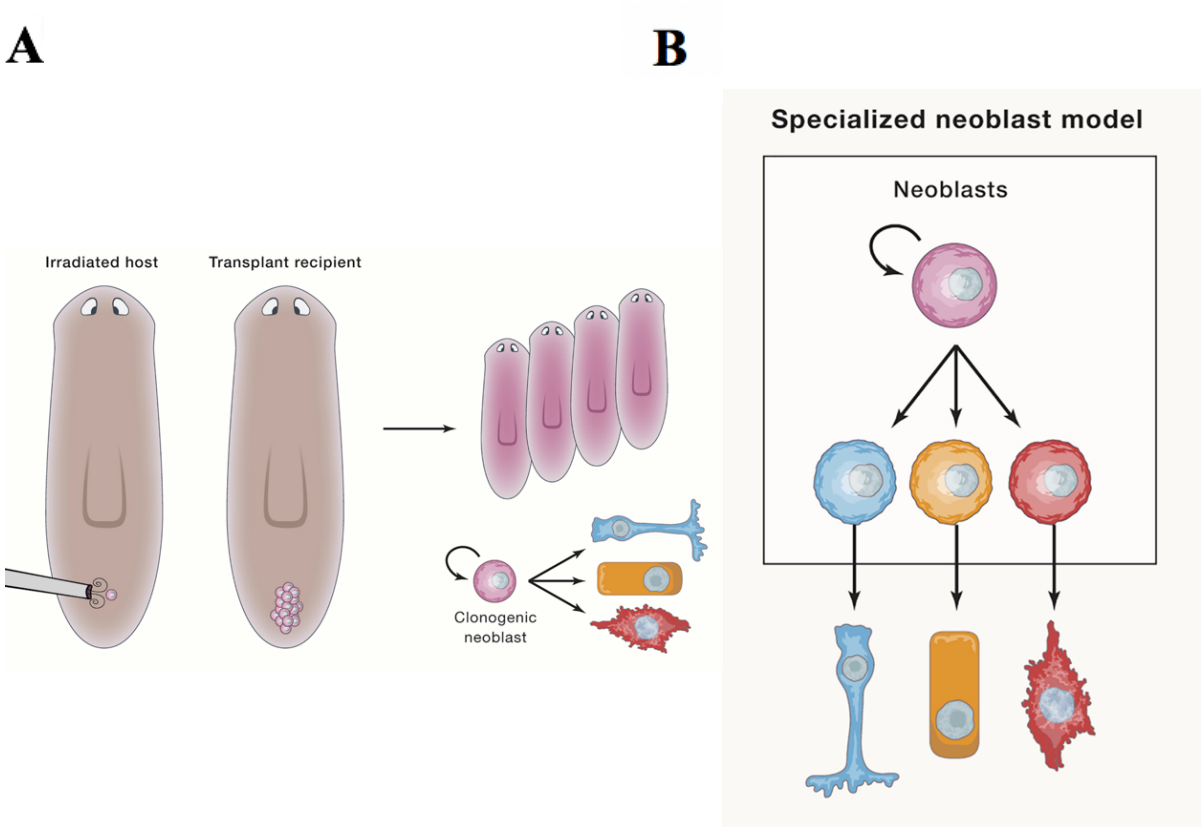

Fig 1.6 Neoblasts Contain a Subpopulation of Totipotent Stem Cells which can give rise to all Planarian Cell Types

A) Cartoon depicting the experiments performed in (Wang, Wagner et al. 2018) showing that a single neoblast transplanted into an irradiated host rescued radiation lethality and reenabled regeneration.
B) Model showing that pluripotent neoblasts self-renew and differentiate into specialized neoblasts which further divide and differentiate into various mature cell types.
Images adapted from (Reddien 2018).

Stages of regeneration

An overview of planarian regeneration is shown in Figure 1.7. Immediately following injury, muscles contract around the wound site to minimize tissue exposure to the external environment (Wurtzel, Cote et al. 2015). Rhabdite cells within the epidermis secrete a mucus which forms a protective layer over the opening, and epithelial cells begin to migrate across the wound to restore a minimal external barrier (Reddien and Sanchez Alvarado 2004). At this 30 minute mark, a set of transcriptional responses can be detected in the epidermis and sub-epidermal muscle, including heat shock and stress response proteins, as well as transcription factors including *jun-1, fos-1,* and multiple *EGR*s (Wenemoser, Lapan et al. 2012). By three hours after injury, a wave of apoptosis is initiated around the injury site, presumably to clear away damaged cells (Pellettieri, Fitzgerald et al. 2010). At six hours post injury, neoblast transcription factor *runt-1* is upregulated, and neoblasts across the body increase their rates of proliferation and begin migration towards the wound site, a response controlled by the activity of the genes *sos-1* and *srf* (Wenemoser, Lapan et al. 2012). Between 6 and 24 hours after injury, components of the WNT signaling pathway, including *wnt1* and *notum*, are expressed which influence patterning of later regenerated tissue (Petersen and Reddien 2011). These responses occur after an injury, regardless of whether tissue was lost or merely damaged (Wenemoser and Reddien 2010).

After the initial generic injury responses, a checkpoint occurs in which the worm assess the status of its injury, and regeneration only proceeds if tissue has been lost which must be replaced. This determination relies on the expression of *follistatin*, which is expressed at all injury sites 6 hours after injury, but has its expression maintained past the 18-hour mark only when tissue is missing (Gavino, Wenemoser et al. 2013). *follistatin* exerts its effects through inhibition of Activin signaling, because *activin* inhibition can rescue regeneration defects caused by *follistatin*

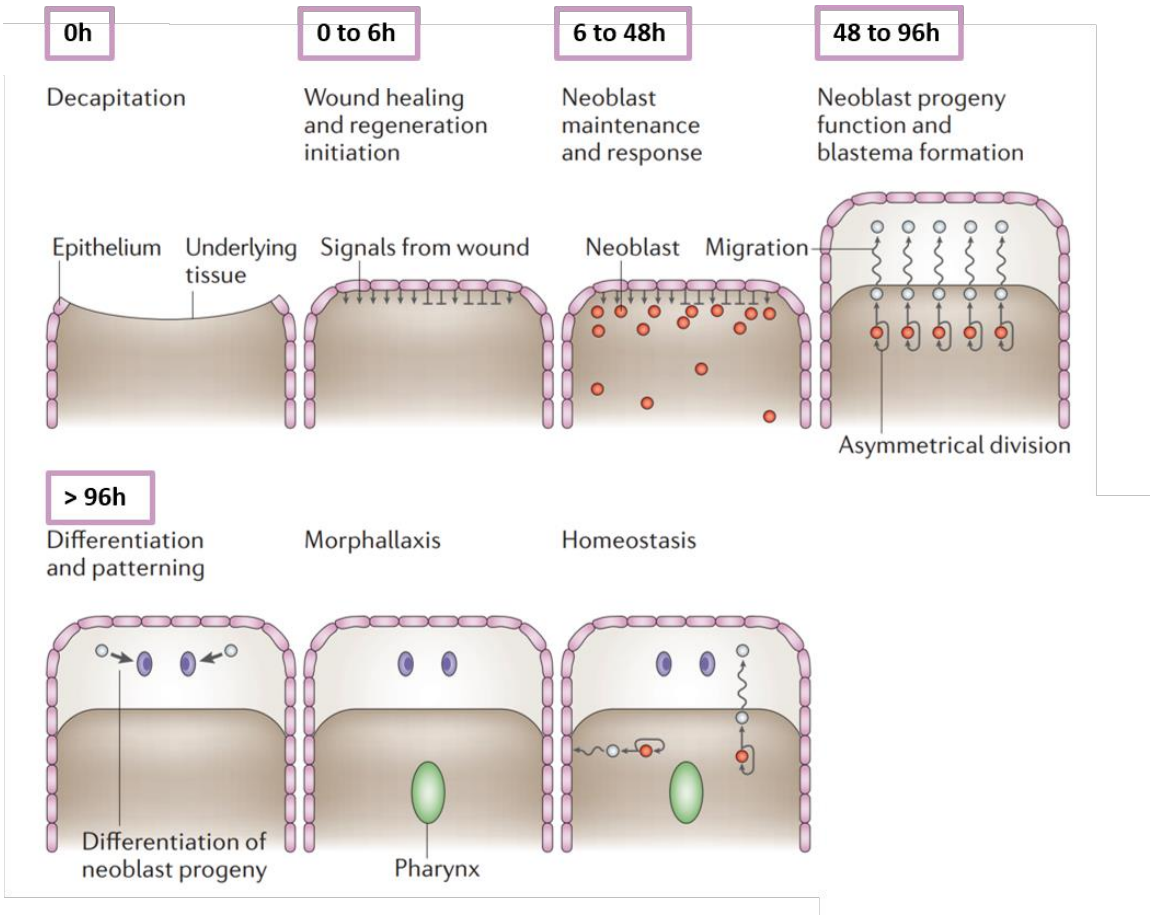

Fig 1.7 Time course of Planarian Regeneration

Cartoon depicts sequential events during regeneration of a head amputation. Early events include wound closure and activation of generic injury responses. Later neoblasts are recruited to the wound to participate in blastema formation, and by 96 hours post injury cells within the blastema have begun differentiating and organizing into replacement structures. Images adapted from (Sanchez Alvarado and Tsonis 2006).

inhibition (Tewari, Stern et al. 2018). In the missing tissue response, mitotic activity of neoblasts, which had been in decline after peaking six hours post injury, is reactivated and reaches a second peak at 48 hours, restoring neoblast populations depleted in the formation of replacement tissue (Wenemoser, Lapan et al. 2012, Tewari, Stern et al. 2018). A body-wide wave of apoptosis occurs, the intensity of which is proportional to the extent of tissue loss (Pellettieri, Fitzgerald et al. 2010) and may serve to provide energy and material for blastema outgrowth through catabolic metabolism.

As neoblasts accumulate at the injury site, a regenerative blastema is formed, within which the neoblasts begin to differentiate. At this time, the identity of the tissues to be regenerated is firmly established, which can involve the formation of signaling centers within the blastema. For instance, regeneration from head amputation will involve the blastema expressing transcription factors *fox-D* and *zic-1* (Vasquez-Doorman and Petersen 2014) to specify a new anterior pole alongside anterior patterning factors *notum* and *sfrp-1.* Under the direction of these transcription factors, appropriate head structures will be organized, and the remainder of the body will undergo morphallaxis to restore initial proportions. Conversely, a posterior-facing injury will create a blastema expressing *pitx* and *islet,* transcription factors which enable the formation of *wnt1* expressing posterior pole cells which organize posterior regeneration (Hayashi, Motoishi et al. 2011). Both the anterior and posterior poles express key factors in muscle cells (Vogg, Owlarn et al. 2014, Sureda-Gomez, Pascual-Carreras et al. 2015) which direct regeneration of replacement structures in the blastema and subsequently maintain homeostatic organization of the anterior-posterior axis. This highlights the importance of muscle cells in planarian patterning and regeneration, which is expanded upon below.

Role of muscle cells in PCG expression and regeneration

While neoblasts confer regenerative ability, prior research has shown that signal transduction cascades that specify axis formation can occur in response to injury when neoblasts have been ablated by ionizing radiation (Petersen and Reddien 2009, Gurley, Elliott et al. 2010). This indicates that patterning information is communicated to neoblasts from another cell type. There exist in planaria a number of genes with regionalized expression patterns and RNAi inhibition phenotypes which disrupt regional patterning, which are therefore known as positional control genes (PCGs) (Reddien 2011, Witchley, Mayer et al. 2013) (Figure 1.8). These include members of the Wnt, BMP, FGF, and Hox gene families (Reddien 2011). A high majority (>90%) of cells stained for expression of each known PCG were identified as muscle cells based on co-labeling with *troponin* or *collagen* (Witchley, Mayer et al. 2013), with remaining expression restricted to particular neuronal subpopulations. This makes a review of planarian body-wall muscle important to understanding the expression and activity of position control genes.

Planarian muscle cells are mononucleated and project a single actinomyosin contractile fiber in a distinct direction (Witchley, Mayer et al. 2013). Different muscle types project longitudinally, along the AP axis, circularly, around the ML/DV axes, or diagonally between the AP and ML axes (Witchley, Mayer et al. 2013, Cebria 2016). Single cell RNAseq has identified transcription factors *myoD* and *nkx1-1* as uniquely specifying longitudinal and circular muscle, respectively (Scimone, Cote et al. 2016). These experiments also revealed expression of specific PCGs within each muscle subtype. Depletion of individual muscle fiber types through RNAi inhibition of *myoD* or *nkx1.1* gave distinct phenotypes, indicating particular roles in patterning and regeneration (Scimone, Cote et al. 2017). Muscle cells are alongside the neoblast compartment and they may communicate through the muscle extra-cellular matrix (Cote, Simental et al. 2019).

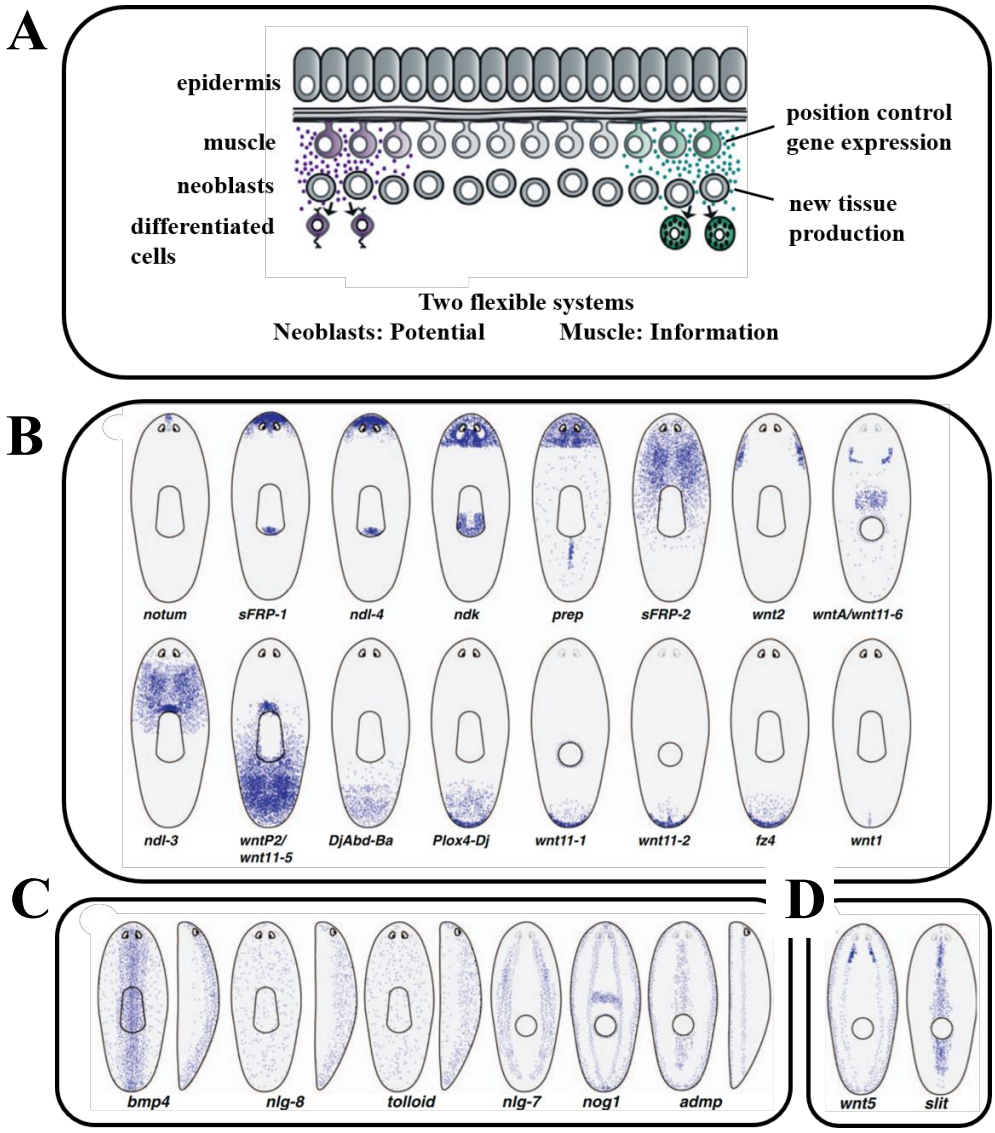

Fig 1.8 Positionally Controlled Genes are Expressed in Muscle and Act as a Patterning Coordinate System

A) A model where PCG expression in muscle communicate positional information to neoblasts to instruct differentiation. Adapted from (Witchley, Mayer et al 2013).
B-D) Cartoon depiction of PCG expression domains along the AP (B) DV (C) or ML (D) axes. Many of these PCGs cause patterning defects when inhibited by RNAi. Images adapted from (Reddien 2011).

The majority of positional control genes expressed in planarian muscle are regionalized with respect to the anterior-posterior axis (Reddien 2011). These include multiple Wnt signaling pathway components, including both Wnt ligands and Wnt signaling inhibitors. Multiple Wnt ligands, *wnt1, wnt11-1,* and *wnt11-2,* are all expressed at the posterior pole, as is the Frizzled receptor *fz4* (Reddien 2018). Wnt ligand *wntP2* is expressed in a gradient from the posterior tip of the tail to the anterior end of the pharynx (Reddien 2018). Multiple members of the secreted frizzled-related protein (SFRP) family, known to inhibit Wnt signaling, putatively through acting as decoy receptors for Wnt ligands, are expressed at the anterior pole or in anterior gradients (Reddien 2011). Another Wnt inhibitor, *notum,* is also expressed at the anterior pole (Hill and Petersen 2015). The significance of the regionalization of these Wnt signaling components will be expanded on in the next section.

Position control genes also regulate regionality along the planarian dorsal-ventral and medial-lateral axes. Signaling ligand *bmp4* is expressed in a graded fashion from the dorsal midline, and inhibition of *bmp4* causes ventralization phenotypes (Reddien, Bermange et al. 2007). Other BMP pathway components, such as *admp*, *tolloid*, *noggin*, and *noggin-like* genes have polarized expression along the DV axis (Reddien 2011). The medial-lateral axis is regulated by midline expression of *slit* (Cebria, Guo et al. 2007) and marked by lateral expression of *wnt5* (Reddien 2011).

Wnt signaling in AP patterning and polarity determination

Prior research has provided a broad overview of the regulation of planarian anterior-posterior patterning (Figure 1.9). RNAi of either the signaling ligand *wnt1* or the intracellular Wnt signaling effector *βcatenin-1* results in regeneration of double headed worms from amputated trunk fragments (Gurley, Rink et al. 2008, Iglesias, Gomez-Skarmeta et al. 2008, Petersen and Reddien 2008). Inhibition of *βcatenin-1* can also cause reorganization of the body axis and emergence of ectopic heads in the absence of injury (Iglesias, Gomez-Skarmeta et al. 2008). Conversely, inhibition of the Wnt signaling inhibitor *APC* leads to double-tailed regeneration (Gurley, Rink et al. 2008), as does inhibition of *notum,* a gene encoding a secreted carboxylesterase that removes a lipid modification from Wnt proteins to prevent their binding to Frizzled receptors (Petersen and Reddien 2011). Collectively, these results suggest that low Wnt activity is permissive for anterior regeneration, while high Wnt signaling activity promotes posterior fates.

This observation is supported by examination of Wnt signaling gradients across the fully regenerated animal. In uninjured worms, the anterior pole is marked by expression of Wnt inhibitors *notum, sfrp-1 and sfrp-2*, while *wnt1, wnt11-1, wnt11-2* and *wntP-2* are expressed in the posterior (Reddien 2018). Reestablishment of these pole expression domains occurs early in the formation of regeneration blastemas and is necessary for head or tail regeneration to proceed, implicating these poles as organizing centers for the production of head or tail tissues (Vasquez-Doorman and Petersen 2014, Sureda-Gomez, Pascual-Carreras et al. 2015). Following injury, *wnt1* is expressed at anterior or posterior-facing injury sites, while *notum* is expressed specifically at anterior-facing wounds, and *notum* activity at the anterior is necessary for subsequent restriction of *wnt1* to the posterior (Petersen and Reddien 2011).

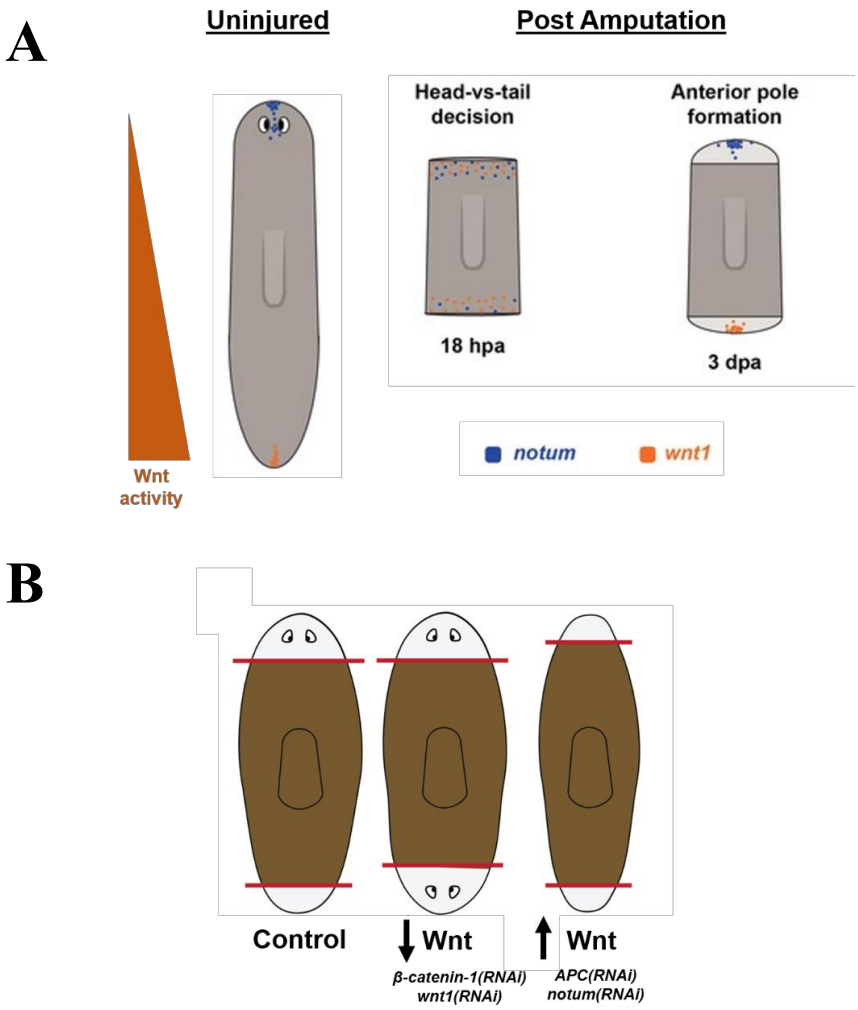

Fig 1.9 Canonical Wnt Signaling Controls Anterior-Posterior Pole Determination

A) In uninjured animals, wnt inhibitor *notum* is expressed at the anterior pole, while *wnt1* is expressed at the posterior pole. Thus creates an animal wide anterior to posterior gradient of increasing wnt activity. In amputated trunk fragments, *notum* is asymmetrically expressed at the anterior facing wound at 18 hours post amputation and becomes restricted to the anterior pole by 3 days post injury. *wnt1* is expressed at both wounds sites equally at 18 hours but becomes restricted to the posterior pole at 3 days post injury. Adapted from (Reddien 2011). B) RNAi conditions which decrease canonical wnt signaling result in ectopic head regeneration at posterior facing wounds. RNAi conditions which increase canonical wnt signaling causes ectopic tail regeneration at anterior facing wounds. Collectively, these results suggest that canonical wnt signaling controls regeneration polarity and a head vs tail regeneration decision. Adapted from (Owlarn and Bartscherer 2016).

Expression of injury induced *wnt1* has been shown to be under the control of Hedgehog signaling, with inhibition of hedgehog activators (*hh, gli, smoothened*) reducing *wnt1* expression at wounds and leading to failed posterior regeneration (Rink, Gurley et al. 2009). Conversely, upregulation of Hedgehog signaling through inhibition of the inhibitor *patched* increases *wnt1* expression and leads to anterior tail regeneration (Rink, Gurley et al. 2009, Yazawa, Umesono et al. 2009). Chemical activation of calcium influx through praziquantel treatment can induce double-headed regeneration in *Dugasia japonica* through alteration of Hedgehog signaling and by extension *wnt1* levels (Zhang, Chan et al. 2011). Gap junction proteins have also been implicated in the process of head/tail determination although their relationship with Wnt signals are not yet known (Oviedo, Morokuma et al. 2010). A preponderance of evidence points to canonical Wnt signaling as the primary determinant of planarian anterior-posterior polarity during homeostasis and regeneration.

In addition to control of overall AP axis polarization, specific Wnts have been implicated in controlling regional identity along the AP axis (Figure 1.10). A Wnt-FGFRL circuit comprising *wnt11-6*, Wnt receptor *fzd5/8-4,* Wnt antagonist *notum* and FGFRL *ndk* has been shown to control head regionalization, limiting the posterior extent of the brain and eyes (Cebria, Kobayashi et al. 2002, Hill and Petersen 2015, Scimone, Cote et al. 2016). Based on double-RNAi experiments with *wnt11-6* and intracellular Wnt signaling factors, the signaling mechanism downstream of *wnt11-6* was proposed to be Dishevelled dependent but βcatenin independent (Hill and Petersen 2015).

Another Wnt/FGFRL regulatory circuit controls regionalization of trunk identity. Inhibition of *wntP-2* (Wnt ligand)*, fzd1/2/7* (Wnt receptor)*, ptk7* (a Wnt co-receptor), or *ndl-3* (FGFRL) causes a posterior trunk duplication, with animals forming secondary mouths and ectopic

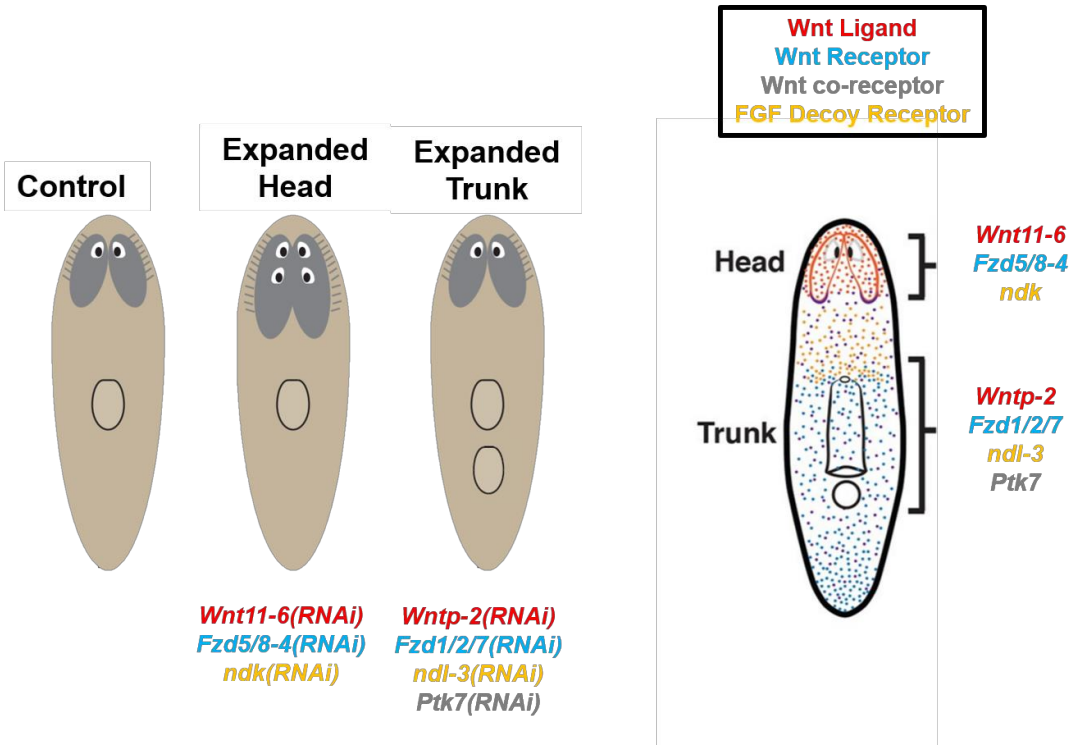

Fig 1.10 Two FGFRL-Wnt circuits control AP Regional Identity in Planaria

Cartoons summarize the characterized RNAi phenotypes of wnt and FGFRL pathway components which control planarian regional identity. *fzd5/8-4, wnt11-6* and *ndk* restrict head identity and their inhibition results in an expanded brain and the formation of ectopic posterior photoreceptors. *fzd1/2/7, ptk, ndl-3* and *wntP-2* restrict trunk identity and their inhibition results in the formation of ectopic posterior mouths and pharynges. Adapted from (Scimone, Cote et al. 2016).

pharynges (Lander and Petersen 2016, Scimone, Cote et al. 2016). Inhibition of factors involved in head or trunk circuits does not affect size or placement of organs within the other region, and perturbation of either system does not affect overall regeneration polarity (Scimone, Cote et al. 2016). The possibility that head and trunk regional circuits can influence each other is suggested by the observation that co-inhibition of *wntP2* can enhance the posterior head regeneration phenotype of *wnt1* RNAi, despite *wntP2* RNAi not itself causing posterior head regeneration (Petersen and Reddien 2009). However, more research is needed to understand the interplay of regional determinants with body-wide anterior-posterior polarization.

Asymmetric injury-induced *notum* expression demarcates wound polarity

Transcriptional profiling of planarian injury induced genes has identified only one factor upregulated after injury in an asymmetric manner with respect to the body axes, the Wnt signaling inhibitor *notum* (Wurtzel, Cote et al. 2015) (Figure 1.11). *notum* is a feedback inhibitor of Wnt signaling, expressed under the control of βcatenin, but able to prevent binding of Wnt ligands to their Frizzled receptors by enzymatically cleaving a key palmitoylate group on the surface of Wnt ligands (Kakugawa, Langton et al. 2015). Injury-induced *notum* is specifically expressed in longitudinal muscle cells, and can be ablated by inhibition of the longitudinal muscle marker *myoD* (Scimone, Cote et al. 2017). Co-inhibition of *wnt1* or *βcatenin* alongside *notum* suppresses the *notum(RNAi)* regeneration phenotype, supporting a role for *notum* acting upstream of canonical Wnt signaling in head versus tail determination (Petersen and Reddien 2011) (Figure 1.12).

Suppression of canonical Wnt signaling through *βcatenin-1* RNAi eliminates *notum* expression (Petersen and Reddien 2009), while overactivation through inhibition of *APC* increases *notum* levels without altering expression asymmetry (Petersen and Reddien 2011). These results

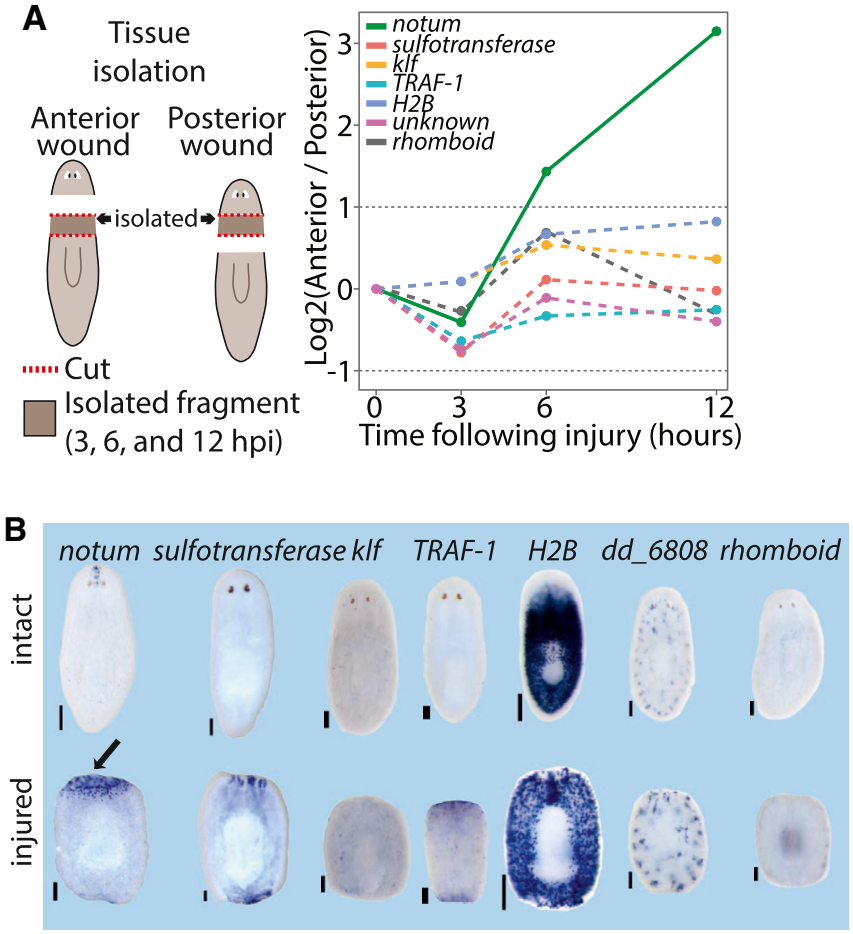

Fig 1.11 *notum* is the Only Planarian Gene with Asymmetric Injury Induced Expression

A) Gene expression profiling of injured tissues in the same location adjacent to wounds of anterior or posterior orientation. Plotted is the $\log_2$ ratio of differential gene expression between the two samples.
B) WISH validation of wound-induced expression on the genes shown in A. Only *notum* showed assymetric expression after injury (black arrow). Scale bars 100 um.
Images from (Wurtzel, Cote et al. 2015).

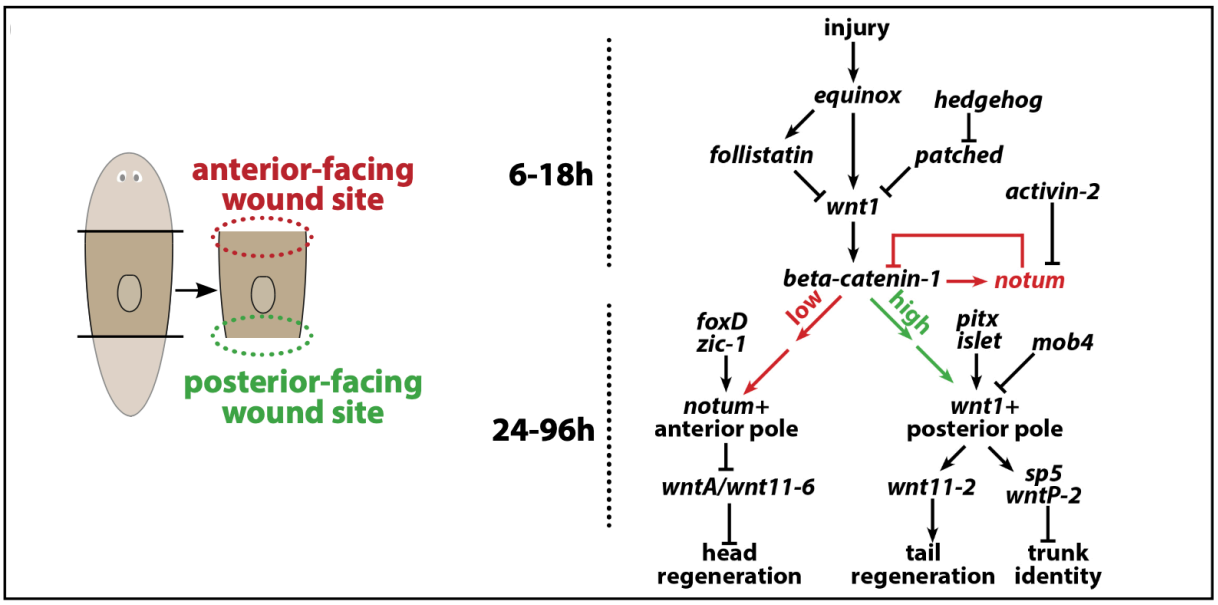

Fig 1.12 Model for Canonical Wnt Signaling Control of Head/Tail Fate Decision

Signaling pathway diagram showing outcomes of low Wnt signaling activity at anterior-facing wound sites (red) and high Wnt signaling activity at posterior-facing wound sites (green) resulting in head or tail regeneration. The expression of *notum* at anterior-facing wounds breaks the symmetry between the wound sites and drives subsequent behavior. Image courtesy of Dr Chris Petersen.

indicate canonical Wnt signaling controls *notum* activation but is not responsible for the polarization of its expression. To date, the only gene identified with an RNAi phenotype affecting *notum* polarization is *activin-2* (Cloutier, McMann et al. 2021), suggesting a role for Activin Signaling in control of *notum*. However, *activin-2* is expressed broadly across the body in a non-polarized manner, making it unclear how Activin signals could be instructive for *notum* polarization.

Dvls are a hub for canonical and non-canonical Wnt signals

Dishevelled proteins are highly conserved intracellular signal transducers which function downstream of Wnts in multiple signaling cascades (Wallingford and Habas 2005). Planarians possesses two dishevelled homologs, *dvl-1* and *dvl-2* with similar but not identical RNAi inhibition phenotypes (Almuedo-Castillo, Salo et al. 2011). Dishevelled proteins contain three conserved domains, each of which can interact with different components of canonical and non-canonical Wnt signaling pathways in a combinatorial fashion to transduce a wide variety of signals with different cellular outcomes (Wallingford and Habas 2005, Gao and Chen 2010) (Figure 1.13).

In canonical Wnt signaling, binding of a Wnt ligand to a Frizzled transmembrane receptor initiates clustering of Fzd and LRP6 proteins within the cell membrane (Gao and Chen 2010). Dvl protein is recruited to the cytoplasmic side of these clusters through binding of the Dvl PDZ domain to the Fzd, with Dvls amino-terminal DIX domain enabling oligomerization of the now membrane-associated Dvl proteins (Sharma, Castro-Piedras et al. 2018). The Dvl oligomers are then able to bind and sequester Axins, blocking Axin-mediated degredation of βcatenin (Gao and Chen 2010), permitting its accumulation, trafficking to the nucleus, and promotion of transcription of Wnt target genes. Recent research has revealed that LRP activity may be dispensable for Fzd

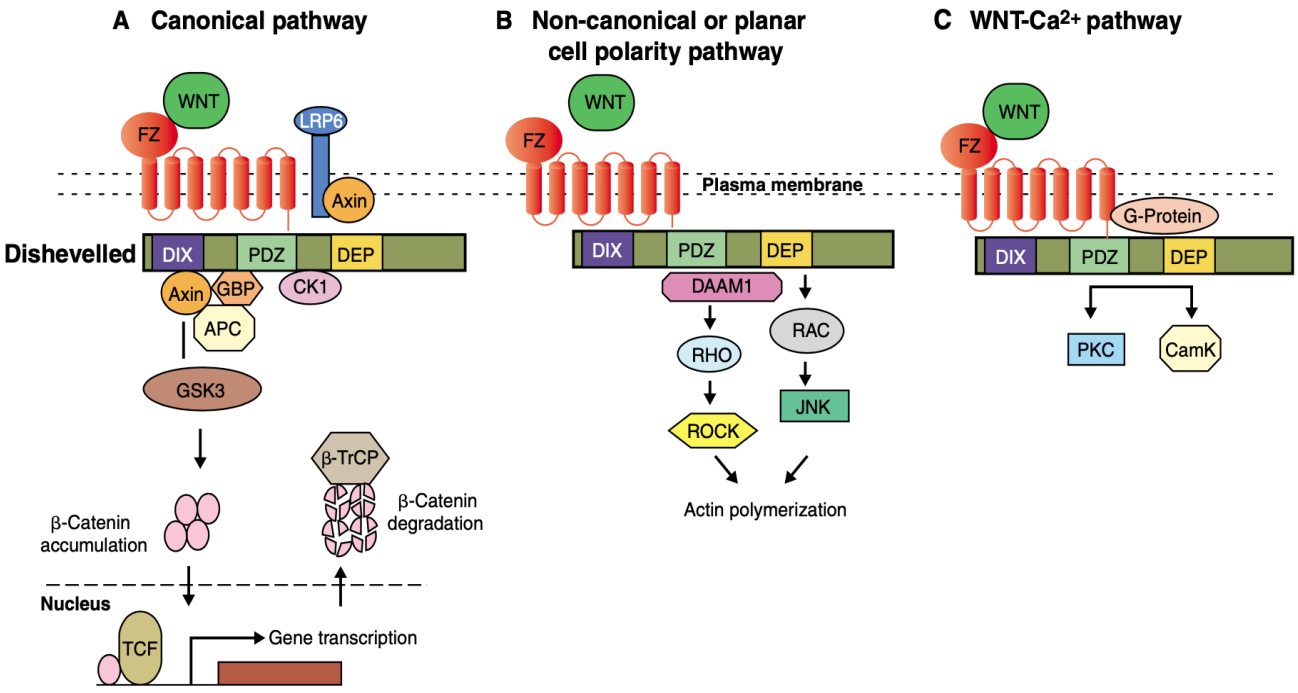

Fig 1.13 Dishevelled acts in Multiple Cellular Signaling Pathways

Cartoon taken from (Wallingford and Habas 2005) depicts that Dishevelled mediates at least three signaling cascades.
A) the canonical Wnt signaling pathway.
B) the non-canonical Wnt pathway known as planar cell polarity.
C) the Wnt-calcium signaling pathway.

mediated recruitment of Dvl and formation of an Axin-inactivating complex (Sharma, Castro-Piedras et al. 2018). Dishevelled proteins are also known to be trafficked to the nucleus, where Dvl has been found to interact with c-Jun and βcatenin, followed by formation of the stable βcatenin/TCF complex and transcriptional activation of Wnt target genes (Gao and Chen 2010). Mutations to the nuclear localization signal within Dvl mutation specifically impaired the βcatenin pathway, in Xenopus embryos (Gao and Chen 2010), suggesting an additional and as yet poorly understood role for nuclear Dvl in control of canonical Wnt signaling.

Dvls also interact with Wnt signals in a βcatenin independent signaling pathway known as planar cell polarity (PCP) where it plays a key role in governing polarity and cytoskeletal rearrangements of a cell (Vu, Mansour et al. 2019). An extracellular PCP signal is received by a Fzd receptor, causing the accumulation of a protein complex at the Fzd receptor which includes Dvls and Diego/Diversin, while the opposite side of the cell localizes a protein complex containing Prickle and Strabismus/Vangl proteins (Aw and Devenport 2017), establishing planar polarization. Several lines of evidence indicate that PCP signaling terminates with control of the actin cytoskeleton, and Dishevelled can activate the well-known actin regulators RHO and RAC, as well as bind DAAM1, a formin-homology protein which can nucleate linear actin cables (Sharma, Castro-Piedras et al. 2018). Dvls activity in the PCP pathway has been shown to control proper polarization of epidermal epithelium in Planaria (Almuedo-Castillo, Salo et al. 2011, Vu, Mansour et al. 2019). Dvls are also known to play a role in multiple additional signaling pathways, such as the Wnt/Ca^{2+} pathway, which may influence the function of canonical Wnt and PCP signaling (Wallingford and Habas 2005). Dvls status as a hub for multiple signaling pathways invited investigation into whether it plays a role in regulation of asymmetric injury-induced *notum* expression, and by extension AP polarity and the head/tail fate decision.

Aim of thesis

The aim of this thesis work is to elucidate mechanisms underlying establishment of AP polarity during planarian regeneration. A particular emphasis is placed on the role of Wnt signaling pathways as regulators of this process.

In chapter 2, we present experiments identifying a role for the planarian Dvl homologs as regulators of polarization of *notum* expression. The Dvl inhibition phenotype is characterized and linked to phenotypes generated by RNAi screening of Wnt ligands. We show a role for the Dvls and multiple Wnts in maintaining *notum* expression at anterior, but not posterior, facing wounds, with consequences for proper head/tail fate decisions. We relate changes in *notum* expression to disruption of muscle morphology and suggest a role for proper muscle patterning in encoding polarity information across the animal. Using sublethal irradiation to temporarily inhibit growth, a critical period of action for the Wnts and Dvls prior to injury is identified.

In chapter 3, in collaborative work with Dr Nicolle Bonar, a model is proposed for the function of *src-1 in* regeneration as a global regulator of anterior patterning in regeneration. It is shown that *src-1* inhibition causes the formation of larger brains with posterior ectopic eyes and a secondary posterior pharynx. These phenotypes are strongly reminiscent of those caused by the inhibition of Wnt and FGFRLs known to control regional patterning in planaria. Further, double RNAi analysis indicates *src-1* is a key patterning regulator linking multiple aspects of posterior determination including body plan regionalization and pole identity. These results suggest that *src-1* may act downstream of known Wnt and FGFRL signals to coordinate regional patterning for regeneration of the body axis.

This work provides new insights into the molecular mechanisms which regulating tissue polarization and the re-establishment of body axes during regeneration.

Chapter 2

Wnt11/Dishevelled signaling acts prior to injury to control wound polarization for the onset of planarian regeneration

Abstract

Regeneration is initiated by wounding, but it is unclear how injury-induced signals precisely convey the identity of the tissues requiring replacement. In the planarian *Schmidtea mediterranea*, the first event in head regeneration is the asymmetric activation of the Wnt inhibitor *notum* in longitudinal body-wall muscle cells, preferentially at anterior-facing versus posterior-facing wound sites. However, the mechanism driving this early symmetry breaking event is unknown. We identify a noncanonical Wnt11/Dishevelled pathway regulating *notum* polarization, which opposes injury-induced *notum*-activating Wnt/βcatenin signals and regulates muscle orientation. Using expression analysis and experiments to define a critical time of action, we demonstrate that Wnt11/Dishevelled signals act prior to injury and in a growth-dependent manner to orient the polarization of *notum* induced by wounding. In turn, injury-induced *notum* dictates polarization used in the next round of regeneration. These results identify a self-reinforcing feedback system driving the polarization of blastema outgrowth and indicate that regeneration uses pre-existing tissue information to determine the outcome of wound-induced signals.

Introduction

Animals capable of whole-body regeneration need mechanisms not only to generate replacement cells but also to specify the identity of tissues within an outgrowing blastema. Regeneration is possible from diverse potential injuries, requiring that animals process signals relaying the size and position of a wound to coordinate the precise replacement of lost tissue. However, the nature of these signals and how they interact with existing tissue is not fully understood. The regeneration of planarian head and tail tissue is a paradigm for understanding blastema formation and fate. The planarian *Schmidtea mediterranea* regenerates from nearly any surgical injury through the use of adult pluripotent stem cells of the neoblast population, the only proliferating cells in planarian adults (Newmark and Sanchez Alvarado 2000, Reddien, Oviedo et al. 2005, Elliott and Sanchez Alvarado 2013, Reddien 2018). In planarians, anterior-facing amputation sites made anywhere along the anteroposterior (AP) axis result in head regeneration, while tail regeneration occurs at any posterior-facing amputation site (Reddien and Sanchez Alvarado 2004). These decisions are independent of the axial location of amputation, and therefore, the orientation of wound sites in some way directs the outcome of subsequent outgrowth.

Head and tail fates for regeneration are themselves driven by a canonical Wnt signaling process, because *βcatenin-1* RNAi causes ectopic head regeneration at posterior-facing wounds, while pathway overactivation through *APC* RNAi causes ectopic regeneration of tails at anterior-facing wounds (Gurley, Rink et al. 2008, Iglesias, Gomez-Skarmeta et al. 2008, Petersen and Reddien 2008). Many of the planarian Wnts are expressed in nested domains in the posterior (*wntP-2/wnt11-5*, *wnt11-1*, *wnt11-2*, *wnt1, wntP-3*) (Petersen and Reddien 2008, Petersen and Reddien 2009, Gurley, Elliott et al. 2010, Petersen and Reddien 2011) and a gradient of βcatenin-1 protein has been detected from the posterior (Sureda-Gomez, Martin-Duran et al. 2016,

Stuckemann, Cleland et al. 2017), suggestive of regulation of canonical Wnt signaling in the process of head and tail formation. In the posterior blastema, high *wnt1* signaling drives formation of a posterior signaling center controlled by differentiation of new *wnt1*$^{+}$ posterior-dorsal-midline muscle cells through the action of STRIPAK/*mob4*, *pitx* and, *islet* factors (Hayashi, Motoishi et al. 2011, Marz, Seebeck et al. 2013, Schad and Petersen 2020), and posterior Wnt signals direct restoration of tail and trunk identity (Sureda-Gomez, Pascual-Carreras et al. 2015, Lander and Petersen 2016, Scimone, Cote et al. 2016). However, *wnt1* is induced early after injury (by 6 hours) and activated generically at all injury sites, suggesting that head regeneration fates from anterior-facing wounds involve a Wnt inhibitory process.

The Wnt inhibitor *notum* is expressed early after injury (6-18 hours) selectively at anterior-facing wound sites and not posterior-facing wound sites (Petersen and Reddien 2011). Subsequently during head regeneration, the action of several transcription factors (*foxD, zic-1, prep, pbx)* differentiates neoblasts into *notum*$^{+}$ cells at the anterior pole, forming an organizing center important for head outgrowth and patterning (Blassberg, Felix et al. 2013, Chen, Wang et al. 2013, Scimone, Lapan et al. 2014, Vasquez-Doorman and Petersen 2014, Vogg, Owlarn et al. 2014). *notum* inhibition leads to a spectrum of anterior regeneration phenotypes, including lack of head regeneration or ectopic tail regeneration (Petersen and Reddien 2011). Administration of *notum* dsRNA by injection immediately after amputation resulted in the regeneration of anterior tails expressing posterior Wnt genes, indicating *notum* can act after injury (Petersen and Reddien 2011). In addition, *notum* acts upstream of *βcatenin-1,* because dual inhibition of both genes phenocopies *βcatenin-1* RNAi to result in ectopic head formation (Petersen and Reddien 2011). Together these results indicate that *notum* acts at very early steps in a regulatory hierarchy driving head regeneration. In addition, a genome-wide expression survey found *notum* to be the only

asymmetrically expressed and early injury-induced gene in planarians, whereas all other examined injury-induced genes are activated equally at any injury site (Wurtzel, Cote et al. 2015). Therefore, the polarity of *notum* expression marks the earliest symmetry breaking event which distinguishes anterior- and posterior-facing wound sites (Petersen and Reddien 2011) and drives the divergent regeneration behavior of the outgrowing blastema.

What is the mechanism driving this early *notum* asymmetry? *notum* injury-induced expression and polarization does not depend on stem cells (Petersen and Reddien 2011), nor on the removal of particular tissues such as the head (Petersen and Reddien 2011). In addition, injury-induced *notum* is expressed exclusively from pre-existing *myoD*$^{+}$ longitudinal muscle cells (Scimone, Cote et al. 2017), suggesting that some latent polarization of muscle and/or other tissues instructs the permissiveness for *notum* activation following injury. In principle, canonical Wnt signals could be candidates for this polarization given that planarian *notum*, like most Notum genes in other organisms, functions as a feedback inhibitor whose expression depends on βcatenin (Petersen and Reddien 2011). However, overactivation of this pathway by *APC* RNAi leads to elevated *notum* at both anterior- and posterior-facing injury sites and a retention of polarization (Petersen and Reddien 2011). Therefore, although βcatenin signaling controls head-versus-tail blastema identity, it likely does not control the polarization of injury-induced *notum* responsible for this decision.

Other signaling pathways are involved in head and tail regeneration and could potentially contribute to this standing polarity. Hedgehog signaling perturbation affects head-versus-tail regeneration through controlling levels of *wnt1* activation but does not regulate *notum* asymmetry (Rink, Gurley et al. 2009, Yazawa, Umesono et al. 2009, Petersen and Reddien 2011). In addition, perturbation of gap junction and calcium signaling impacts regeneration polarity but through

impacting *wnt1* expression and/or *notum* activation rather than *notum* polarity (Oviedo, Morokuma et al. 2010, Zhang, Chan et al. 2011, Durant, Bischof et al. 2019). Several additional factors including *foxD* and *zic-1* have been identified as important for head regeneration but appear to act on downstream steps, because they do not influence the early expression of *notum* from pre-existing anterior-facing muscle cells (Scimone, Lapan et al. 2014, Vasquez-Doorman and Petersen 2014, Vogg, Owlarn et al. 2014). Activin signaling plays a critical role in regulating *notum* expression polarity because *activin-2* RNAi leads to mispolarized blastemas and elevated injury-induced *notum* expression at posterior-facing injury sites (Cloutier, McMann et al. 2021). However, *activin-2* is expressed broadly in the animal, so it is unclear whether this factor provides an instructive cue for polarization (Cloutier, McMann et al. 2021). In addition, the Activin pathway inhibitor *follistatin* is expressed at any injury site where it drives the mitotic and cell death responses specific to conditions of tissue removal and drives the process of head regeneration by suppressing *wnt1* expression independent of *notum* asymmetry (Tewari, Stern et al. 2018). Therefore, the nature of tissue polarization that leads to injury-induced *notum* expression asymmetry remains unknown.

Noncanonical βcatenin-independent Wnt signaling pathways mediated by Dishevelled (Dvl) function in numerous developmental contexts including planar cell polarity (Wallingford and Habas 2005, Devenport 2014, Aw and Devenport 2017, Sharma, Castro-Piedras et al. 2018). In planarians, A/P polarization of the ciliated ventral epidermis is mediated by Dishevelled (Almuedo-Castillo, Salo et al. 2011, Vu, Mansour et al. 2019), but it is unknown whether such a pathway could control the polarity of the *notum* expression following injury that is functionally linked to blastema fate determination. In addition, whether some or all of the planarian Wnts function equally in tissue polarization and/or the activation of *notum* is not known.

We report here that the planarian Dishevelled homologs exert a distinct action on *notum* expression compared to *βcatenin-1*, with *dvl-1;dvl-2(RNAi)* animals undergoing apolarization of injury-induced *notum* expression responses, including ectopic *notum* expression at posterior-facing wounds, and also disorganization of muscle fibers. We identify a cohort of planarian Wnts which act positively to promote *notum* expression at wound sites (*wnt1* and *wntP-2/wnt11-5)* and two posteriorly expressed Wnt11 homologs (*wnt11-1* and *wnt11-2)* that negatively regulate *notum* at posterior-facing wound sites, likely through action of *dvl-1* and *dvl-2* in a non-canonical Wnt pathway. Under irradiation treatments depleting stem cells prior to injury, the effect of Dvl/Wnt11 inhibition to reverse *notum* polarity is lost. In addition, the re-expression of *wnt11-1* and *wnt11-2* through regeneration occurs after the *notum* expression decision, together indicating that these factors likely act prior to injury to establish latent cues which influence injury-induced *notum* polarity. The use of pre-existing signals to influence injury-induced genes is analogous to the maternal contributions to early embryogenesis, in which information from a prior stage integrates and informs a new phase of growth.

Results

Dvl inhibition leads to mispolarization of injury-induced *notum* from longitudinal muscle

We hypothesized that Wnt-related pathways might participate in controlling the polarity of injury-induced *notum* expression and tested this using RNAi. As observed previously, *βcatenin-1* inhibition prevented *notum* expression at anterior-facing wounds, and *APC* inhibition resulted in over-expression of *notum* at both anterior- and posterior-facing wounds while retaining expression asymmetry (Figure 2.1). To more broadly perturb Wnt-related signaling pathways, we inhibited the two planarian Dishevelled homologs (*dvl-1* and *dvl-2*), and this treatment resulted in a dramatically distinct phenotype of ectopic *notum* expression throughout the regenerating fragment (Figure 2.2). Because *dvl-1* and *dvl-2* likely act upstream of *βcatenin-1* to activate canonical Wnt signaling (Wallingford and Habas 2005, Gurley, Rink et al. 2008), this result suggested Dvl must additionally have a distinct *βcatenin-1*-independent role in the regulation of *notum* expression. Uninjured *dvl-1;dvl-2(RNAi)* worms also had ectopic *notum*$^+$ cells (Figure 2.2), so we further examined the types of cells expressing *notum* under these conditions (Figure 2.3). In control animals, *notum* expression occurred only at the anterior-facing wounds (AFW), and nearly all (>95%) *notum*$^+$ cells also expressed the muscle marker *collagen* (Figure 2.3), in line with previous experiments (Witchley, Mayer et al. 2013). In amputated *dvl-1;dvl-2(RNAi)* trunk fragments 40% of *notum*$^+$ cells at either wound site (Figure 2.3, insets i and iii) colocalized with *collagen*$^+$ muscle cells. By contrast, *notum*$^+$ cells away from the wound site of (*dvl-1;dvl-2(RNAi)* animals were *collagen*-negative (Figure 2.3, inset ii), as were *notum*$^+$ cells present in the pre-pharyngeal region of uninjured *dvl-1;dvl-2(RNAi)* worms (Figure 2.3). *notum* is co-expressed in *chat*$^+$ neurons of the brain in normal animals (Hill and Petersen 2015), so we tested whether ectopic *notum* expressed

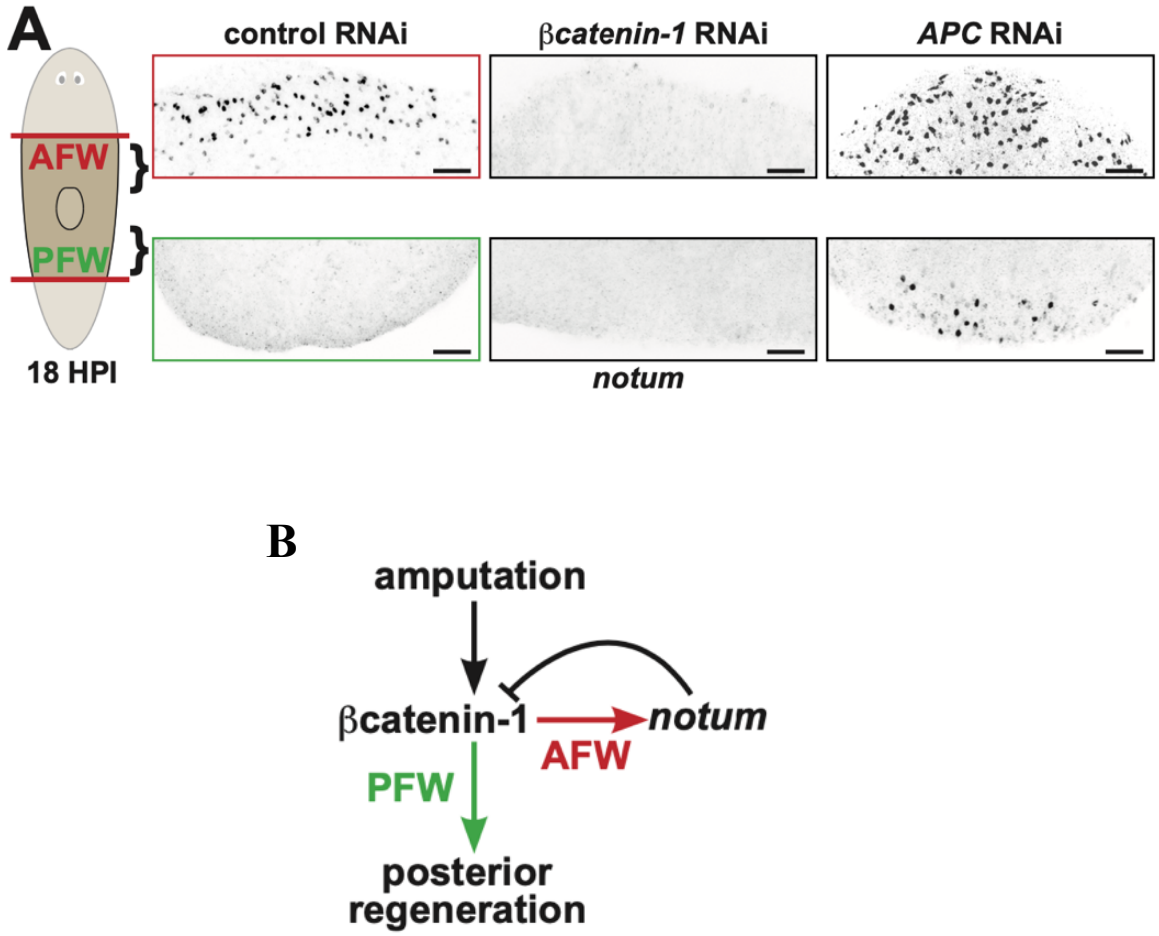

Fig 2.1 Pre-existing Model of Wnt Signaling Control of *notum* expression

A) *in situ* hybridizations showing *notum* is asymmetrically expressed by 18 hours post-injury (HPI) at anterior-facing wounds (AFW) versus posterior-facing wounds (PFW) after transverse amputation. Inhibition of *βcatenin-1* or *APC* leads to under- or over-expression of *notum* without affecting overall *notum* expression polarity. Scale bars 100 microns.
B) model from prior work in which high *notum* expression at AFWs after injury leads to low βcatenin activity and anterior regeneration, and low *notum* expression at PFWs allows high βcatenin activity resulting in posterior regeneration.

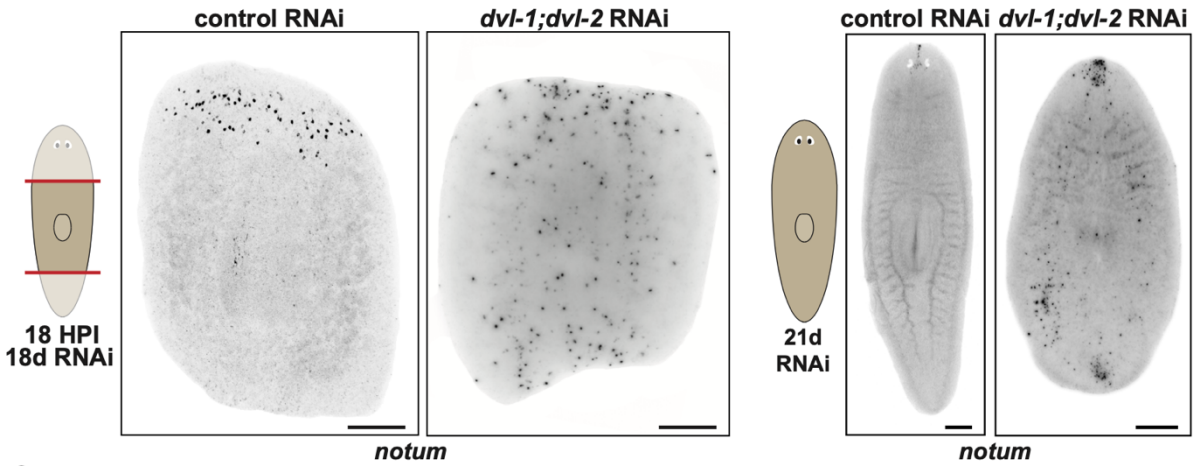

Fig 2.2 Inhibition of the Dvls Leads to Ectopic *notum* Expression

in situ hybridizations to detect *notum* expression at 18 hours post-injury (left) or in uninjured (right) *dvl-1;dvl-2(RNAi)* versus control RNAi animals 21 days after beginning dsRNA feeding (21d). Scale bars 300 microns.

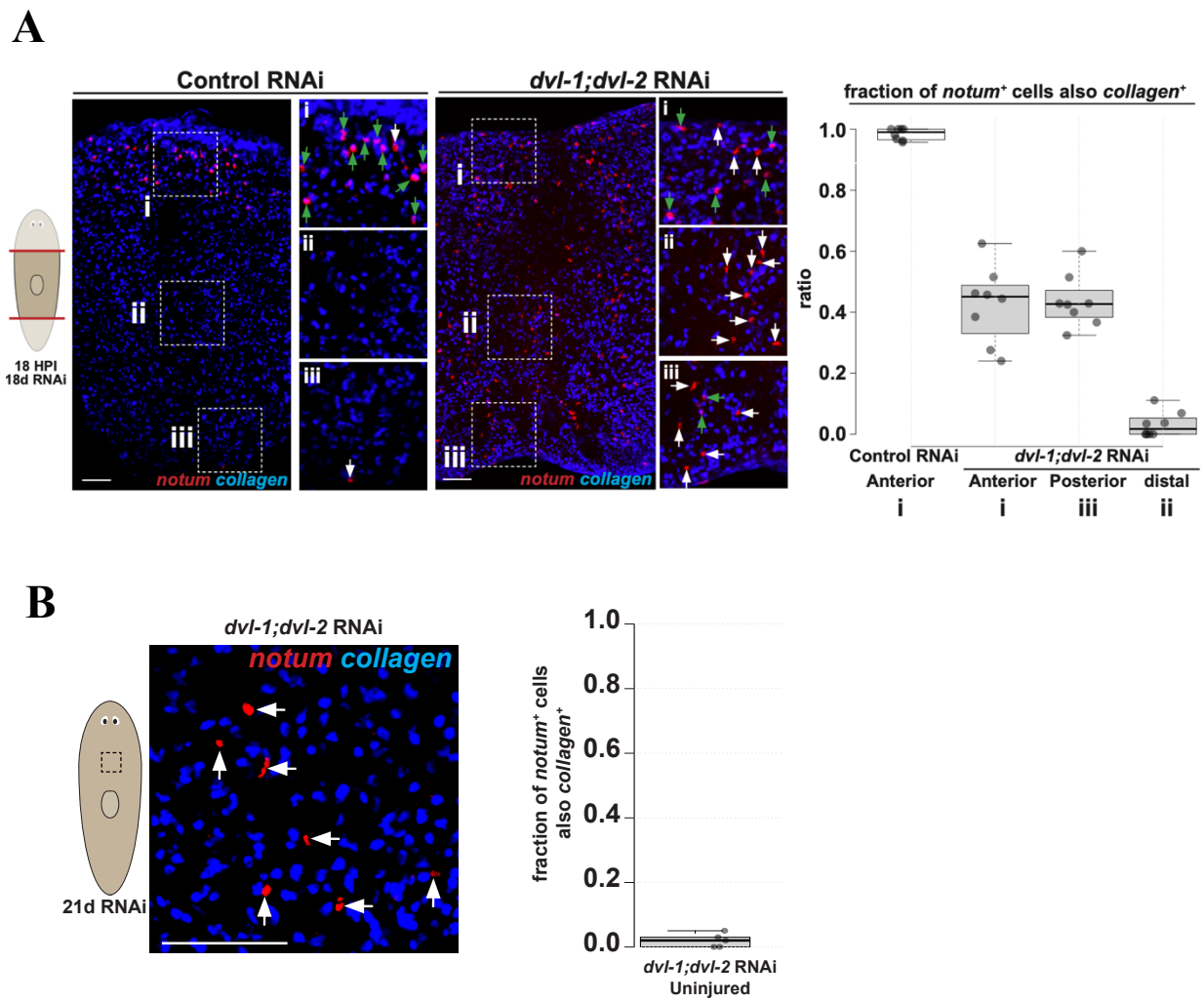

Fig 2.3 Inhibition of the Dvls Leads to Ectopic *notum* Expression in Muscle at Wound Sites, in Non-Muscle Cells Throughout the Body

A) double FISH of control versus *dvl-1;dvl-2(RNAi)* regenerating trunk fragments at 18 hours post-amputation after 18 days of RNAi to detect *notum* and *collagen*. Insets depict locations at anterior-facing wounds (i), regions distal from wound sites (ii), and at posterior-facing wounds (iii), shown at 300% zoom. Scale bars 100 microns. Green arrows mark *notum*$^+$ *collagen*$^+$ muscle cells, while white arrows mark cells which express *notum* but not *collagen*. Graph shows quantification of fraction of notum$^+$ cells expressing collagen. In *dvl-1;dvl-2(RNAi)* animals, approximately 40% of *notum*-expressing cells near wound sites (i, iii) were *collagen*$^+$ muscle cells while ectopic *notum*$^+$ cells located away from wound sites (ii) were *collagen*$^-$.
B) double FISH to detect *notum* and muscle marker *collagen* in the pre-pharyngeal region of *dvl-1;dvl-2(RNAi)* uninjured animals after 21 days of RNAi. Scale bar 100 microns. White arrows indicate *notum*$^+$*collagen*$^-$ cells. *notum*$^+$ cells formed centrally in *dvl-1;dvl-2(RNAi)* animals in the absence of injury are likely not muscle cells.

in non-muscle cells might be expressed in *chat*$^{+}$ neurons and found that approximately 15% of *notum*$^{+}$ cells in *dvl-1;dvl-2(RNAi)* animals were *chat*$^{+}$ neurons (Figure 2.4), accounting for approximately a quarter of the *notum*$^{+}$ *collagen*$^{-}$ population. Together, we conclude that Dvl inhibition causes expression of *notum* both in *chat*+ neurons and in an unidentified cell type, and also results in inappropriate expression of *notum* in *collagen*$^{+}$ muscle cells proximal to wound sites.

We then examined numbers of *notum*-expressing muscle cells near injury sites at 18-hours post-amputation. Strikingly, inhibition of the Dvls resulted in elevated numbers of *notum*-expressing muscle cells at posterior-facing wounds while decreasing *notum* expression at anterior-facing wounds (Figure 2.5). Whereas perturbation of canonical Wnt signaling concordantly modified the expression of *notum* at all injury sites (Figure 2.1) (Petersen and Reddien 2011), inhibition of Dishevelled homologs reduced or eliminated the polarization of *notum* expression (Figure 2.5). In addition, at posterior-facing wounds, Dishevelled inhibition had an opposite effect on *notum* expression compared to *βcatenin-1* RNAi, likely indicating action via distinct processes. By examining anterior- and posterior-facing wounds generated at different axis locations, we found that inhibition of the Dvls caused similar disruptions to *notum* expression polarity across the body (Figure 2.5). We conclude that Dishevelled regulates the orientation of injury-induced *notum* expression.

We undertook additional analysis to determine whether wound-site localized expression of *notum* in muscle cells occurred in response to injury (Figure 2.6). Compared to *dvl-1;dvl-2(RNAi)* animals fixed immediately after injury (0 hours), *dvl-1;dvl-2(RNAi)* fragments fixed at 18 hours had elevated numbers of *notum*$^{+}$*collagen*$^{+}$ cells at both anterior- and posterior-facing wound sites (Figure 2.6). Therefore, Dvl inhibition causes both anterior- and posterior-facing wound sites to

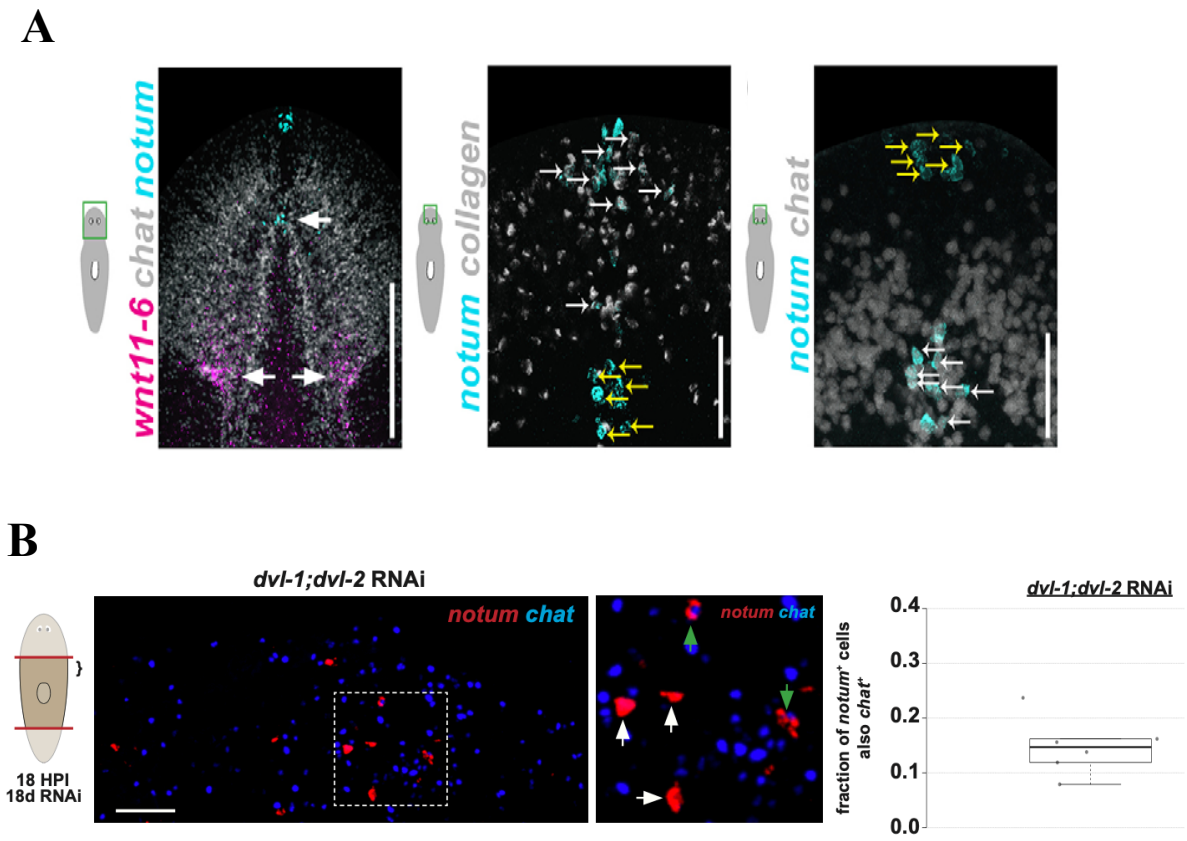

Fig 2.4 A Minority of Ectopic *notum* Expressing Cells Generated by Dvl Inhibition are *chat*$^{+}$ neurons

A) figure from (Hill and Petersen 2015) showing two populations of *notum* expressing cells. *notum/collagen* double positive cells in the anterior pole, and *notum/chat* double positive cells in the center of the brain.
B) double FISH to detect *notum* and the neuronal marker *chat* in *dvl-1;dvl-2(RNAi)* animals. Scale bar 100 microns. Green arrows mark *notum*$^{+}$ *chat*$^{+}$ cells, while white arrows mark cells which express *notum* but not *chat*. Graph on the right shows fraction of *notum*$^{+}$ cells colocalizing with *chat* expression. *notum*$^{+}$ *chat*$^{+}$ cells could be identified and represented ~15% of *notum*$^{+}$ cells in *dvl-1;dvl-2(RNAi)* animals. Therefore, a majority of *notum*$^{+}$ *collagen*$^{-}$ cells in these animals were not *chat*$^{+}$.

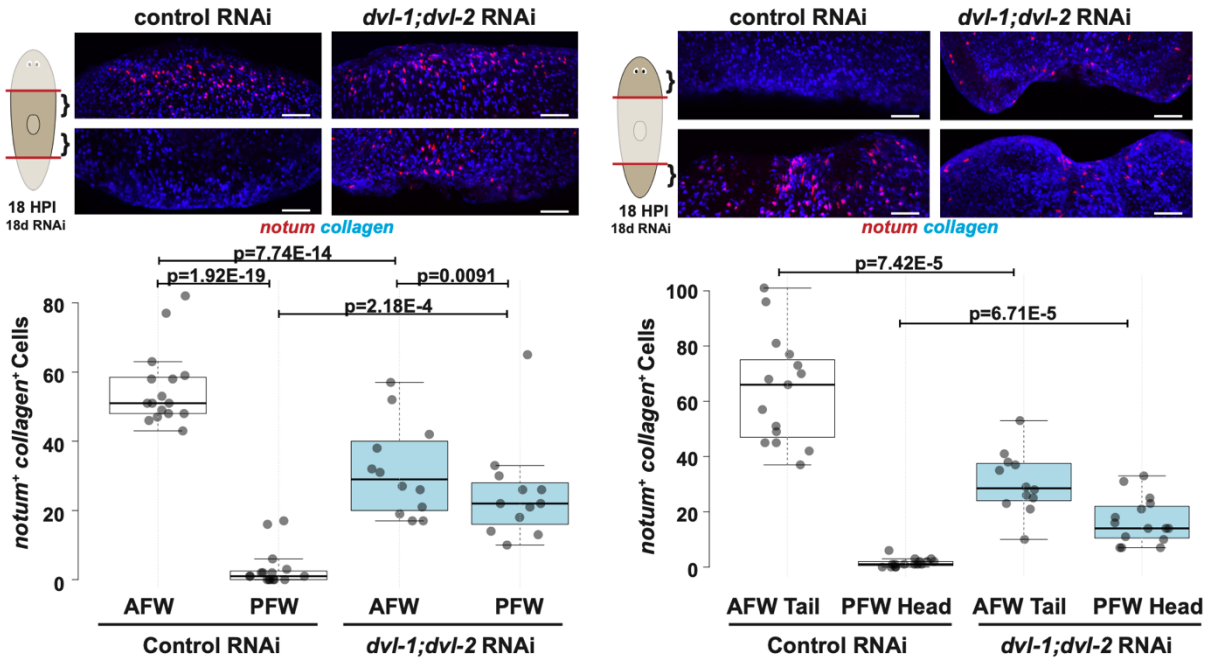

Fig 2.5 Inhibition of the Dvls Depolarizes *notum* Expression with Respect to AP Wound Site

Double-FISH of *notum* and *collagen* after indicated treatments. Scale bars 100 microns. Bottom graphs show quantification of *notum*$^+$ *collagen*$^+$ cells. Box plot shows median values (middle bars) and first to third interquartile ranges (boxes); whiskers indicate 1.5× the interquartile ranges and dots are individual data points. p-values were computed from two-tailed unpaired t-tests between the conditions indicated by brackets. Dvl RNAi resulted in reduced *notum* expression from anterior-facing wounds and elevated expression from posterior-facing wounds.

be able to induce the expression of *notum* in *collagen*$^+$ muscle cells after injury. We observed this same trend in animals amputated at different AP axis locations, indicating Dvl controls *notum* polarization throughout the body and not only regionally (Figure 2.6). By contrast, non-muscle *notum* expressing cells (i.e., *collagen*-negative and *notum*-positive cells) were not significantly upregulated between 0 and 18 hours after injury in *dvl-1;dvl-2(RNAi)* animals (Figure 2.7; Trunk AFWs p=0.374, Trunk PFW p=0.934, Tail AFW p=0.204, Trunk PFW p=0.438), indicating that *notum* expression in non-muscle cells after Dvl RNAi is not strongly induced by injury. Together, these data indicate that Dvl polarizes injury-induced *notum* expression specifically in muscle and across the body axis.

We next considered whether Dvl inhibition caused mispolarized injury-induced *notum* in the *myoD*$^+$ longitudinal muscle cells which typically express *notum*, or alternatively enabled *notum* expression in some other muscle cell types. Using double-FISH we detected *notum* expressed from *myoD*$^+$ muscle cells at posterior-facing wounds in *dvl-1;dvl-2(RNAi)* animals (Figure 2.8). Therefore, longitudinal muscles inappropriately activate *notum* after Dvl inhibition. Using double-FISH we also compared the fraction of total *notum*$^+$ cells near wounds sites detected as *myoD*$^+$ longitudinal muscle cells or detected as expressing the pan-muscle marker *collagen.* We found equal fractions of *notum*$^+$*myoD*$^+$ cells and *notum*$^+$*collagen*$^+$ cells compared to total wound-proximal *notum*$^+$ cells after Dvl RNAi (~40% of all *notum*$^+$ cells in each case) (Figure 2.8), arguing that a primary role of Dvl in this process is to polarize longitudinal muscle cells for appropriate expression of *notum*.

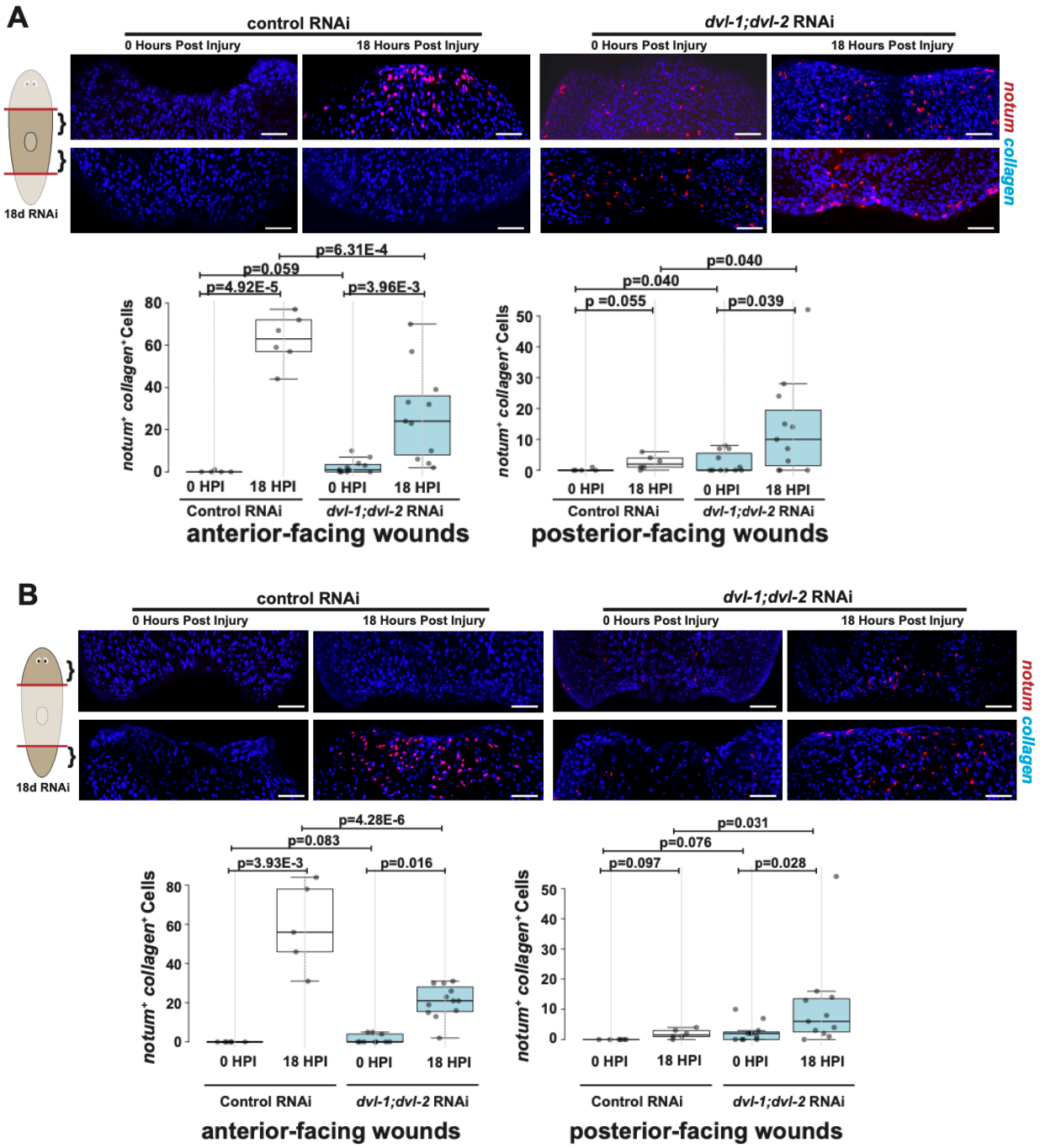

Fig 2.6 Ectopic *notum* Expression in Muscle is Injury Induced

Double FISH to detect *notum* and *collagen* in control versus *dvl-1;dvl-2(RNAi)* animals fixed at 0 hours or 18 hours post-injury, with quantification of double-positive cells from each wound site in each condition and fragment type as indicated by the cartoons. The excess *notum* expression in 18-hour regenerating *dvl-1;dvl-2(RNAi)* animals was induced by injury in trunk fragments (p=0.039) and head fragments (p=0.028). Scale bars 100uM in all images.

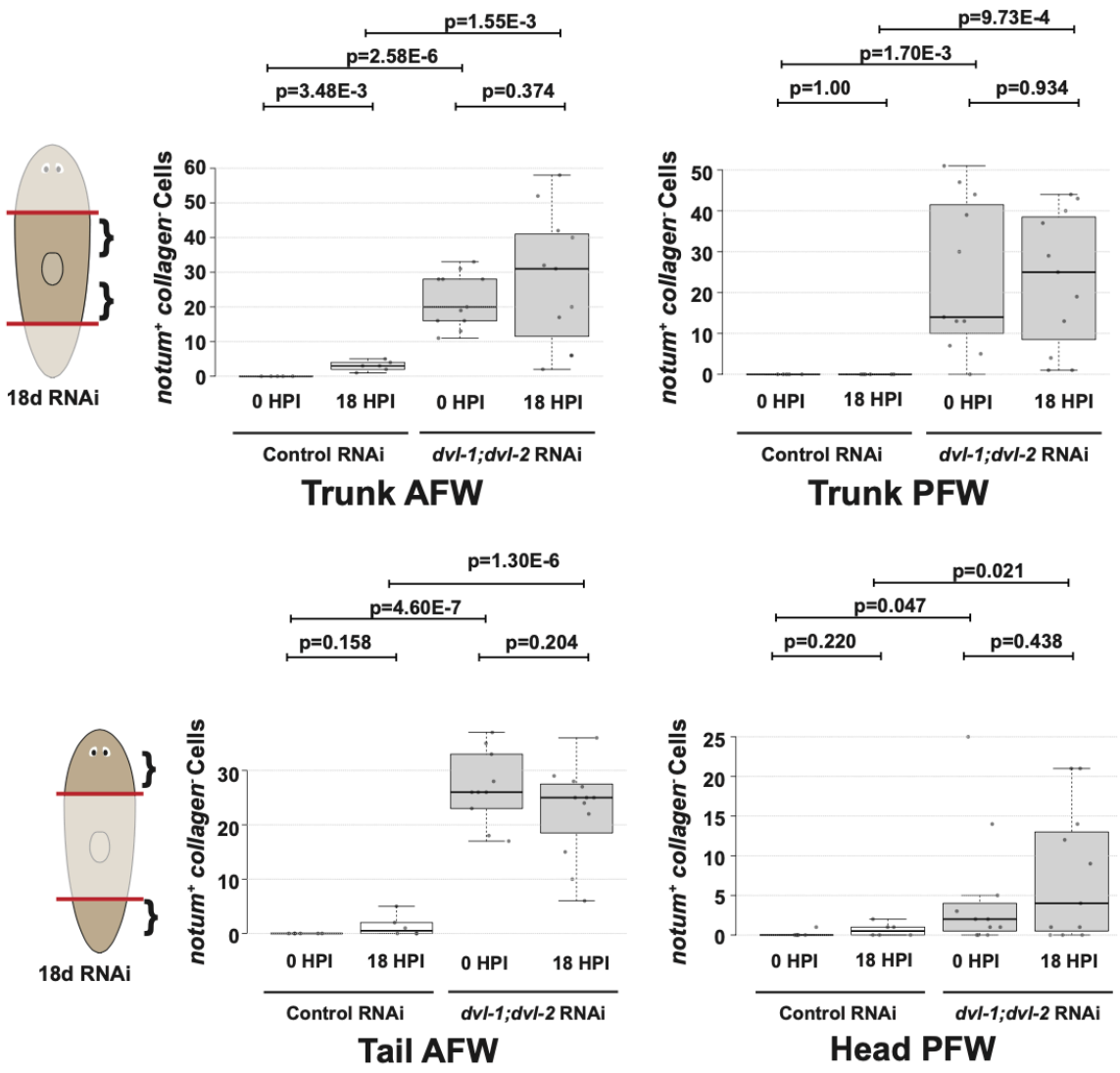

Fig 2.7 Non-muscle *notum* Expression Driven by Dvl Inhibition is not Injury Responsive

Quantification of *notum*$^{+}$ *collagen*$^{-}$ (non-muscle) cells from the anterior- and posterior-facing wound sites of trunk, tail, and head fragments as indicated. In *dvl-1;dvl-2(RNAi)* worms *notum*$^{+}$ *collagen*$^{-}$ cells were present prior to injury (0 HPI) and in equal abundance by 18 hours post-injury.

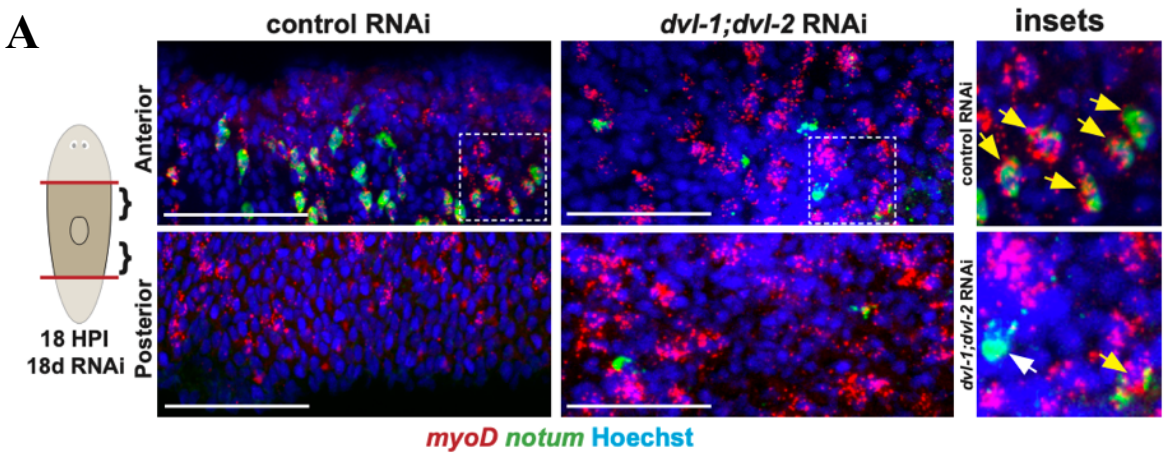

Fig 2.8 Under Dvl Inhibition, *notum* is Expressed in Longitudinal Muscle

A) Double FISH showing injury sites 18 hours post amputation to detect *notum* along with the longitudinal-muscle-body marker *myoD* and counterstained with Hoechst. Scale bars, 50 microns. Insets show 300% zoom, white boxes mark location of insets. Yellow arrows mark *notum*$^+$ *myoD*$^+$ cells, while white arrows mark cells which express *notum* but not *myoD*. B) Graph shows fraction of *notum*$^+$ cells colocalizing with *myoD* expression at individual wound sites and a comparison to colocalization of *notum* and *collagen* at these locations from data from Figure 1. *notum*$^+$ cells co-expressed either *myoD* or *collagen* to a similar degree (~40%) at anterior- and posterior-facing wound sites in *dvl-1;dvl-2(RNAi)* worms.

Dvl inhibition disrupts AP patterning and muscle morphology

We sought to evaluate the overall outcome of regeneration after combined *dvl-1* and *dvl-2* inhibition under the same dsRNA dosing schedule in which mispolarized injury-induced *notum* was detected. By day 14 of regeneration, 21% (12/57) of *dvl-1;dvl-2(RNAi)* animals regenerated posterior-facing heads, but other animals in this cohort formed posterior forked tail blastemas (21%, 12/57), failed posterior regeneration (12%, 7/57), failed posterior and anterior regeneration (33%, 19/57), or underwent lysis resulting in death (11%, 6/57); only a single worm (2%, 1/57) regenerated normally (Figure 2.9). This range of morphological phenotypes is consistent with observations from prior studies (Gurley, Rink et al. 2008, Almuedo-Castillo, Salo et al. 2011, Vu, Mansour et al. 2019). Pleiotropy of the *dvl-1;dvl-2(RNAi)* phenotype may reflect Dishevelled's role in multiple signaling and cell-adhesion pathways, with successful posterior head regeneration requiring a particular titration of *dvl-1;dv-l-2* dsRNA sufficient to alter polarity without compromising the overall capacity to regenerate.

We sought to confirm whether *dvl-1;dvl-2(RNAi)* treatment robustly disrupted anterior-posterior polarity even in fragments which did not form substantial blastemas. To do so, worms were administered six doses of *dvl-1;dvl-2* dsRNA, amputated, and trunk fragments were collected for analysis at day eight of regeneration. *In situ* hybridization with anterior pole markers *notum, sfrp-1,* and *foxD* revealed that *dvl-1;dvl-2(RNAi)* trunk fragments generated two anterior poles, even when regeneration blastemas were small or absent, while also not expressing the posterior marker *wntP-2/wnt11-5* (Figure 2.10). The penetrance of the double-anterior pole phenotype at day eight of regeneration exceeded that of double-headed worms at day 14, indicating that some fragments made inverted polarity determinations but subsequently failed to proceed with regeneration. These results accord with previous investigations in which *dvl-1;dvl-2(RNAi)* trunks

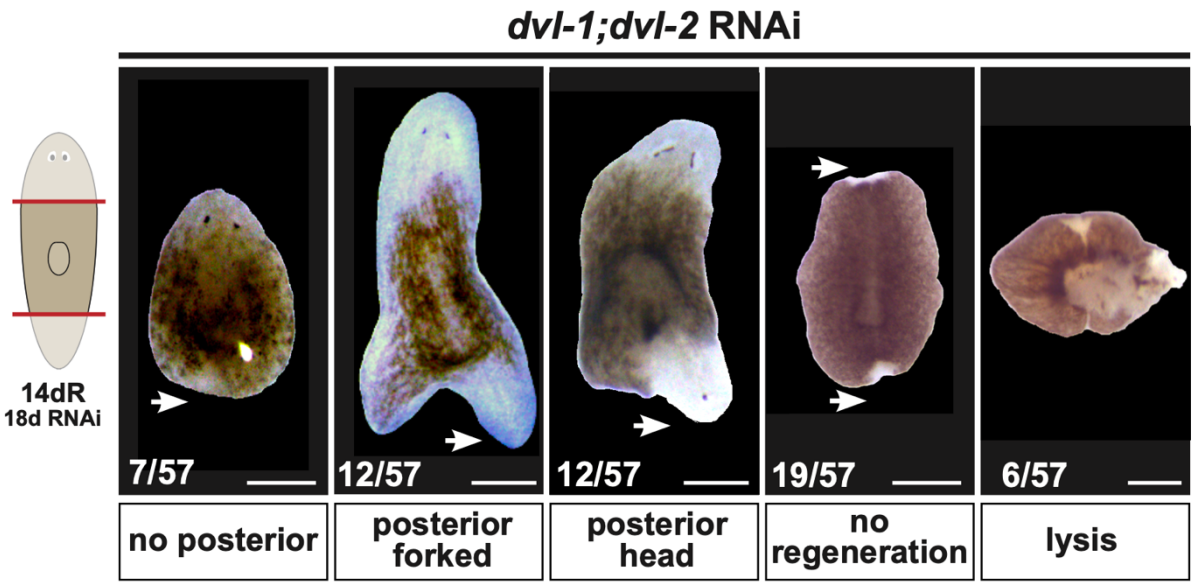

Fig 2.9 Dvl Inhibition Causes Regeneration Defects, Including Polarity Reversal

A spectrum of regeneration phenotypes from *dvl-1;dvl-2* RNAi observed at day 14 of regeneration (14dR): regeneration of posterior heads, forked blastemas, and anterior and/or posterior blastema failure. Numbers of animals qualitatively scored in each condition are indicated.

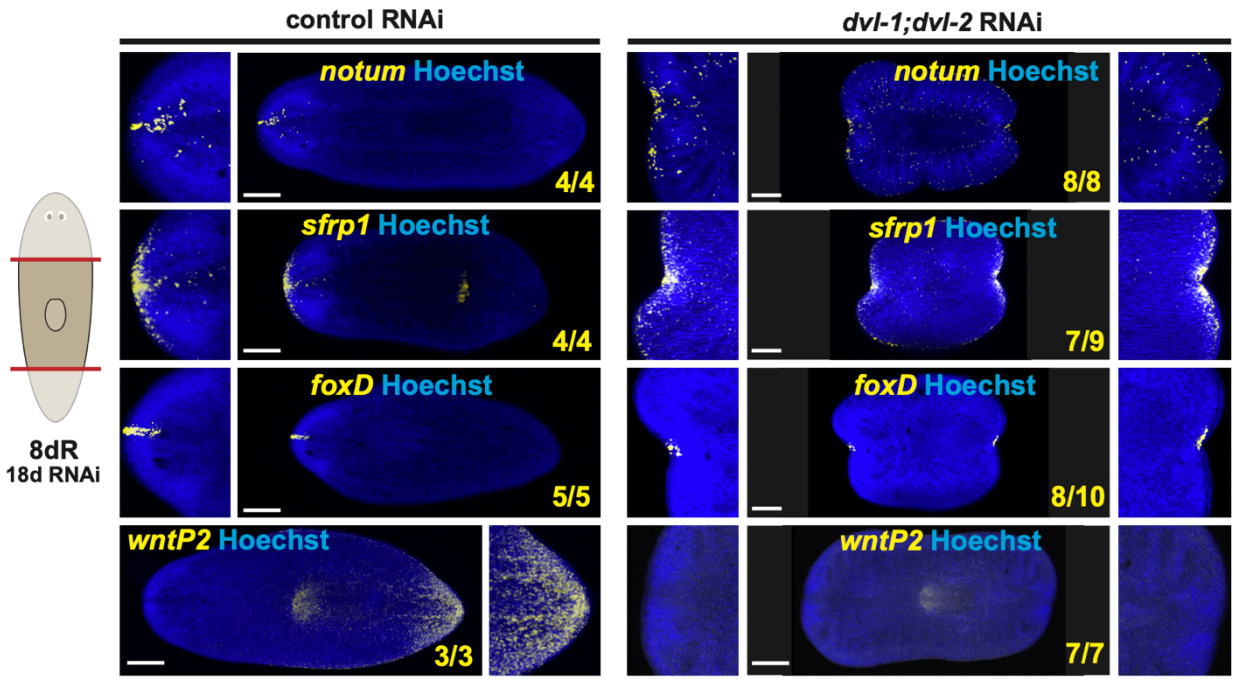

Fig 2.10 Dvl Inhibition Leads to Anterior Pole Identity at Regenerating PFWs

in situ hybridizations from control versus *dvl-1;dvl-2(RNAi)* trunk fragments fixed at day eight of regeneration using probes to detect anterior (*notum, sfrp1, foxD)* or posterior (*wntP-2*) identity and counterstained with Hoechst. Scorings indicate number of animals with expression as shown, and the left/right insets show a 200% zoom of the anterior and/or posterior of the main panel.

formed two anterior poles without blastemas displaying visible head features (Almuedo-Castillo, Salo et al. 2011). By contrast, *βcatenin-1* RNAi causes regeneration of heads at posterior-facing wound sites and not failed regeneration (Petersen and Reddien 2008). From these observations, we conclude that Dishevelled inhibition leads to ectopic injury-induced *notum* expression as well as a robust phenotype of anterior/posterior mispolarization and also failed posterior and anterior outgrowth.

dvl-1 and *dvl-2* both had broad expression by FISH (Figure 2.11), consistent with a prior single-cell RNAseq atlas showing expression of these genes in several major cell-type categories (Figure 2.12) (Fincher, Wurtzel et al. 2018). Both Dishevelled homologs had expression in muscle cell clusters by scRNAseq, and we verified by co-FISH that both were expressed in *collagen*$^{+}$ muscle (Figure 2.12). Expression of these genes was also broad throughout early regeneration (Figure 2.11). These results suggest Dishevelled factors could function in a variety of tissues, including in muscle.

Given this spectrum of regeneration phenotypes as well as the mispolarization of injury-induced *notum* after Dvl RNAi, we reasoned that Dvl inhibition may affect the architecture of the muscle system. To test this possibility, we stained control and *dvl-1;dvl-2(RNAi)* animals for muscle fibers using the 6G10 antibody (Ross, Omuro et al. 2015), which labels circular and diagonal muscle and more weakly marks longitudinal muscle. Musculature in control animals had a highly regular alignment of muscle fibers whose angles with respect to the AP axis binned into discrete categories according to their subtype (longitudinal around 0 degrees, diagonal around +/- 45 degrees, circular around +/- 90 degrees). By contrast, *dvl-1;dvl-2(RNAi)* animals had disorganization of fibers so that they were reduced in abundance and not well aligned across their lengths, leading to a broad distribution of fiber angles (Figure 2.13). Although no markers of

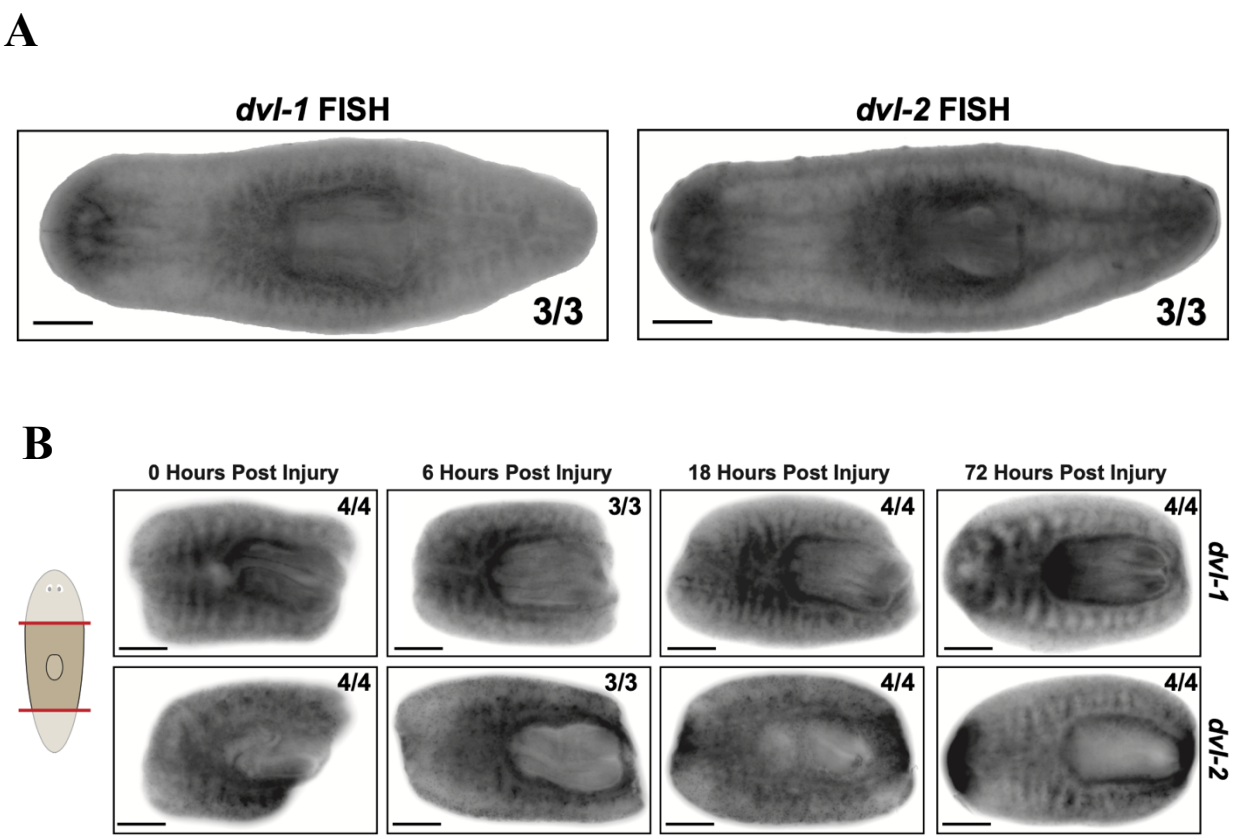

Fig 2.11 *dvl-1* and *dvl-2* are Broadly Expressed Before and After Injury

A) Dvl expression following injury. FISH of *dvl-1* and *dvl-2* shows a broad distribution of Dvl mRNAs. Scale bars 300 microns.
B) FISH showing that *dvl-1* and *dvl-2* transcripts were expressed following injury. Scale bars 300 microns.

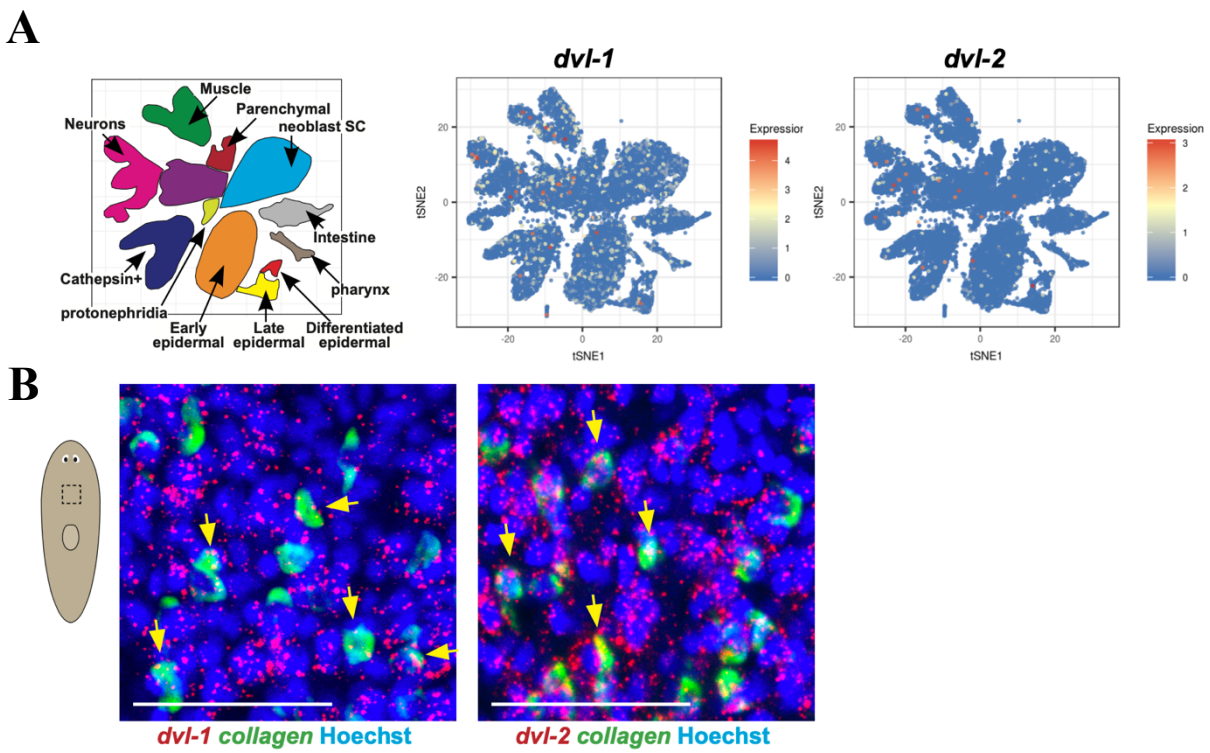

Fig 2.12 *dvl-1* and *dvl-2* are Expressed in Multiple Cell Types, Including Muscle

A) single-cell RNAseq plots from a planarian cell atlas (digiworm.wi.mit.edu) show expression of *dvl-1* and *dvl-2* across multiple classes of cell types, including muscle (left, cartoon annotates clusters and muscle cluster drawn in green).
B) double FISH detects *dvl-1* and *dvl-2* in *collagen*$^{+}$ muscle cells. Scale bars 50 microns.

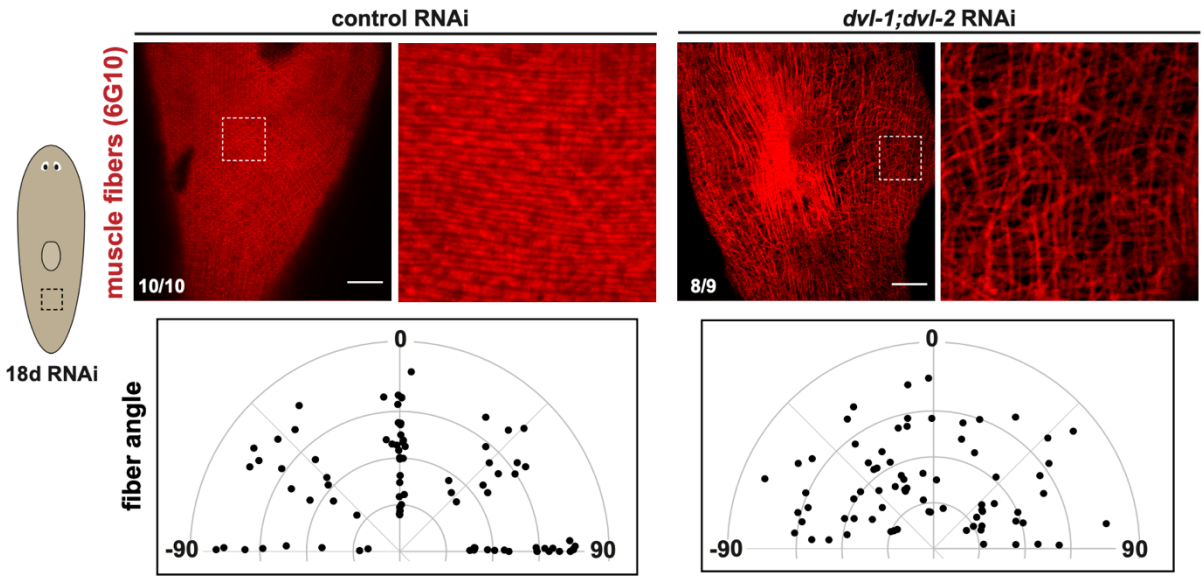

Fig 2.13 Inhibition of Dvls Disorganizes Muscle Morphology

Top, Immunofluorescence using 6G10 mouse monoclonal antibody to detect muscle fiber organization of the in homeostatic control versus *dvl-1;dvl-2(RNAi)* animals after 18 days of RNAi. Insets show 400% zoom, white boxes mark location of insets. Number of animals scored in each condition are indicated. Scale bars 100 microns. Bottom, quantifications of a collection of muscle fiber angles measured from 3-4 fields of view approximately 20x20 microns in size across 3 animals per condition. Each dot represents individual muscle fibers, plotted with angles in degrees and jittered over a random radial position to display measurements of similar value. In control RNAi animals, fiber angles cluster according to muscle subtype: longitudinal (0 degrees), circular (-90 and 90 degrees), and diagonal (-45 and 45 degrees). By contrast, Dvl inhibition caused disorganization of the muscle fiber network such that fiber angles no longer appeared clustered. Scale bars, 300 microns in all images.

muscle fiber polarity are known, these results are consistent with a model in which Dvl inhibition leads to a body transformation involving disorganization of the muscle system which could contribute to mispolarized *notum* expression.

Distinct Wnts promote or inhibit polarized *notum* expression

Dishevelled and *βcatenin-1* play distinct roles in the injury-induced expression of *notum,* so we hypothesized that various planarian Wnt genes might also have distinct roles in this process, reflecting operation through separate pathways. To test this idea, we inhibited the nine planarian Wnt genes by RNAi and examined the effects on *notum* expression at 18-hours post-amputation (Figures 2.14-2.19). *wnt1* expression is induced by injury at around the same timeframe as *notum,* is co-expressed with injury-induced *notum*, and acts oppositely in head-versus-tail determination (Petersen and Reddien 2009). *wnt1* RNAi reduced but did not eliminate injury-induced *notum* expression at anterior-facing wounds and did not modify expression at posterior-facing wounds (Figure 2.14). Based on *wnt1* RNAi's incomplete effect on *notum* expression, we speculated that *wnt1* might act in conjunction with other Wnt genes to drive *notum* expression following injury. A prior screen of Wnt roles in head-versus-tail regeneration revealed that *wnt1* acts with *wntP-2,* a gene with an animal-wide posterior-to-anterior expression gradient, to suppress head formation (Petersen and Reddien 2009). Phylogenetic analysis has either placed *wntP-2* (also referred to as *wnt11*-5) as a Wnt11 family member (Gurley, Elliott et al. 2010) or a Wnt4 family member (Riddiford and Olson 2011). *wnt1* inhibition causes posterior head regeneration with incomplete penetrance, from ~30% (Petersen and Reddien 2009) to 75% (Figure 2.15), whereas *wnt1;wntP-2(RNAi)* animals regenerate posterior heads with nearly 100% penetrance (Figure 2.15) (Petersen and Reddien 2009). Because these two Wnts jointly participate in head-versus-tail determination,

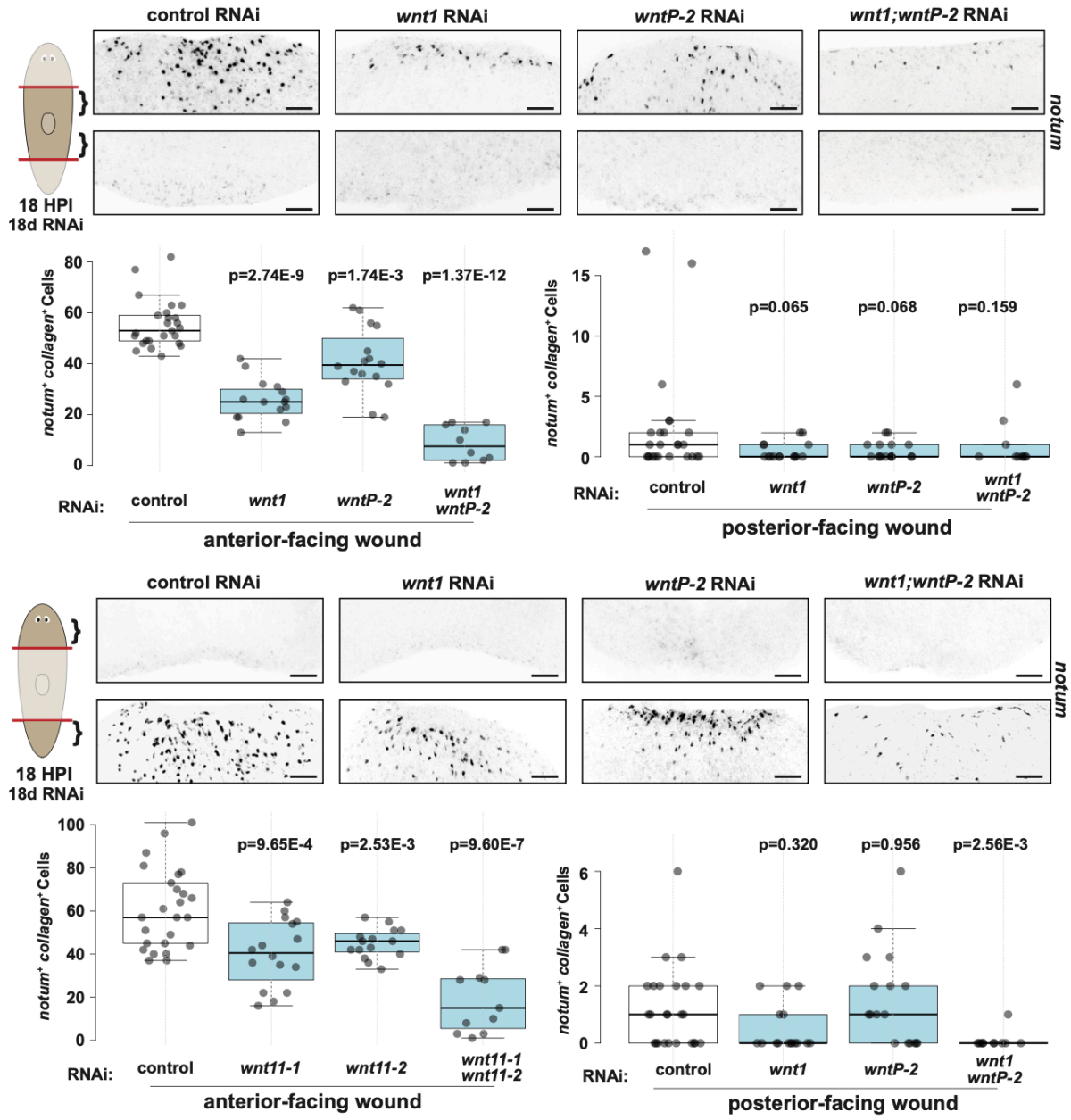

Fig 2.14 *wnt-1* and *wntP-2* Promote *notum* Expression at Anterior-facing Wounds

Single-channel images from double FISH to detect *notum* and *collagen* 18 hours post-injury in trunk (top) or head and tail (bottom) fragments inhibited for *wnt1*, *wntP-2,* or both factors simultaneously. Scale bars, 100 microns. Bottom graphs show quantification of *notum*$^+$ *collagen*$^+$ cells.

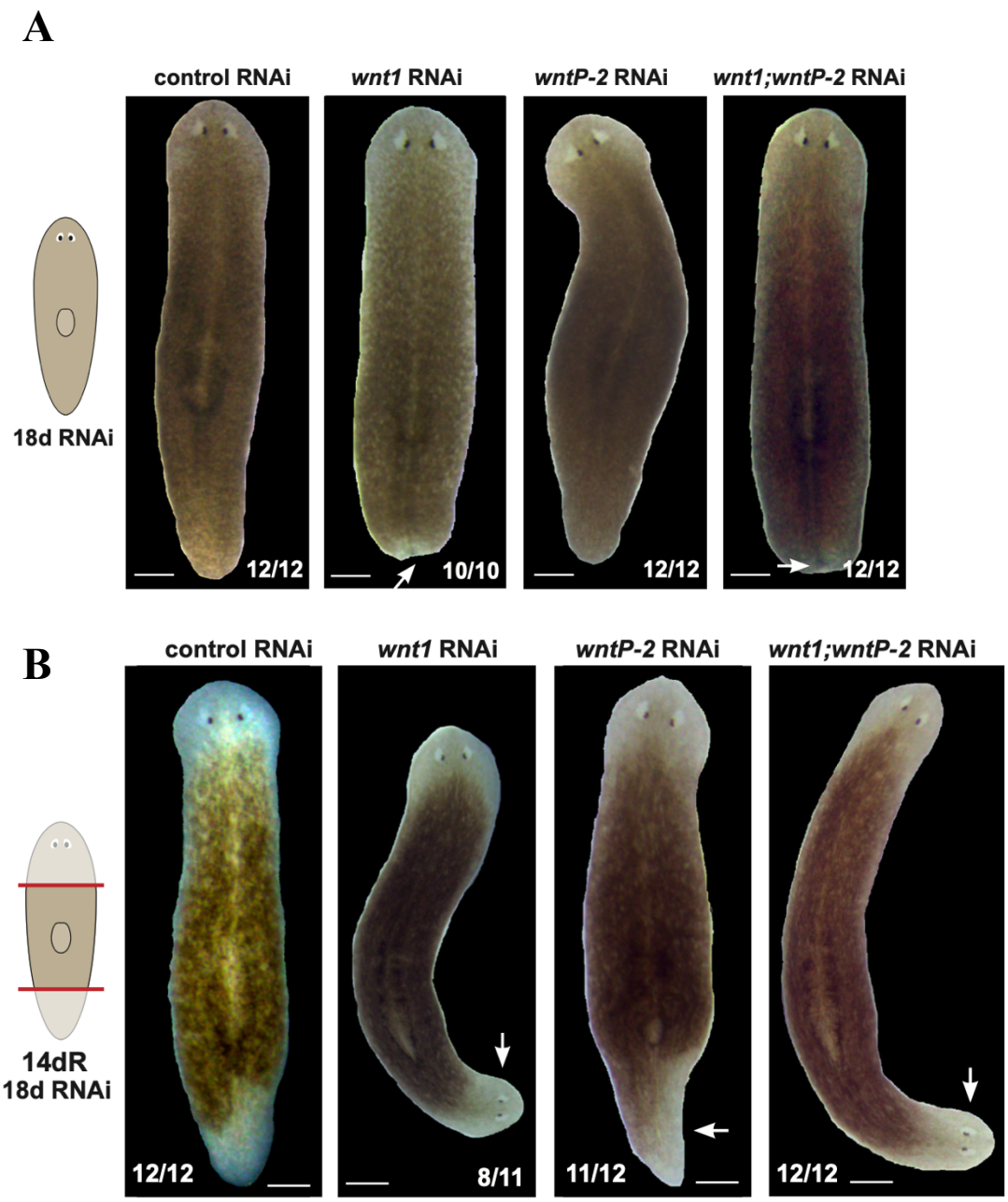

Fig 2.15 *wnt1* and *wntP-2* Promote Posterior Fate

Live images of animals after 18 days of homeostatic inhibition (A) or after 2 weeks of regeneration following 18 days of RNAi (B). *wnt1* RNAi caused a blunted tail morphology in homeostatic inhibition conditions. *wnt1* RNAi caused regeneration of posterior heads, co-inhibition of *wnt1* and *wntP-2* enhanced the penetrance of double-headed regeneration. Scale bars 300uM in all images.

we tested their combined effects on *notum* expression. *wntP-2* inhibition alone modestly decreased *notum* expression, and *wnt1;wntP-2* RNAi nearly eliminated injury-induced *notum* at anterior-facing wounds without affecting posterior-facing wounds (Figure 2.14). In addition, *wnt1;wntP-2* RNAi similarly reduced injury-induced *notum* expression at amputation sites located at different positions along the AP axis, suggesting the function of these genes on *notum* expression is not regional-specific (Figure 2.14). The re-establishment of the *wntP-2* expression gradient during regeneration takes place on a longer timescale than injury-induced *notum* expression (Gurley, Elliott et al. 2010), so it is possible that *wntP-2*'s role in this process either precedes injury or involves post-transcriptional activation. *wntP-2* expression could be detected at regions far into the anterior (Figure 2.16) and is expressed in both circular and longitudinal muscle cells (Scimone, Cote et al. 2017), while *wnt1* expression is activated near wound sites in the same timeframe as injury-induced *notum* (Figure 2.16) where it is co-expressed with *notum* (Petersen and Reddien 2011). These results together suggest a mechanism for *notum* activation by injury involving both wound-induced *wnt1* and homeostatic *wntP-2* acting with *βcatenin-1* following injury.

Inhibition of five other Wnt genes had either no effect on *notum* expression, small effects, or effects that were specific to axis position (Figure 2.17). Inhibition of *wnt5*, *wntP-3,* and *wnt2-1* had no effect on expression of *notum* at anterior-facing wounds or posterior-facing wounds. Inhibition of *wntP-4* caused a statistically significant (p=2.86E-3) but small reduction to *notum* activation at the anterior-facing wound site of regenerating trunk fragments (~15% reduction to median number of *notum*-expressing cells). *wntP-4* RNAi also caused a morphological phenotype of impaired tail blastema formation (Figure 2.17). Inhibition of *wnt11-6* (also termed *wntA*) (Kobayashi, Saito et al. 2007, Adell, Salo et al. 2009, Hill and Petersen 2015) resulted in normal *notum* expression at anterior-facing wounds, and normal lack of expression at posterior-facing

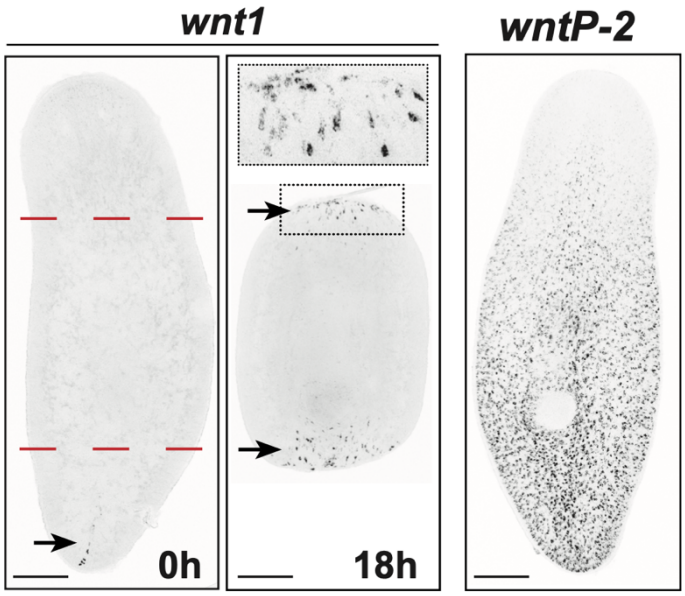

Fig 2.16 *wnt1* and *wntP-2* are Expressed in the Posterior, *wnt1* is also Injury Induced

in situ hybridizations of *wnt1* and *wntP-2* in uninjured animals and animals fixed 18 hours post-injury as indicated. Scale bars, 300 microns. *wnt1* is an injury-induced gene activated with similar kinetics to *notum*, and *wntP-2* is expressed in an animal-wide gradient from the posterior prior to injury.

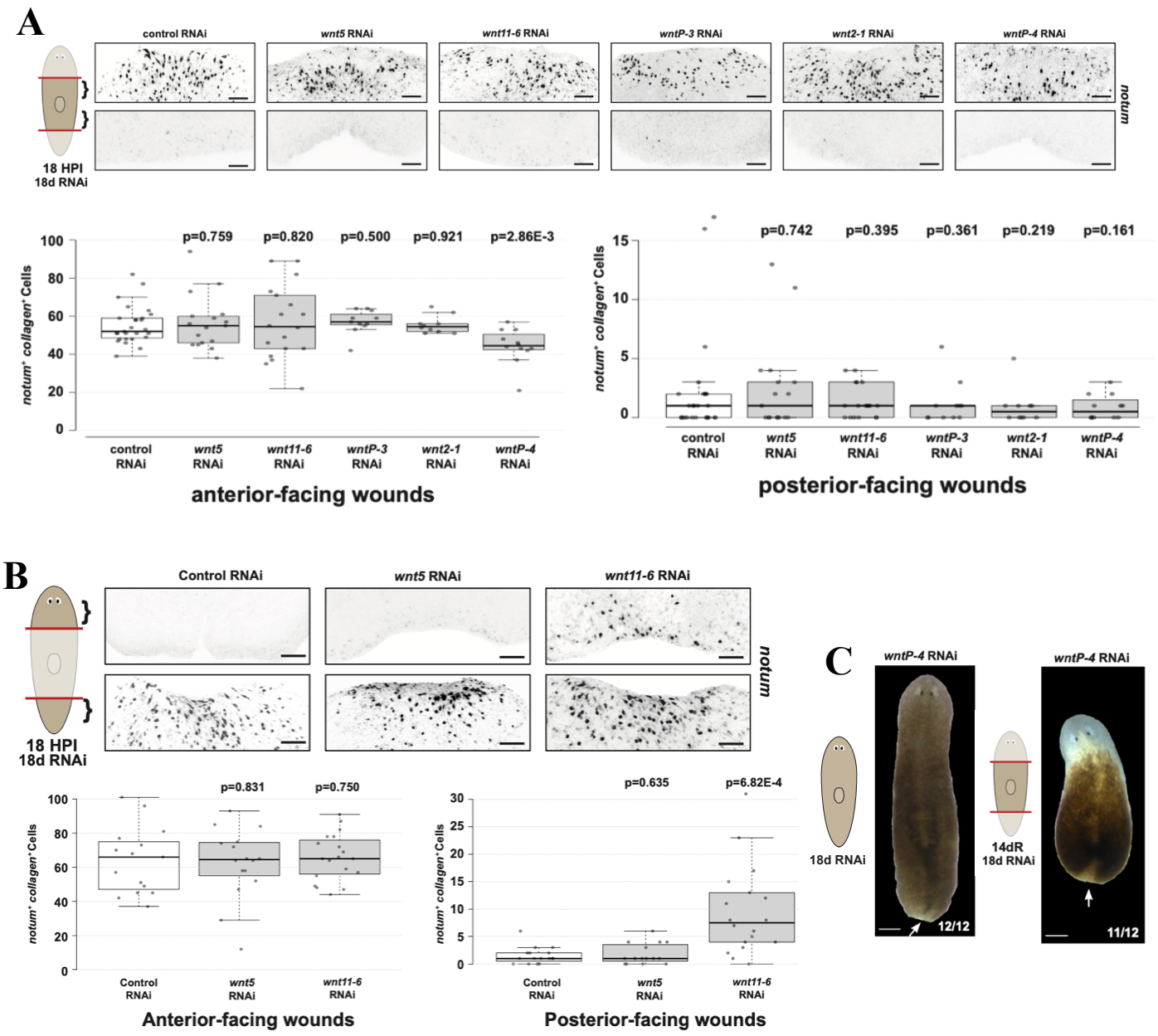

Fig 2.17 Inhibition of Multiple Wnts Produces Minor or Regionalized Effects

A-B) Single-channel images from double FISH to detect *notum* and *collagen* after inhibition of planarian Wnt genes fixed 18 hours post-amputation and after 18 days of RNAi in trunk (A) or head and tail (B) fragments. Bottom graphs show quantification of numbers of *notum*$^+$ *collagen*$^+$ cells. Scale bars 100uM in all images. *wnt5, wntP-3, wnt2-1, and wnt11-6* RNAi did not impact expression of *notum* at posterior- or anterior-facing wounds in regenerating trunk fragments. *wntP-4* RNAi weakly reduced numbers of *notum*-expressing cells from anterior-facing wounds of regenerating trunk fragments. *Wnt11-6* RNAi elevated numbers of *notum*-expressing cells from posterior-facing wounds of regenerating head fragments.
C) homeostatic and regeneration phenotypes of *wntP-4* RNAi.

wounds in regenerating trunk fragments, but caused elevated expression of *notum* at posterior-facing wounds of regenerating head fragments (Figure 2.17). Therefore, *wnt11-6* has a regional-specific suppressive role to limit *notum* expression, but likely cannot account for *notum* polarization at all injury sites. *wnt11-6*/*wntA* factors have been described to play a role in anterior head and eye patterning and not in posterior identity determination, consistent with this factor influencing pattern formation regionally (Kobayashi, Saito et al. 2007, Adell, Salo et al. 2009, Hill and Petersen 2015).

RNAi of two Wnt ligands, *wnt11-1* and *wnt11-2,* resulted in ectopic *notum* expression at posterior-facing wounds, but did not affect *notum* expression at anterior-facing wounds (Figure 2.18). Inhibition of either of these Wnt11s individually produced this phenotype, and co-inhibition produced a stronger phenotype of *notum* overexpression, suggesting *wnt11-1* and *wnt11-2* act together to suppress *notum* at posterior-facing wounds. In experiments conducted after 18 days of RNAi, the *wnt11-1;wnt11-2(RNAi)* phenotype of *notum* overexpression at posterior-facing wounds was statistically significant (p=1.36E-4) but produced relatively few *notum*$^{+}$ cells (~15 cells on average) compared to normal anterior-facing wounds (~60 cells on average) (Figure 2.18), suggesting insufficient length of knockdown for a full strength phenotype. Therefore, we inhibited *wnt11-1* and *wnt11-2* by RNAi for a more extended time (30 days) and found this extended inhibition resulted in a higher number of *notum*$^{+}$ cells at posterior-facing wounds (~40 cells on average), closer in abundance to the *notum*$^{+}$ cells normally present at anterior-facing wound sites. In addition, this longer RNAi treatment still did not modify numbers of *notum*$^{+}$ cells at anterior-facing wound sites (Figure 2.19). We conclude that progressive long-term inhibition of *wnt11-1* and *wnt11-2* may gradually deplete a process important for suppressing the induction of *notum* at posterior-facing wound sites following injury. In *wnt11-1;wnt11-2(RNAi)* animals, the expression

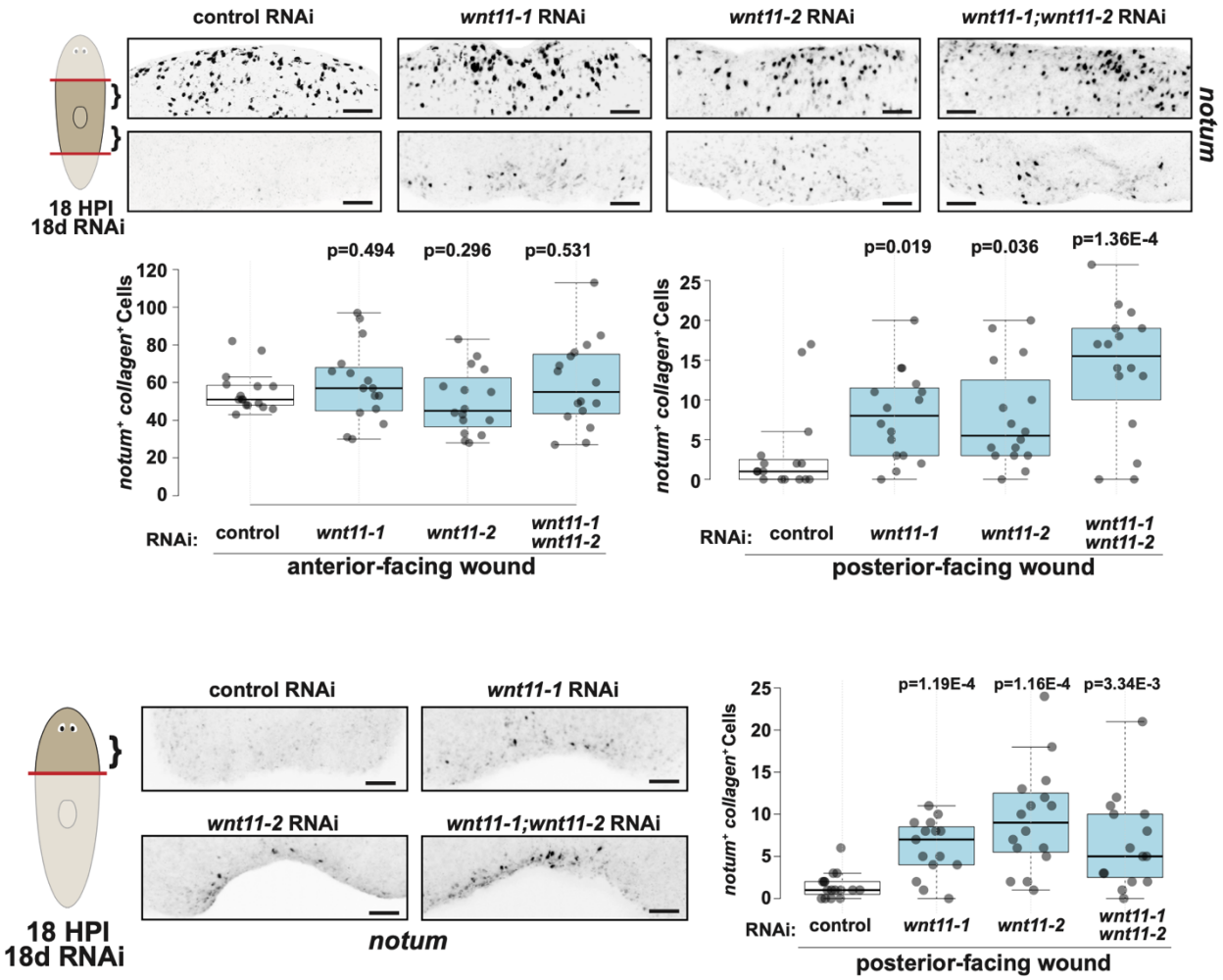

Fig 2.18 *wnt11-1* and *wnt11-2* Restrict *notum* Expression at Posterior-facing Wounds

Single-channel images from double-FISH to detect *notum* and *collagen* 18 hours post-injury in animals treated with *wnt11-1* and/or *wnt11-2* dsRNA for 18 days prior to amputation. Scale bars, 100 microns in all images. Bottom graphs show quantification of *notum*$^+$ *collagen*$^+$ cells. Inhibition of *wnt11-1* and *wnt11-2* led to increased *notum* expression at posterior-facing wounds, including at posterior facing wounds generated distantly from the posterior of the animal.

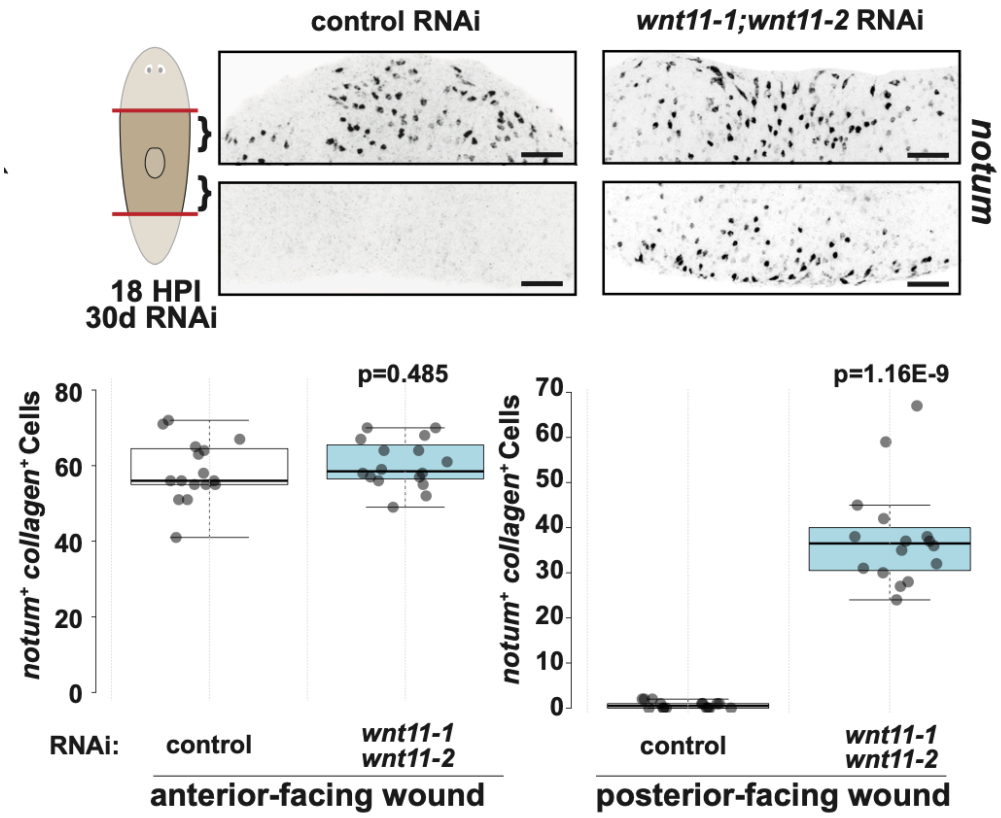

Fig 2.19 Extended RNAi Administration Strengthens *wnt11-1 wnt11-2* Inhibition Phenotype

Single-channel images from double-FISH to detect *notum* and *collagen* 18 hours post-injury in animals treated with *wnt11-1* and/or *wnt11-2* dsRNA for 30 days. Prolonging RNAi increased the strength of the ectopic *notum* phenotype.

of injury-induced *notum* at posterior-facing wounds occurred almost entirely in *myoD*$^+$ longitudinal muscle cells (Figure 2.20). A similar frequency of wound-proximal *notum*$^+$ cells were *collagen*$^+$, indicating Wnt11 signals control polarization of injury responses primarily within longitudinal muscle, rather than preventing expression in other muscle cell types. Wnt11-1 and Wnt11-2 are highly similar at the protein level, consistent with the possibility of redundant functions (Gurley, Elliott et al. 2010). These phenotypes were in contrast to RNAi phenotypes of other Wnt signaling components such as *APC* RNAi, which drove ectopic *notum* expression at posterior wounds along with a general increase in *notum* at anterior-facing wound sites and elsewhere in the body (Petersen and Reddien 2011). Therefore, *wnt11-1* and *wnt11-2* control *notum* expression polarity through selective inhibition of expression at posterior-facing wounds, rather than affecting overall levels of *notum* activation. We also tested whether Wnt11s or Dvls regulate numbers of longitudinal muscle cells to examine whether elevated *notum* expression responses could arise indirectly from higher numbers of *myoD*$^+$ cells. *dvl-1;dvl-2(RNAi)* animals had a reduction in *myoD*$^+$ cells, in line with the observation of overall lower density of muscle fibers in these animals (Figure 2.13), in spite of also resulting in greater numbers of *notum*-expressing cells at posterior-facing wounds (Figure 2.21). Furthermore, *wnt11-1;wnt11-2(RNAi)* animals had normal numbers of *myoD*$^+$ cells, together indicating Wnt11/Dvl signaling likely does not control *notum* polarization responses only by altering muscle density (Figure 2.21).

wnt11-1 and *wnt11-2* are expressed in graded domains from the posterior in animals prior to injury (Figure 2.22) (Gurley, Elliott et al. 2010). In addition, prior studies determined these factors are expressed in body-wall muscle cells (Witchley, Mayer et al. 2013, Scimone, Cote et al. 2017), and single-cell RNAseq from a planarian cell atlas (Fincher, Wurtzel et al. 2018) and double-FISH confirmed *wnt11-1* and *wnt11-2* are expressed in *collagen*$^+$ muscle (Figure 2.22).

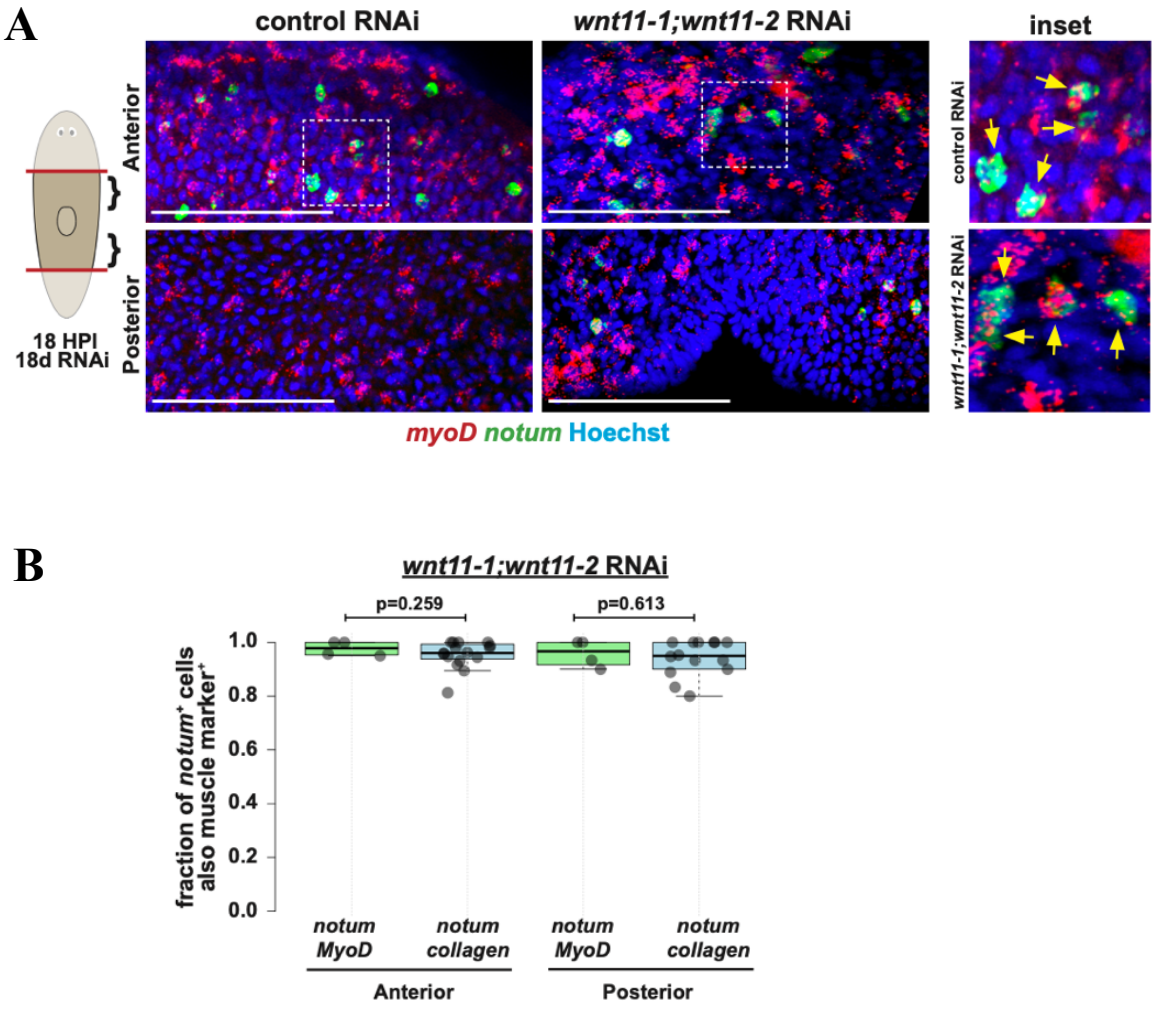

Fig 2.20 Under *wnt11-1 wnt11-2* Double Inhibition, *notum* is Expressed in Longitudinal Muscle

A) co-expression of *notum* in *myoD*$^+$ longitudinal muscle cells at wound sites after *wnt11-1;wnt11-2(RNAi)*.
B) quantifications of fractions of *notum*$^+$ cells detected as *collagen*$^+$ or *myoD*$^+$ by double-FISH. P-values were calculated by two-tailed unpaired t-tests between each condition at either wound site. Scale bars 50 microns.

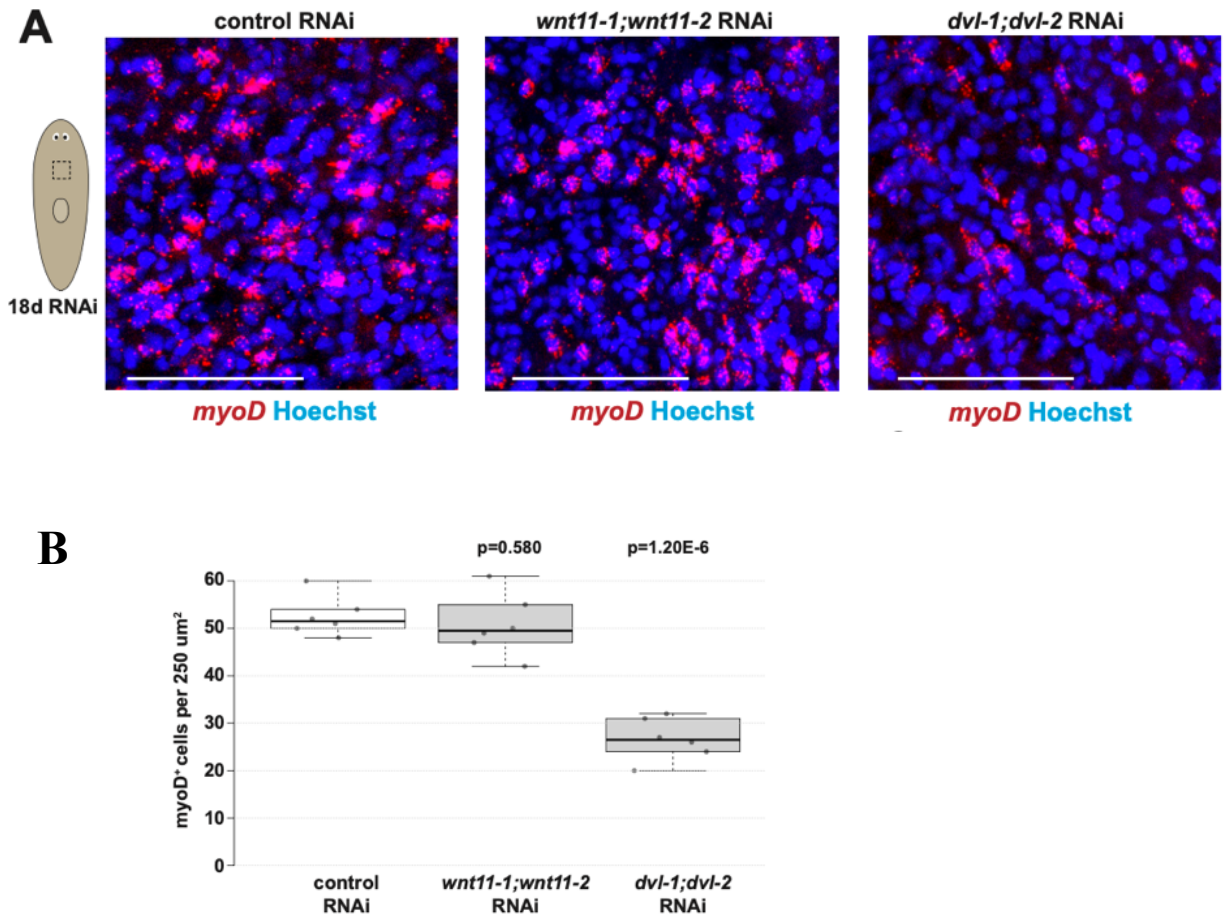

Fig 2.21 Inhibition of the Dvls, but not the Wnt11s, Decreases Longitudinal Muscle Density

A) FISH to detect *myoD* expression after *wnt11-1;wnt11-2* RNAi and *dvl-1;dvl-2* RNAi.
B) box plot shows median values (middle bars) and first to third interquartile ranges (boxes); whiskers indicate 1.5× the interquartile ranges and dots are data points obtained by measurement of prepharyngeal field of view from individual animal specimens. p-values were calculated using two-tailed unpaired t-tests comparing each condition to the control condition. *Dvl-1/dvl-2* RNAi reduced numbers of *myoD*$^+$ cells. Scale bars 50 microns.

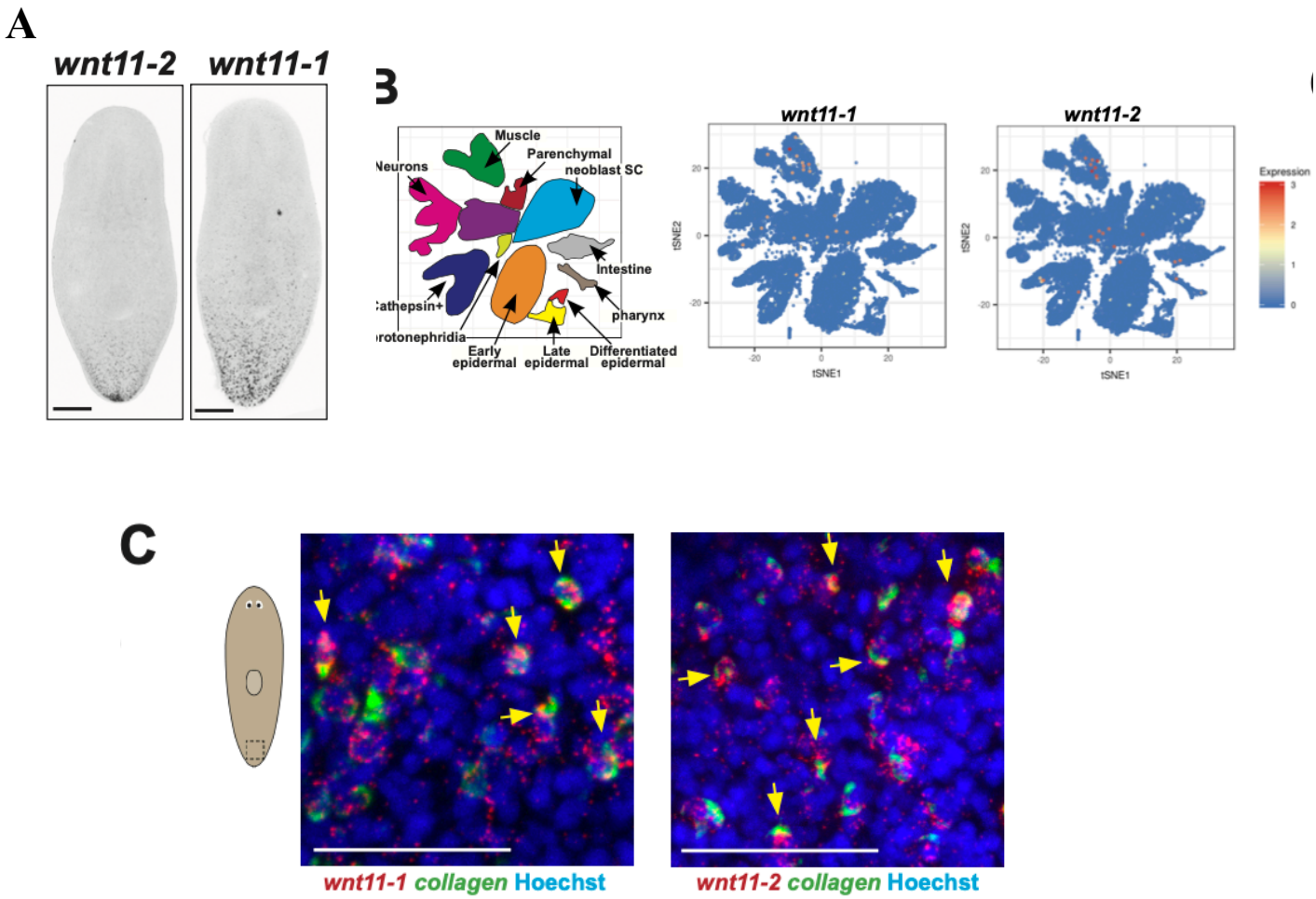

Fig 2.22 *wnt11-1* and *wnt11-2* are Expressed in the Posterior in Muscle Cells

A) *in situ* hybridizations of *wnt11-1* and *wnt11-2* in uninjured animals. Scale bars, 300 microns. Both genes are expressed in the posterior.
B) single-cell RNAseq plots from a planarian cell atlas (digiworm.wi.mit.edu) show expression of *wnt11-1* and *wnt11-2* in muscle (left, cartoon annotates clusters and muscle cluster drawn in green).
C) double-FISH showing colocalization of *wnt11-1* and *wnt11-2* in *collagen*$^{+}$ muscle. Scale bars 50uM.

wnt11-1 is expressed specifically in *nkx1.1*$^{+}$ circular muscle cells and in an *nkx1.1*-dependent manner, while *wnt11-2* expression was depleted only by co-inhibition of both longitudinal muscle determinant *myoD* along with *nkx1.1* (Scimone, Cote et al. 2017). Despite their prominent expression in the posterior and non-detection by in situ hybridization at further anterior locations, inhibition of these Wnts caused *notum* expression at posterior-facing wound sites from throughout the AP axis, including the posterior wounds of head fragments (Figure 2.18). These results suggest Wnt11s exert their influence across the body and could act as polarizing cues for negative regulation of *notum* after injury.

Inhibition of two Wnt11 factors can induce posterior head regeneration

We examined the consequences to regeneration after dual inhibition of the two Wnt11s, at first using a dosing schedule in which dsRNAs were delivered for 18 days prior to amputation (Figure 2.23). Under these conditions, *wnt11-2* inhibition lead to tail regeneration failure and a posterior bulged morphology reminiscent of *dvl-1;dvl-2(RNAi)* phenotypes, and *wnt11-1* inhibition permitted tail regeneration to occur but caused a narrowing of tail morphology, similar to reported results (Adell, Salo et al. 2009, Sureda-Gomez, Pascual-Carreras et al. 2015). Dual inhibition of *wnt11-1* and *wnt11-2* for 18 days of RNAi resulted in tail retraction and bulged posterior phenotypes prior to amputation, followed by failed tail regeneration after amputation, while head regeneration occurred normally in these animals (Figure 2.23). Animals with failed posterior regeneration did not express anterior markers *sFRP-1, foxD,* or *notum* in the posterior and maintained posterior *wntP-2* expression (Figure 2.24). In these animals, the muscle architecture appeared normal in the anterior but had altered organization in the posterior (Figure 2.25). However, we note that the muscle system was much more disorganized in *dvl-1;dvl-2* RNAi

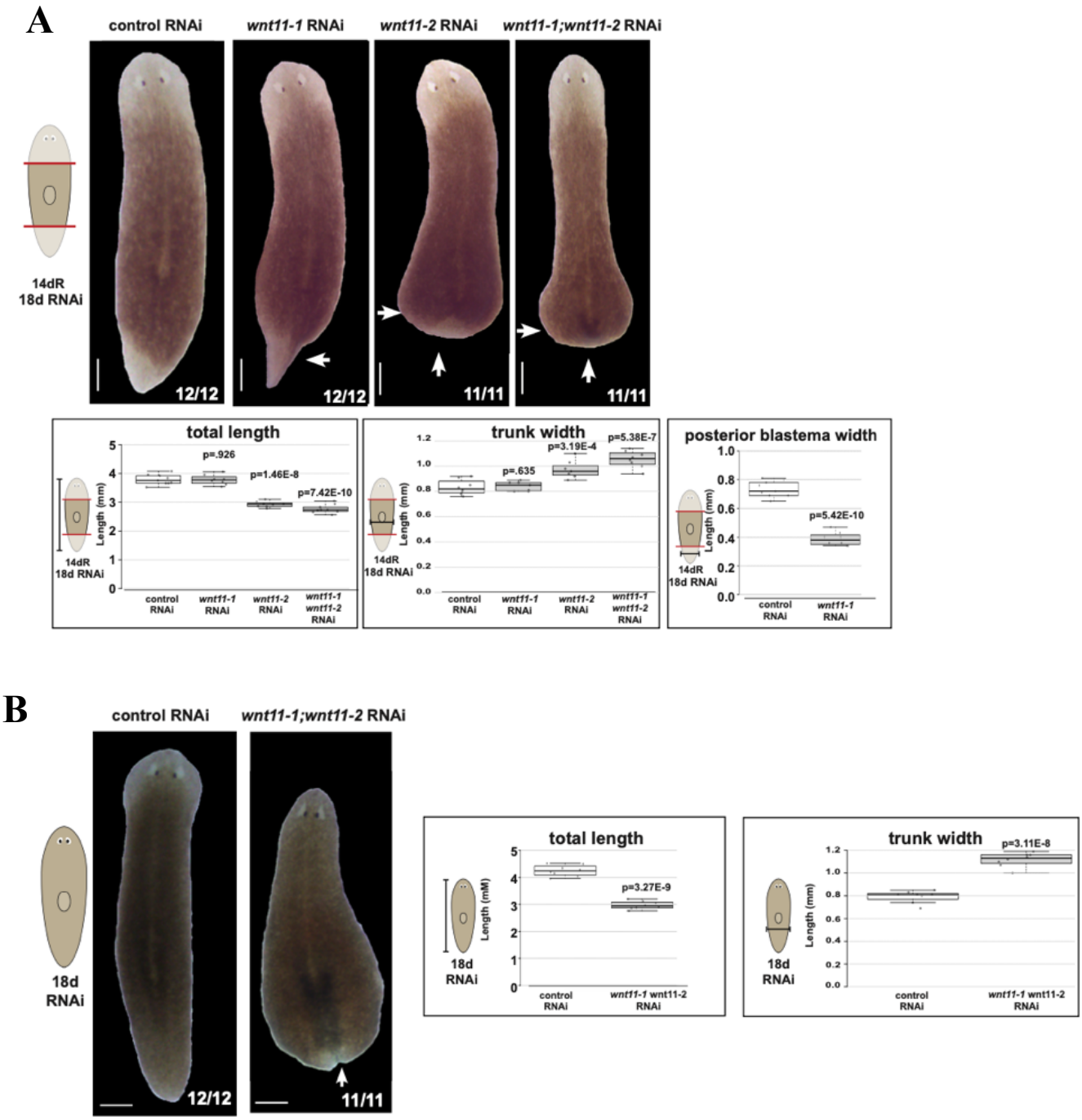

Fig 2.23 *wnt11-1* and *wnt11-2* Promote Posterior Identity and Regeneration

Morphological defects in uninjured worms (A) or at 14 days of regeneration (B) after inhibition of Wnt11 factors. *wnt11-1* RNAi caused a pointed posterior blastema, and *wnt11-2* RNAi or *wnt11-1;wnt11-2* double RNAi caused failure of tail regeneration and also lateral bulging near the injury site. Quantifications of length and width for each condition shown below. Scale bars 300uM.

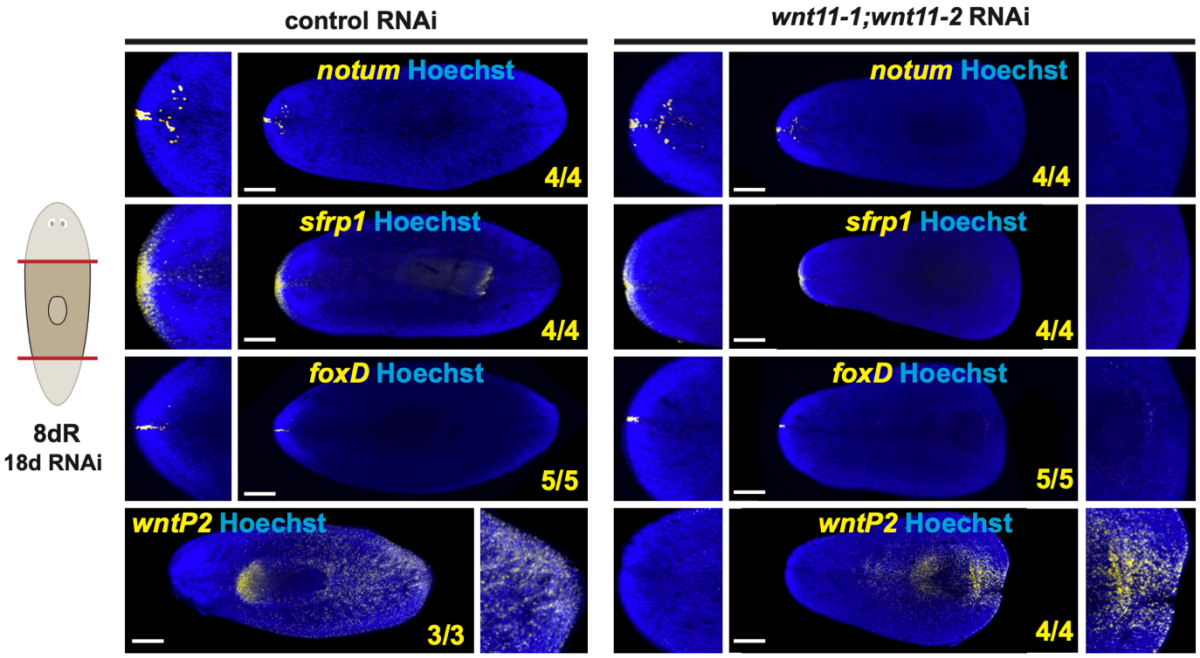

Fig 2.24 Inhibition of *wnt11-1* and *wnt11-2* over 18 Days Does Not Affect Pole Identity

in situ hybridizations from control versus *wnt11-1;wnt11-2(RNAi)* animals fixed at eight days of regeneration using probes to detect anterior (*notum, sfrp1, foxD)* or posterior (*wntP-2*) identity and counterstained with Hoechst. Scorings indicate number of animals with expression as shown, and the left/right insets show a 200% zoom of the anterior and/or posterior of the main panel. Scale bars 300uM.

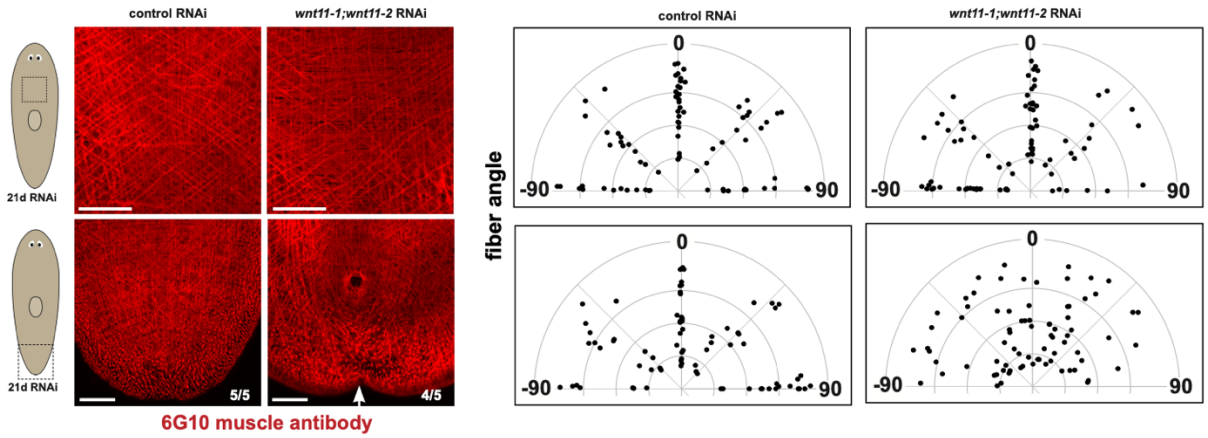

Fig 2.25 Inhibition of the Wnt11s Disrupts Muscle Morphology in the Posterior but not the Anterior

Muscle fiber organization in control versus *wnt11-1;wnt11-2(RNAi)* animals determined by immunostaining with 6G10 antibody. Images taken as indicated prepharyngeally or at the tail tip in uninjured animals, with numbers of animals scored in each condition indicated. Muscle fiber morphology broadly correlates with the overall blunted and bulged posterior defect observed in *wnt11-1;wnt11-2(RNAi)* animals, while prepharyngeal locations have apparently normal fiber network organization. Right, quantifications of muscle fiber orientation as in Figure 2.13. Dots show angle orientations with respect to the AP axis of individually measured muscle fibers from 3-4 20x20micron fields of view from 2-3 animals per condition, with radial position jittered randomly. Scale bars 100uM.

(Figure 2.13) than in *wnt11-1;wnt11-2* RNAi. Given that *notum* mis-polarization can occur to some extent in the anterior regions of *wnt11-1;wnt11-2(RNAi)* animals with apparently normal muscle fiber organization, we suggest Wnt11 genes might affect aspects of muscle polarity not evident only from the overall fiber network morphology. Because we found that prolonged *wnt11-1;wnt11-2* RNAi dosing resulted in a more pronounced expression of *notum* at posterior-facing wound sites, we tested these animals for regeneration defects after 30 days of RNAi (Figure 2.26). Under these conditions, *wnt11-1;wnt11-2(RNAi)* animals regenerated posterior heads (17%, 3/17 animals) which stained positive for expression of the anterior tip marker *sFRP-1*, or instead failed to form a posterior blastema (83%, 14/17 animals) and had a bulged posterior morphology. Therefore, long-term inhibition of Wnt11 increases the severity of the *notum* mis-polarization phenotype and causes inversion of posterior blastema identity. Because *βcatenin-1* inhibition causes head/tail transformations while instead eliminating *notum* expression, we suggest *wnt11-1* and *wnt11-2* likely control blastema and *notum* polarity through a βcatenin-independent noncanonical Wnt pathway mediated by Dishevelled.

Wnt11/Dishevelled act prior to injury and through growth to control injury-induced *notum*

We reasoned that Dvl/Wnt11 factors could either act after injury in polarity-determining signaling induced by wounding within muscle cells, or alternatively might set up axis polarization prior to injury in a manner read out by injury-induced *notum*, for example through establishing tissue polarization during ongoing homeostasis prior to injury. dsRNA dosing experiments revealed that the *dvl-1;dvl-2(RNAi)* phenotype of *notum* mis-polarization strengthened between administering dsRNA doses for 9 and 18 days prior to injury suggestive of progressive emergence

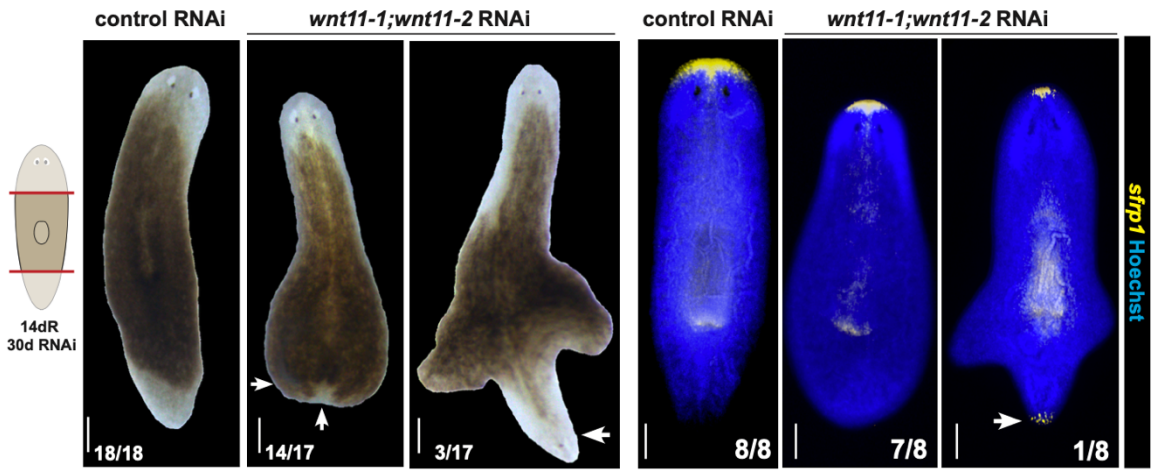

Fig 2.26 Extended Inhibition of the Wnt11s Leads to Posterior Head Regeneration

Left, *wnt11-1;wnt11-2(RNAi)* animals formed posterior-facing heads (3/17 animals, arrow) and failed posterior regeneration (14/17, arrow) after 30 days of RNAi followed by 14 days of response after amputation. Right, FISH detecting anterior marker *sfrp-1* marking posterior head of a *wnt11-1;wnt11-2(RNAi)* animal (arrow). Scale bars 300 microns in all images.

of the phenotype (Figure 2.27). Similar results showing strengthening of the *notum* misexpression phenotype over progressively longer periods of gene inhibition were observed after *wnt11-1;wnt11-2* RNAi (Figures 2.18-2.19). These results are suggestive of a model in which both Dvl and Wnt11 homologs act over a longer term to establish *notum* polarity, but they could instead be due to a slow turnover of the Dvl and Wnt11 proteins.

To further delineate these two models, we reasoned that if Wnt11/Dvl signaling were triggered by injury to suppress *notum* expression at posterior-facing wounds, this would likely occur through the regulation of muscle cells already present at the time of injury rather than any new muscle produced during the first 6-18hours after surgery. Indeed, normally polarized activation of injury-induced *notum* does not depend on stem-cell mediated tissue production, shown previously through experiments that depleted neoblasts by irradiation followed by examination of *notum* injury responsiveness (Vasquez-Doorman and Petersen 2014). Instead, the decision to activate *notum* at wound sites takes place in longitudinal muscle already present at the time of injury. We therefore sought to determine whether the Dvl and Wnt11 RNAi phenotypes of *notum* mispolarization were similarly independent of neoblast-dependent tissue production or instead required this process. We first tested the effects of Dishevelled inhibition in animals subjected to a sublethal dose of irradiation (1350 rads), a treatment known to decrease neoblast abundance and temporarily halt production of new muscle cells (Cloutier, McMann et al. 2021). We initiated this irradiation treatment on day two of an 18-day dsRNA dosing period, followed by amputation and fixation at 18 hours post-injury (Figure 2.28, Irradiation “early”). As expected from prior studies (Vasquez-Doorman and Petersen 2014), irradiation caused a moderate reduction to *notum* expression at anterior-facing wounds control animals without altering the lack of expression at posterior-facing wounds, confirming that normal injury-induced *notum* polarization

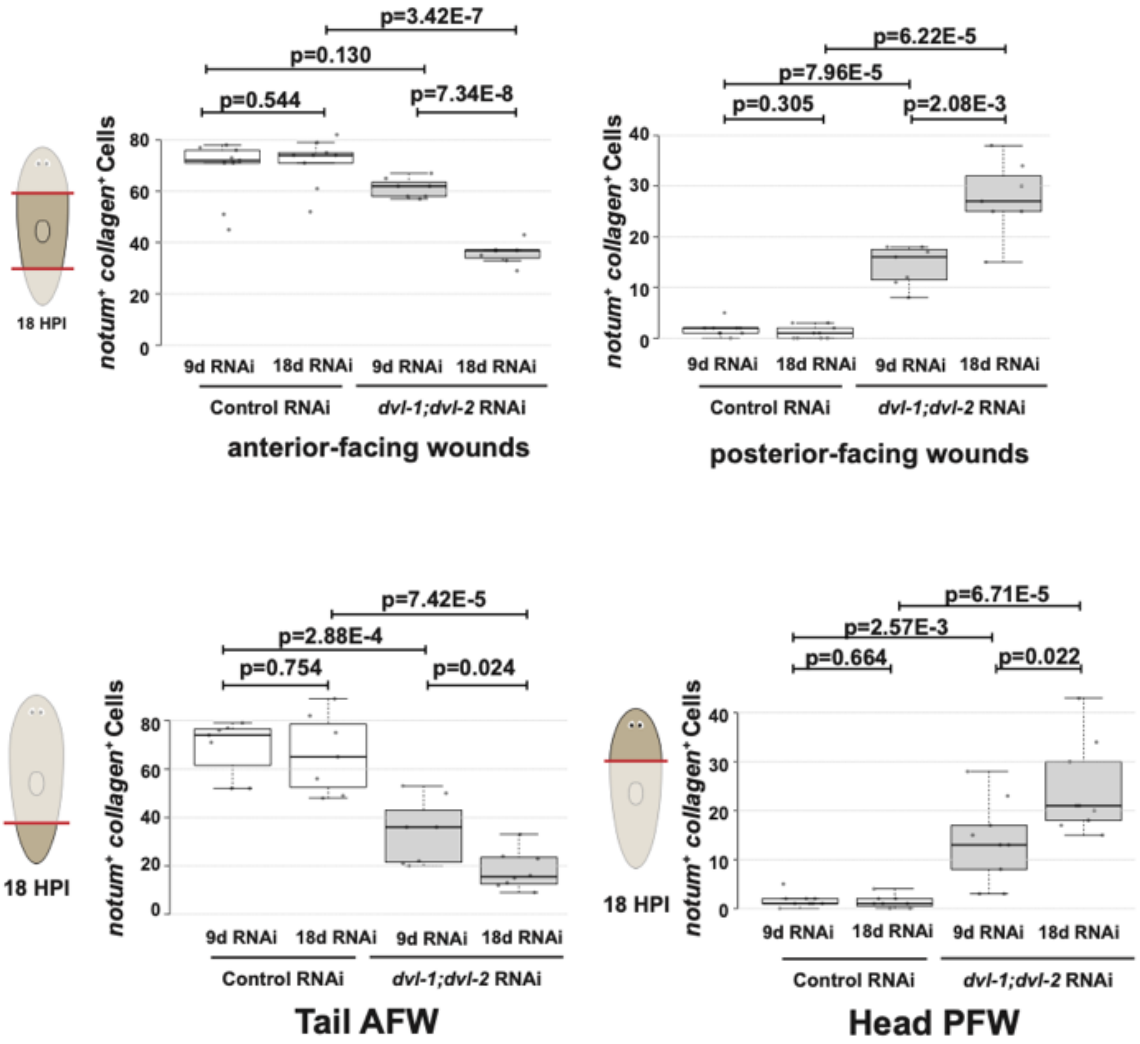

Fig 2.27 Dvl Inhibition Phenotypes Strengthen with Longer RNAi Administration

Examination of the effect of dsRNA feeding schedule on the *notum* expression phenotype. Animals were treated with dsRNA for 9 days (3 doses) or 18 days (6 doses) of dsRNA then amputated and fixed at 18 hours post-injury and stained by double FISH for *notum* and *collagen* expression. Numbers of *notum*$^+$ *collagen*$^+$ cells were counted at each injury site as shown in the graphs. Elevated numbers of *notum*-expressing cells could be observed at head PFW and trunk PFW by three dsRNA feedings and this number was greater after six dsRNA feedings.

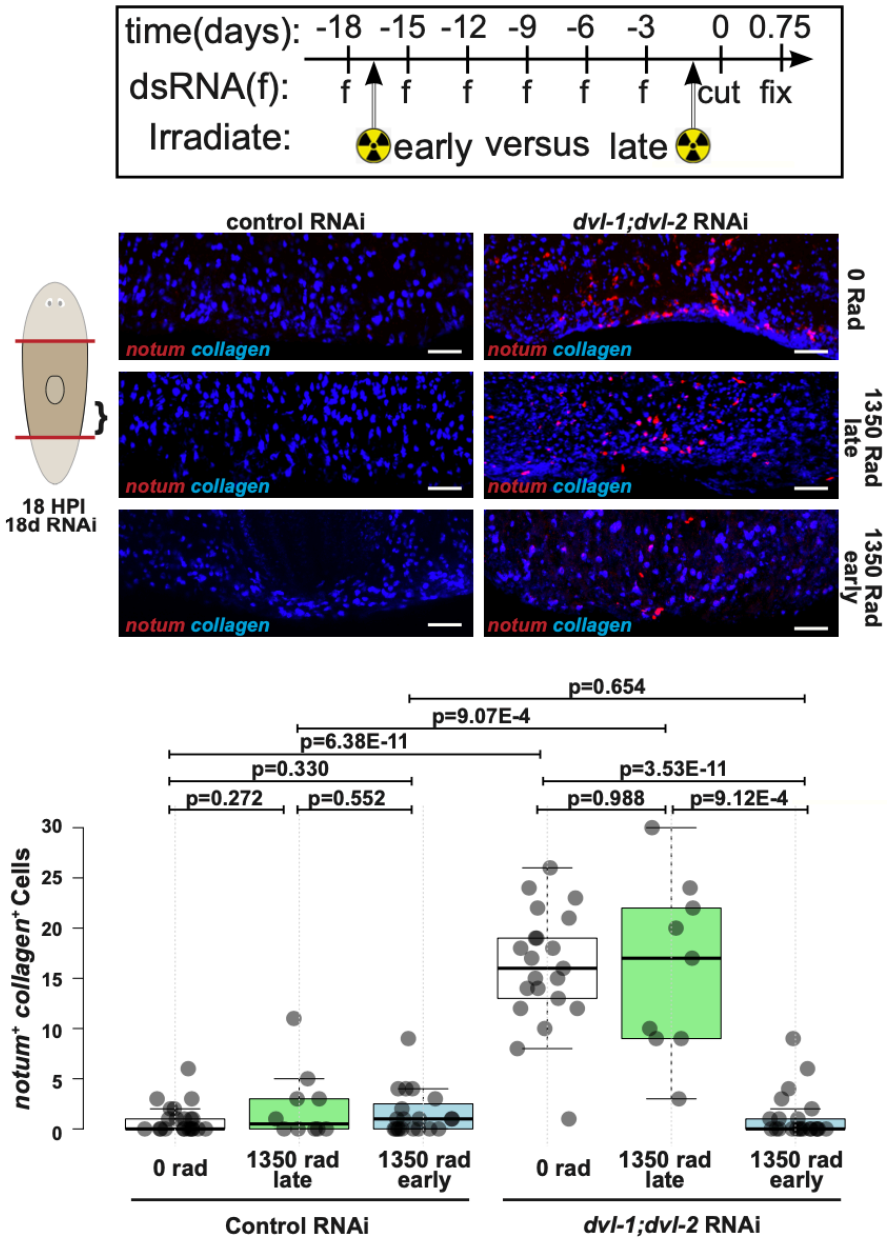

Fig 2.28 Sublethal Irradiation During a Critical Window Inhibits *dvl-1;dvl-2(RNAi)* phenotype of *notum* Expression at Posterior-facing Wounds

Examining the effects of the timing of sublethal irradiation on expression of *notum* after control or *dvl-1;dvl-2(RNAi)*. Cartoons depict two experimental strategies in which the timing of 1350 Rads sublethal X-ray irradiation (radiation sign) was varied to occur either at the beginning ("early") or after the end ("late") of an 18-day period of six feedings (f) of dsRNA, prior to amputation (cut), fixation (fix) at 18 hours post-injury, and double FISH for *notum* and *collagen* expression. Quantification of *notum*$^+$ *collagen*$^+$ cells from each treatment is shown for the posterior-facing wounds from amputated trunk fragments.

can take place under conditions of reduced cell turnover (Figure 2.29). Correspondingly, the irradiation treatment in control RNAi animals decreased the density of muscle fibers without apparently altering their orientations (Figure 2.30). Irradiation of *dvl-1;dvl-2(RNAi)* animals completely suppressed the phenotype of excess *notum*$^{+}$ cells at posterior-facing wound sites (p=3.53E-11), reducing levels of *notum* to those in matched irradiated control animals (p=0.654) (Figure 2.27, irradiated "early"). By contrast, the phenotype of ectopic *notum* expression occurred (p=9.07E-4) in Dvl RNAi animals administered with the equivalent dose of radiation the day prior to injury (Figure 2.28, irradiated "late") and led to a similar abundance of ectopic *notum*$^{+}$ cells as in unirradiated Dvl RNAi animals (p=0.988) (Figure 2.28). Therefore, the Dvl RNAi phenotype mis-polarizing *notum* expression is irradiation sensitive, and this sensitivity occurs during a timeframe between 1 and 17 days prior to injury. Similarly, the *wnt11-1;wnt11-2(RNAi)* phenotype was also eliminated by irradiation treatments initiated during an 18 day period of RNAi administration (Figure 2.31). The irradiation sensitivity of the *notum* repolarization effect was also observed in either *dvl-1;dvl-2(RNAi)* and *wnt11-1;wnt11-2(RNAi)* animals from posterior-facing injury sites located in the anterior of the animal, so this effect was not specific to a particular animal region (Figures 2.32). In addition, irradiation also prevented the onset of morphological phenotypes of posterior reduction and widening from *wnt11-1;wnt11-2* RNAi, as well as lateral ruffling phenotypes from *dvl-1;dvl-2* RNAi (Figure 2.33), indicating these phenotypes correlate with the phenotype of mispolarized *notum* expression.

One possible interpretation of these results is that Dvl or Wnt11 RNAi causes newly differentiating muscle to form in a mispolarized manner, leading to the subsequent mispolarization of injury-induced *notum.* Alternatively, it is possible that irradiation affects the Dvl or Wnt11 RNAi phenotype progression in some other way. We note that the normal process which both

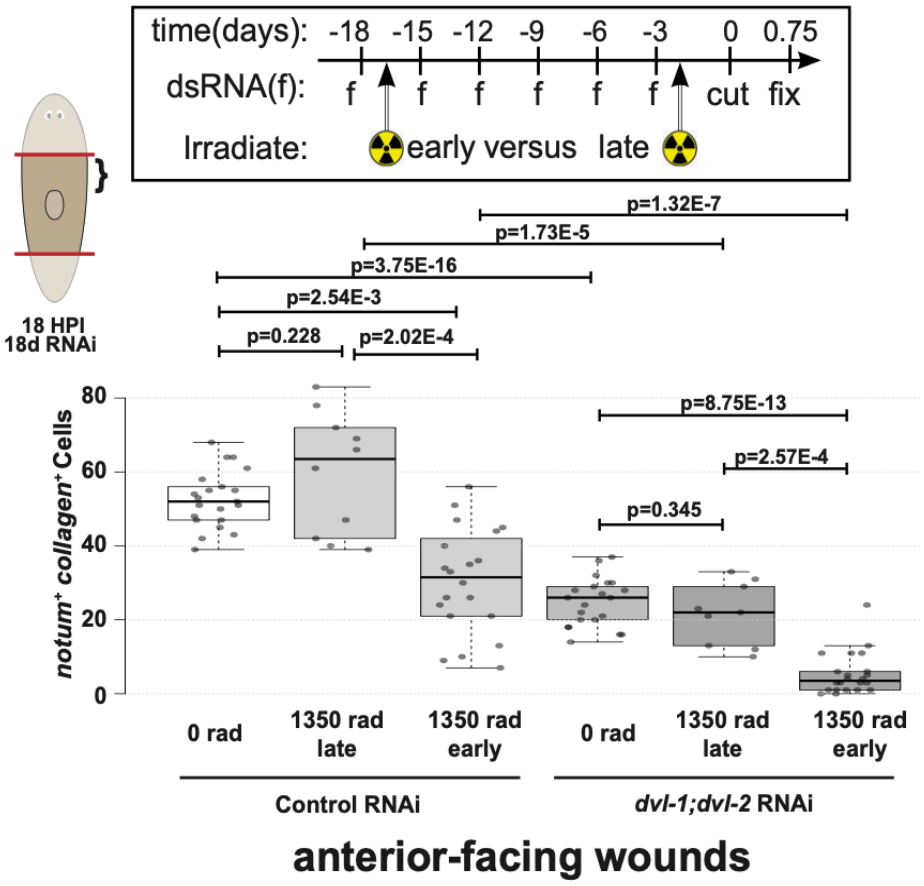

Fig 2.29 Sublethal Irradiation Reduces *notum* Expression at Anterior-Facing Wounds

Examining the effects of the timing of sublethal irradiation on expression of *notum* at anterior-facing wounds after control or *dvl-1;dvl-2(RNAi)*. Cartoons depict two experimental strategies in which the timing of 1350 Rads sublethal X-ray irradiation (radiation sign) was varied to occur either at the beginning ("early") or after the end ("late") of an 18-day period of six feedings (f) of dsRNA, prior to amputation (cut), fixation (fix) at 18 hours post-injury, and double FISH for *notum* and *collagen* expression. Quantification of *notum*$^+$ *collagen*$^+$ cells from each treatment is shown for the posterior-facing wounds from amputated trunk fragments.

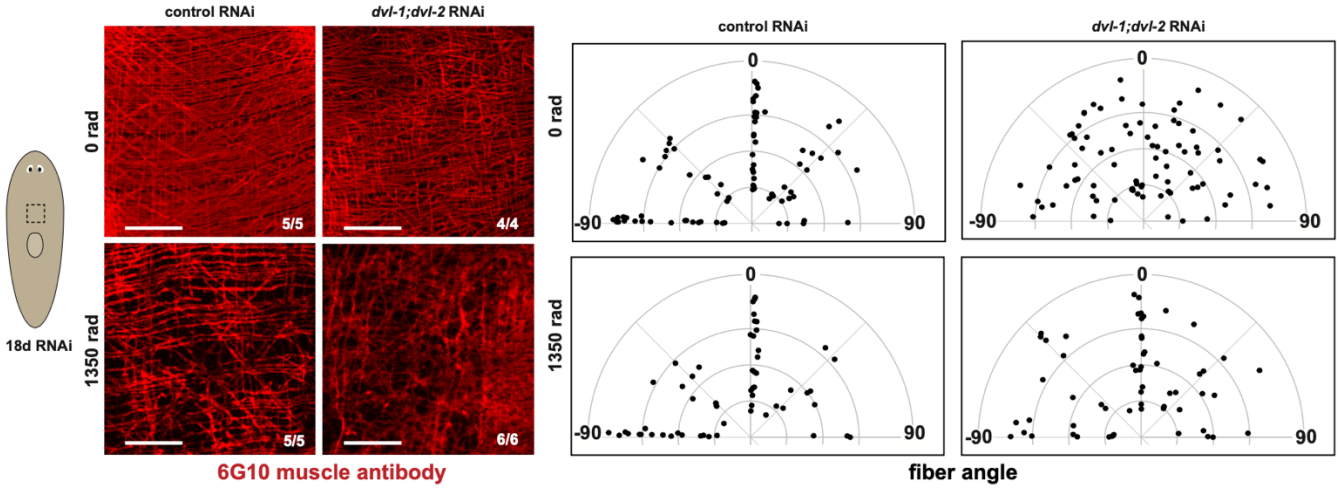

Fig 2.30 Irradiation Partially Rescues Dvl Inhibition Phenotype of Muscle Disorganization

Animals were treated with RNAi and 0 or 1350 rads as in Figure 5, then stained with 6G10 antibody. Numbers of animals scored in each condition are indicated. The density of the fiber network was reduced by irradiation in control(RNAi) animals compared to 0 rad controls. *dvl-1;dvl-2* RNAi led to disorganization in unirradiated animals, and irradiation led to a reduced density network also disorganized. Right, quantifications of muscle fiber angle as in Figure 2.13. Dots show angle orientations with respect to the AP axis of individually measured muscle fibers from 3-4 20x20micron fields of view from 2-3 animals per condition, with radial position jittered randomly in order to display datapoints with similar angles. Scale bars 100uM in all images.

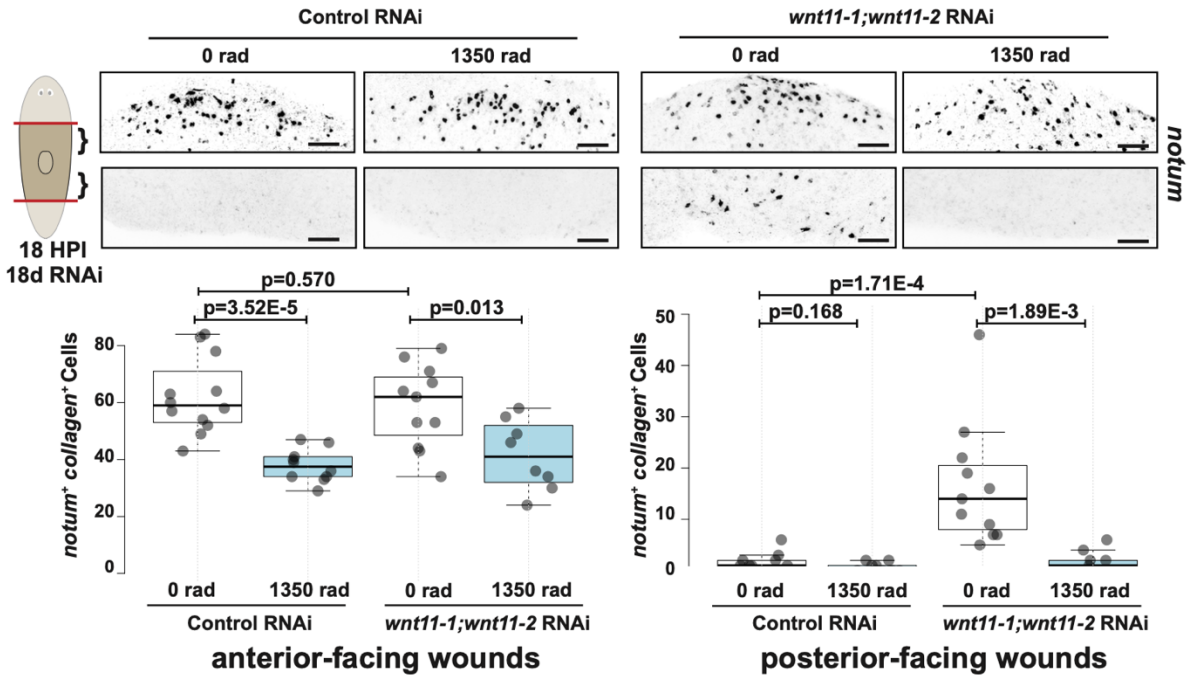

Fig 2.31 Sublethal Irradiation Inhibits *wnt11-1;wnt11-2(RNAi)* phenotype of *notum* Expression at Posterior-facing Wounds

Irradiation experiments carried out as in the "early" dose treatment testing irradiation sensitivity of *wnt11-1;wnt11-2* phenotypes on *notum* expression. Scale bars 100 um.

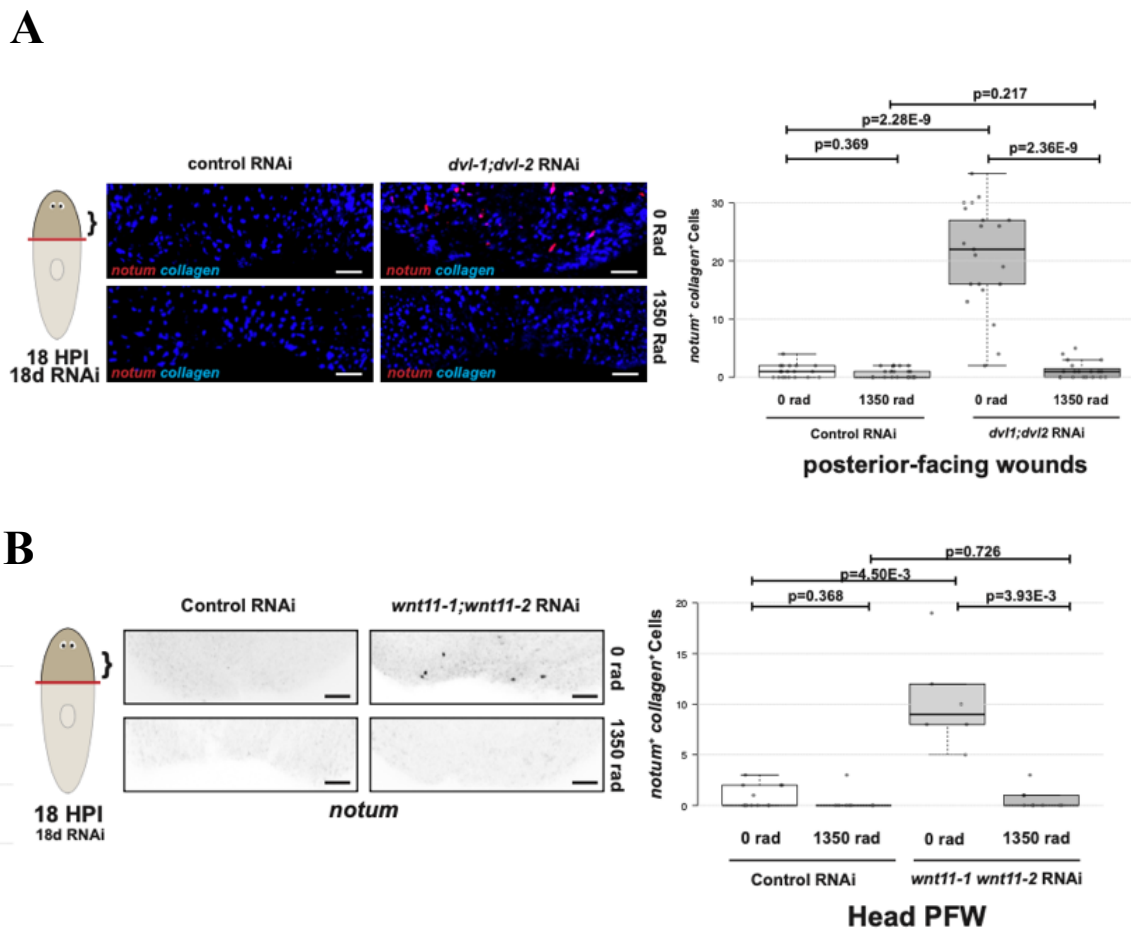

Fig 2.32 Irradiation Affects RNAi Phenotypes at Posterior Wounds of Head Fragments As it Does Trunk Fragments

Analysis of *notum*$^{+}$*collagen*$^{+}$ cell numbers at posterior-facing wounds of head fragments treated and fixed as in the "early" irradiation treatment described previously after *dvl-1;dvl-2* inhibition (A) or after *wnt11-1;wnt11-2* inhibition (B). Scale bars 100 microns in all images.

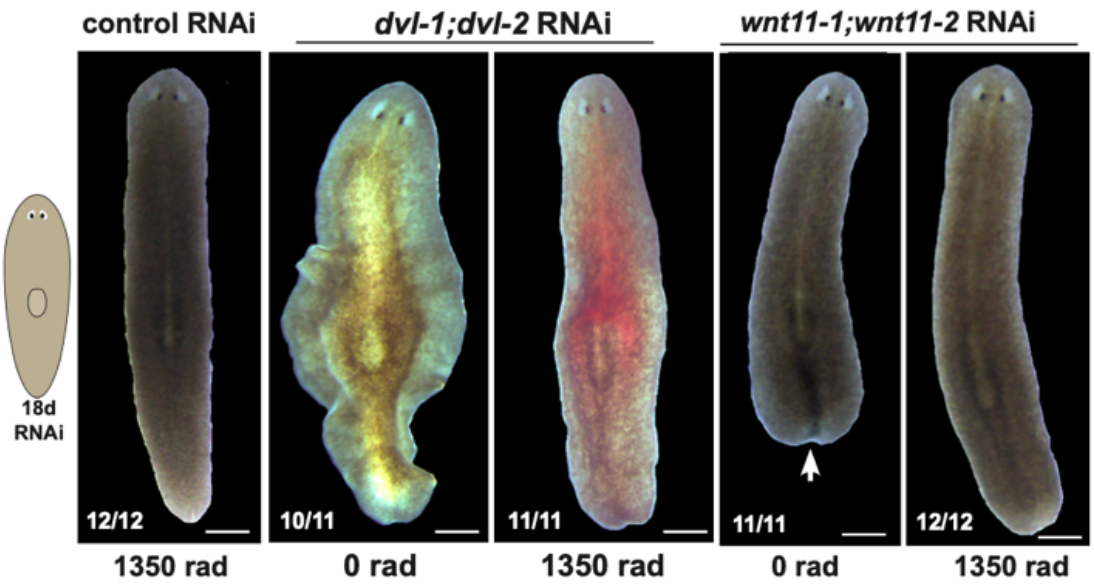

Fig 2.33 Irradiation Suppresses Morphological Changes Driven by Dvl or Wnt11 Inhibition

Morphological phenotypes after homeostatic inhibition of Dvl or Wnt11 factors as indicated, with or without 1350 rads sublethal irradiation 17 days prior. Irradiation suppressed the posterior blunting phenotype (arrow) from *wnt11-1;wnt11-2* inhibition. Scale bars 300 microns.

dvl-1;dvl-2(RNAi) animals appear with unusual coloration due to abnormal lighting (both) and being recently fed before imaging (right). Coloration does not reflect an RNAi phenotype.

activates *notum* and ensures its normal polarity at anterior-facing wound sites was not eliminated following this treatment (Figure 2.31), so irradiation does not intrinsically block all injury-induced *notum* expression from longitudinal muscle present at the time of wounding. In addition, irradiation itself did not affect the mRNA expression of Dishevelled homologs or *wnt11-1* and *wnt11-2*, consistent with a model in which Wnt11 and *notum* expression occur within muscle cells extant before and after wounding (Figure 2.34). We cannot rule out the possibility that depletion of Dvl and Wnt11 proteins is dependent on stem cell dependent tissue replacement. However, RNAi experiments have been conducted in sublethally irradiated planarians previously and have successfully uncovered genes controlling the self-renewal and differentiation of remaining neoblasts (Wagner, Ho et al. 2012, Lei, Thi-Kim Vu et al. 2016, Chan, Ma et al. 2021), indicating that RNAi can result in reduction to gene function in irradiated planarians, but Dvl and Wnt11 proteins may be exceptions. However, this interpretation also implies that the Dvl and Wnt11 protein cohorts engaged in polarizing *notum* activation would likely have been produced prior to injury.

Together, these experiments argue against, but do not fully rule out, a possible model in which injury elicits Wnt11/Dvl signals in muscle that directly control *notum* polarization. Instead, we suggest that Wnt11 expression from the posterior indirectly establishes axis polarization prior to injury, resulting in asymmetric expression of *notum* after injury. We further examined Wnt11's possible order of action in regeneration through analysis of Wnt and *notum* expression dynamics after injury. Posterior Wnt genes are known to re-establish their expression domains during posterior regeneration (Petersen and Reddien 2008, Gurley, Elliott et al. 2010). We measured the timing of *wnt11-1* and *wnt11-2* re-expression following amputation compared to *notum* activation using in situ hybridizations in a matched cohort of regenerating animals. In animals amputated

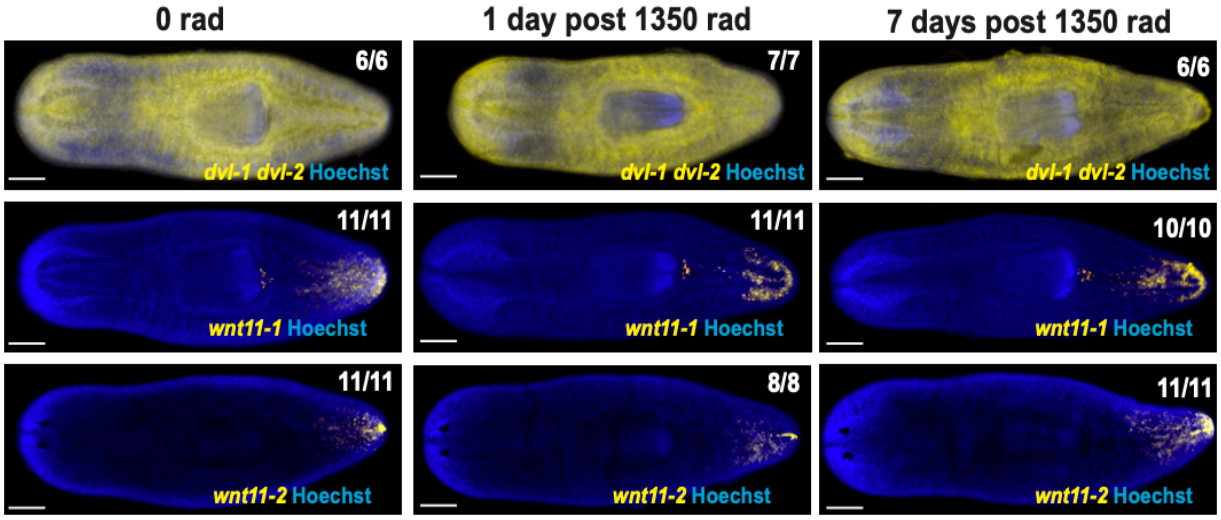

Fig 2.34 Irradiation Does not Alter Expression of Dvls or Wnt11s

FISH to detect Dvl expression (equal mixture of *dvl-1* and *dvl-2* riboprobes), *wnt11-1* and *wnt11-2* after 0 or 1350 rads at the indicated days after exposure. Number of animals representing each image shown, bars 300 microns. Irradiation did not eliminate expression of these factors.

pre-pharyngeally and examined for divergent posterior and anterior regeneration responses, asymmetric *notum* expression activated by 5-hours and peaked at 18-hours, while *wnt11-1* and *wnt11-2* expression near the wound-site was absent during these early times and only emerged later by 72-hours (Figure 2.35). These experiments, together with the timed irradiation experiments, argue that a body-wide polarization involving Wnt11 cues from the posterior acts via a noncanonical Wnt pathway prior to injury to influence the symmetry breaking event of asymmetric injury-induced *notum* activation.

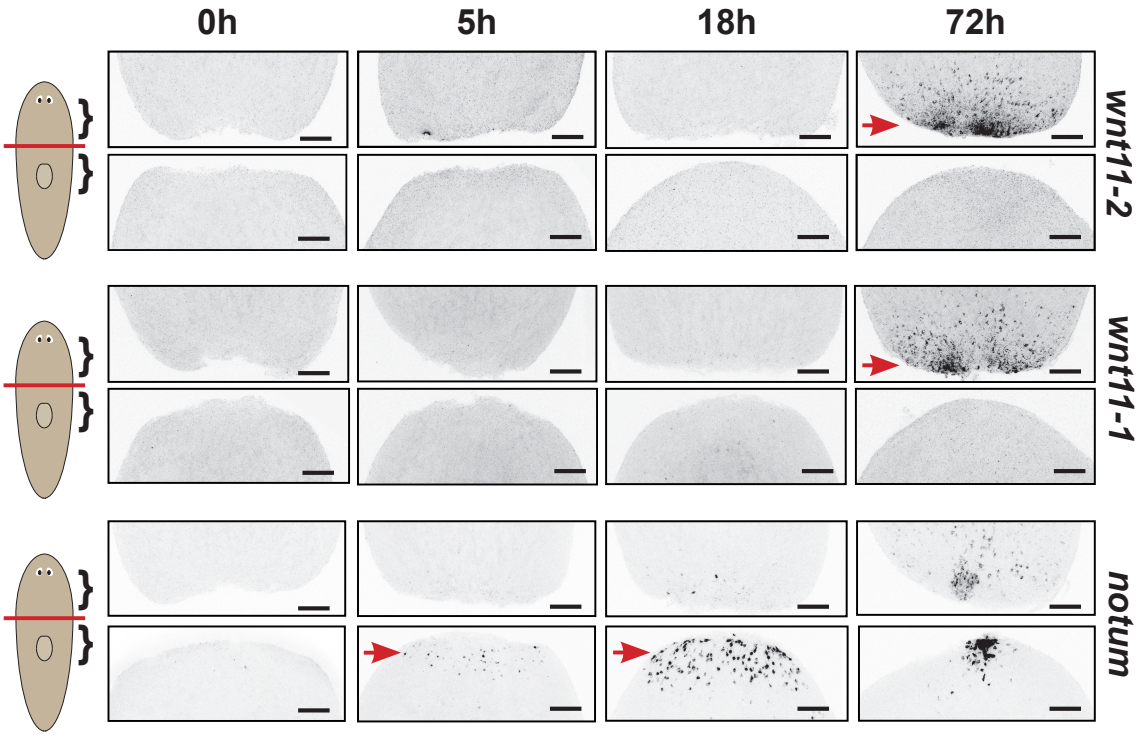

Fig 2.35 Re-expression of *wnt11-1* and *wnt11-2* During Regeneration Occurs After Expression of Injury-induced *notum*.

Time-course FISH detecting first appearance (arrows) of new expression of tested factors in regeneration indicating *wnt11-1* and *wnt11-2* re-expression occurs after *notum* activation. Panels represent 5/5 animal fragments tested. Scale bars 100 um.

Discussion

Our analysis suggests a model in which Wnt factors have distinct roles with respect to *notum* activation (Figure 2.36). Candidate searching identified *notum* as a strongly anterior-polarized injury-induced gene in planarians (Petersen and Reddien 2011), and a subsequent search using RNAseq revealed *notum* to be the only planarian injury-induced gene with prominent and early anterior/posterior-asymmetry (Wurtzel, Cote et al. 2015). Therefore, planarians likely possess an animal-wide polarity system established prior to injury and/or involving post-transcriptional control after injury which elicits a polarization of *notum* expression at wound sites. Injury-induced *wnt1* and an animal-wide gradient of *wntP-2* provide activating cues for *notum* expression after injury dependent on *βcatenin-1* (Figure 2.36). Our results furthermore indicate Dvl and two posteriorly expressed Wnt11 factors have βcatenin independent roles in suppressing *notum* expression at posterior-facing wound sites (Figure 2.36). We suggest that Wnt11/Dvl likely controls polarization in uninjured tissue that is read out through the asymmetric activation of *notum*, perhaps through dictating the A/P polarization of newly differentiated longitudinal muscle cells, or alternatively through another polarized cell type such as epidermis, which is known to be homeostatically polarized by Dishevelled (Almuedo-Castillo, Salo et al. 2011). However, given that Wnt11s are expressed from muscle and influence polarization of *notum* in muscle, we suggest this communication likely takes place across muscle cells.

Our study advances on prior work implicating planarian Dishevelled in epidermal polarization (Almuedo-Castillo, Salo et al. 2011, Vu, Mansour et al. 2019) by showing its specific function in a non-canonical, Wnt11-mediated role in suppressing the injury-induced expression of *notum* used for controlling head-versus-tail blastema identity determination. We suggest that the decrease in expression of *notum* at anterior-facing wounds in Dvl RNAi could occur because of its

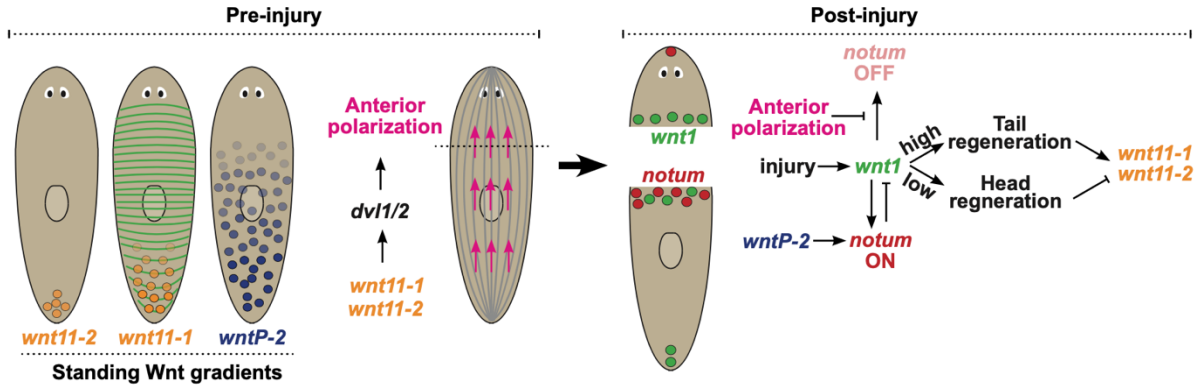

Fig 2.36 Model of Antero-Posterior Polarity Determination During Regeneration

Model depicting the roles of Wnt genes in activating and polarizing *notum* in longitudinal muscle cells early in regeneration. Standing gradients of *wnt11-1, wnt11-2*, and *wntP-2* are present prior to injury. Signals activating expression of *notum* include the *wnt1* gene induced by injury in muscle cells as well as the *wntP-2* gene, expressed in a body-wide gradient. *wnt11-1, wnt11-2*, and Dishevelled homologs *dvl-1* and *dvl-2* repress expression of *notum* at posterior-facing wound sites. Based on expression in regeneration and irradiation sensitivity of their RNAi phenotypes, we suggest the influence of Wnt11/Dvl on *notum* polarity occurs prior to injury through initiating and/or propagating anterior polarization to account for the influence these factors exert on sites distant from Wnt11 expression domains. *wnt11-1* is expressed from circular muscle and injury-induced *notum* is expressed from longitudinal muscle. The polarized expression of *notum* by 6-18 hours after injury leads to suppression of *wnt1* activity at anterior-facing wounds and subsequent anterior regeneration, while low levels of *notum* at posterior-facing wounds permit higher *wnt1* activity, leading to posterior regeneration. Subsequently by 72 hours, blastemas either express or do not express Wnt11 as an outcome of tail or head growth, respectively. Therefore, *notum* and Wnt11 mutually antagonize in order to sustain polarization across successive rounds of regeneration. Scale bars, 100 microns

role in canonical Wnt signaling that activates *notum* or alternatively that Dvl RNAi randomizes *notum* expression with respect to injury sites. By contrast, *wnt11-1* and *wnt11-2* suppress *notum* expression specifically at posterior-facing wounds while *wnt1* and *wntP-2* activate expression at anterior-facing wound sites. One possible model is that injury-induced *wnt1* provides a cue that attempts to activate *notum* at any injury site, but that pre-existing information from *wnt11-1/wnt11-2* and *wntP-2* provide a polarized environment that enables longitudinal muscles to distinguish their orientation with respect to a wound site. Furthermore, our findings that Dvl and *wnt11-1;wnt11-2* RNAi phenotypes are suppressed by irradiation are suggestive of a model in which stem cell dependent tissue turnover helps to reinforce tissue polarization over time, which for example could be achieved by enabling newly born longitudinal muscle cells to polarize in the appropriate direction. Thus, patterns sustained through differentiation and growth could contribute to the interpretation of injury signals. Pre-existing signals have been implicated in the placement of newly born *notum*$^{+}$*foxD*$^{+}$ anterior pole cells in head regeneration, regulated by BMP and Wnt5 signals which are present prior to injury, but it is unclear whether this regulation is through the new or pre-existing component of these signals (Almuedo-Castillo, Salo et al. 2011). Our data defining a critical time for Dvl/Wnt11 activity on *notum* expression asymmetry, based on the timing of irradiation sensitivity, as well as timeseries expression data of Wnt11 versus *notum* in regeneration, demonstrates that signals important for instructing regeneration can act prior to injury.

Our results implicate Wnt11 factors as polarizing determinants used for regeneration after injury. In vertebrates, Wnt11 factors can act through canonical (Tao, Yokota et al. 2005) or noncanonical (Heisenberg, Tada et al. 2000, Matsui, Raya et al. 2005, Witzel, Zimyanin et al. 2006) signals in development via Dvl signaling and are required for proper axis polarization and

formation. In addition, the neural tube provides a source of Wnt11 critical for aligning the lateral outgrowth of myofibers, indicating Wnt11s can drive muscle polarization (Gros, Serralbo et al. 2009). In accordance with our results, Wnt11 factors may have an ancient and conserved role in controlling the polarity and architecture of muscle. The involvement of separate injury-induced and constitutive gradients of Wnt signaling from muscle for controlling axis polarity in regeneration has been observed in the Acoel *Hofstenia miamia*, and so the overall strategy could be an ancient feature of whole-body regeneration in Bilaterians (Srivastava, Mazza-Curll et al. 2014, Raz, Srivastava et al. 2017, Tewari, Owen et al. 2019, Ramirez, Loubet-Senear et al. 2020).

Our results also point to the importance of orthogonal muscle fibers in controlling injury-induced polarity. *notum* is expressed in longitudinal muscle cells after injury, suggesting that orientation of these fibers may be important for the early polarization of *notum* activation. *wnt11-1* is expressed primarily from circular muscle cells, and inhibition of the circular muscle differentiation factor *nkx1-1* leads to *wnt11-1* expression loss (Scimone, Cote et al. 2017). RNAseq of *nkx1-1(RNAi)* animals revealed additional factors expressed specifically in circular muscle (Scimone, Cote et al. 2017). However, *wnt11-2* transcript was not as strongly downregulated by this treatment, suggesting it is expressed in other muscle cell types, and instead *wnt11-2* was downregulated after inhibition of both *nkx1.1* and *myoD* (Scimone, Cote et al. 2017). In addition, depletion of circular muscle through *nkx1.1* RNAi led to a weak phenotype of elevated *notum* expression at posterior-facing wound sites that could be a consequence of reducing both *wnt11-1* and *wnt11-2* levels (Scimone, Cote et al. 2017). *nkx1.1* RNAi also depletes expression of *activin-2*, another factor regulating tissue polarization that impacts injury-induced *notum* expression and is expressed from circular muscle (Scimone, Cote et al. 2017). Together these results highlight the

importance of signals from circular muscle to direct the injury-induced properties of orthogonally arranged longitudinal muscle.

We anticipate several possible mechanisms for conveyance of polarity across the body to influence injury-induced *notum* expression. Polarity could be propagated from the Wnt11 source from cell to cell across in a process resembling planar cell polarity, for example across successive longitudinal muscle fibers. Alternatively, a gradient of Wnt11 protein throughout the body could help to orient the polarization of distant receiving longitudinal muscle cells. Given that low amounts of *wnt11-1* expression have been observed even far into the anterior of animals (Stuckemann, Cleland et al. 2017), it is also possible that longitudinal muscle cells are directly polarized from contact with *wnt11-1* or *wnt11-2* expressing cells. Finally, it is possible that longitudinal muscle lacks intrinsic polarization but is instead instructed by other polarized tissue such as the epidermis (Almuedo-Castillo, Salo et al. 2011, Vu, Mansour et al. 2019). Future higher resolution analyses of the architecture of the muscle system, as well as investigation of additional determinants of polarity, could help resolve these possibilities.

The identification of posterior Wnt11s as determinants regulating early injury-induced *notum* suggests a self-assembly feedback mechanism in which regeneration relies upon but also reinforces tissue polarity. Tissue polarity emerges from the posterior Wnt11 determinants signaling through Dvl to regulate A/P orientation through growth. After transverse injury, the wound-induced factor *wnt1* and AP gradient gene *wntP-2* act through canonical Wnt signaling to try to activate *notum.* At anterior-facing wounds, the Dvl/Wnt11 polarity axis permits expression of *notum*, which then represses *wnt1* and likely other regional Wnt genes to generate an environment low for *βcatenin-1* activity, which enables head regeneration and consequently lack of new *wnt11-1* and *wnt11-2* expression. At posterior-facing wounds, pre-existing Wnt11 mediated

polarity represses *notum* expression, allowing *wnt1* expression to drive determination of a new posterior, leading to new expression of *wnt11-1* and *wnt11-2* and consequently a reinforcement of polarization that can instruct the next round of regeneration. This process of mutual inhibition between *notum* and Wnt11, bridging information before and after injury, would enable a fidelity of regeneration outcomes to be sustained across potentially large numbers of generations of asexually reproducing adults.

Regeneration involves critical inputs from injuries, including gene expression states induced by wounding (Petersen and Reddien 2009, Petersen and Reddien 2011, Wenemoser, Lapan et al. 2012, Wurtzel, Cote et al. 2015, Benham-Pyle, Brewster et al. 2021). However, our results additionally suggest a critical role for signals operating prior to injury that can help to instruct wound-induced outputs. Adult pattern formation is essential for regeneration to restore the appropriate missing parts following tissue removal. Our results suggest that regenerative ability may arise from the coupling of constitutive patterning information with injury-induced signals.

Materials and Methods

Cloning, riboprobes and dsRNA

Genes were cloned from planarian cDNA generated by reverse transcription of bulk RNA preparations as previously described (Petersen and Reddien 2011), and PCR fragments were cloned into pGEM-T-easy. Constructs to inhibit *wnt11-1*, *wnt11-2*, *wntP-2*, *wnt1, βcatenin-1, APC, dvl-1*, and *dvl-2* were previously described (Gurley, Rink et al. 2008, Petersen and Reddien 2008, Petersen and Reddien 2009, Petersen and Reddien 2011). Riboprobes were generated by *in vitro* antisense transcription using digoxigenin- or fluorescein-labeled nucleotides and isolated by ethanol precipitation. dsRNA was generated by *in vitro* transcription to produce sense and antisense transcripts which were ethanol precipitated and then annealed at 72C.

RNAi

RNAi was performed by feeding worms a mixture of dsRNA (16%), red food dye (4%) and homogenized liver paste (80%). Worms were starved at least 7 days before RNAi feeding, then fed every third day for six feedings spanning 18 days. dsRNA coding for *C. elegans unc-22* was used as a negative control, as this sequence is absent in the *S. mediterranea* genome. Animals waited 3 days post-feeding, and on the 21st day after feeding began were fixed uninjured for analysis, or amputated transversely into head, trunk, and tail fragments.

Fluorescence in situ hybridization

Animals were sacrificed in 5% NAC in PBS, fixed in 4% formaldehyde and bleached in 6% H_2O_2 in methanol. Animals were transitioned into riboprobe solution and hybridization was conducted

overnight at 56°C. Secondary labeling was conducted using anti-digoxigenin-POD (at 1:1000) or anti-fluorescein-POD (at 1:2000) antibodies in MABT containing 10% horse serum and 10% Western Blocking Reagent (Roche). Signal was developed by tyramide amplification with 1:1000 rhodamine-tyramide (DIG probes) or 1:2000 fluorescein-tyramide (FL probes). For double FISH secondary antibody binding and tyramide amplification steps were performed sequentially, separated by enzyme quenching for 45 minutes in 4% formaldehyde. Nuclear counterstaining was performed using Hoechst 33342 at 1:1000 in PBSTx.

Immunostaining

Animals were sacrificed in .75M HCl, fixed in Carnoy's solution (60% ethanol, 30% chloroform, 10% glacial acetic acid) and bleached in 6% H_2O_2 in methanol. Animals were blocked for 6 hours in PBST (1x PBS, .3% Triton X-100) plus 10% horse serum followed by overnight incubation with primary antibody mouse monoclonal 6G10 at 1:1000 in blocking solution, washout, and overnight incubation with secondary antibody rabbit anti-mouse HRP at 1:1000 in blocking solution. Signal was developed by tyramide amplification with 1:1000 rhodamine-tyramide. Nuclear counterstaining was performed using Hoechst 33342 at 1:1000 in PBSTx.

Image acquisition and cell counting

Live images were obtained on a Leica M210F dissecting microscope equipped with a Leica DFC295 camera. Adjustments to brightness and contrast made using Fiji/ImageJ. FISH images obtained on a Leica DM5500B compound microscope with Optigrid structured illumination or a Leica TCS SPE confocal microscope. Images are maximum projections of a z-stack adjusted for brightness and contrast using Fiji/ImageJ. For quantification of *notum*$^+$ cells, the ~200-micron

region near wound sites were imaged at 10x on a Leica TCS SPE confocal microscope with one-micron Z-stacks. Animals were imaged both dorsally and ventrally, then *notum*$^{+}$ cells were manually counted, annotated, and scored in ImageJ for colocalization with either *collagen, chat*, or *myoD* as indicated, and cell counts from each side were summed for a total count of cells per wound site.

Irradiation assay

Animals were irradiated using a Radsource RS-2000 X-ray irradiator to deliver 1350 rads to worms maintained in 1x Montjuic salts at 20°C.

Chapter 3

Src acts with Wnt signaling to pattern the planarian anteroposterior axis

This work was conducted in collaboration with Dr. Nicolle Bonar and published in *Development.* See citation below. Individual contributions to the work are indicated in the Figure Legends

Bonar N. A., Gittin D. I., and C. P. Petersen (2022). "Src acts with WNT/FGFRL signaling to pattern the planarian anteroposterior axis." Development **149**(7)

Abstract

Tissue patterning to establish the AP axis is critical in planarian regeneration for animals to replace correctly regionalized tissues in response to injury. Canonical Wnt signaling through βcatenin establishes anterior versus posterior pole identities through *notum* and *wnt1* signaling. Two additional Wnt/FGFRL signaling pathways separately control positional regionalization of head and trunk domains, but the downstream mechanisms controlling their function are unclear. Here we identify two of 10 planarian Src homologs that restrict head and trunk identities to anterior positions without substantially affecting AP pole identity. Src proteins are tyrosine kinases that function at the hubs of multiple pathways, relaying signals from cell surface receptors to control diverse cellular outputs. *src-1(RNAi)* animals formed larger brains than control animals with neuronal tissue and extra eyes extending posteriorly, strongly reminiscent of RNAi phenotypes for *ndk*, *wnt11-6/wntA*, and *fzd5/8-4* RNAi. Furthermore, *src-1 RNAi* resulted in posterior duplication of the pharynx similar to *wnt11-5/wntP-2*, *ndl-3* and *ptk7* RNAi phenotypes. *src-1* was required for the restriction of expression of multiple anterior PCGs, indicating its importance for maintenance of regional identity along the AP axis. Double-RNAi analysis indicated *src-1* function impacts multiple aspects patterning. We suggest that *src-1* acts downstream of both head and trunk patterning pathways to enable proper regeneration of the A-P axis.

Introduction

Robust pattern control is fundamental to the process of regeneration (Wolpert 1969). Animals must be able to quickly re-establish tissue identity and proper polarity after injury for regeneration to proceed successfully. Further, regardless of regeneration abilities, many animals must also maintain regional identity throughout adult life as they replace and specify new cells to replenish old tissue. Planarians present a powerful system for studying these patterning control mechanisms, as they possess a remarkable ability to regenerate any missing body part and are in a state of constant cellular turnover to replace aged tissues (Reddien and Sanchez Alvarado 2004, Reddien 2011). Planarian regeneration abilities extend from a population of pluripotent stem cells, termed neoblasts (Wagner, Wang et al. 2011). However, neoblasts are not believed to contain the positional information necessary for regeneration to occur correctly. Instead, muscle cells have been found to be the source of patterning information and are hypothesized to relay positional information to neoblasts to guide their regional differentiation (Witchley, Mayer et al. 2013, Scimone, Cote et al. 2017). Therefore, distinct cell types control positional information versus the production of new tissues. However, the signaling mechanisms controlling positional information in muscle and the reestablishment of patterning after injury are not yet fully understood.

Nonetheless, significant progress has been made into identifying core signaling pathways that control AP axis establishment in planarians, mainly featuring variants of Wnt signaling. Several of the nine planarian Wnt genes are expressed overlapping domains from the posterior, while several Wnt inhibitors demarcate nested anterior domains. In recent years, the functions of many of these factors have been elucidated. A canonical βcatenin-dependent Wnt signaling pathway controls the head-versus-tail identity of blastemas after transverse amputation. Downregulation of Wnt pathway components β*catenin-1*, *wnt1, Evi/wntless, Dvl-1/2* or *teashirt*

causes regeneration of ectopic heads (Petersen and Reddien 2008, Petersen and Reddien 2009, Gurley, Elliott et al. 2010, Iglesias, Almuedo-Castillo et al. 2011, Owen, Wagner et al. 2015, Reuter, Marz et al. 2015) whereas up-regulation of canonical Wnt signaling via RNAi inhibition of the Wnt negative regulators *notum* and *APC* causes the regeneration of ectopic tails (Gurley, Rink et al. 2008, Petersen and Reddien 2011). *wnt1* and *notum* are both transcriptionally induced by injury where they likely participate in the control of the polarization or orientation of the outgrowing blastemal tissue. Additionally, *wnt1* and *notum* are expressed at the posterior and anterior termini (termed poles) where they may function to control region-specific patterning or act at the tip of a hierarchy of AP factors.

Additional Wnt-dependent pathways may function downstream or in parallel to the pole identity and tissue polarization controlled by *wnt1*, and these pathways also involve FGFRL family members. *wnt11-6* (also known as *wntA*) and associated factors limit the regionalization of head tissue. Inhibition of *wnt11-6* or the *fzd5/8-4* Wnt receptor causes posterior expansion of the brain and the formation of ectopic posterior eyes (Kobayashi, Saito et al. 2007, Adell, Salo et al. 2009, Scimone, Cote et al. 2016). Similarly, RNAi of *nou-darake (ndk),* a member of the FGFRL- family of putative FGF decoy receptors, also resulted in a similar brain expansion phenotype (Cebria, Kobayashi et al. 2002). The Wnt inhibitor *notum* also appears to act in the head regionalization pathway independent of its roles in *wnt1/*polarity signaling. First, *notum(RNAi)* decapitated animals that escape formation of tails succeed in growing a brain that is too small, and second, head fragments that do not express injury-induced *notum* are responsive to *notum* inhibition to form smaller than normal brains. Additionally, co-inhibition of *wnt11-6* suppresses the *notum(RNAi)* phenotypes of small brain and ectopic anterior photoreceptors whereas co-inhibition

of *wnt1* does not modify these phenotypes (Hill and Petersen 2015, Atabay, LoCascio et al. 2018, Hill and Petersen 2018).

A separate set of Wnt-related and FGFRL genes control trunk identity in planarians. Inhibition of *ndl-3* (a FGFRL protein), *ptk7* (a kinase dead wnt co-receptor), *wntP-2* (Wnt ligand) and *fzd1/2/7* (Wnt receptor) causes posterior trunk duplication, with animals forming secondary mouths and ectopic pharynges (Lander and Petersen 2016, Scimone, Cote et al. 2016). These findings suggest that a body-wide system of Wnt-FGFRL signaling conveys positional information needed for regeneration and homeostatic tissue maintenance. However, two important questions remain unanswered. First, it is not known how the Wnts and FGFRLs identified in these studies interact with one another or if they act in parallel to control positional identity and body regionalization. Second, the relationship between Wnt/FGFRL signaling along the AP axis and canonical Wnt signaling at the axis termini remains unresolved. Here we identify *src-1* as a global suppressor of anterior identities that links multiple aspects of posterior determination including, head and trunk regionalization and pole identity. Further, we propose that *src-1* likely acts downstream of multiple pathways linking both canonical and non-canonical wnt signaling to control anterior identity in planaria.

Results

Planarian *src-1* suppresses head and trunk identity

To identify regulators of neuronal regeneration in planarians, we conducted an RNAi screen of 63 kinases and identified a patterning phenotype, the formation of ectopic posterior eyes, after inhibition of a Src family homolog that we named *src-1.* We cloned and sequenced *src-1* and phylogenetic analysis identified nine other src family kinases (Figure 3.1). We then used src-1(RNAi) to examine *src-1* requirements in patterning. qPCR verified *src-1* RNAi knockdown (Figure 3.2). Normal animals regenerate two eyes as observed in live animals and measured by double fluorescence *in situ* hybridization (FISH) detecting both *opsin*$^{+}$ (eye photosensory neurons) and *tyrosinase* (eye pigment cup cells). By contrasts, src-*1(RNAi)* animals formed ectopic posterior eyes in addition to their normal eyes (Figure 3.3, A and D). The src-*1(RNAi)* phenotype was strongly reminiscent of phenotypes observed for *ndk*, *wnt11-6*, and *fzd5/8-4* RNAi which also resulted in the formation of a larger brain (Cebria, Kobayashi et al. 2002, Hill and Petersen 2015). Therefore, we sought to determine whether *src-1(RNAi)* animals similarly formed a larger brain. We investigated the size of the brain in *src-1(RNAi)* animals by examining the expression of *gluR,* a marker of the lateral brain branches, and found that *src-1(RNAi)* animals formed a larger brain than controls during head regeneration (Figure 3.3, B-D) and in the absence of injury (Figure 3.4, A). These results were further confirmed by measurement of *cintillo*$^{+}$ neurons (Figure 3.4, B) Thus, we conclude that *src-1* acts to suppress head identity.

Given *src-1's* ability to suppress head identity, we next sought to test the specificity of *src-1* in controlling AP patterning and examined *src-1(RNAi)* animals for defects in the assignment of trunk identity. Several factors have been implicated in trunk identity determination which do not appear to influence head patterning: *fzd-1/2/7, ndl3, ptk7,* and *wntp2* (Lander and Petersen 2016).

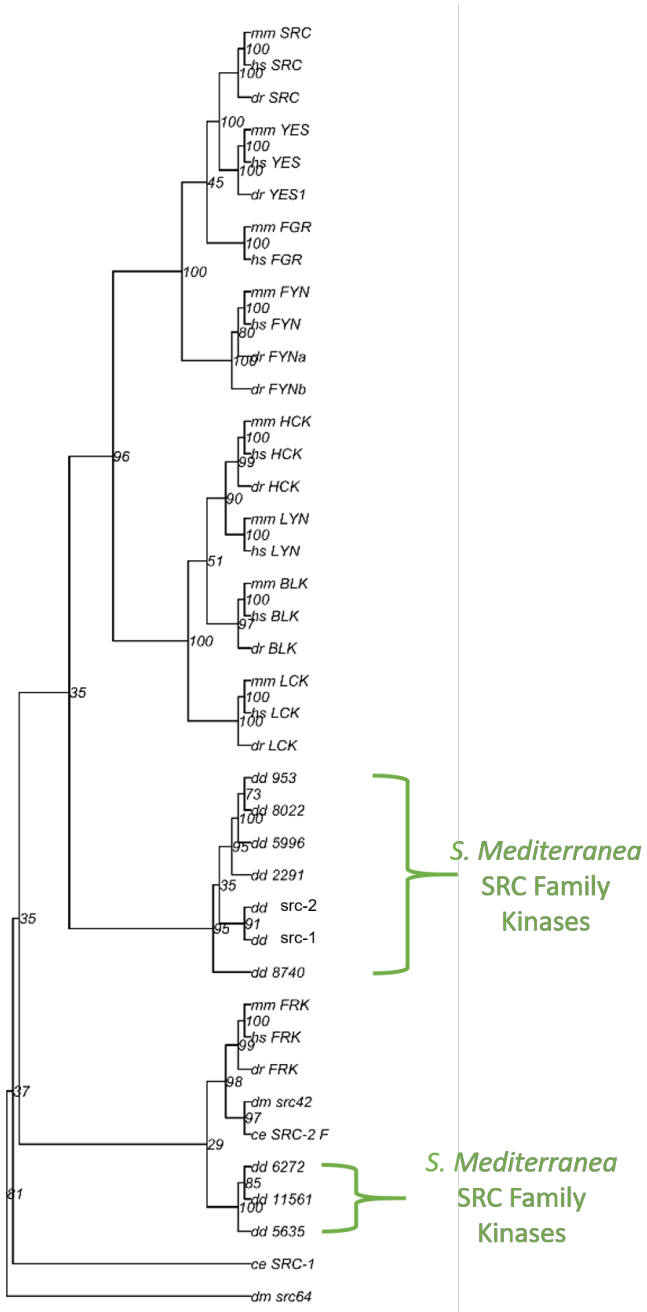

Fig 3.1 Phylogeny of *Schmidtea mediterranea* Src Family Kinases

Phylogenetic tree of planarian src family kinases. Predicted protein sequences for dd_Smed_v6_3147_0_1 (*src-1)* and dd_Smed_v6_3363_0_1 (*src-2*) were aligned to Src family kinase sequences from well-annotated proteomes. Alignment performed and figure created by Dr. Alex Karge.

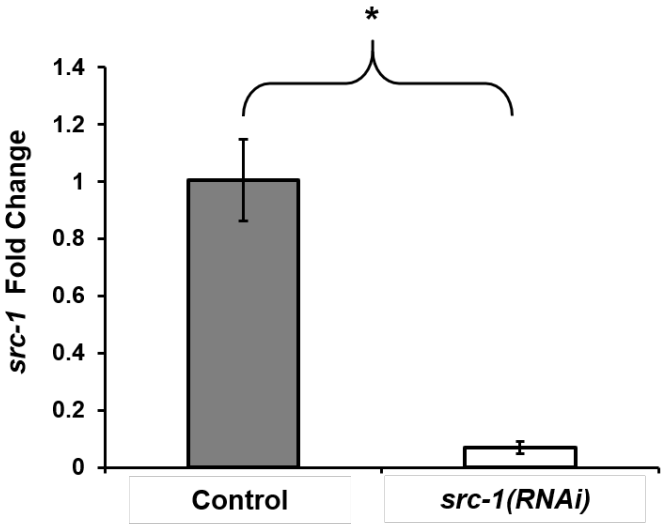

Fig 3.2 *src-1* RNAi Knockdown

qPCR verified RNAi knockdown of *src-1*, * $p<0.05$, two-tailed t-test.
Experiment performed by David Gittin

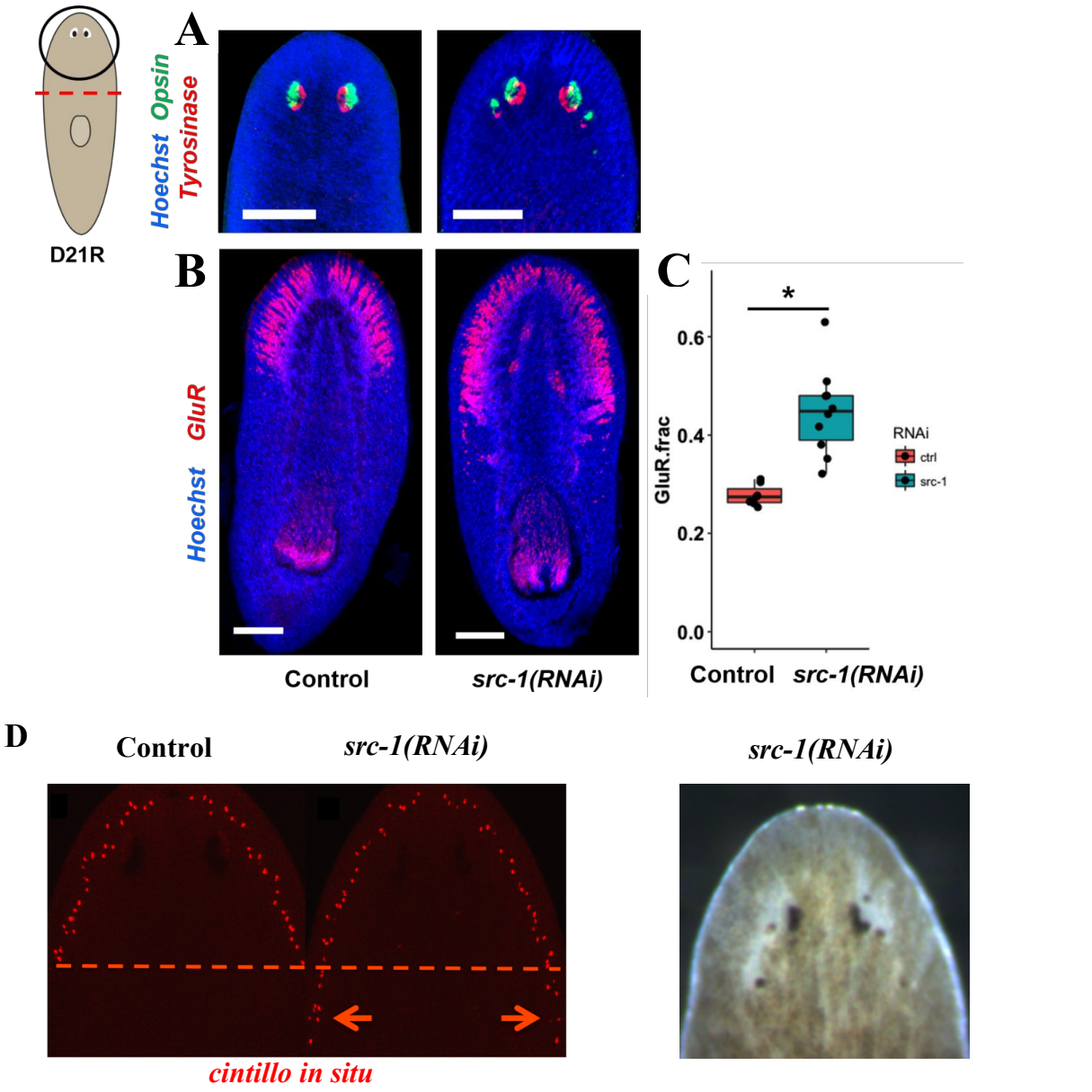

Fig 3.3 *src-1* is a Regulator of Head Identity

A) *src-1(RNAi)* animals undergoing tail regeneration formed ectopic posterior photoreceptors. Scale bars: 150 um.
B) *src-1(RNAi)* animals undergoing tail regeneration formed a larger brain as evident by *GluR* expression, a marker of planarian brain branches. Scale Bars: 300 um.
C) Quantification of brain size by *GluR* expression as proportional to body length. * $p<0.05$, two-tailed t-test.
D) Initial observations of brain expansion and posterior ectopic eyes in *src-1(RNAi)* animals which inspired experiments in A-C. Left, size matched control and *src-1(RNAi)* animals aligned to show expanded brain after RNAi treatment, *cintillo* cells extend beyond dotted line marking normal posterior extent of the brain (arrows). Right, *src-1* RNAi causes ectopic eye formation. A-C experiments performed by Dr. Nicolle Bonar; D experiments performed by David Gittin

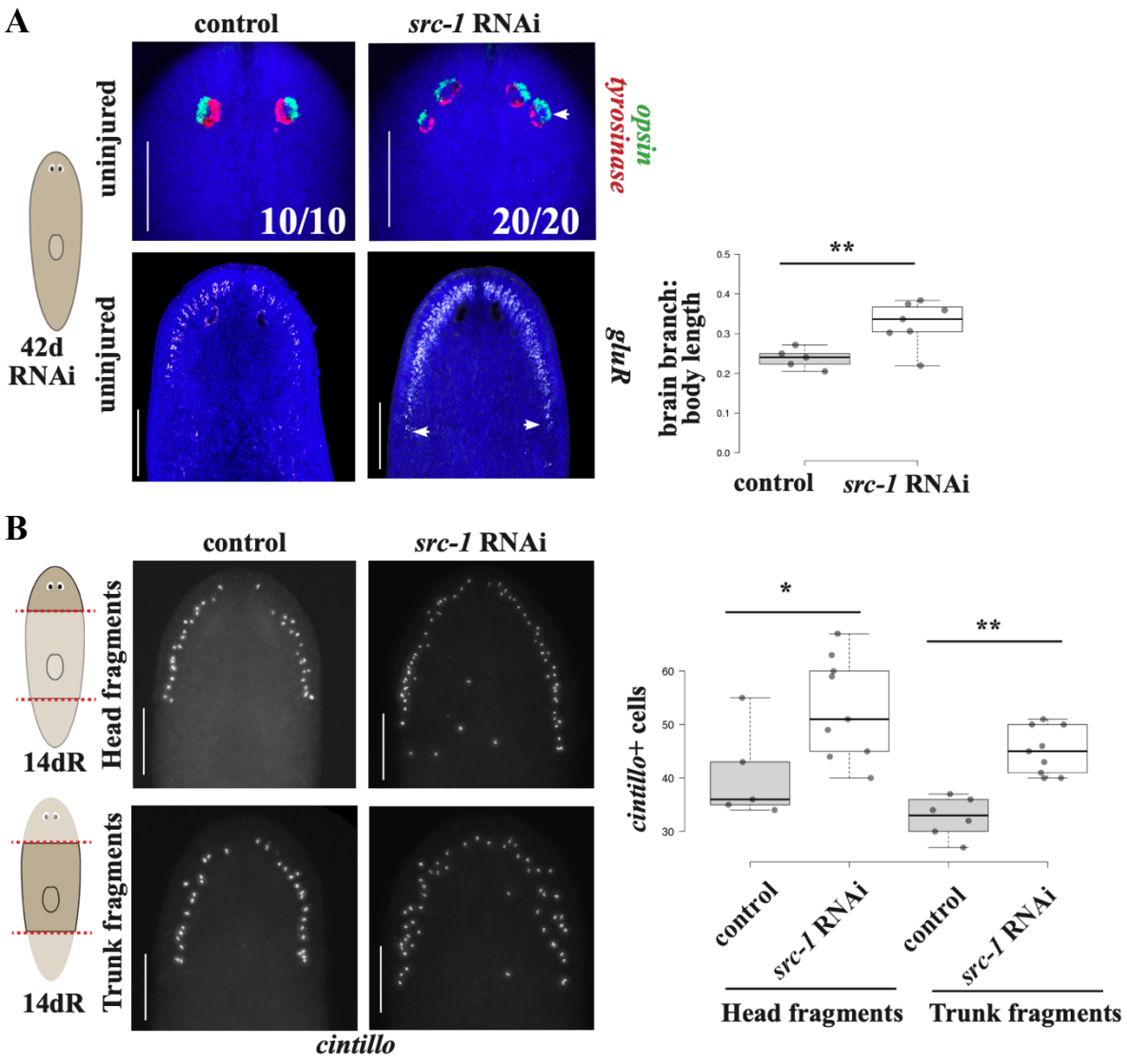

Fig 3.4 Further Evidence *src-1* is a regulator of Head Identity.

A) *src-1(RNAi)* form ectopic posterior photoreceptors and undergo brain expansion in the absence of injury.
B) Regenerating *src-1(RNAi)* head and tail fragments form a larger brain as evidenced by number of *cintillo*$^{+}$ chemosensory neurons.
Experiments performed by David Gittin

By contrast, the two planarian dishevelled factors likely function in both head and trunk regionalization pathways because simultaneous inhibition of *dishevelled-1* and *dishevelled-2* results in head expansion and trunk expansion (Almuedo-Castillo, Salo et al. 2011). *src-1(RNAi)* regenerating trunk fragments formed a secondary posterior pharynx (marked by *laminin*) at 20% penetrance (Figure 3.5) and were also observed to be capable of forming secondary mouths. Thus, we conclude that like *dvl-1/2, src-1* anteriorly limits both trunk and head identity.

Because we found *src-1* to be a regulator of anterior patterning, we investigated whether the other Src family kinases in *S. mediterranea* might redundantly control patterning. We used RNAi to inhibit five additional Src family kinases, only one of which mimicked the effects of *src-1* RNAi, and we named this gene *src-2*. *src-2(RNAi)* animals formed ectopic posterior eyes (3 of 10) and formed a larger brain (Figure 3.6) similar to *src-1(RNAi)* animals. Therefore, *src-2* negatively regulates head regional identity in planarians. We did not detect any trunk expansion or duplication phenotypes in *src-2(RNAi)* animals, however, it is possible that putative roles in trunk regionalization were not detected because of a small sample size. *src-1* head expansion phenotypes were more highly penetrant (~90-100% of animals) compared with *src-2* RNAi effects (~30%). This difference could be due to differential RNAi silencing efficiencies or degree of involvement in each pathway.

We next investigated whether *src-1* could act a positional control gene (PCG) to regulate anterior patterning. PCGs are genes that are expressed in muscle cells in a gradient like fashion that act as a system of body coordinates and positional information to control regeneration and tissue turnover (Witchley, Mayer et al. 2013). We found *src-1* to be broadly expressed throughout the animal, except for the pharynx, but not in a gradient-like fashion, differing from known PCGs (Figure 3.7, A). *src-1* expressed in both muscle and non-muscle cells (Figure 3.7, B) as measured

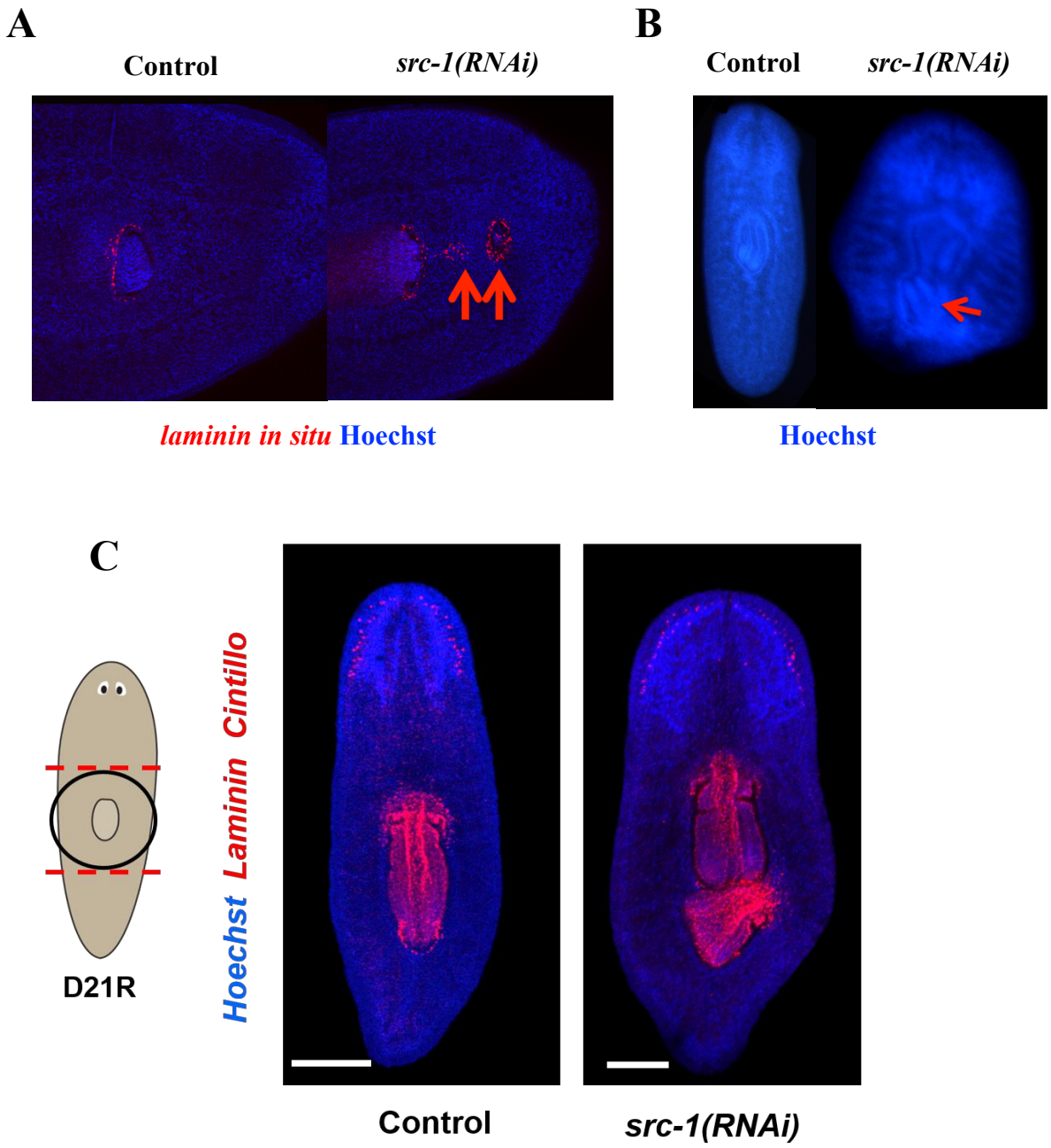

Fig 3.5 *src-1* is a Regulator of Trunk Identity

A-B) initial observations suggesting duplication of trunk structures (A mouth, B pharynx) in *src-1(RNAi)* animals.
A) *in situ* hybridizations marking *laminin* expression with Hoechst as a counterstain.
B) Hoechst stain allowing visualization of pharynx.
C) regenerating *src-(RNAi)* trunk fragments formed a posterior secondary pharynx (2 of 10 animals) as marked by *laminin* expression and a larger brain (10 of 10 animals) as marked by *cintillo* expression. Scale bars: 300 um.
A-B experiments performed by David Gittin. C experiments performed by Dr. Nicolle Bonar

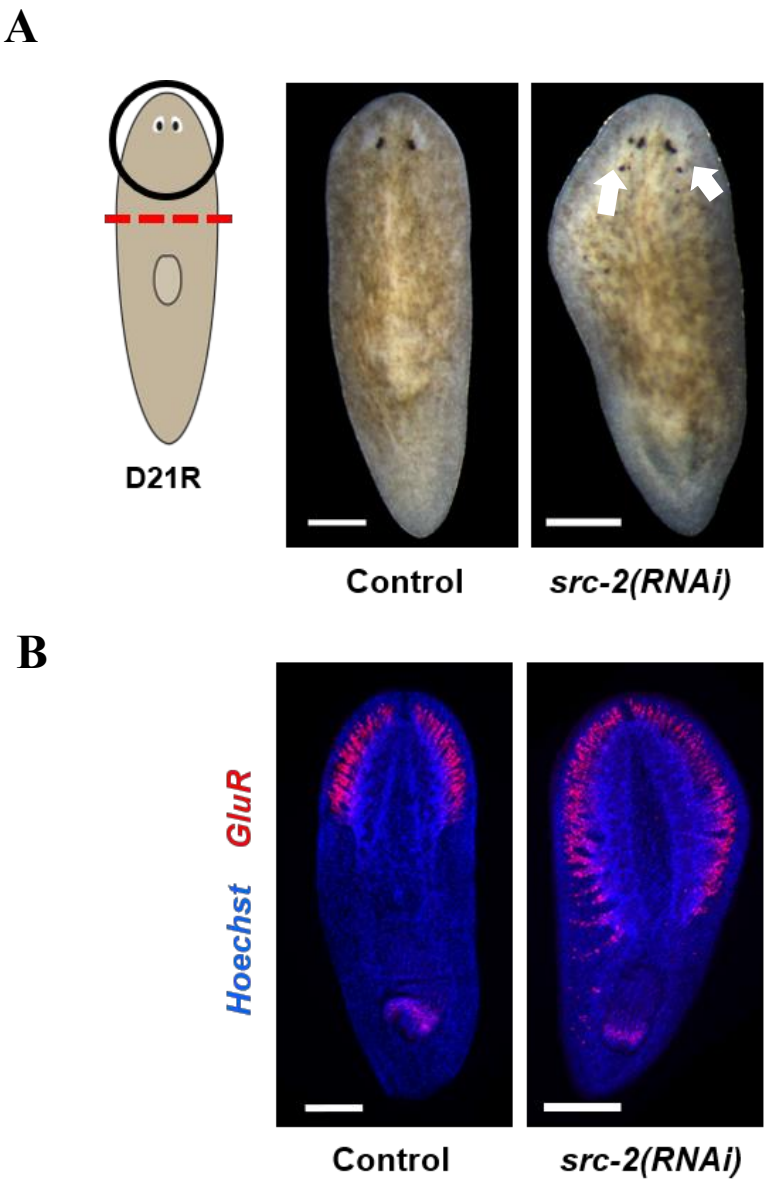

Fig 3.6 *src-2* is a Regulator of Head Identity

A) live images of control and *src-1(RNAi)* animals undergoing tail regeneration at day 21 post amputation. *src-1(RNAi)* animals formed ectopic posterior photoreceptors (arrows). B) *src-1(RNAi)* animals undergoing tail regeneration at day 21 post amputation formed a larger brain as evident by an in-situ hybridization for expression of *GluR*, a marker of planarian brain branches. Scale bars: 300 um.
Experiments performed by Dr. Nicolle Bonar

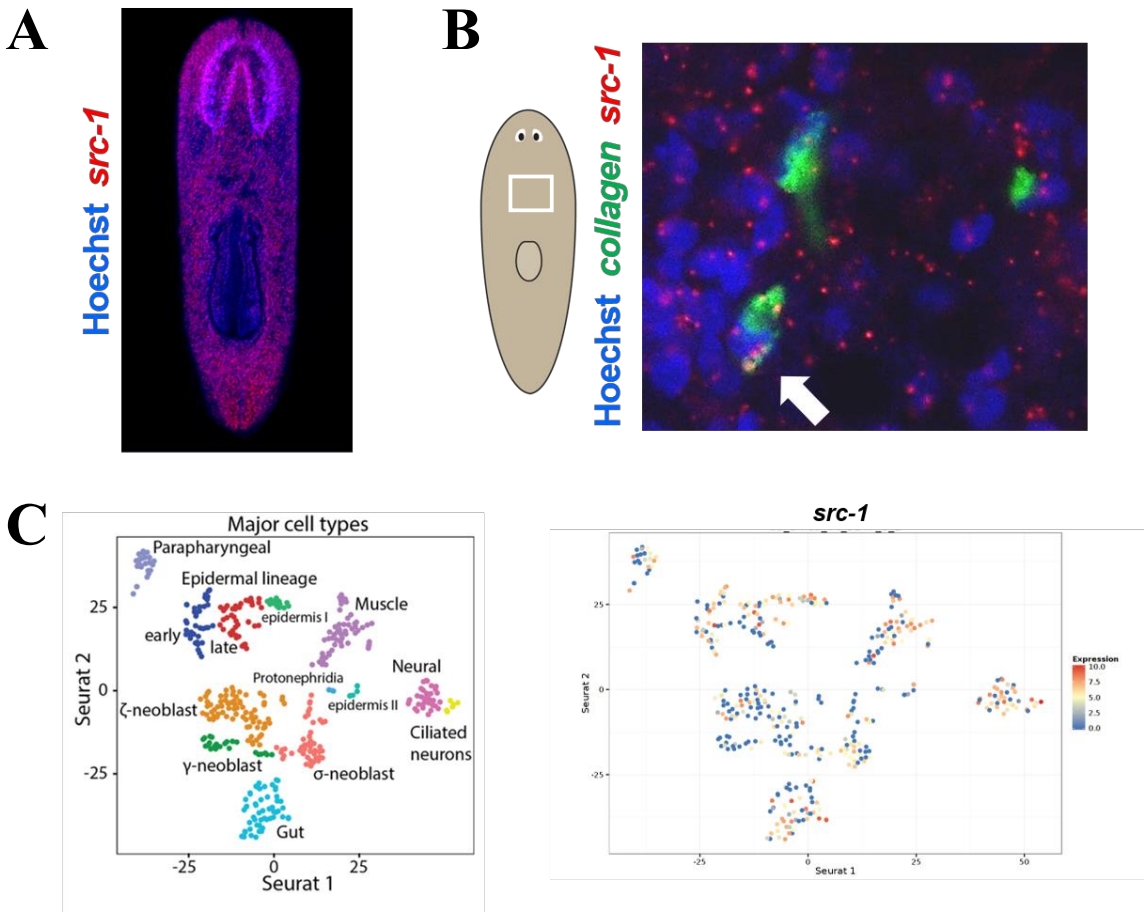

Fig 3.7 *src-1* is Broadly Expressed in Both Muscle and Non-Muscle Cells.

A) FISH to detect *src-1* expression, showing broad expression throughout the planarian body plan except for the pharynx.
B) Double FISH to detect the expression of *src-1* and *collagen* in uninjured animals, with cartoons indicating the approximate location of the imaged regions. *src-1* mRNA expression was punctate and broad. Some *collagen*$^{+}$ cells could be identified with overlapping detection of *src-1* (arrows).
C) Single-cell RNA-seq expression profiling as measured from a prior study (Wurtzel, Cote et al. 2015) measured *src-1* transcripts.
Experiments performed by Dr. Nicolle Bonar

by FISH and co-expression with the muscle marker *collagen*. These data confirm single-cell RNA sequencing experiments which found *src-1* to be widely expressed in a wide variety of cell types, including muscle (Wurtzel, Cote et al. 2015) (Figure 3.7, C). These results suggest that *src-1* may act in muscle cells to regulate anterior identity in planarians, or alternatively influence patterning in tissues other than muscle, and/or that *src-1* may have additional cellular functions in other cell types.

Muscle fibers have been shown to have distinct patterning roles during regeneration. Inhibition of PCGs expressed in muscle cells can lead to the expansion of both head and trunk region (Cebria, Kobayashi et al. 2002, Hill and Petersen 2015, Lander and Petersen 2016, Scimone, Cote et al. 2016). Treatments to prevent differentiation of muscle cells also result in patterning defects. For example, *myoD* RNAi to prevent formation of longitudinal muscle fibers results in failure to express *follistatin* and *notum* within injured longitudinal muscle cells and thereby resulting in failed anterior outgrowth at amputation sites. In addition, *nxk1-1* RNAi prevents differentiation of circular muscle fibers, leading to midline bifurcation and the formation of two-heads at the anterior axis (Scimone, Cote et al. 2017). Therefore, we sought to examine whether the head and trunk expansion phenotype observed in *src-1(RNAi)* animals could be the result of loss of muscle fibers or muscle cell bodies. Immunostainings showed that longitudinal, circular, and diagonal muscle fibers were apparently normal in regenerating *src-1(RNAi)* animals (Figure 3.8, A). In addition, muscle cell bodies labeled by the presence of *collagen* mRNA were also unchanged in regenerating *src-1(RNAi)* animals (Figure 3.8, B). This suggests that *src-1* is regulating anterior patterning not through affecting muscle formation but instead by either changing the signaling within muscle or another cell type.

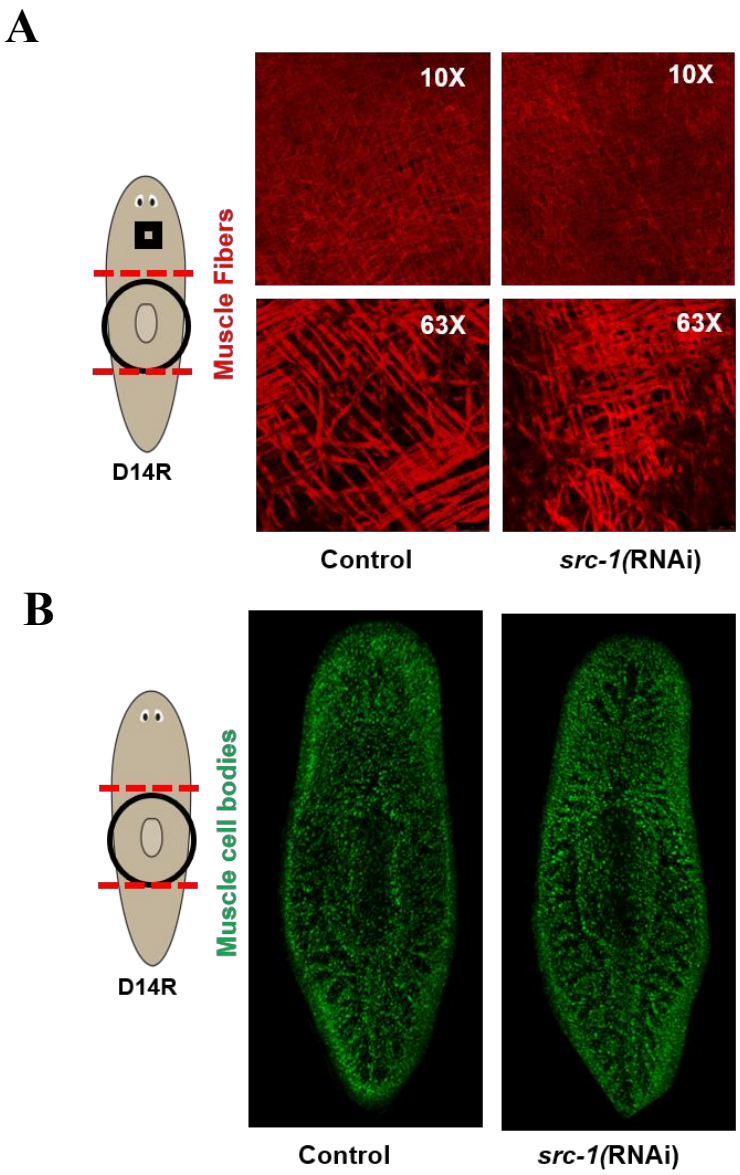

Fig 3.8 *src-1* Inhibition Does Not Affect Muscle Integrity

A) muscle fibers (anti-6G10) are unchanged in *src-1(RNAi)* regenerating animals as compared to controls with circular, longitudinal, and diagonal fibers all visible.
B) muscle cell bodies (FISH for *collagen* expression) are unchanged in *src-1(RNAi)* regenerating animals as compared to controls.
Experiments performed by Dr. Nicolle Bonar

src-1 can pattern the AP axis independently from pole identity

We theorized that the expansion of the head region in *src-1(RNAi)* animals may be a result of changes in the anterior pole. We sought to determine whether the establishment of the anterior pole was normal in *src-1(RNAi)* animals by examining the expression of *notum,* which is asymmetrically expressed at the anterior wound site 18 hours after amputation and is required for the establishment of the anterior pole (Petersen and Reddien 2011). We found *notum* to be asymmetrically expressed in *src-1(RNAi)* animals at 18 hours post amputation at similar levels to controls (Figure 3.9), consistent with the observation that *src-1* RNAi animals did not have impaired axis polarization. We also observed *notum* to be expressed at the anterior poles at 72 hours post amputation regardless of *src-1* inhibition (Figure 3.9). We then examined the anterior pole in *src-1(RNAi)* regenerating trunk fragments 14 days after amputation, after the head has completely regenerated, and in uninjured animals. In *src-1(RNAi)* animals, *notum* pole expression was laterally expanded, and *notum* anterior brain expression appeared expanded in concert with the expanded brain in such animals (Figure 3.9). These results suggest that *src-1* is not required for the establishment of the anterior pole but restricts the lateral expansion of the anterior pole after brain formation and independently of regeneration.

In contrast to *notum*, *wnt-1* is expressed at both the anterior and posterior facing wound sites after amputation and is required for the formation of the posterior pole in regenerating animals. Regenerating *src-1(RNAi)* animals had normal wound-induced *wnt-1* expression at 18-hours post- amputation and formed a posterior pole by 72 hours post amputation (Figure 3.10). Furthermore, after 14 days of regeneration or homeostatic inhibition, *src-1(RNAi)* animals had a normal posterior pole as compared to controls (marked by *wnt-1* expression) (Figure 3.10). Thus,

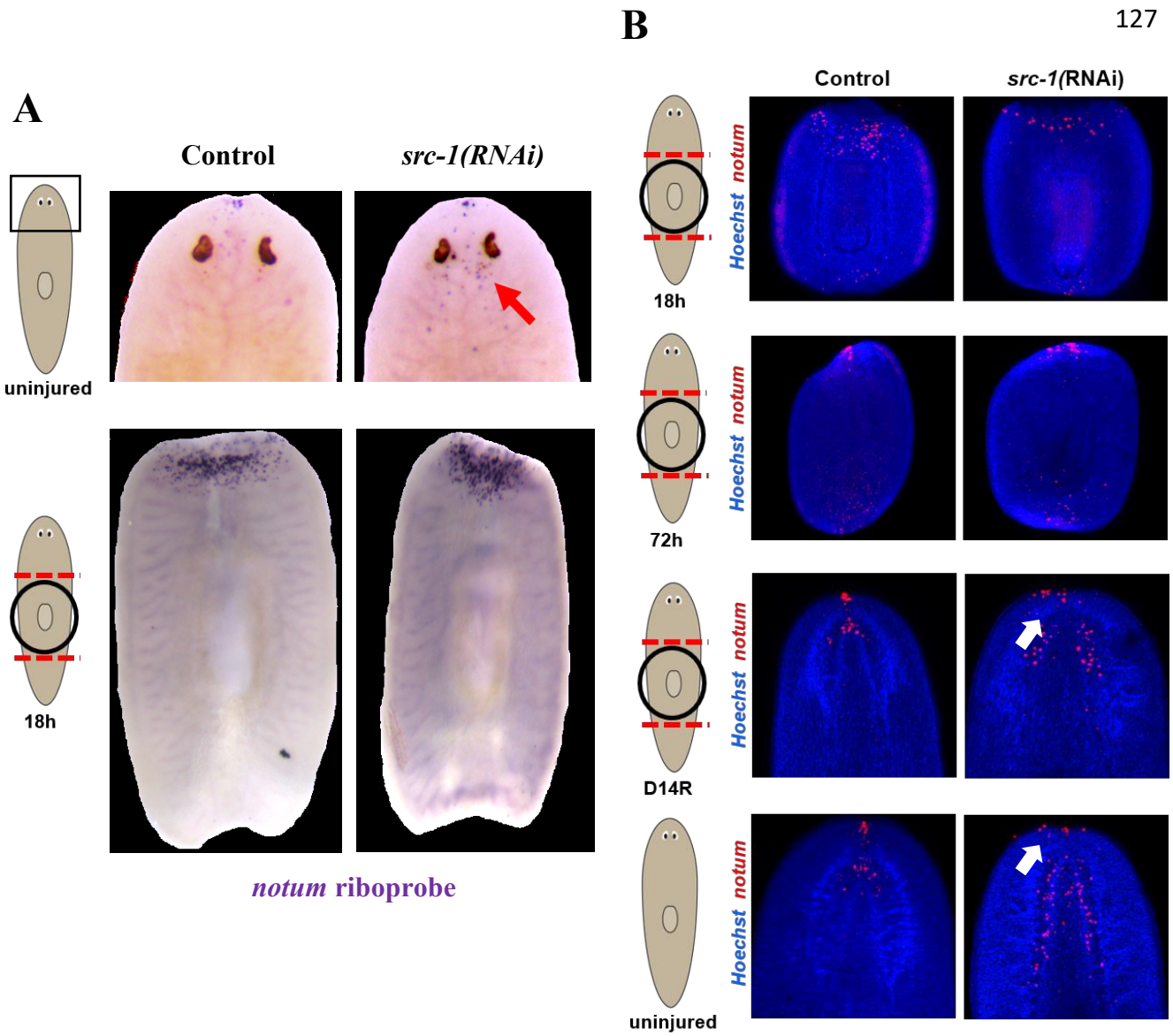

Fig 3.9 *src-1* Restricts the Anterior Pole

A) initial observations which lead to experiments shown at the right. Colorimetric *in situ* for *notum* expression in control and *src-1(RNAi)* uninjured animals and 18 hour trunk fragments. Red arrow marks increased *notum* expression.
B) *src-1(RNAi)* trunk fragments have normal wound induced *notum* expression (FISH) at 18 hours post amputation and form an anterior pole at 72 hours post amputation but have more body wide *notum* expression than controls. *src-1(RNAi)* animals regenerating their head and uninjured animals have an expanded anterior pole and more brain notum at 14 days post amputation (arrows).
A experiments performed by David Gittin. B experiments performed by Dr. Nicolle Bonar

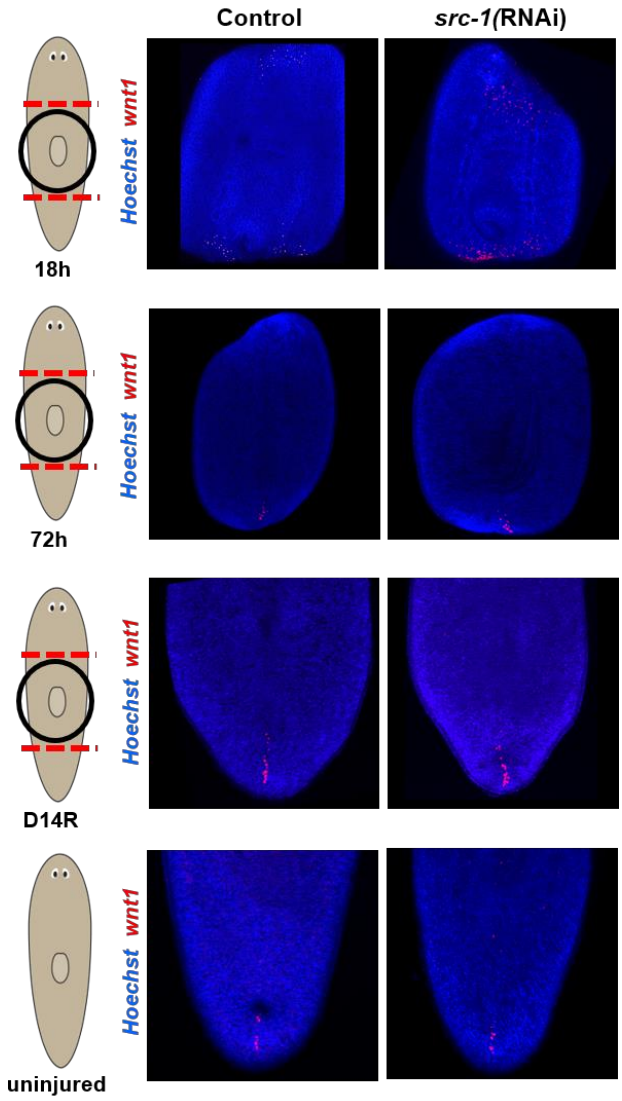

Fig 3.10 *src-1* Inhibition Does Not Affect the Posterior Pole

src-1(RNAi) trunk fragments have normal wound induced *wnt-1* expression at 18 hours post amputation and form a posterior pole at 72 hours post amputation similar to controls. *src-1(RNAi)* animals regenerating their tails and uninjured animals have a posterior pole as marked by the expression of *wnt1*.
Experiments performed by Dr. Nicolle Bonar

src-1 does not affect the establishment or maintenance of the posterior pole. Posterior and anterior pole formation depends on *βcatenin* and *APC* suggesting that *src-1* can act independently of these factors.

src-1 regulates expression of body-wide AP patterning factors

Given the expansion of the anterior pole in *src-1(RNAi)* animals, we next sought to examine whether the domains of anteriorly positionally controlled genes (PCGs) were similarly expanded in *src-1(RNAi)* animals. We examined the anterior PCGs *ndk* and *ndl-5* which are expressed in both brain and muscle cells. Both regenerating and uninjured *src-1(RNAi)* animals had expanded *ndk* and *ndl-5* domains that extended more posteriorly towards the pharynx than control animals (Figure 3.11). These results suggest that *src-1* patterning function is not limited to the brain or eyes but likely acts more generally to restrict the domains of anterior PCGs and regulate regional patterning identity in planarians.

We next investigated possible *src-1*-dependent regulation of trunk patterning factors *ndl3, ptk7,* and *wntP-2* (Lander and Petersen 2016, Scimone, Cote et al. 2016). *src-1* inhibition resulted in the reduction of the anterior boundary of *ndl3* and *ptk7* within the pre-pharyngeal region but did not impact the posterior boundary of these mRNAs in both regenerating and uninjured animals (Figure 3.12). These observations suggest *src-1* acts to restrict the anterior domain in planaria and allows for the possibility the *src-1* could be activating *ndl-3* and *ptk-7* expression in order to control trunk identity. We then examined the effect of *src-1* inhibition on the trunk PCGs, *wntP-2*, expressed in a posterior-to-anterior gradient in planaria. *wntP-2* expression was unchanged in *src-1(RNAi)* uninjured animals or decapitated animals regrowing their heads but reduced to nearly undetectable levels in decapitated head fragments regenerating their tails (Figure 3.13). *axin-B* is

a negative regulator of Wnt/βcatenin signaling in planarians whose inhibition results in two-tailed planarians, and it is expressed similarly to *wntP-2* in a posterior-to- anterior gradient (Almuedo-Castillo, Salo et al. 2011). Axins are well-known as feedback inhibitors of βcatenin signaling, so the expression of Axin was of interest to consider for determining the pathway involvement of *src.* Unlike *βcatenin-1* RNAi, *src-1* inhibition did not eliminate *axin-B* expression, but because of variable staining and the difficulty in detecting the *axin-B* transcript in these experiments, we could not unambiguously rule out the possibility that *src-1* inhibition mildly modifies *axinB* expression in some way. However, this analysis suggests that *src-1* inhibition likely does not eliminate *βcatenin* signaling along the body axis, similar to similar prior observations made after *wntP-2* and *ptk7* RNAi (Lander and Petersen 2016) (Figure 3.13).

Because *src-1(RNAi)* animals could regenerate an apparently normal posterior pole, we were interested to determine whether expression of other posterior PCGs would be affected after *src-1* RNAi. The expression of the posterior PCGs, *fzd-4,* and *wnt11-1* was unchanged in uninjured *src-1(RNAi)* animals and also in tail fragments regenerating their heads at 14 days amputation (Figure 3.14). However, *src-1(RNAi)* head fragments undergoing tail regeneration had reduced *fzd-4* and *wnt11-1* expression (Figure 3.14). These observations suggest that *src-1* may regulate or allow for the expression and activation of posterior PCGs such as *fzd-4* and *wnt11-1* in regeneration, perhaps independently or downstream of posterior pole formation.

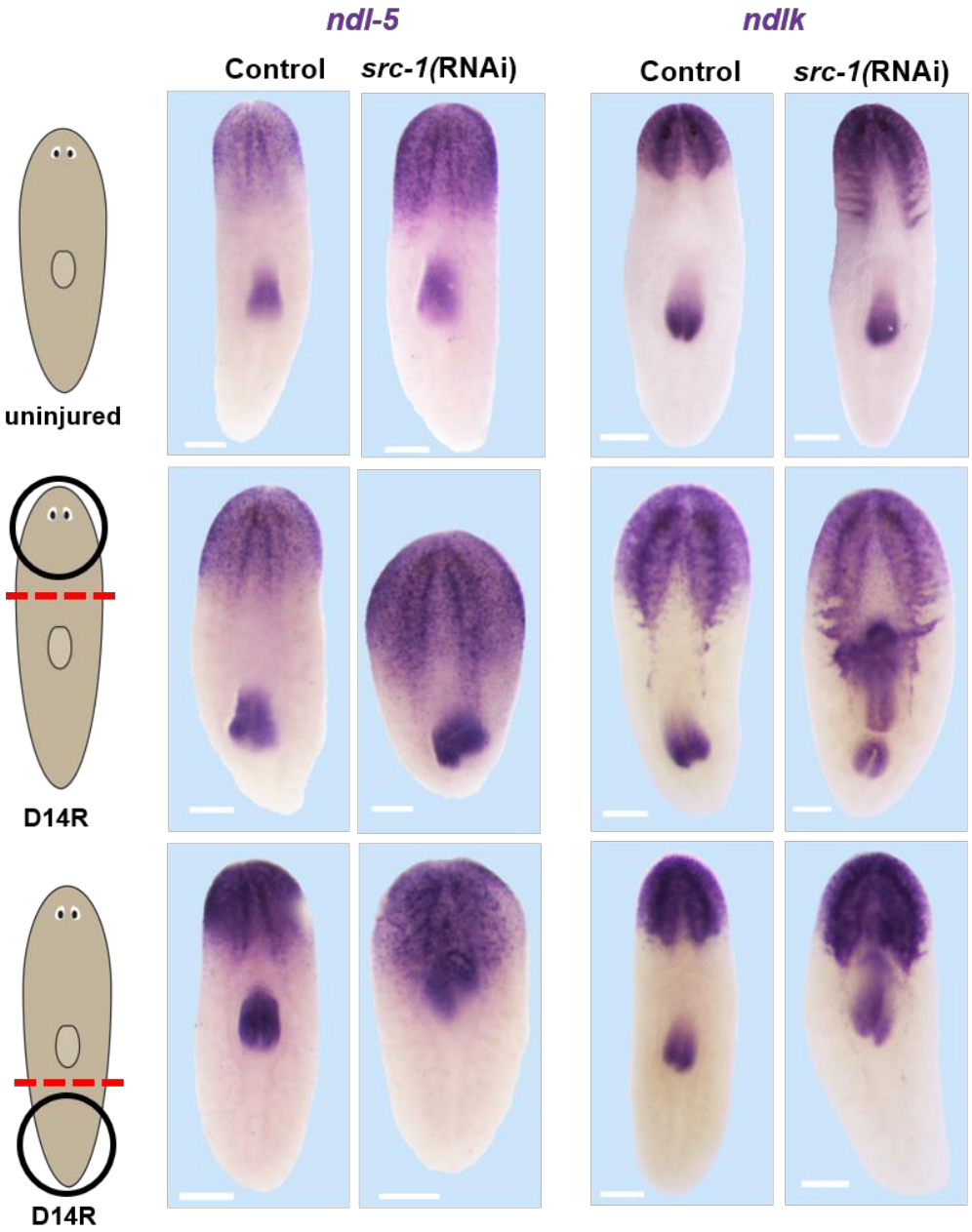

Fig 3.11 *src-1* Restricts Anterior Positionally Controlled Genes

src-1(RNAi) uninjured animals, regenerating head and tail fragments 14 days post amputation have expanded *ndl-5* and *ndk* domains as compared to controls as determined by WISH. Scale bars: 300 um.
Experiments performed by Dr. Nicolle Bonar

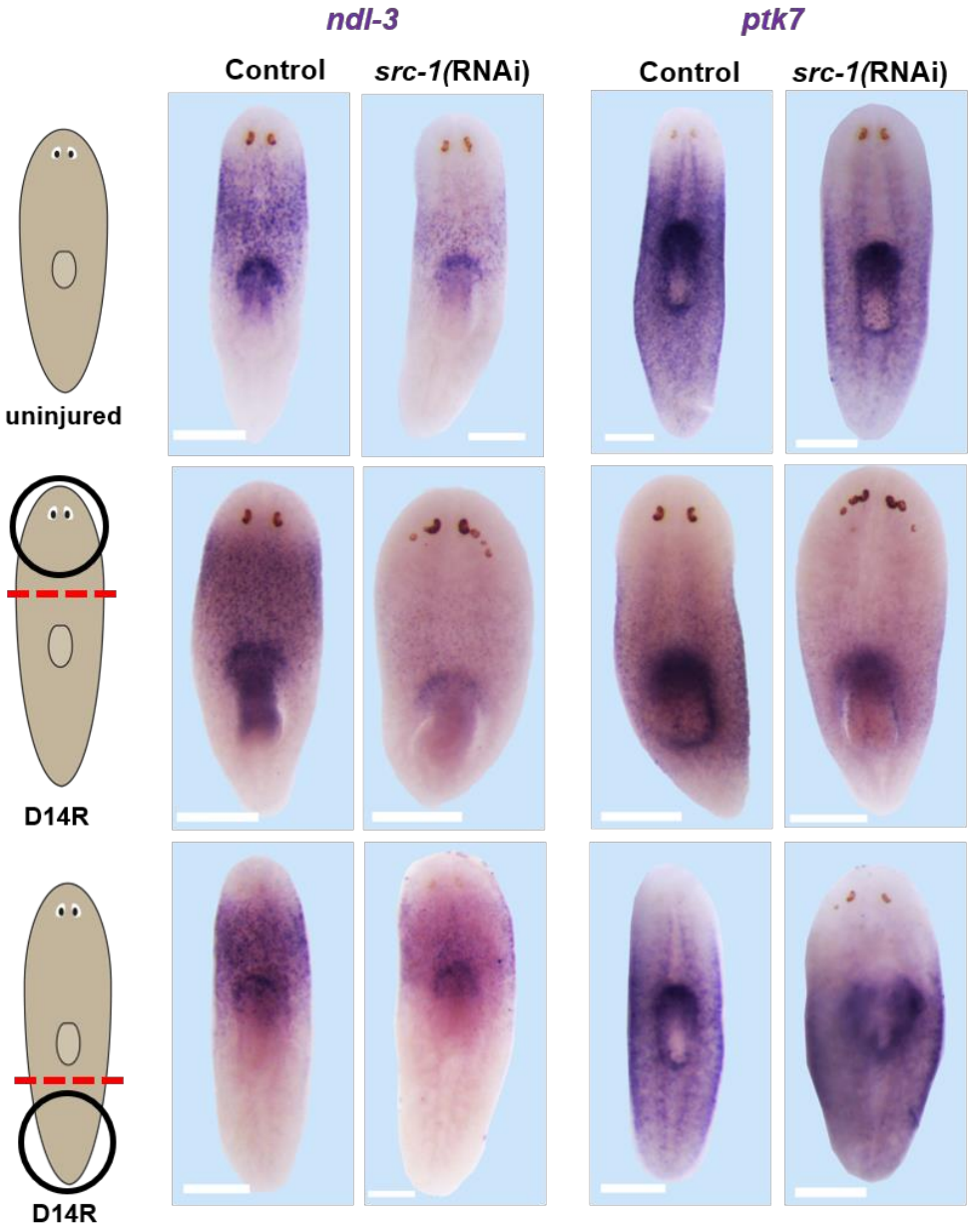

Fig 3.12 *src-1* Suppresses Trunk Positionally Controlled Genes

src-1(RNAi) uninjured animals, regenerating head and tail fragments 14 days post amputation have contracted anterior *ndl-3* and *ptk7* domains as compared to controls as determined by WISH. Scale bars: 300 um.
Experiments performed by Dr. Nicolle Bonar

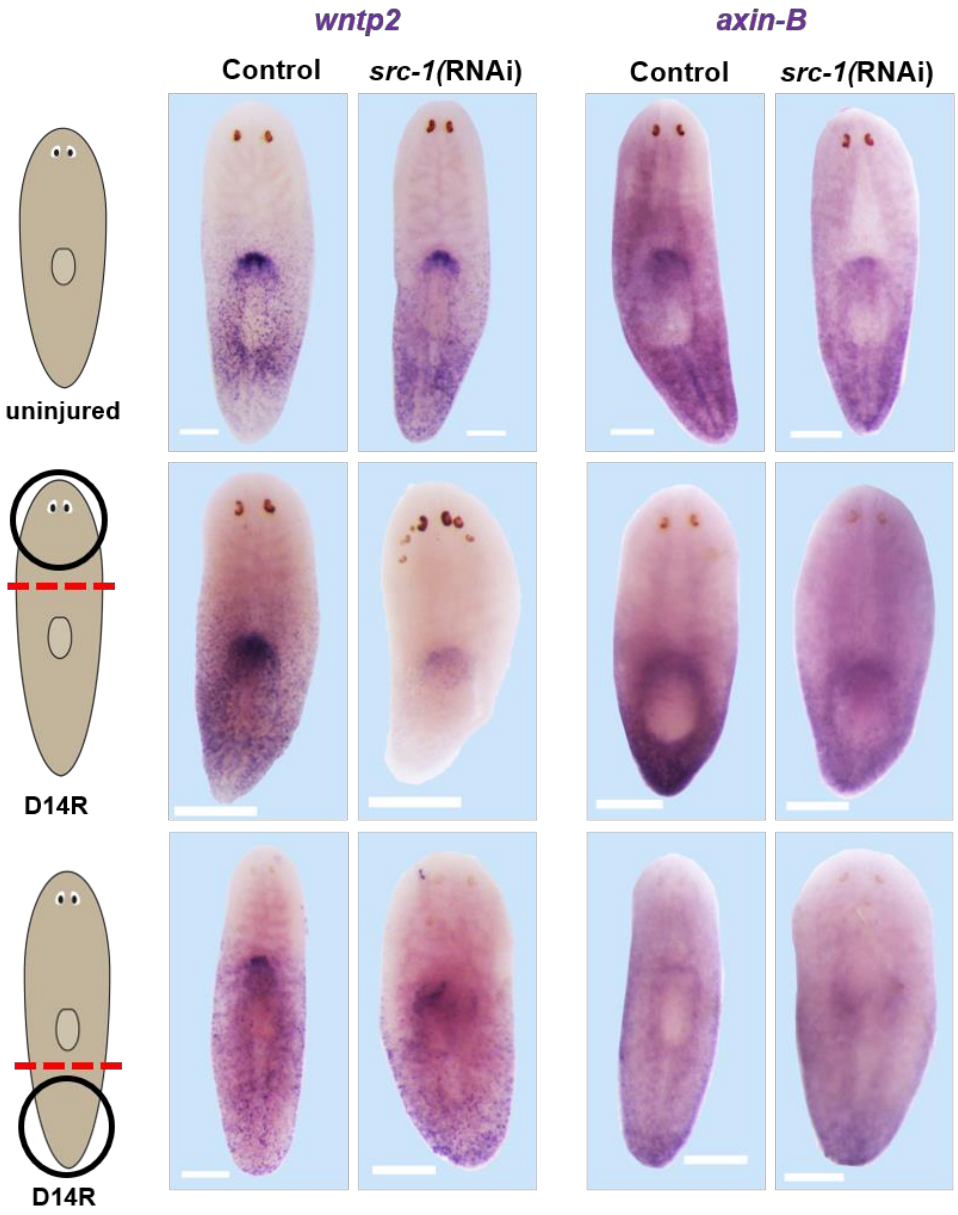

Fig 3.13 *src-1* Effects Expression of Medial-Posterior Genes

src-1(RNAi) uninjured animals and regenerating tail fragments have no change in *wntp-2* expression. *src-1(RNAi)* regenerating head fragments have reduced posterior *wntp-2* expression. *src-1(RNAi)* uninjured animals and regenerating head and tail fragments have variable *axin-B* expression as determined by WISH. Scale bars: 300 um.
Experiments performed by Dr. Nicolle Bonar

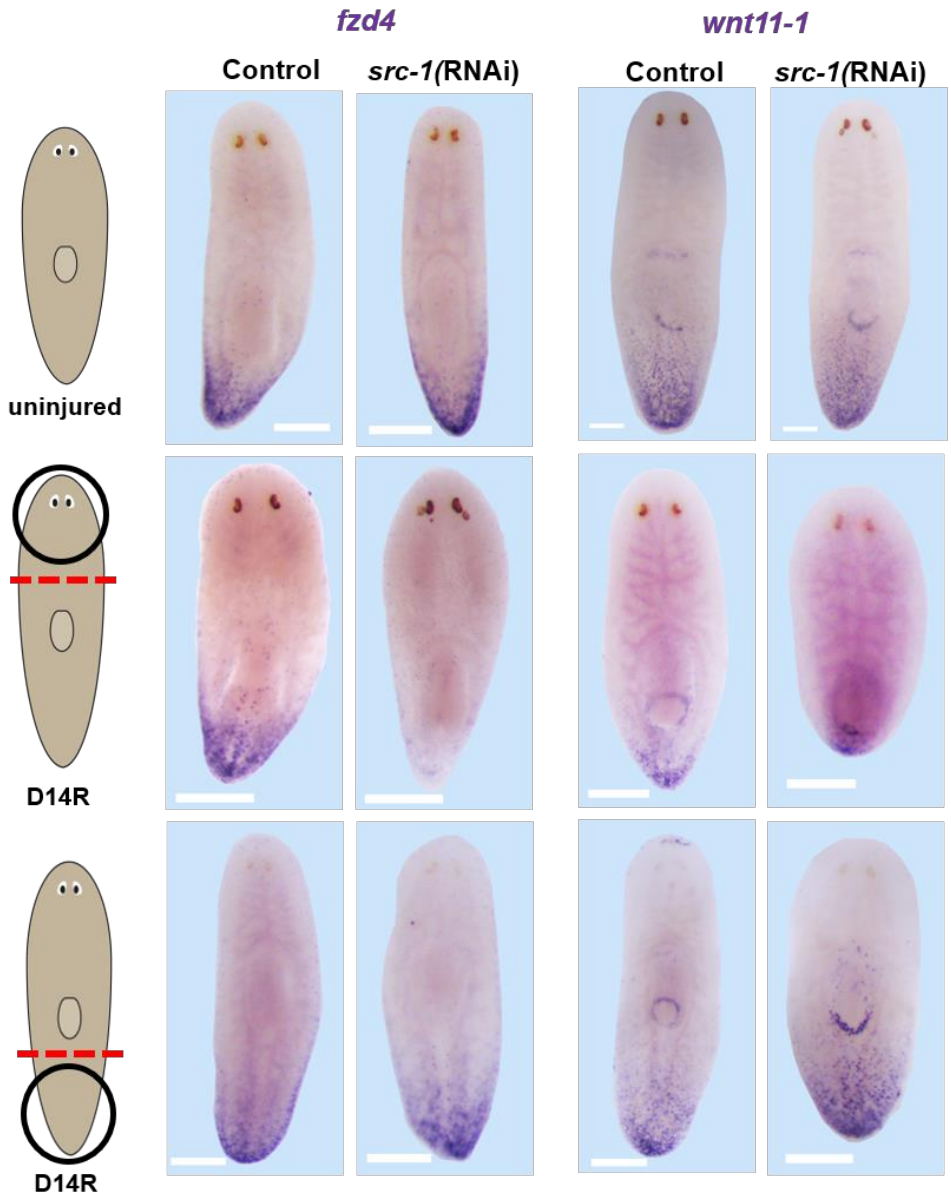

Fig 3.14 *src-1* Regulates Posterior Positionally Controlled Genes in Regeneration

src-1(RNAi) uninjured animals and regenerating tail fragments 14 days post amputation have normal *fzd4* and *wnt11-1* expression as determined by WISH. *src-1(RNAi)* regenerating head fragments 14 days post amputation have reduced *fzd4* and *wnt11-1* expression. Scale bars: 300 um.
Experiments performed by Dr. Nicolle Bonar

src-1 likely acts independently of *notum/wnt11-6* in head patterning

Srcs are intracellular tyrosine kinase that can act as a signaling hub of multiple pathways and influence many cellular processes (Parsons and Parsons 2004). Given that *src-1* inhibition expands the anterior domain of PCGs, and results in brain expansion and posterior ectopic eye phenotypes reminiscent of *ndk* and *wnt11-6* RNAi (Cebria, Kobayashi et al. 2002, Hill and Petersen 2015), we sought to determine whether *src-1* might signal downstream of either factor. To address this question, we designed an epistasis experiment using double RNAi. *notum(RNAi)* head fragments form an ectopic set of eyes within the head tip anterior to the pre-existing photoreceptors, whereas wnt11-6(RNAi) head fragments undergoing brain remodeling form an ectopic set of eyes posterior to the pre-existing eyes. Concurrent inhibition of *notum* and *wnt11-6* suppresses the anterior ectopic photoreceptor and small brain phenotype caused by *notum* inhibition and instead results in an increased brain size like *wnt11-6(RNAi)* animals. Therefore, *wnt11-6* likely acts downstream and oppositely to *notum* (Hill and Petersen 2015).

Thus, we wanted to determine whether the concurrent inhibition of notum and src would produce similar results. *src-1(RNAi)* head fragments, like *wnt11-6(RNAi)* head fragments, form an ectopic set of posterior photoreceptors posterior to the original photoreceptors. However, simultaneous inhibition of *notum* and *src-1* in amputated head fragments produced several RNAi phenotypes: 24 of 42 animals exhibited a synthetic phenotype with both posterior and anterior photoreceptors, 9 of 42 animals had a *notum(RNAi)* phenotype with only anterior photoreceptors, 6 of 42 animals exhibited a *src-1(RNAi)* phenotype and had only posterior photoreceptors, and 3 of 42 animals appeared normal (Figure 3.15). The observation of a synthetic phenotype after inhibition of both src-1 and notum but not after inhibition of notum and *wnt11-6* suggests that src-1 might not signal exclusively downstream of *wnt11-6* within the head. In support of this,

simultaneous inhibition of *notum* and *src-1* in amputated head fragments led to a brain size (as measured by *cintillo*$^{+}$ cell number) that was neither small like *notum(RNAi)* nor large like *src-1(RNAi)* but instead a size in between the two RNAi phenotypes (Figure 3.16). This further suggests that src-1 can act to restrict brain size and head identity independently of notum.

We next sought to determine whether *src-1* could instead act only downstream of *ndk.* However, there are no known negative regulators of *ndk*, so we wanted to determine if notum itself likely acts upstream, downstream or independent of *ndk.* Similar to simultaneous inhibition of *notum* and *src-1*, simultaneous inhibition of *notum* and *ndk* in amputated head fragments produced several RNAi phenotypes; 5 of 48 animals exhibited a synthetic phenotype with both posterior and anterior photoreceptors, 30 of 48 animals had a *notum(RNAi)* phenotype with only anterior photoreceptors, 5 of 48 animals exhibited a *ndk(RNAi)* phenotype and had only posterior photoreceptors, and 8 of 48 animals appeared normal (Figure 3.17). The presence of a synthetic phenotype and anterior photoreceptor *notum(RNAi)* like phenotype suggests that *ndk* does not act exclusively downstream of notum and can act independently of notum to restrict head identity. And double inhibition of these factors in amputated head fragments undergoing brain remodeling led to a brain size (as measured by *cintillo*$^{+}$ cell number) that was neither small like *notum(RNAi)* or large like *ndk(RNAi)* but instead a size in between the two RNAi phenotypes (Figure 3.18). These results allow for the possibility that src-1 could be acting downstream, upstream, or independently of *ndk.*

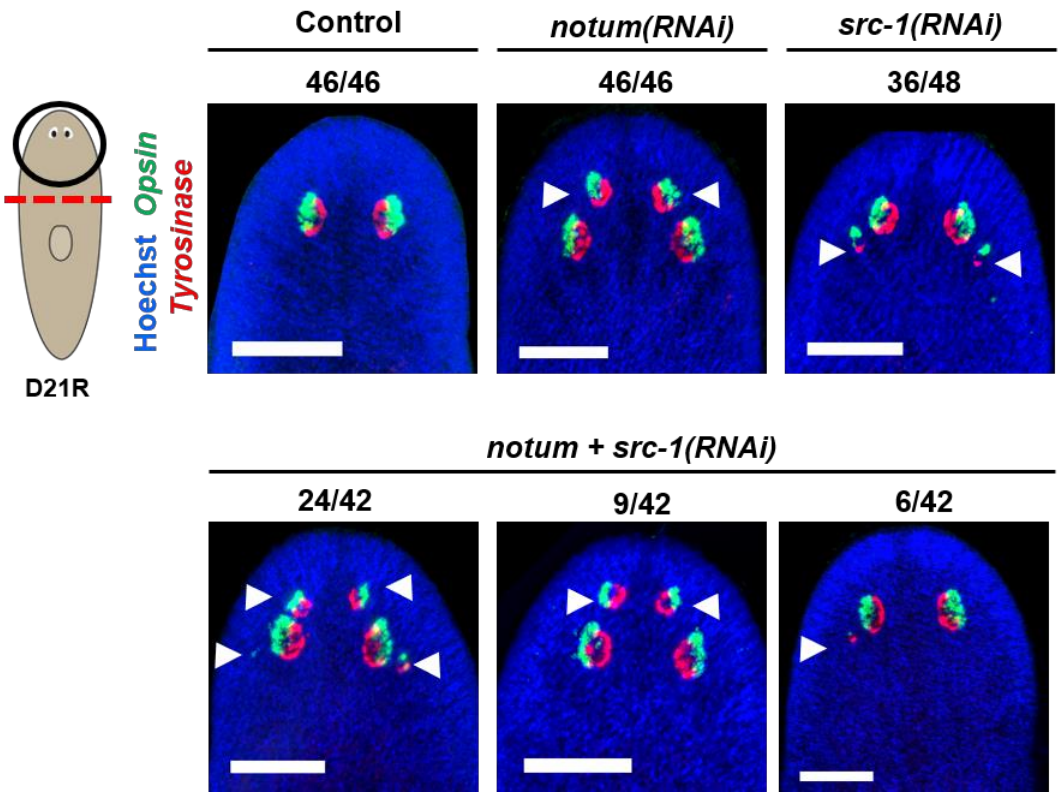

Fig 3.15 Simultaneous Inhibition of *notum* and *src-1* Creates a Synthetic Eye Phenotype

FISH to detect expression of opsin (green), a marker of photoreceptor neurons, and tyrosine (red), a marker of pigment cup cells, in control, *src-1;notum(RNAi)* regenerating head fragments. Hoechst (blue) used as a counterstain to detect nuclei. Ectopic regenerated eyes (white arrows). *notum(RNAi)* caused the formation of anterior ectopic eyes, and *src-1(RNAi)* caused the formation of posterior ectopic eyes, simultaneous inhibition of *src-1* and *notum(RNAi)* resulted in a synthetic phenotype in 24/42 animals with both anterior and posterior ectopic eyes. Scale bars: 150 um.
Experiments performed by Dr. Nicolle Bonar

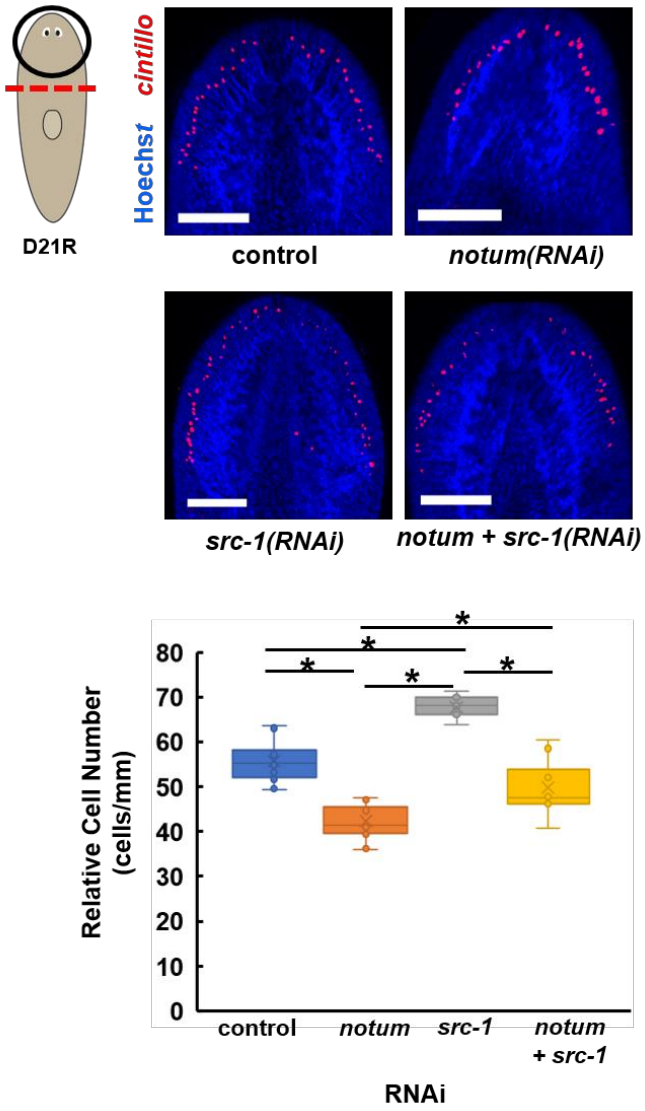

Fig 3.16 Simultaneous Inhibition of *notum* and *src-1* Creates an Intermediate Brain Size Phenotype

Top, FISH to detect expression of *cintillo* (red), a marker of chemosensory neurons, in control, *src-1, notum,* and *src-1;notum(RNAi)* regenerating head fragments. Bottom, quantification of *cintillo*$^{+}$ cell number normalized to animal size. *, $p<0.05$. Scale bars: 150 um. *notum* RNAi caused the formation of a smaller brain, *src-1(RNAi)* caused the formation of a larger brain, simultaneous inhibition of *src-1* and *notum(RNAi)* resulted in an intermediate brain size between those of single RNAi phenotypes.
Experiments performed by Dr. Nicolle Bonar

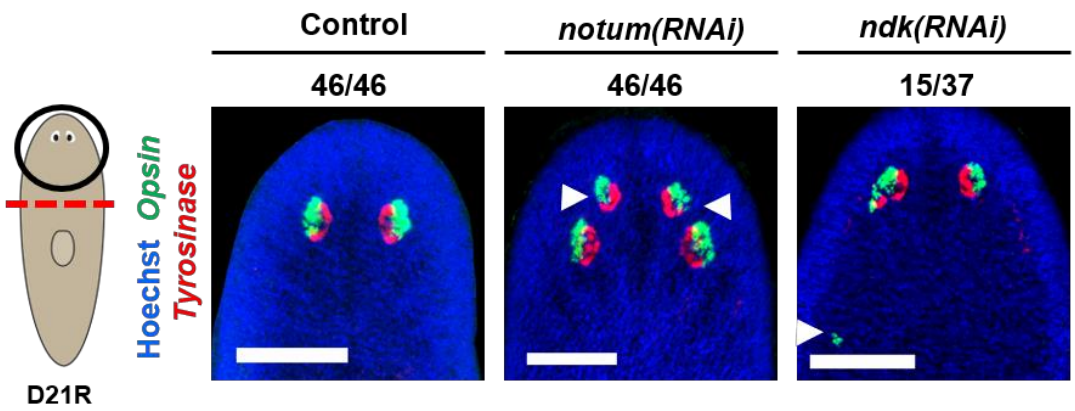

Fig 3.17 Simultaneous Inhibition of *notum* and *ndk* Creates a Synthetic Eye Phenotype

FISH to detect expression of *opsin* (green), a marker of photoreceptor neurons, and *tyrosinase* (red), a marker of pigment cup cells, in control, *ndk, notum* and *ndk;notum(RNAi)* regenerating head fragments. Hoechst (blue) used as a counterstain to detect nuclei. Ectopic regenerated eyes (white arrows). *notum(RNAi)* caused the formation of anterior ectopic eyes, and *ndk(RNAi)* caused the formation of posterior ectopic eyes. Simultaneous inhibition of *notum* and *ndk* resulted in a synthetic phenotype in 5/48 animals with both anterior and posterior ectopic eyes. Scale bars: 150 um.
Experiments performed by Dr. Nicolle Bonar

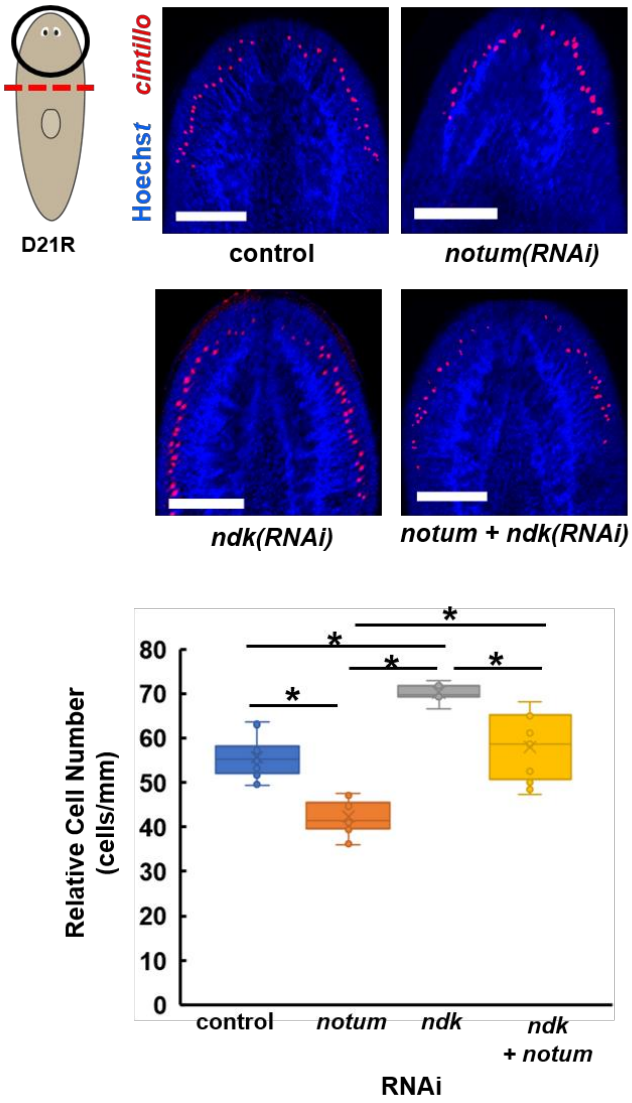

Fig 3.18 Simultaneous Inhibition of *notum* and *ndk* Creates an Intermediate Brain Size Phenotype

Top, FISH to detect expression of *cinitillo* (red), a marker of chemosensory neurons, in control, *ndk, notum* and *ndk;notum(RNAi)* regenerating head fragments. Bottom, quantification of *cintillo*$^{+}$ cell number normalized to animal size. *, P<0.05. Scale bars: 150 um. *notum(RNAi)* caused the formation of a smaller brain, and *ndk(RNAi)* caused the formation of a larger brain as compared to the control, simultaneous inhibition of *src-1* and *ndk* resulted in an intermediate sized brain in between the brain size of individual RNAi phenotypes.
Experiments performed by Dr. Nicolle Bonar

src-1 inhibition broadly sensitizes animals to AP pattern disruption

We next examined the genetic interaction between *src-1* and *ndk* through simultaneous inhibition. Double RNAi of these factors lead to a dramatic phenotype in regenerating head fragments, in which large numbers of ectopic posterior photoreceptors were formed, extending almost the entire length of the AP axis (Figure 3.19). This effect, as measured by number of ectopic photoreceptors, was greater than either individual RNAi phenotype or simple addition of the two effects. This suggested that *src-1* and *ndk* act through separate and partially redundant pathways to restrict anterior identity, such that loss of both produces a synthetic phenotype.

In some cases, simultaneous inhibition of *src-1* with *wnt11-6, ndk* or *src-2* led to patterning phenotypes distinct from head expansion. At a low penetrance, such animals underwent a polarity reversal in which animals regenerated a posterior-facing head rather than a tail (Figure 3.20). Other animals undergoing co-inhibition of *src-1* and either *wnt11-6*, *ndk*, *fzd5/8-4* or *src-2* formed ectopic pharynges at a low penetrance reminiscent to *wntP-2, ptk7, or ndl-3* RNAi (Figure 3.21). These results indicate the *src-1* can interact with multiple head patterning factors to restrict not only head but also trunk identity.

Next, we explored the effects of simultaneous *src-1* inhibition with the patterning factors known to restrict trunk but not head identity in planarians (Lander and Petersen 2016, Scimone, Cote et al. 2016). Simultaneous inhibition of *src-1* and either *ndl-3, ptk7* or *wntP-2* RNAi had no additional effect on the size of the head domain as determined by brain size measurements (Figure 3.22). *src-1* inhibition enhanced the ectopic pharynx phenotype after inhibition of *ndl-3* and *ptk7* but did not strongly enhance the already highly penetrant *wntP-2(RNAi)* ectopic pharynx phenotype (Figure 3.23). These results indicate the *src-1* can participate with other trunk PCGs to control trunk patterning, likely independent of head regionalization.

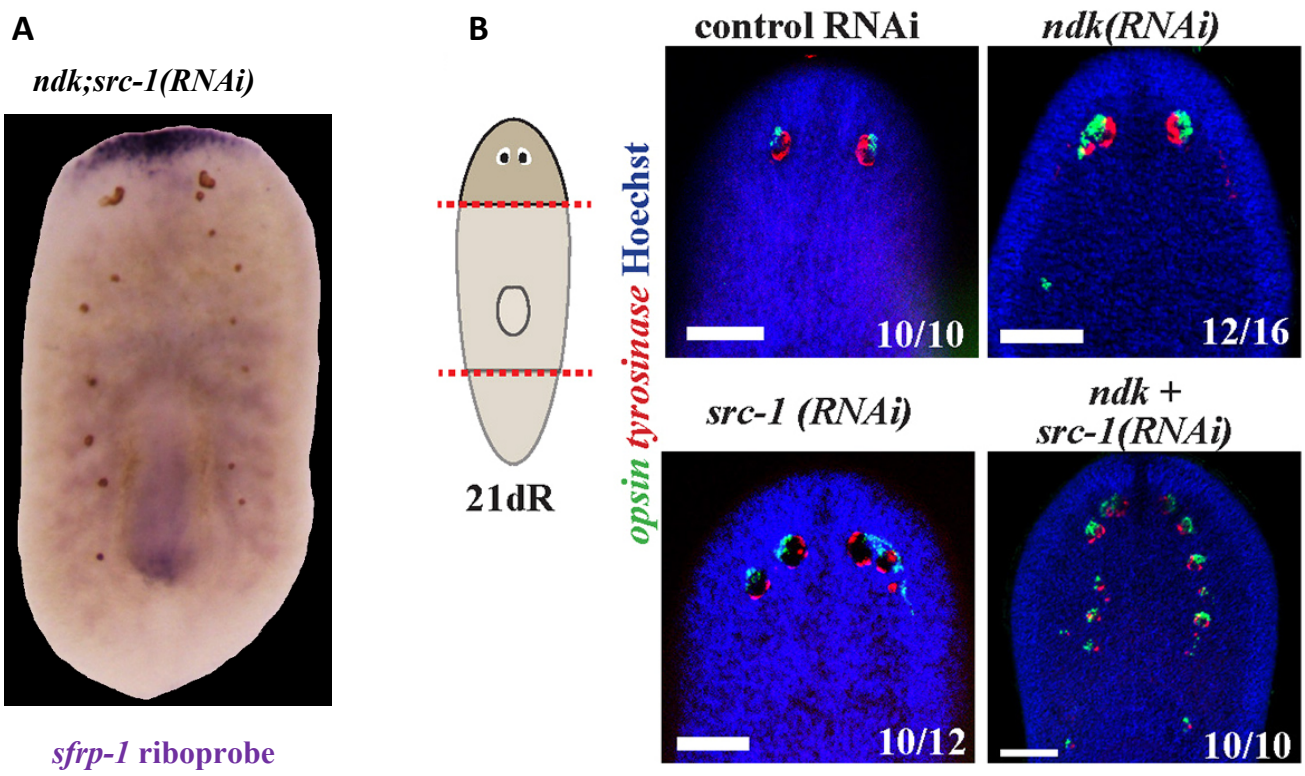

Fig 3.19 Simultaneous Inhibition of *src-1* and *ndk* Leads to Dramatic Posterior Photoreceptor Phenotype

A) Colorimetric *in situ* hybridization for *sfrp-1* in regenerated *src-1;ndk(RNAi)* head fragment. Note 13 ectopic eyes visible as brown circles.
B) FISH to detect expression of *opsin* (green), a marker of photoreceptor neurons, and *tyrosinase* (red), a marker of pigment cup cells, in control, *ndk, src-1* and *ndk;src-1(RNAi)* regenerating head fragments. Hoechst (blue) used as a counterstain to detect nuclei. Simultaneous inhibition of *src-1* and *ndk* created a synthetic phenotype of numerous ectopic eyes extending into the posterior of the animal.
Experiments performed by David Gittin

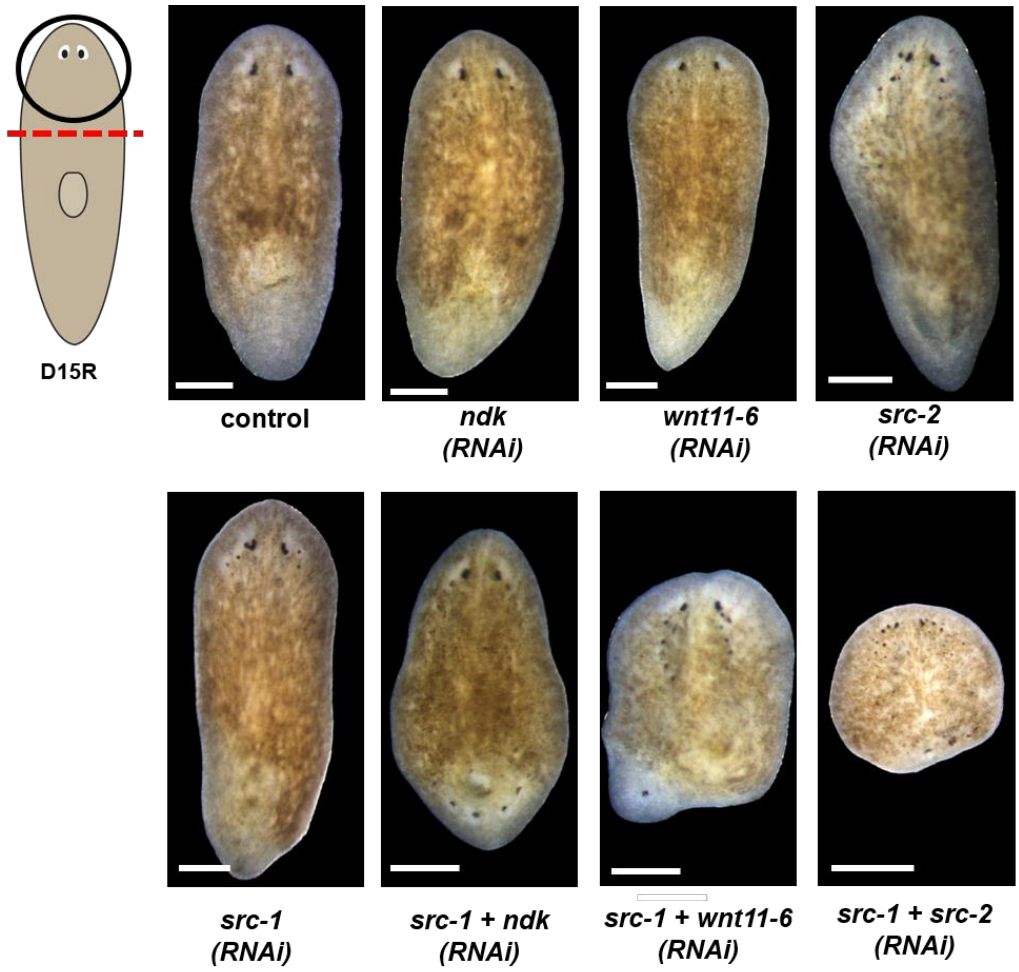

Fig 3.20 Simultaneous *src-1* Inhibition with Anterior Suppressors Can Cause a Polarity Reversal

Live images or regenerating head fragments at day 21 post amputation for the RNAi conditions indicated. Simultaneous inhibition of *src-1* with *wnt11-6, ndk,* or *src-2,* in some cases (<10%) resulted in a polarity reversal as evident by the formation of ectopic eyes at the posterior blastema. Scale bars: 300 um.
Experiments performed by Dr. Nicolle Bonar

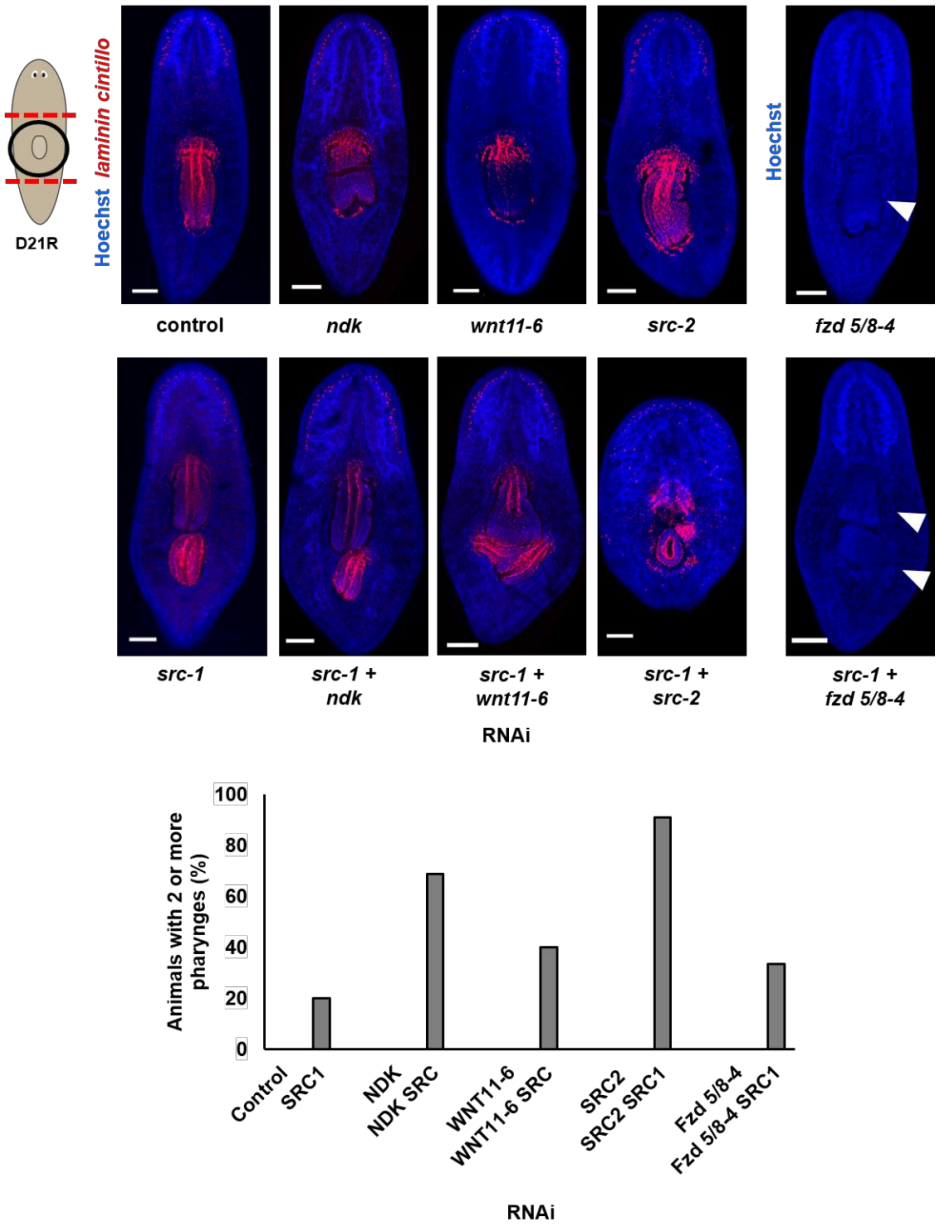

Fig 3.21 Simultaneous *src-1* Inhibition with Anterior Suppressors Expands Trunk Identity

Top, FISH to detect expression of *laminin* (red), a pharynx marker, and *cintillo* (red), a marker of chemosensory neurons, in trunk fragments at day 21 post amputation in the RNAi condition indicated. Hoechst (blue) used as a counterstain to detect nuclei. Simultaneous inhibition of *src-1* with *wnt11-6, ndk, fzd5/8-4* or *src-2,* resulted in the formation of ectopic posterior pharynges. Bottom, percent of animals with two or more pharynges for the RNAi condition indicated. Scale bars: 150 um.
Experiments performed by Dr. Nicolle Bonar

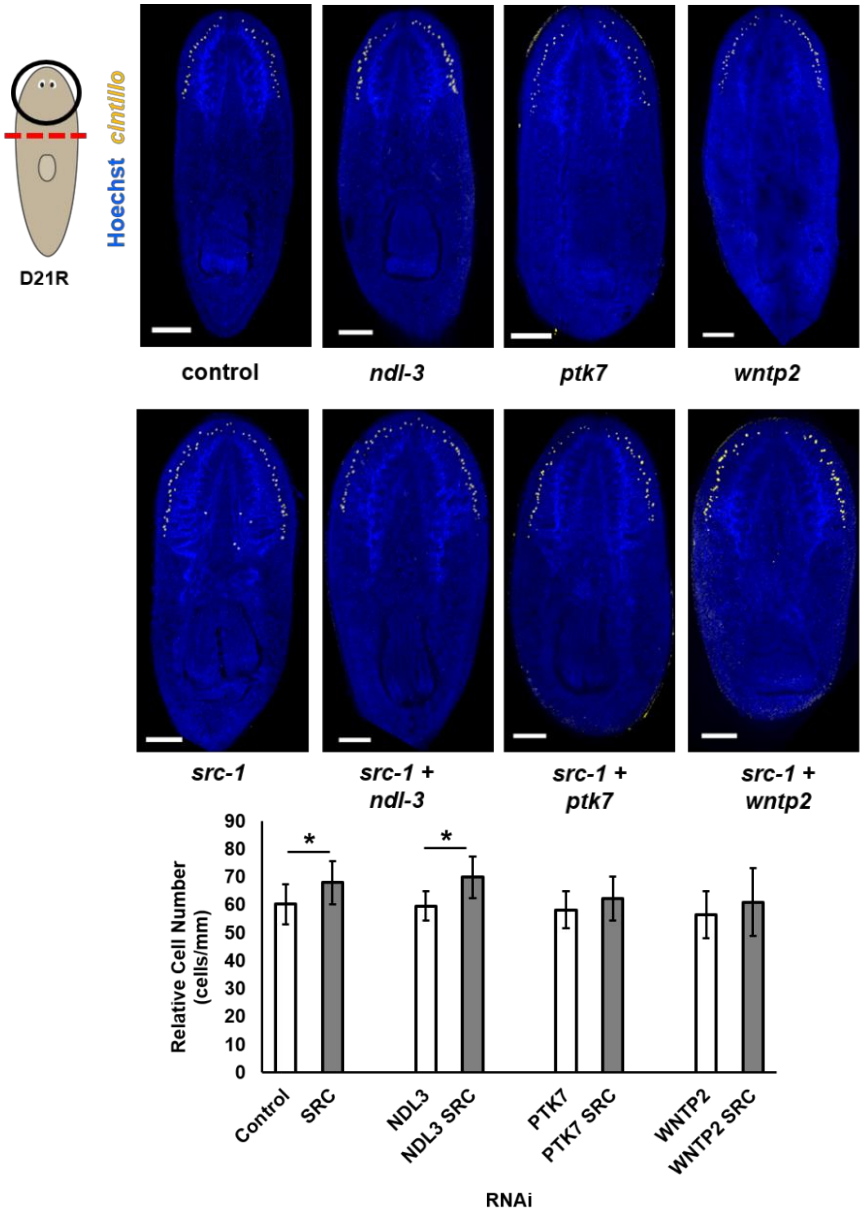

Fig 3.22 Simultaneous *src-1* Inhibition with Trunk Identity Suppressors does not Enhance Brain Size

Top, FISH to detect expression of *cintillo* (yellow), a marker of chemosensory neurons, in head fragments at day 21 post amputation in the indicated RNAi conditions. Hoechst (blue) used as a counterstain to detect nuclei. Bottom, quantification of *cintillo*+ cell number normalized to animal size. *, $p<0.05$. Scale bars: 150 um. Simultaneous inhibition of *src-1* with patterning factors known to restrict trunk identity, *ndl-3, ptk7,* or *wntp-2*, did not result in the formation of a larger brain greater than the effects of *src-1(RNAi)* alone. Scale bars: 150 um. Experiments performed by Dr. Nicolle Bonar

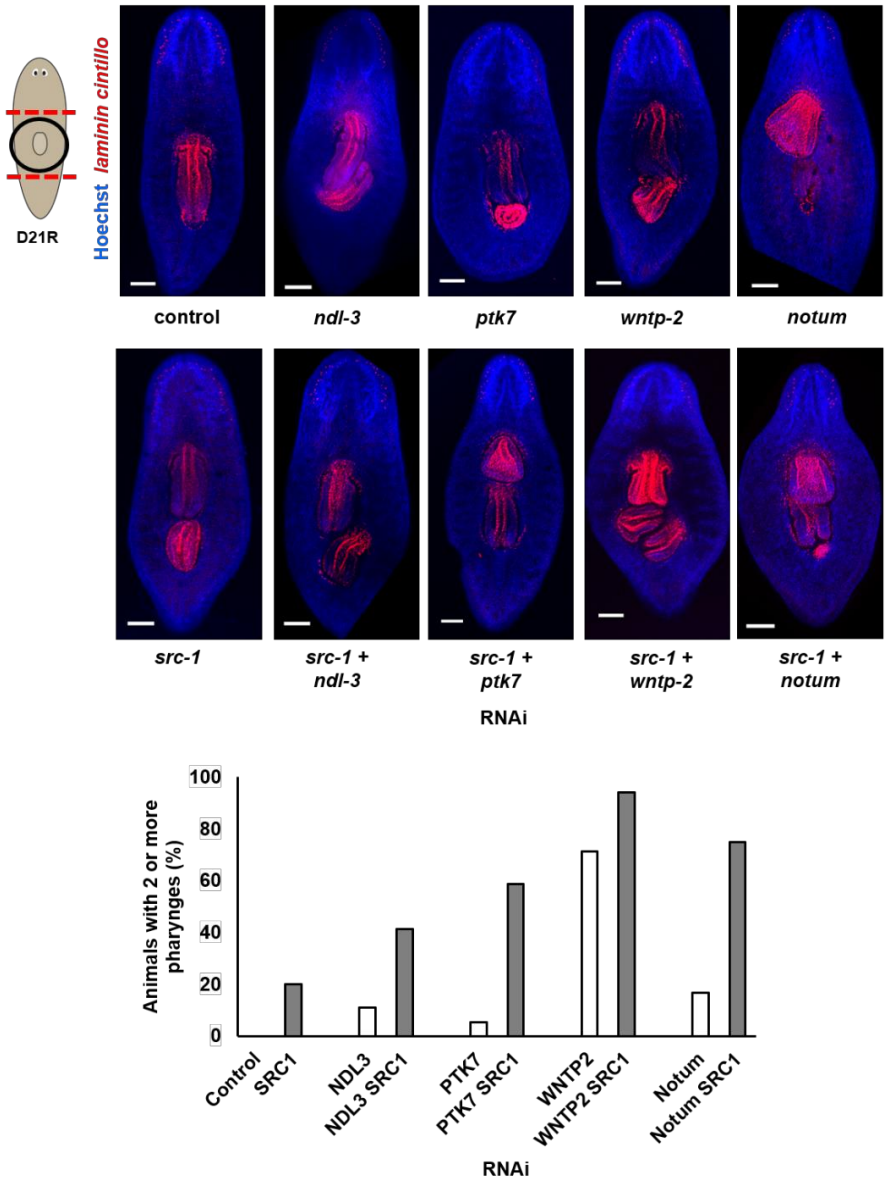

Fig 3.23 Simultaneous *src-1* Inhibition with Regulators of Trunk Identity Enhances the Formation of Ectopic Pharynges.

Top, FISH to detect expression of *laminin* (red), a pharynx maker, and *cintillo* (red), a marker of chemosensory neurons, in trunk fragments at day 21 post amputation in the RNAi condition indicated. Hoechst (blue) used as a counterstain to detect nuclei. Simultaneous inhibition of *src-1* with *ndl-3, ptk7, wntp-2* or *notum*, resulted in the formation of ectopic posterior pharynges at a greater penetrance than *src-1, ndl-3, ptk7, wntp-2* or *notum* alone. Bottom, percent of animals with two or more pharynges for the RNAi condition indicated. Scales bars: 300 um. Experiments performed by Dr. Nicolle Bonar

Possible relationships between *src-1* and AP polarity

At a low penetrance (1 in 20 animals), *src-1(RNAi)* regenerating trunk fragments regenerated an ectopic posterior head along with a posterior tail to form a novel two-headed, one-tailed animal that we termed "3-pronged" (Figure 3.24). This phenotype is distinct from *βcatenin-1* RNAi, but suggested a potential weak involvement for *src-1* in determining AP axis polarization. We tested whether simultaneous inhibition *of src-1* with other patterning factors could cause more penetrant polarity reversals. We had already observed a low penetrance polarity reversal after simultaneous inhibition of *src-1* along with either *wnt11-6, ndk,* or *src-2* inhibition. *wnt-1* is responsible for the formation of the posterior pole (Petersen and Reddien 2009), and *wnt1* inhibition causes regeneration of a posterior head at low penetrance (1 in 9 animals in this experiment). Co-inhibition of *src-1* and *wnt-1* dramatically enhanced this phenotype, caused the formation of a posterior head in 8 of 10 animals. Similarly, dual inhibition of *src-1* and trunk identity factors *fzd1/2/7* and *ptk7* also resulted in the formation of a posterior head at high penetrance, an effect not seen at all for *ptk7* inhibition alone (Figure 3.24). Furthermore, we found that dual inhibition of *src-1* and *ndl-2* (an anterior PCG with no known function) resulted in a higher penetrance of the 2-headed, one-tailed phenotype. Together these results suggest *src-1* may participate in AP axis polarization pathways. Cross-regulatory interactions among PCGs have not yet been fully explored, but prior work found that like *wntP-2* RNAi can dramatically enhance the *wnt1(RNAi)* double-headed phenotype, similar to *src-1* RNAi. These data implicate *src-1* is a global patterning regulator in planaria linking multiple aspects of posterior determination including restricting head and trunk identity and regulating polarity decision.

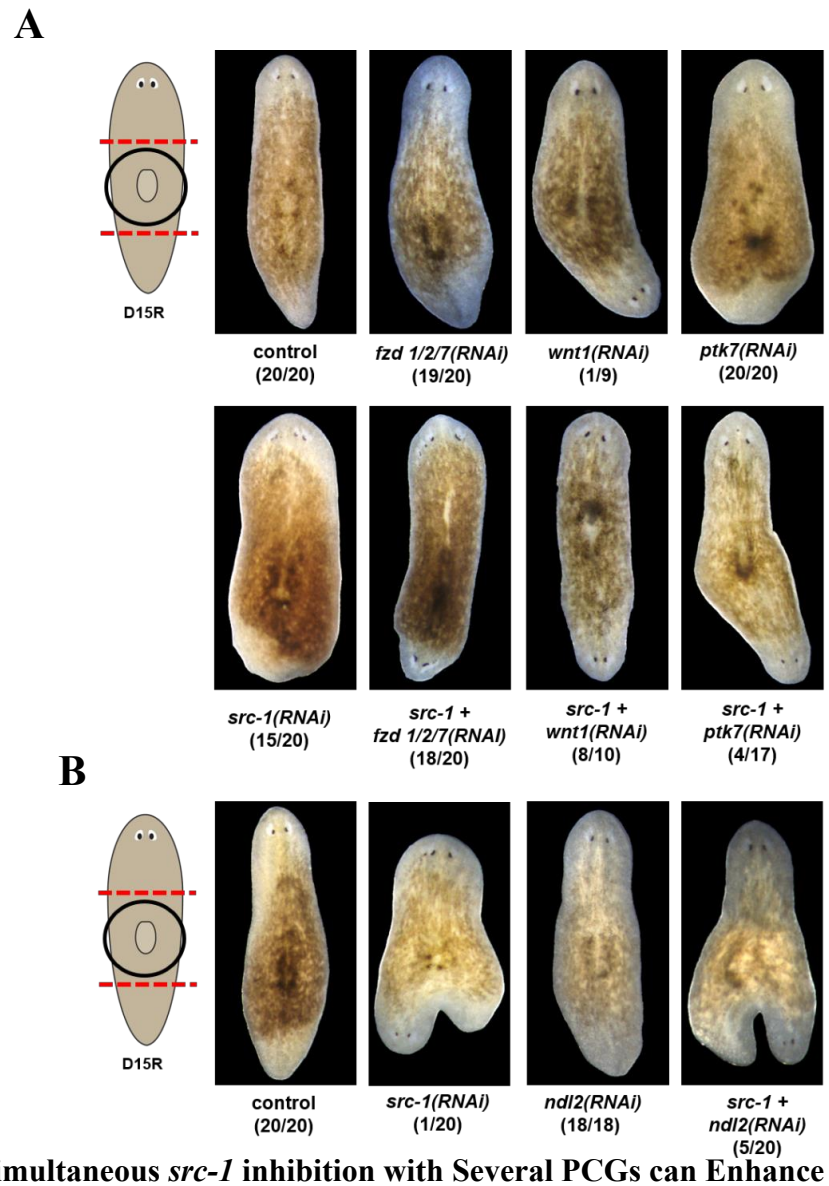

Fig 3.24 Simultaneous *src-1* inhibition with Several PCGs can Enhance Polarity Reversal

Live images of regenerating trunk fragments at day 15 post amputation for the RNAi conditions indicated.

A) *wnt1(RNAi)* caused the regeneration of a posterior head at low penetrance (1/9). Co-inhibition of *src-1* and *wnt1* enhanced this phenotype causing the formation of a posterior head in 8/10 animals. Simultaneous inhibition of *src-1* and trunk identity factors *fzd1/2/7* and *ptk7* resulted in the formation of a posterior head at high penetrance.
B) Bottom, at a low penetrance (1 in 20 animals), *src-1(RNAi)* animals regenerated an ectopic posterior head and a posterior tail to form two-headed, one-tailed animal, this phenotype was enhanced with simultaneous inhibition of *src-1* and *ndl-2* (5 of 20 animals).
Experiments performed by Dr. Nicolle Bonar

Discussion

Together, these findings suggest a role for *src-1* in controlling anterior patterning during planarian regeneration (Figure 3.25). We found *src-1* to acts as a global negative regulator of anterior patterning as its inhibition resulted in the expansion of both head and trunk identity. These effects were largely independent of hallmarks of head-tail AP axis polarization: injury-induced *wnt1* or *notum* expression and the formation of *wnt1* and *notum* poles. However, *src-1* could participate with other factors to control head/tail polarity. Canonical Wnt signaling is responsible for the head versus tail polarity decision in planarian regeneration (Petersen and Reddien 2008, Petersen and Reddien 2009, Petersen and Reddien 2011) while two Wnt and FGFRL "gene circuits" have been shown to be responsible for positional control of both the head and trunk region (Lander and Petersen 2016, Scimone, Cote et al. 2016). It is unclear if positional control of the head region occurs through canonical or non-canonical Wnt signaling.

Given that Src is an intracellular kinase known to act a downstream of multiple receptors we sought to determine whether *src-1* could be acting a regulator of anterior patterning through involvement in canonical Wnt signaling, non-canonical Wnt signaling or FGFRL signaling.

The canonical Wnt signaling pathway stimulates the nuclear accumulation of βcatenin to allow for Wnt-induced gene transcription. Upon Wnt binding to Frizzled receptors, recruitment of Dishevelled leads to disassembly of the βcatenin destruction complex through the sequestration of Axin, thus allowing βcatenin to translocate to the nucleus to activate gene expression via the activation of the TCF/LEF transcription factors (Gao and Chen 2010).

One possible connection between Src and canonical Wnt signaling is that Src has been found to bind to and activate vertebrate Dishevelled-2 (Dvl2), potentiating activation of canonical Wnt downstream (Yokoyama and Malbon 2009). Notably, inhibition of planarian *dvl-2* caused the

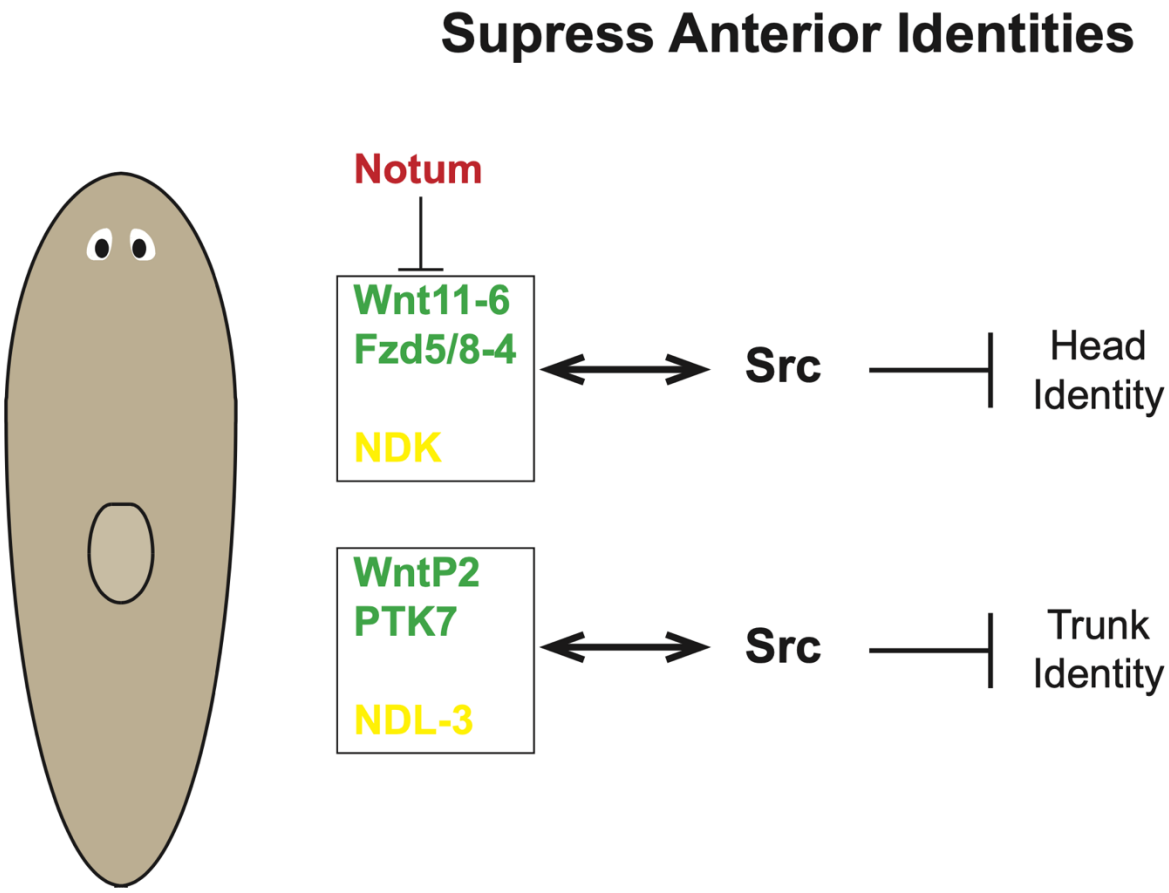

Fig 3.25 SRC: A Suppressor of Anterior Identities

We propose a role for *src-1* in planarian regeneration as a global suppressor of anterior identities where it acts act with known Wnt/FGFRL circuits to restrict the expansion of both head and trunk identity.
Figure courtesy of Dr. Nicolle Bonar

simultaneous formation of a secondary ectopic pharynx and posterior ectopic photoreceptors (Almuedo-Castillo, Salo et al. 2011) similar to the *src-1(RNAi)* phenotype. Furthermore, reduced doses of *βcatenin* dsRNA have been reported to result in the formation of an ectopic posterior mouth and pharynx primordium (Almuedo-Castillo, Salo et al. 2011). Similarly, reduced doses of *notum* dsRNA can also result in the formation of an ectopic anterior mouth and pharynx primordium (Figure 3.23). This suggests that an intermediate level of canonical Wnt signaling could be needed for proper trunk identity and pharynx formation, consistent with an observed gradient of βcatenin protein from the tail into the head (Stuckemann, Cleland et al. 2017). This concurs with results obtained from a study (Sureda-Gomez, Pascual-Carreras et al. 2015), which found that inhibition of three posteriorly expressed Wnts (*Smed-wnt1*, *Smed-wnt11-2*, and *Smed-wnt11-1*) resulted in the formation of secondary pharynges. These authors proposed that these three Wnts could act in a βcatenin-dependent manner, nuclearizing Smed-βcatenin1 in different domains along the AP axis to control trunk identity. Our results show synergistic effects when *src-1* is simultaneously inhibited with *wnt1* or *fzd1/2/7*, causing an increased penetrance of a polarity reversal (Figure 3.24). Similarly, inhibition of *src-1* with *wntP-2* led to an expanded trunk region and a higher penetrance of the double pharynx phenotype (Figure 3.23). Dual inhibition of *src-1* and *notum* also produced enhanced a trunk duplication, although it is not yet clear whether this may have been a posterior or anterior duplication. This data could be consistent with a model in which in some contexts *src-1* can act downstream of canonical Wnt signaling potentially through *dishevelled-2* to control trunk identity and posterior polarity determination.

However, our data is not consistent with a model whereby *src-1* acts exclusively downstream of canonical Wnt signaling to control anterior identity and polarity. Simultaneous inhibition of *src-1* with the Wnt inhibitor *notum* created a synthetic phenotype whereby ~50% of

animals formed both *src-1(RNAi)* like posterior ectopic eyes and *notum(RNAi)* like anterior ectopic eyes (Figure 3.15). The presence of a synthetic phenotype suggests that *src-1* is not acting exclusively downstream of *notum* to control regional identity and could also be acting through non-canonical Wnt signaling or FGFRL signaling to regulate regional identity. Interestingly, Dishevelled has also been shown to act in non-canonical Wnt signaling and to mediate a Wnt5-derailed/Related to tyrosine kinase (RYK)–dependent signal (Gao and Chen 2010). Planarian *wnt5* is thought to define the lateral-medial axis in planarian regeneration (Gurley, Elliott et al. 2010), and inhibition of *dishevelled-1* in planaria has been shown to recapitulate aspects of the *wnt5(RNAi)* phenotype such as lateral separation of the planarian brain lobes (Almuedo-Castillo, Salo et al. 2011). The fact that the *src-1(RNAi)* phenotype produced ectopic posterior photoreceptors that are positioned at a lateral angle (Figure 3.3) and not directly posterior to the original photoreceptors might also be indicative for a role of *src-1* downstream of lateral *wnt-5* signals and posterior *wnt11-6* signals. Further, *src-1* inhibition also caused a lateral expansion of the anterior pole (Figure 3.9), an effect previously observed in *wnt5* RNAi.

In addition to a regulatory role for *src-1* downstream of both canonical and non-canonical signaling, we considered the possibility that the *src-1* could act downstream of an unidentified receptor or FGFRLs. FGFRL such as *ndk* and *ndl-3* have been shown to regulate regional identity in planaria (Cebria, Kobayashi et al. 2002, Lander and Petersen 2016, Scimone, Cote et al. 2016); however, the mechanism by which this signaling occurs is unclear. FGFRLs have been shown to act as decoy receptors in Xenopus embryos. The FGFRL1 ectodomain is shed from the cell membrane and binds to some FGF ligands with high affinity, including FGF2, FGF3, FGF4, FGF8, FGF10, and FGF22 to regulate FGF signaling (Steinberg, Zhuang et al. 2010). However, inhibition of FGF or FGFRs in planaria have not resulted in patterning phenotypes. The intracellular domain

of human FGFRL1 has been found to interact with Spred1 which may allow for intracellular signaling (Zhuang, Villiger et al. 2011). Further, in beta-cell insulin granules, the intracellular domain of FGFRL1 can bind SHP-1 via a SH2 domain to activate ERK signaling (Silva, Altamentova et al. 2013). Given the synergist effects of *src-1* inhibition with *ndk* and *ndl-3* (Figures 3.19, 3.22, 3.23) and the similar synergistic RNAi phenotypes seen with *ndk* and *fzd5/8-4* (Scimone, Cote et al. 2016) it is possible that there is cross-talk between Wnt and FGFRL signaling pathways to control body regionalization in planaria and that these may be mediated through *src-1*. On the other hand, the examination of the extra photoreceptor defect in *src-1* RNAi revealed more similarities with the *wnt11-6* phenotype than the *ndk* phenotype. First, *ndk* RNAi generated posterior photoreceptors located more distantly than either *wnt11-6* or *src-1* RNAi. Second, both *wnt11-6* and *src-1* RNAi tended to shift the location of eye regeneration more posteriorly, unlike *ndk* RNAi. These observations suggest *src-1* acts distinctly from *ndk.* However further experiments will be needed to elucidate this hypothesis.

Given the pleiotropic effects of *src-1* RNAi and a role for Src inhibition in regulating endocytosis (Schmid 2017) it could be hypothesized that widespread cellular changes in endocytic trafficking of receptors could result in the *src-1(RNAi)* patterning and blastema organization defects. However, we believe this mechanism is unlikely as clathrin-mediated endocytic signals were found to be required for both regeneration and to maintain homeostasis in planaria (Inoue, Hayashi et al. 2007) and we don't observe these changes in *src-1(RNAi)* animals.

Thus, taken together, we propose a role for *src-1* in globally suppressing anterior identity and regulating posterior determination through downstream activation of multiple pathways including both non-canonical and canonical Wnt signaling and possibly FGFRLs.

Materials and Methods

Planarian culture

Asexual strain CIW4 of the planarian *Schmidtea mediterranea* were maintained in 1× Montjuic salts at 19°C as described (Petersen and Reddien 2011). Planarians were fed a liver paste and starved for at least 7 days before experiments.

Cloning

Src-1 and SFK sequences were identified by blast using transcriptome assemblies of the planarian genome (respectively SMU15027599 and SMU15038708 at SmedGD, http://smedgd.stowers.org (Robb, Gotting et al. 2015); equivalent to dd_Smed_v6_2017_0_1 and dd_Smed_v6_3365_0_1 at PlanMine, http://planmine.mpi-cbg.de (Brandl, Moon et al. 2016)).

Riboprobes

Riboprobes and double-stranded RNA (dsRNA) for *src-1* were generated by *in vitro* transcription (NxGen, Lucigen) as described previously (Petersen and Reddien 2011). Riboprobes and dsRNAs for *src-1* were cloned by RTPCR into pGEM-T-easy. Other riboprobes (*chat, cintillo, gluR, opsin, tyrosinase, collagen, laminin, notum, wnt1, ndk, ndl-5, fzd4, wntp2, axinb, ptk7*) were as previously described (Oviedo, Newmark et al. 2003, Cebria, Guo et al. 2007, Reddien, Bermange et al. 2007, Wang, Zayas et al. 2007, Collins, Hou et al. 2010, Gurley, Elliott et al. 2010, Wenemoser and Reddien 2010, Petersen and Reddien 2011, Lapan and Reddien 2012, Currie and Pearson 2013, Marz, Seebeck et al. 2013)

RNAi

RNAi was performed either by dsRNA feeding. For RNAi, dsRNA was synthesized from *in vitro* transcription reactions (NxGen, Lucigen). dsRNA corresponding to *Caenorhabditis elegans unc-22*, not present in the planarian genome, served as a negative control. Unless noted otherwise, animals were fed a mixture of liver paste and dsRNA six times in 14 days prior to amputation of heads and tails 4 h after the final feeding.

In situ hybridization and immunostaining

Colorimetric (NBT/BCIP) or fluorescence *in situ* hybridizations were performed as described (Lander and Petersen 2016) after fixation in 4% formaldehyde and bleaching (Pearson, Eisenhoffer et al. 2009) using blocking solution containing 10% horse serum and western blot blocking reagent (Roche) (King and Newmark 2013). Digoxigenin- or fluorescein-labeled riboprobes were synthesized as described (Pearson, Eisenhoffer et al. 2009) and detected with anti- digoxigenin-HRP (1:2000, Roche/Sigma-Aldrich 11207733910, lot 10520200), anti-fluorescein- HRP (1:2000, Roche/Sigma-Aldrich 11426346910, lot 11211620) or anti-digoxigenin-AP (1:4000, Roche/Sigma-Aldrich 11093274910, lot 11265026). Hoechst 33342 (Invitrogen) was used at 1:1000 as a counterstain. For immunostainings, animals were fixed in Carnoy's solution as described (Hill and Petersen 2015), using tyramide amplification to detect labeling with rabbit anti-6G10 (1:3000, Cell Signaling D2C8, lot 3377S).

Image analysis

Live animals and NBT/BCIP-stained animals were imaged with a Leica M210F dissecting microscope and a Leica DFC295, with adjustments to brightness and contrast using Adobe

Photoshop. Whole animal fluorescence imaging was performed on either a Leica DM5500B compound microscope with Optigrid structured illumination system or a Leica laser scanning SPE confocal microscope at 40x or 63x, and presented images are maximum projections of a Z-series with adjustments to brightness and contrast using ImageJ and Photoshop. Plots were generated in Microsoft Excel or R (ggplot2).

Cell counting

cintillo^{+} cells in the brain were counted manually and normalized to the square root of the animal area determined using Hoechst staining and CellProfiler (Lamprecht, Sabatini et al. 2007).

Real-time PCR

Total RNA was extracted by mechanical homogenization in Trizol (Life Technologies), DNase-treated (TURBO DNAse, Ambion), and reverse transcribed with oligo-dT primers (Multiscribe reverse transcriptase, Applied Biosystems), and qPCR was performed using Eva Green PCR Master Mix (Biotium) from nine regenerating fragments in four replicates. Relative mRNA abundance was calculated using the delta-Ct method after verification of primer amplification efficiency, normalizing to ubiquilin expression. Reactions producing Ct values flagged by Grubb's outlier test with alpha outlier test with alpha <0.05 were discarded from analysis as described (Burns, Nixon et al. 2005). *P*-values below 0.05 by a two-tailed *t*-test were considered as significant.

Eye Regeneration Assays

Modified from (Hill and Petersen 2018). Briefly, worms were immobilized on ice for resection. Eyes were removed using a hypodermic needle. All animals were tracked individually and imaged one day prior to eye removal, one day after eye removal to confirm resection of eye tissue, and 22 days post-surgery to determine the regenerative outcome.

Chapter 4

General Discussion

Scope of thesis

The planarian flatworm *Schmidtea mediterranea* possesses remarkable regenerative ability, enabling recreation of an entire organism from a small fragment. This process involves correctly assessing AP orientation within the injured fragment to direct regeneration of appropriate head or tail structures. While strong evidence exists for Wnt signaling activity as the primary driver of AP polarity, it is still unclear how regenerating fragments recapitulate Wnt activity gradients after loss of the regions expressing key Wnt ligands. In particular, how Wnt signaling antagonist *notum* is asymmetrically expressed after injury to designate anterior-facing wounds.

This thesis aims to address the question of how injury-induced *notum* expression is regulated. Specifically, we show that activity of the genes *wnt11-1, wnt11-2, dvl-1* and *dvl*-2 during a critical period before injury is necessary to restrict injury-induced *notum* expression and maintain proper AP polarity during regeneration. Additionally, we identify a role for *src-1* as a global suppressor of anterior identities that acts with Wnt/FGFRL signaling. Together, these observations suggest a model by which AP polarity information is encoded across the body through polarization of signaling cues within body-wall muscle, which are then read out to control expression of Wnt signaling components in response to injury. This establishes anterior and posterior poles and a broad body-wide AP gradient of Wnt signaling activity, which is further integrated with regional cues to direct proper regeneration of structures along the AP axis.

Determinants of Antero-Posterior Polarity in Planarian Regeneration

Dvl/Wnt11 signaling restricts *notum* expression at posterior-facing wounds through a βcatenin independent mechanism

The importance of the asymmetric injury-induced expression of *notum* for the regeneration head/tail fate decision was identified by previous planarian researchers (Petersen and Reddien 2009). However, understanding of the molecular underpinning of this asymmetry was rudimentary, only extending to placing *notum* activation downstream of canonical Wnt signaling through βcatenin (Petersen and Reddien 2011). Through the investigations detailed in chapter 2, this understanding has been significantly expanded. While this work confirmed observations that βcatenin activity is necessary for *notum* expression, it additionally uncovered an as-yet unreported role for non-canonical Wnt signaling in control of *notum* polarization.

Key to these findings was the observation of an unexpected phenotype of *notum* overexpression and depolarization in *dvl-1;dvl-2(RNAi)* worms. While the planarian Dvls had previously been examined for a role in polarity determination (Almuedo-Castillo, Salo et al. 2011, Vu, Mansour et al. 2019) no research had been specifically conducted into their role in muscle cells or possible impact on *notum* expression. Seeing a dvl inhibition phenotype of *notum* over-expression, so radically at odds with the *notum* phenotype of *βcatenin-1* RNAi, suggested that some Wnts may signal through Dvls to oppose *notum* expression, inspiring an in-depth screening of the contributions of each individual Wnt ligand. This effort confirmed previous observations of the activity of *wnt1* and *wntP2* (Petersen and Reddien 2009) in enabling *notum* expression at anterior-facing wounds, as well as uncovering novel roles for *wnt11-1* and *wnt11-2* in restricting ectopic notum expression at posterior-facing wounds, without apparently contributing to AFW

expression, a novel phenotype. The techniques utilized in this research, in particular the use of double fluorescent *in situ* hybridization to co-label *notum* and muscle markers, are likely to be reused by subsequent researchers in the Petersen lab and the planaria community more generally as a robust and quantitative method for assessing *notum* expression at wound sites.

This mechanism is dependent on the growth of polarity-informing muscle cells

The mechanism(s) by which Dvl and Wnt11 activity regulate *notum* expression are still not completely elucidated, but considerable progress has been made through tying the RNAi phenotypes of these genes to reorganization of muscle morphology and identifying a dependence on a critical period of growth prior to injury. The use of sublethal irradiation to temporarily block neoblast proliferation, and thus production of new differentiated cells and growth generally, has been useful for the study of planaria in multiple contexts (Reddien and Sanchez Alvarado 2004). In this work, it enabled us to distinguish between two broad hypotheses of Dvl and Wnt11 activity, namely whether they exerted their effects on *notum* expression through controlling standing polarity within muscle cells, or through specifying proper polarization of newly created muscle cells. The elimination of ectopic *notum* expression RNAi phenotypes in irradiated worms strongly pointed towards the second possibility. This was supported by observations that irradiation could also partially block alteration of muscle orientation and overall body morphology caused by RNAi of *wnt11-1, wnt11-2, dvl-1* and *dvl-2*. Notably, irradiation only altered these RNAi phenotypes when administered well in advance of injury; not if given the day prior. This supports the idea that irradiation effects RNAi phenotypes by blocking new cell production and tissue turnover in the altered signaling environment, and not by direct irradiation effects, such as ablation of neoblasts.

src-1 acts downstream of multiple planarian Wnts to control tissue patterning

Investigations into the activity of the planarian gene *src-1* emerged out of a larger RNAi screen of receptor tyrosine kinases conducted by past lab members and were initially unrelated to this study of injury-induced *notum* expression. However, in the course of this research a commonality emerged, with both stories describing part of the overall process of anterior-posterior identity specification during regeneration. While the dvls and posterior wnt11s control body-wide AP patterning and re-specification of polarity during regeneration, *src-1* appears to act downstream of Wnt-FGFRL signaling in multiple regional contexts, though always with the same function of restricting anterior fate. This serves as a reminder that specifying the planarian AP axis is a complex and multistage process, with multiple signaling pathways likely working together in partial redundancy at different stages of regeneration/homeostatic maintenance and in body-wide vs regional contexts.

Significance of Work

The findings presented here provide the first comprehensive assessment of the role of all known Wnt signaling ligands in regulation of injury induced *notum* expression. We identify novel roles for genes *wnt11-1* and *wnt11-2* in restricting *notum* expression at posterior facing wounds, independent of overall *notum* expression. We also identify a novel role for the planarian Dvls in maintaining polarization of the *notum* injury response independent of their role in canonical Wnt Signaling. For these factors, we identify a critical period of action prior to injury, providing evidence that homeostatic mechanisms encode polarity information within the planarian tissues to be read out when needed to guide regeneration. Further, our work identifies a role for Src in suppressing anterior identity downstream of multiple pathways.

Future Directions

The findings in this work make important contributions towards the understanding of polarity determination and patterning in planarian regeneration, but many questions remain. This work has identified a key role for the signaling ligands *wnt11-1* and *wnt11-2* in regulating injury induced *notum* expression across the body. However, both of these genes are expressed only in relatively small domains near the posterior pole (Figure 2.20). This raises the question: how is signaling from posteriorly expressed *wnt11-1* and *wnt11-2* communicated across the body?

One possibility is that Wnt11-1 and Wnt11-2 proteins, while created in the posterior, are then moved across the body, broadly distributed to be able to exert effects at any position along the AP axis. The size of the Wnt proteins should limit creation of a body-wide gradient by simple diffusion (Gurley, Elliott et al. 2010), but active transport could be employed to create a long-distance protein gradient. To investigate this possibility, it would be necessary to develop

antibodies against these proteins compatible with whole-mount immunostaining. Unfortunately, the pool of available planarian antibodies is limited, and previous attempts to develop antibodies against Wnt ligands have repeatedly proven unsuccessful. Research in this vein was successful in creation of a βcatenin antibody capable of detecting protein levels through western blot, but incompatible with immunostaining (Stuckemann, Cleland et al. 2017), which could nonetheless be used to establish the presence of a βcatenin protein gradient along the anterior-posterior axis. A similar strategy could potentially be employed for the Wnt11 ligands.

Another alternative is that the Wnt11-1 and Wnt11-2 proteins are localized to the posterior, near their site of transcription, but communicate signals which are propagated across the body. A possible mechanism is suggested by the interaction of these factors with the planarian Dishevelleds. Dvls are known to be active within the planar cell polarity pathway, a signaling pathway which can transmit polarization information across long distances and is implicated in control of polarity within planarian epidermis (Vu, Mansour et al. 2019). Initial screens of planar cell polarity components have failed to yield *notum* expression phenotypes (experiments not included in this report), but the possibility remains that this is due to insufficient length of knockdown or a high degree of PCP factor redundancy, and that future research may identify a role for PCP in muscle polarization. Supporting this idea, Dvl activity is known to be essential for proper AP patterning during the development of multiple animal species (Wallingford and Habas 2005).

Investigation of muscle morphology through use of the 6G10 antibody has revealed that muscle becomes disorganized under the inhibition of the Dvls and Wnt11s, but that changes in injury induced *notum* expression from muscle fibers can precede visible disorganization (Figure 2.24). More detailed techniques to examine muscle morphology or orientation could reveal

changes in longitudinal muscle contemporaneous with alterations in its *notum* expressivity. For instance, a possible role of planar cell polarity in controlling muscle orientation could be investigated through staining of muscle fibers with antibodies for pathway components such as Diego/Diversin, the Vgls, or Prickled and observing whether these proteins localize to distinct complexes at either end of the muscle fiber.

A final possibility to be investigated is whether *notum* is truly the sole factor distinguishing anterior and posterior wound sites after injury. While repeated transcriptomic evaluation of injury sites has to date identified *notum* as unique in its expression asymmetry (Wurtzel, Cote et al. 2015, Fincher, Wurtzel et al. 2018), the possibility cannot be ruled out that other an as-yet unidentified genes react in a way specific to wound site orientation. If such genes are ever identified their requirement for proper regeneration should be determined, and epistatic relationship to *notum* and other Wnt signaling components in the head/tail fate decision should be investigated.

This work identified *src-1* as a global suppressor of anterior identities in planaria. *src-1* encodes an intracellular signaling kinase that likely acts downstream of both canonical and non-canonical Wnt signaling to restrict anterior identities in planarians. However, it is still unclear what signaling acts through or downstream of *src-1*. The identification of functional antibodies to detect Src activation states, as well as defining negative regulators of *src-1* signaling, would be invaluable for determining how *src-1* interacts with known or novel signaling pathways. In addition, *src-1* is only one of ten planarian Src family kinases, and these have not been fully explored. *src-2* also negatively regulates anterior patterning, though RNAi phenotypes after inhibition of this gene manifest with lower penetrance and expressivity (Figure 3.6). However, five of the ten planarians Src family kinases remain to be investigated for their effects on patterning. Determining the

function of the other Src family kinases could help to elucidate the roles of *src-1* in controlling positional information.

As is often the case in research, each question answered begets more questions. The knowledge gained in this thesis represents a step along a greater pathway to fully understanding the mechanisms of regeneration.

References

Adell, T., E. Salo, M. Boutros and K. Bartscherer (2009). "Smed-Evi/Wntless is required for beta-catenin-dependent and -independent processes during planarian regeneration." Development **136**(6): 905-910.

Agata, K., Y. Saito and E. Nakajima (2007). "Unifying principles of regeneration I: Epimorphosis versus morphallaxis." Dev Growth Differ **49**(2): 73-78.

Almuedo-Castillo, M., E. Salo and T. Adell (2011). "Dishevelled is essential for neural connectivity and planar cell polarity in planarians." Proc Natl Acad Sci U S A **108**(7): 2813-2818.

Atabay, K. D., S. A. LoCascio, T. de Hoog and P. W. Reddien (2018). "Self-organization and progenitor targeting generate stable patterns in planarian regeneration." Science **360**(6387): 404-409.

Aw, W. Y. and D. Devenport (2017). "Planar cell polarity: global inputs establishing cellular asymmetry." Curr Opin Cell Biol **44**: 110-116.

Benham-Pyle, B. W., C. E. Brewster, A. M. Kent, F. G. Mann, Jr., S. Chen, A. R. Scott, A. C. Box and A. Sanchez Alvarado (2021). "Identification of rare, transient post-mitotic cell states that are induced by injury and required for whole-body regeneration in Schmidtea mediterranea." Nat Cell Biol **23**(9): 939-952.

Blassberg, R. A., D. A. Felix, B. Tejada-Romero and A. A. Aboobaker (2013). "PBX/extradenticle is required to re-establish axial structures and polarity during planarian regeneration." Development **140**(4): 730-739.

Bode, H. R. (2009). "Axial patterning in hydra." Cold Spring Harb Perspect Biol **1**(1): a000463.

Brandl, H., H. Moon, M. Vila-Farre, S. Y. Liu, I. Henry and J. C. Rink (2016). "PlanMine--a mineable resource of planarian biology and biodiversity." Nucleic Acids Res **44**(D1): D764-773.

Burkhardt-Holm, P., Y. Oulmi, A. Schroeder, V. Storch and T. Braunbeck (1999). "Toxicity of 4-chloroaniline in early life stages of zebrafish (Danio rerio): II. Cytopathology and regeneration of liver and gills after prolonged exposure to waterborne 4-chloroaniline." Arch Environ Contam Toxicol **37**(1): 85-102.

Burns, M. J., G. J. Nixon, C. A. Foy and N. Harris (2005). "Standardisation of data from real-time quantitative PCR methods - evaluation of outliers and comparison of calibration curves." BMC Biotechnol **5**: 31.

Cebria, F. (2016). "Planarian Body-Wall Muscle: Regeneration and Function beyond a Simple Skeletal Support." Front Cell Dev Biol **4**: 8.

Cebria, F., T. Guo, J. Jopek and P. A. Newmark (2007). "Regeneration and maintenance of the planarian midline is regulated by a slit orthologue." Dev Biol **307**(2): 394-406.

Cebria, F., C. Kobayashi, Y. Umesono, M. Nakazawa, K. Mineta, K. Ikeo, T. Gojobori, M. Itoh, M. Taira, A. Sanchez Alvarado and K. Agata (2002). "FGFR-related gene nou-darake restricts brain tissues to the head region of planarians." Nature **419**(6907): 620-624.

Chan, A., S. Ma, B. J. Pearson and D. Chan (2021). "Collagen IV differentially regulates planarian stem cell potency and lineage progression." Proc Natl Acad Sci U S A **118**(16).

Chen, C. C., I. E. Wang and P. W. Reddien (2013). "pbx is required for pole and eye regeneration in planarians." Development **140**(4): 719-729.

Cloutier, J. K., C. L. McMann, I. M. Oderberg and P. W. Reddien (2021). "activin-2 is required for regeneration of polarity on the planarian anterior-posterior axis." PLoS Genet **17**(3): e1009466.

Collins, J. J., 3rd, X. Hou, E. V. Romanova, B. G. Lambrus, C. M. Miller, A. Saberi, J. V. Sweedler and P. A. Newmark (2010). "Genome-wide analyses reveal a role for peptide hormones in planarian germline development." PLoS Biol **8**(10): e1000509.

Cote, L. E., E. Simental and P. W. Reddien (2019). "Muscle functions as a connective tissue and source of extracellular matrix in planarians." Nat Commun **10**(1): 1592.

Currie, K. W. and B. J. Pearson (2013). "Transcription factors lhx1/5-1 and pitx are required for the maintenance and regeneration of serotonergic neurons in planarians." Development **140**(17): 3577-3588.

Das, S. K. and H. G. Brown (1978). "Management of lost finger tips in children." Hand **10**(1): 16-27.

Devenport, D. (2014). "The cell biology of planar cell polarity." J Cell Biol **207**(2): 171-179.

Douglas, B. S. (1972). "Conservative management of guillotine amputation of the finger in children." Aust Paediatr J **8**(2): 86-89.

Durant, F., J. Bischof, C. Fields, J. Morokuma, J. LaPalme, A. Hoi and M. Levin (2019). "The Role of Early Bioelectric Signals in the Regeneration of Planarian Anterior/Posterior Polarity." Biophys J **116**(5): 948-961.

Elliott, S. A. and A. Sanchez Alvarado (2013). "The history and enduring contributions of planarians to the study of animal regeneration." Wiley Interdiscip Rev Dev Biol **2**(3): 301-326.

Fincher, C. T., O. Wurtzel, T. de Hoog, K. M. Kravarik and P. W. Reddien (2018). "Cell type transcriptome atlas for the planarian Schmidtea mediterranea." Science **360**(6391).

Forsthoefel, D. J., A. E. Park and P. A. Newmark (2011). "Stem cell-based growth, regeneration, and remodeling of the planarian intestine." Dev Biol **356**(2): 445-459.

Forsthoefel, D. J., F. A. Waters and P. A. Newmark (2014). "Generation of cell type-specific monoclonal antibodies for the planarian and optimization of sample processing for immunolabeling." BMC Dev Biol **14**: 45.

Fritzenwanker, J. H., M. Saina and U. Technau (2004). "Analysis of forkhead and snail expression reveals epithelial-mesenchymal transitions during embryonic and larval development of Nematostella vectensis." Dev Biol **275**(2): 389-402.

Gao, C. and Y. G. Chen (2010). "Dishevelled: The hub of Wnt signaling." Cell Signal **22**(5): 717-727.

Gavino, M. A., D. Wenemoser, I. E. Wang and P. W. Reddien (2013). "Tissue absence initiates regeneration through follistatin-mediated inhibition of activin signaling." Elife **2**: e00247.

Grohme, M. A., S. Schloissnig, A. Rozanski, M. Pippel, G. R. Young, S. Winkler, H. Brandl, I. Henry, A. Dahl, S. Powell, M. Hiller, E. Myers and J. C. Rink (2018). "The genome of Schmidtea mediterranea and the evolution of core cellular mechanisms." Nature **554**(7690): 56-61.

Gros, J., O. Serralbo and C. Marcelle (2009). "WNT11 acts as a directional cue to organize the elongation of early muscle fibres." Nature **457**(7229): 589-593.

Gurley, K. A., S. A. Elliott, O. Simakov, H. A. Schmidt, T. W. Holstein and A. Sanchez Alvarado (2010). "Expression of secreted Wnt pathway components reveals unexpected complexity of the planarian amputation response." Dev Biol **347**(1): 24-39.

Gurley, K. A., J. C. Rink and A. Sanchez Alvarado (2008). "Beta-catenin defines head versus tail identity during planarian regeneration and homeostasis." Science **319**(5861): 323-327.

Hariharan, I. K. and F. Serras (2017). "Imaginal disc regeneration takes flight." Curr Opin Cell Biol **48**: 10-16.

Hayashi, T., M. Asami, S. Higuchi, N. Shibata and K. Agata (2006). "Isolation of planarian X-ray-sensitive stem cells by fluorescence-activated cell sorting." Dev Growth Differ **48**(6): 371-380.

Hayashi, T., M. Motoishi, S. Yazawa, K. Itomi, C. Tanegashima, O. Nishimura, K. Agata and H. Tarui (2011). "A LIM-homeobox gene is required for differentiation of Wnt-expressing cells at the posterior end of the planarian body." Development **138**(17): 3679-3688.

Heisenberg, C. P., M. Tada, G. J. Rauch, L. Saude, M. L. Concha, R. Geisler, D. L. Stemple, J. C. Smith and S. W. Wilson (2000). "Silberblick/Wnt11 mediates convergent extension movements during zebrafish gastrulation." Nature **405**(6782): 76-81.

Hill, E. M. and C. P. Petersen (2015). "Wnt/Notum spatial feedback inhibition controls neoblast differentiation to regulate reversible growth of the planarian brain." Development **142**(24): 4217-4229.

Hill, E. M. and C. P. Petersen (2018). "Positional information specifies the site of organ regeneration and not tissue maintenance in planarians." Elife **7**.

Hwang, W. Y., Y. Fu, D. Reyon, M. L. Maeder, P. Kaini, J. D. Sander, J. K. Joung, R. T. Peterson and J. R. Yeh (2013). "Heritable and precise zebrafish genome editing using a CRISPR-Cas system." PLoS One **8**(7): e68708.

Iglesias, M., M. Almuedo-Castillo, A. A. Aboobaker and E. Salo (2011). "Early planarian brain regeneration is independent of blastema polarity mediated by the Wnt/beta-catenin pathway." Dev Biol **358**(1): 68-78.

Iglesias, M., J. L. Gomez-Skarmeta, E. Salo and T. Adell (2008). "Silencing of Smed-betacatenin1 generates radial-like hypercephalized planarians." Development **135**(7): 1215-1221.

Illingworth, C. M. (1974). "Trapped fingers and amputated finger tips in children." J Pediatr Surg **9**(6): 853-858.

Inoue, T., T. Hayashi, K. Takechi and K. Agata (2007). "Clathrin-mediated endocytic signals are required for the regeneration of, as well as homeostasis in, the planarian CNS." Development **134**(9): 1679-1689.

Jopling, C., E. Sleep, M. Raya, M. Marti, A. Raya and J. C. Izpisua Belmonte (2010). "Zebrafish heart regeneration occurs by cardiomyocyte dedifferentiation and proliferation." Nature **464**(7288): 606-609.

Kakugawa, S., P. F. Langton, M. Zebisch, S. A. Howell, T. H. Chang, Y. Liu, T. Feizi, G. Bineva, N. O'Reilly, A. P. Snijders, E. Y. Jones and J. P. Vincent (2015). "Notum deacylates Wnt proteins to suppress signalling activity." Nature **519**(7542): 187-192.

Kawakami, Y., J. Capdevila, D. Buscher, T. Itoh, C. Rodriguez Esteban and J. C. Izpisua Belmonte (2001). "WNT signals control FGF-dependent limb initiation and AER induction in the chick embryo." Cell **104**(6): 891-900.

Kawakami, Y., C. Rodriguez Esteban, M. Raya, H. Kawakami, M. Marti, I. Dubova and J. C. Izpisua Belmonte (2006). "Wnt/beta-catenin signaling regulates vertebrate limb regeneration." Genes Dev **20**(23): 3232-3237.

Kierdorf, U., H. Kierdorf and T. Szuwart (2007). "Deer antler regeneration: cells, concepts, and controversies." J Morphol **268**(8): 726-738.

Kikuchi, K., J. E. Holdway, A. A. Werdich, R. M. Anderson, Y. Fang, G. F. Egnaczyk, T. Evans, C. A. Macrae, D. Y. Stainier and K. D. Poss (2010). "Primary contribution to zebrafish heart regeneration by gata4(+) cardiomyocytes." Nature **464**(7288): 601-605.

King, R. S. and P. A. Newmark (2013). "In situ hybridization protocol for enhanced detection of gene expression in the planarian Schmidtea mediterranea." BMC Dev Biol **13**: 8.

Kobayashi, C., Y. Saito, K. Ogawa and K. Agata (2007). "Wnt signaling is required for antero-posterior patterning of the planarian brain." Dev Biol **306**(2): 714-724.

Kragl, M., D. Knapp, E. Nacu, S. Khattak, M. Maden, H. H. Epperlein and E. M. Tanaka (2009). "Cells keep a memory of their tissue origin during axolotl limb regeneration." Nature **460**(7251): 60-65.

Kroehne, V., D. Freudenreich, S. Hans, J. Kaslin and M. Brand (2011). "Regeneration of the adult zebrafish brain from neurogenic radial glia-type progenitors." Development **138**(22): 4831-4841.

Lamprecht, M. R., D. M. Sabatini and A. E. Carpenter (2007). "CellProfiler: free, versatile software for automated biological image analysis." Biotechniques **42**(1): 71-75.

Lander, R. and C. P. Petersen (2016). "Wnt, Ptk7, and FGFRL expression gradients control trunk positional identity in planarian regeneration." Elife **5**.

Lapan, S. W. and P. W. Reddien (2012). "Transcriptome analysis of the planarian eye identifies ovo as a specific regulator of eye regeneration." Cell Rep **2**(2): 294-307.

Layden, M. J., F. Rentzsch and E. Rottinger (2016). "The rise of the starlet sea anemone Nematostella vectensis as a model system to investigate development and regeneration." Wiley Interdiscip Rev Dev Biol **5**(4): 408-428.

Lei, K., H. Thi-Kim Vu, R. D. Mohan, S. A. McKinney, C. W. Seidel, R. Alexander, K. Gotting, J. L. Workman and A. Sanchez Alvarado (2016). "Egf Signaling Directs Neoblast Repopulation by Regulating Asymmetric Cell Division in Planarians." Dev Cell **38**(4): 413-429.

Marques, I. J., E. Lupi and N. Mercader (2019). "Model systems for regeneration: zebrafish." Development **146**(18).

Marz, M., R. Schmidt, S. Rastegar and U. Strahle (2011). "Regenerative response following stab injury in the adult zebrafish telencephalon." Dev Dyn **240**(9): 2221-2231.

Marz, M., F. Seebeck and K. Bartscherer (2013). "A Pitx transcription factor controls the establishment and maintenance of the serotonergic lineage in planarians." Development **140**(22): 4499-4509.

Matsui, T., A. Raya, Y. Kawakami, C. Callol-Massot, J. Capdevila, C. Rodriguez-Esteban and J. C. Izpisua Belmonte (2005). "Noncanonical Wnt signaling regulates midline convergence of organ primordia during zebrafish development." Genes Dev **19**(1): 164-175.

Morgan, T. H. (1898). "Developmental Mechanics." Science **7**(162): 156-158.

Morgan, T. H. (1901). "Regeneration and Liability to Injury." Science **14**(346): 235-248.

Moss, J. B., P. Koustubhan, M. Greenman, M. J. Parsons, I. Walter and L. G. Moss (2009). "Regeneration of the pancreas in adult zebrafish." Diabetes **58**(8): 1844-1851.

Newmark, P. A. and A. Sanchez Alvarado (2000). "Bromodeoxyuridine specifically labels the regenerative stem cells of planarians." Dev Biol **220**(2): 142-153.

Newmark, P. A., Y. Wang and T. Chong (2008). "Germ cell specification and regeneration in planarians." Cold Spring Harb Symp Quant Biol **73**: 573-581.

Oviedo, N. J., J. Morokuma, P. Walentek, I. P. Kema, M. B. Gu, J. M. Ahn, J. S. Hwang, T. Gojobori and M. Levin (2010). "Long-range neural and gap junction protein-mediated cues control polarity during planarian regeneration." Dev Biol **339**(1): 188-199.

Oviedo, N. J., P. A. Newmark and A. Sanchez Alvarado (2003). "Allometric scaling and proportion regulation in the freshwater planarian Schmidtea mediterranea." Dev Dyn **226**(2): 326-333.

Owen, J. H., D. E. Wagner, C. C. Chen, C. P. Petersen and P. W. Reddien (2015). "teashirt is required for head-versus-tail regeneration polarity in planarians." Development **142**(6): 1062-1072.

Owlarn, S. and K. Bartscherer (2016). "Go ahead, grow a head! A planarian's guide to anterior regeneration." Regeneration (Oxf) **3**(3): 139-155.

Parsons, S. J. and J. T. Parsons (2004). "Src family kinases, key regulators of signal transduction." Oncogene **23**(48): 7906-7909.

Pearson, B. J., G. T. Eisenhoffer, K. A. Gurley, J. C. Rink, D. E. Miller and A. Sanchez Alvarado (2009). "Formaldehyde-based whole-mount in situ hybridization method for planarians." Dev Dyn **238**(2): 443-450.

Pellettieri, J., P. Fitzgerald, S. Watanabe, J. Mancuso, D. R. Green and A. Sanchez Alvarado (2010). "Cell death and tissue remodeling in planarian regeneration." Dev Biol **338**(1): 76-85.

Petersen, C. P. and P. W. Reddien (2008). "Smed-betacatenin-1 is required for anteroposterior blastema polarity in planarian regeneration." Science **319**(5861): 327-330.

Petersen, C. P. and P. W. Reddien (2009). "A wound-induced Wnt expression program controls planarian regeneration polarity." Proc Natl Acad Sci U S A **106**(40): 17061-17066.

Petersen, C. P. and P. W. Reddien (2011). "Polarized notum activation at wounds inhibits Wnt function to promote planarian head regeneration." Science **332**(6031): 852-855.

Poss, K. D., L. G. Wilson and M. T. Keating (2002). "Heart regeneration in zebrafish." Science **298**(5601): 2188-2190.

Ramirez, A. N., K. Loubet-Senear and M. Srivastava (2020). "A Regulatory Program for Initiation of Wnt Signaling during Posterior Regeneration." Cell Rep **32**(9): 108098.

Raz, A. A., M. Srivastava, R. Salvamoser and P. W. Reddien (2017). "Acoel regeneration mechanisms indicate an ancient role for muscle in regenerative patterning." Nat Commun **8**(1): 1260.

Reddien, P. W. (2011). "Constitutive gene expression and the specification of tissue identity in adult planarian biology." Trends Genet **27**(7): 277-285.

Reddien, P. W. (2018). "The Cellular and Molecular Basis for Planarian Regeneration." Cell **175**(2): 327-345.

Reddien, P. W., A. L. Bermange, A. M. Kicza and A. Sanchez Alvarado (2007). "BMP signaling regulates the dorsal planarian midline and is needed for asymmetric regeneration." Development **134**(22): 4043-4051.

Reddien, P. W., A. L. Bermange, K. J. Murfitt, J. R. Jennings and A. Sanchez Alvarado (2005). "Identification of genes needed for regeneration, stem cell function, and tissue homeostasis by systematic gene perturbation in planaria." Dev Cell **8**(5): 635-649.

Reddien, P. W., N. J. Oviedo, J. R. Jennings, J. C. Jenkin and A. Sanchez Alvarado (2005). "SMEDWI-2 is a PIWI-like protein that regulates planarian stem cells." Science **310**(5752): 1327-1330.

Reddien, P. W. and A. Sanchez Alvarado (2004). "Fundamentals of planarian regeneration." Annu Rev Cell Dev Biol **20**: 725-757.

Reuter, H., M. Marz, M. C. Vogg, D. Eccles, L. Grifol-Boldu, D. Wehner, S. Owlarn, T. Adell, G. Weidinger and K. Bartscherer (2015). "Beta-catenin-dependent control of positional information along the AP body axis in planarians involves a teashirt family member." Cell Rep **10**(2): 253-265.

Riddiford, N. and P. D. Olson (2011). "Wnt gene loss in flatworms." Dev Genes Evol **221**(4): 187-197.

Rink, J. C., K. A. Gurley, S. A. Elliott and A. Sanchez Alvarado (2009). "Planarian Hh signaling regulates regeneration polarity and links Hh pathway evolution to cilia." Science **326**(5958): 1406-1410.

Rink, J. C., H. T. Vu and A. Sanchez Alvarado (2011). "The maintenance and regeneration of the planarian excretory system are regulated by EGFR signaling." Development **138**(17): 3769-3780.

Robb, S. M., K. Gotting, E. Ross and A. Sanchez Alvarado (2015). "SmedGD 2.0: The Schmidtea mediterranea genome database." Genesis **53**(8): 535-546.

Robb, S. M. and A. Sanchez Alvarado (2002). "Identification of immunological reagents for use in the study of freshwater planarians by means of whole-mount immunofluorescence and confocal microscopy." Genesis **32**(4): 293-298.

Ross, K. G., K. C. Omuro, M. R. Taylor, R. K. Munday, A. Hubert, R. S. King and R. M. Zayas (2015). "Novel monoclonal antibodies to study tissue regeneration in planarians." BMC Dev Biol **15**: 2.

Salo, E. (2006). "The power of regeneration and the stem-cell kingdom: freshwater planarians (Platyhelminthes)." Bioessays **28**(5): 546-559.

Sanchez Alvarado, A. (2003). "The freshwater planarian Schmidtea mediterranea: embryogenesis, stem cells and regeneration." Curr Opin Genet Dev **13**(4): 438-444.

Sanchez Alvarado, A. and P. A. Newmark (1999). "Double-stranded RNA specifically disrupts gene expression during planarian regeneration." Proc Natl Acad Sci U S A **96**(9): 5049-5054.

Sanchez Alvarado, A. and P. A. Tsonis (2006). "Bridging the regeneration gap: genetic insights from diverse animal models." Nat Rev Genet **7**(11): 873-884.

Schad, E. G. and C. P. Petersen (2020). "STRIPAK Limits Stem Cell Differentiation of a WNT Signaling Center to Control Planarian Axis Scaling." Curr Biol **30**(2): 254-263 e252.

Schmid, S. L. (2017). "Reciprocal regulation of signaling and endocytosis: Implications for the evolving cancer cell." J Cell Biol **216**(9): 2623-2632.

Scimone, M. L., L. E. Cote and P. W. Reddien (2017). "Orthogonal muscle fibres have different instructive roles in planarian regeneration." Nature **551**(7682): 623-628.

Scimone, M. L., L. E. Cote, T. Rogers and P. W. Reddien (2016). "Two FGFRL-Wnt circuits organize the planarian anteroposterior axis." Elife **5**.

Scimone, M. L., S. W. Lapan and P. W. Reddien (2014). "A forkhead transcription factor is wound-induced at the planarian midline and required for anterior pole regeneration." PLoS Genet **10**(1): e1003999.

Sharma, M., I. Castro-Piedras, G. E. Simmons, Jr. and K. Pruitt (2018). "Dishevelled: A masterful conductor of complex Wnt signals." Cell Signal **47**: 52-64.

Silva, P. N., S. M. Altamentova, D. M. Kilkenny and J. V. Rocheleau (2013). "Fibroblast growth factor receptor like-1 (FGFRL1) interacts with SHP-1 phosphatase at insulin secretory granules and induces beta-cell ERK1/2 protein activation." J Biol Chem **288**(24): 17859-17870.

Srivastava, M., K. L. Mazza-Curll, J. C. van Wolfswinkel and P. W. Reddien (2014). "Whole-body acoel regeneration is controlled by Wnt and Bmp-Admp signaling." Curr Biol **24**(10): 1107-1113.

Steinberg, F., L. Zhuang, M. Beyeler, R. E. Kalin, P. E. Mullis, A. W. Brandli and B. Trueb (2010). "The FGFRL1 receptor is shed from cell membranes, binds fibroblast growth factors (FGFs), and antagonizes FGF signaling in Xenopus embryos." J Biol Chem **285**(3): 2193-2202.

Stocum, D. L. (2004). "Amphibian regeneration and stem cells." Curr Top Microbiol Immunol **280**: 1-70.

Stoick-Cooper, C. L., R. T. Moon and G. Weidinger (2007). "Advances in signaling in vertebrate regeneration as a prelude to regenerative medicine." Genes Dev **21**(11): 1292-1315.

Stoick-Cooper, C. L., G. Weidinger, K. J. Riehle, C. Hubbert, M. B. Major, N. Fausto and R. T. Moon (2007). "Distinct Wnt signaling pathways have opposing roles in appendage regeneration." Development **134**(3): 479-489.

Stuckemann, T., J. P. Cleland, S. Werner, H. Thi-Kim Vu, R. Bayersdorf, S. Y. Liu, B. Friedrich, F. Julicher and J. C. Rink (2017). "Antagonistic Self-Organizing Patterning Systems Control Maintenance and Regeneration of the Anteroposterior Axis in Planarians." Dev Cell **40**(3): 248-263 e244.

Sureda-Gomez, M., J. M. Martin-Duran and T. Adell (2016). "Localization of planarian beta-CATENIN-1 reveals multiple roles during anterior-posterior regeneration and organogenesis." Development **143**(22): 4149-4160.

Sureda-Gomez, M., E. Pascual-Carreras and T. Adell (2015). "Posterior Wnts Have Distinct Roles in Specification and Patterning of the Planarian Posterior Region." Int J Mol Sci **16**(11): 26543-26554.

Swapna, L. S., A. M. Molinaro, N. Lindsay-Mosher, B. J. Pearson and J. Parkinson (2018). "Comparative transcriptomic analyses and single-cell RNA sequencing of the freshwater planarian Schmidtea mediterranea identify major cell types and pathway conservation." Genome Biol **19**(1): 124.

Tanaka, E. M. and P. W. Reddien (2011). "The cellular basis for animal regeneration." Dev Cell **21**(1): 172-185.

Tao, Q., C. Yokota, H. Puck, M. Kofron, B. Birsoy, D. Yan, M. Asashima, C. C. Wylie, X. Lin and J. Heasman (2005). "Maternal wnt11 activates the canonical wnt signaling pathway required for axis formation in Xenopus embryos." Cell **120**(6): 857-871.

Tewari, A. G., J. H. Owen, C. P. Petersen, D. E. Wagner and P. W. Reddien (2019). "A small set of conserved genes, including sp5 and Hox, are activated by Wnt signaling in the posterior of planarians and acoels." PLoS Genet **15**(10): e1008401.

Tewari, A. G., S. R. Stern, I. M. Oderberg and P. W. Reddien (2018). "Cellular and Molecular Responses Unique to Major Injury Are Dispensable for Planarian Regeneration." Cell Rep **25**(9): 2577-2590 e2573.

Trevino, M., D. J. Stefanik, R. Rodriguez, S. Harmon and P. M. Burton (2011). "Induction of canonical Wnt signaling by alsterpaullone is sufficient for oral tissue fate during regeneration and embryogenesis in Nematostella vectensis." Dev Dyn **240**(12): 2673-2679.

Tu, S. and S. L. Johnson (2011). "Fate restriction in the growing and regenerating zebrafish fin." Dev Cell **20**(5): 725-732.

van Wolfswinkel, J. C., D. E. Wagner and P. W. Reddien (2014). "Single-cell analysis reveals functionally distinct classes within the planarian stem cell compartment." Cell Stem Cell **15**(3): 326-339.

Vasquez-Doorman, C. and C. P. Petersen (2014). "zic-1 Expression in Planarian neoblasts after injury controls anterior pole regeneration." PLoS Genet **10**(7): e1004452.

Vogg, M. C., S. Owlarn, Y. A. Perez Rico, J. Xie, Y. Suzuki, L. Gentile, W. Wu and K. Bartscherer (2014). "Stem cell-dependent formation of a functional anterior regeneration pole in planarians requires Zic and Forkhead transcription factors." Dev Biol **390**(2): 136-148.

Vu, H. T., S. Mansour, M. Kucken, C. Blasse, C. Basquin, J. Azimzadeh, E. W. Myers, L. Brusch and J. C. Rink (2019). "Dynamic Polarization of the Multiciliated Planarian Epidermis between Body Plan Landmarks." Dev Cell **51**(4): 526-542 e526.

Wagner, D. E., J. J. Ho and P. W. Reddien (2012). "Genetic regulators of a pluripotent adult stem cell system in planarians identified by RNAi and clonal analysis." Cell Stem Cell **10**(3): 299-311.

Wagner, D. E., I. E. Wang and P. W. Reddien (2011). "Clonogenic neoblasts are pluripotent adult stem cells that underlie planarian regeneration." Science **332**(6031): 811-816.

Wallingford, J. B. and R. Habas (2005). "The developmental biology of Dishevelled: an enigmatic protein governing cell fate and cell polarity." Development **132**(20): 4421-4436.

Wang, I. E., D. E. Wagner and P. W. Reddien (2018). "Clonal Analysis of Planarian Stem Cells by Subtotal Irradiation and Single-Cell Transplantation." Methods Mol Biol **1774**: 479-495.

Wang, J. and I. Conboy (2010). "Embryonic vs. adult myogenesis: challenging the 'regeneration recapitulates development' paradigm." J Mol Cell Biol **2**(1): 1-4.

Wang, Y., R. M. Zayas, T. Guo and P. A. Newmark (2007). "nanos function is essential for development and regeneration of planarian germ cells." Proc Natl Acad Sci U S A **104**(14): 5901-5906.

Wenemoser, D., S. W. Lapan, A. W. Wilkinson, G. W. Bell and P. W. Reddien (2012). "A molecular wound response program associated with regeneration initiation in planarians." Genes Dev **26**(9): 988-1002.

Wenemoser, D. and P. W. Reddien (2010). "Planarian regeneration involves distinct stem cell responses to wounds and tissue absence." Dev Biol **344**(2): 979-991.

Witchley, J. N., M. Mayer, D. E. Wagner, J. H. Owen and P. W. Reddien (2013). "Muscle cells provide instructions for planarian regeneration." Cell Rep **4**(4): 633-641.

Witzel, S., V. Zimyanin, F. Carreira-Barbosa, M. Tada and C. P. Heisenberg (2006). "Wnt11 controls cell contact persistence by local accumulation of Frizzled 7 at the plasma membrane." J Cell Biol **175**(5): 791-802.

Wolpert, L. (1969). "Positional information and the spatial pattern of cellular differentiation." J Theor Biol **25**(1): 1-47.

Wurtzel, O., L. E. Cote, A. Poirier, R. Satija, A. Regev and P. W. Reddien (2015). "A Generic and Cell-Type-Specific Wound Response Precedes Regeneration in Planarians." Dev Cell **35**(5): 632-645.

Yazawa, S., Y. Umesono, T. Hayashi, H. Tarui and K. Agata (2009). "Planarian Hedgehog/Patched establishes anterior-posterior polarity by regulating Wnt signaling." Proc Natl Acad Sci U S A **106**(52): 22329-22334.

Yokoyama, N. and C. C. Malbon (2009). "Dishevelled-2 docks and activates Src in a Wnt-dependent manner." J Cell Sci **122**(Pt 24): 4439-4451.

Zeng, A., H. Li, L. Guo, X. Gao, S. McKinney, Y. Wang, Z. Yu, J. Park, C. Semerad, E. Ross, L. C. Cheng, E. Davies, K. Lei, W. Wang, A. Perera, K. Hall, A. Peak, A. Box and A. Sanchez Alvarado (2018). "Prospectively Isolated Tetraspanin(+) Neoblasts Are Adult Pluripotent Stem Cells Underlying Planaria Regeneration." Cell **173**(7): 1593-1608 e1520.

Zhang, D., J. D. Chan, T. Nogi and J. S. Marchant (2011). "Opposing roles of voltage-gated Ca2+ channels in neuronal control of regenerative patterning." J Neurosci **31**(44): 15983-15995.

Zhuang, L., P. Villiger and B. Trueb (2011). "Interaction of the receptor FGFRL1 with the negative regulator Spred1." Cell Signal **23**(9): 1496-1504.